Networked Implementation of Continuous-Time Distributed Algorithms: A Hybrid System Approach

by

Mani Hemanth Dhullipalla

A thesis submitted in partial fulfillment of the requirements for the degree of

Doctor of Philosophy

in

Control Systems

Department of Electrical and Computer Engineering
University of Alberta

Abstract

With the advancements in functional capabilities of computing and communication devices, there has been a widespread interest in research and implementation of distributed (control and optimization) algorithms. These algorithms frequently find themselves in applications such as distributed computation, sensor estimation, and multi-vehicle/multi-agent coordination. In particular, the continuous-time (CT) variants of these algorithms are studied when physical entities (also referred to as agents), such as autonomous vehicles, whose dynamics naturally evolve over continuous-time, are involved. However, direct implementation of such CT variants necessitates continuous information exchange which is seldom possible. Therefore, this thesis focuses on investigating CT distributed algorithms that employ time- or event-based strategies for discrete-time communication over networks.

We begin by designing event-based broadcast strategies. First, we consider a CT nonlinear system that can be stabilized with a known static state-feedback controller. We employ an emulation-based technique to implement the known controller with intermittent state updates; these updates are governed by event-triggering conditions (or ETCs which are mathematical conditions based on system variables) that dictate when the system can broadcast its state to the controller. Subsequently, we extend the study to the case of multi-agent systems (MASs) where the agents intermittently broadcast the information to their neighbors over a network. Depending on an agent's ability

or inability to sense states (or relative states) of fellow agents, we design two different event-triggering mechanisms (ETMs) that help the agent in making decisions over broadcasts. We demonstrate the effectiveness of the proposed framework by offering two case studies on consensus of agents governed by nonlinear dynamics.

In the aforementioned studies, the focus is on designing event-based broadcast strategies and, therefore, we have assumed that the states are broadcasted without being affected by the network itself. However, in practice, these broadcasts are often prone to several network-induced imperfections. In this thesis, we also investigate aspects of two such imperfections, namely, quantized broadcasts and transmission delays. In this regard, first, we study the problem of consensus among nonlinear agents that broadcast quantized information upon event occurrence. Second, we present a framework for distributed control of nonlinear agents where the state broadcasts take place at pre-defined sampling instants (namely, time-based broadcast strategies) and are susceptible to transmission delays.

Finally, we consider a distributed optimization problem over a class of directed networks where the agents are assigned private cost functions. The agents employ CT accelerated gradient algorithm to asymptotically reach global minima; the convergence of such an algorithm is first established. Subsequently, the distributed control framework proposed earlier is adopted to enable event-based broadcasting of local decision variables.

The effectiveness of the proposed methods in this thesis are demonstrated through case studies, numerical examples and, in some cases, counter-examples. Through these findings, we believe that CT distributed algorithms can be digitally implemented with some ease while simultaneously conserving energy and/or communication resources.

Preface

The ideas in Chapters 3, 4, and 6 have evolved from my discussions with Dr. Hao Yu. With the exception of Chapter 2, the introduction in Chapter 1 and the algorithms, the theoretical analyses, and the case studies in this thesis are part of my original work.

- Chapter 3 has been published as: Mani H. Dhullipalla, Hao Yu and Tongwen Chen. Dynamic periodic event-triggered control for nonlinear plants with state feedback. *IFAC PapersOnLine*, 53(2):2814–2819, 2020.

- Chapter 4 has been published as: Mani H. Dhullipalla, Hao Yu and Tongwen Chen. A framework for distributed control via dynamic periodic event-triggering mechanisms. *Automatica*, 146:110548, 2022.

- Chapter 5 has been accepted for publication as: Mani H. Dhullipalla, Hao Yu and Tongwen Chen. Event-triggered consensus of nonlinear agents with quantized broadcasts: a hybrid system approach. *22nd IFAC World Congress*, Japan, July 2023.

- Chapter 6 has been submitted for publication as: Mani H. Dhullipalla, Hao Yu and Tongwen Chen. Distributed control under transmission delays: a model-based hybrid systems approach. *IEEE Transactions on Automatic Control.*

- Chapter 7 has been submitted for publication as: Mani H. Dhullipalla, Hao Yu and Tongwen Chen. Accelerated gradient flows for weight-balanced digraphs with event-based broadcasting. *IEEE Transactions on Control of Network Systems.*

Dedicated to my family:
Amma, Nanna, Harsha & Kumar.

Acknowledgements

Over the course of this pursuit, several individuals have encouraged and assisted me, both, in my research and in my personal life. I would like to thank every single one of them. In this regard, first and foremost, I would like to express my sincere gratitude towards my supervisor, Dr. Tongwen Chen. His patience, sustained encouragement and advising over the last few years have helped me immensely in shaping my research goals, learning from my failures, fueling my love for control theory and have, collectively, been vital in the completion of this thesis. Along the same note, I would also like to thank Dr. Qing Zhao and Dr. Zhan Shu for graciously accepting our request to be a part of my PhD supervisory committee and for offering their precious time and valuable feedback on my work.

Subsequently, I would like to extend my gratitude towards my colleague and collaborator Dr. Hao Yu for numerous discussions we had (and continue to have) over research problems of common interest and for his suggestions, comments and criticisms on my work and ideas that have helped me refine and evolve them efficiently. Apart from being my colleague at work, I also consider him to be a good friend. I would like to thank all current and previous members of our research group: Junyi, Jing, Rezwan, Haniyeh, Li, Hari, Habib, Jinyuan, Ziyi, Donny, Yashar, Jiang Lin, Boyuan, Hossein, and Jun for their kindness, conversations, and, occasionally, sharing a coffee/lunch.

I also wish to acknowledge the financial support from Natural Sciences and Engineering Research Council of Canada (NSERC) and Alberta EDT Major Innovation Fund. Their support has been essential for me to pursue my research in Canada.

Finally, and on a personal note, I need to express my gratitude and appreciation for everything that my family has done for me; this thesis is dedicated to them. I would also like to acknowledge and appreciate the efforts of two professors from my alma mater: 1) Dr. C. S. Shankar Ram who has initiated me into the world of control theory, and 2) Dr. S. J. Subramanian who has always been my support system, both, during my time at the institute and later in life. My warmest appreciation also extends to my friends: the Marauders (and their spouses), my beloved insti-junta (especially, Nakama and Ruby who have patiently absorbed my rants over the years before expressing their own), Hima, Shazi, Ali, and to all the friends I made in Edmonton (Sowmya, Sumanth, Gokul, Sanat, Shibu, Krishna, Hari, Damayantee, Alan and others); they have all helped me stay mentally resilient and have stood by my side through the thick and thin of life.

Contents

List of Tables

List of Figures

List of Symbols

$\mathbb{R}$ ($\mathbb{R}_{\geq 0}$)	Set of real (respectively, non-negative real) numbers
$\mathbb{R}^n$	Set of $n-$tuples of real numbers
$\mathbb{Z}$ ($\mathbb{Z}_{\geq 0}$)	Set of integer (respectively, non-negative integer) numbers
$\lvert x\rvert$	Euclidean norm of vector $x \in \mathbb{R}^n$
$\langle x, y\rangle$	Inner product of vectors $x, y \in \mathbb{R}^n$
$\mathcal{L}$ ($\mathcal{L}_{\text{os}}$)	Lipschitz (respectively, one-sided Lipschitz) constant
Λ_M^A	Largest eigenvalue of square matrix A
$\mathcal{G}$	Undirected or directed network
$\mathcal{V}$	Set of vertices/agents in the network $\mathcal{G}$
$\mathcal{E}$	Set of edges or communication links in $\mathcal{G}$
L	Weighted graph Laplacian matrix
A	Weighted graph adjacency matrix
Λ_2	Algebraic connectivity of undirected network $\mathcal{G}$
$a_\xi(\mathsf{L})$	Generalized algebraic connectivity of directed network $\mathcal{G}$
$\mathcal{N}_{\text{in}}^i$ ($\mathcal{N}_{\text{out}}^i$)	In-neighbor set (respectively, out-neighbor set) of agent i
$\mathbf{0}$ ($\mathbf{1}$)	Vector of zeros (respectively, ones) of a suitable dimension
$\mathbb{I}_m$	Identity matrix of dimension m
$\otimes$	Kronecker product
$\rightrightarrows$	Used in context of set-valued mapping

List of Acronyms

AGA	Accelerated gradient algorithm
AGF	Accelerated gradient flow (namely, CT AGA)
CT	Continuous-time
DOP	Distributed optimization problem
ETM	Event-triggering mechanism
ETC	Event-triggering condition
LMI	Linear matrix inequality
MAS	Multi-agent system
MAD	Maximum allowable delay
MASP	Maximum allowable sampling period
MLB	Modified-Lagrangian based
NCS	Networked control system
NIP	Network-induced imperfection
SDC	Sampled-data control
ZOH	Zero-order-hold

Chapter 1

Introduction

In this chapter, we introduce research background on distributed control and optimization algorithms and on networked control systems (NCSs). Subsequently, we present a literature survey to summarize the recent developments in event-triggered and sampled-data distributed control and optimization. Thereafter, we list the contributions of this thesis and subsequently provide its outline.

1.1 Research Background

Distributed algorithms have a long history in the field of computer science, particularly, concerning aspects of distributed computation. The central idea here is to breakdown a problem into several smaller ones and appropriately distribute them over a network of processors (also referred to as agents or nodes) in order to potentially reduce the computational burden demanded by the problem, see [56], [3]. Often, in such scenarios, the processors ought to achieve consensus upon some quantities (e.g., on decision variables in distributed optimization, see [80]) while being mindful of their own dynamics. The notion of consensus among dynamical systems was formally studied in [89], [71] and it plays an important role in continuous-time (CT) distributed control and optimization algorithms which form the crux of this thesis.

1.1.1 Distributed Algorithms

Typically, CT distributed algorithms find themselves in cyber-physical applications involving agents (such as unmanned aerial/underwater vehicles, robots, and power grids) whose dynamics naturally evolve in continuous-time, see [15, 41, 87] and the reference therein. These algorithms are often centered around various consensus-based problems such as average consensus in [71,83], average-max-min and finite-time consensus in [13], output consensus in [46], bipartite consensus in [118] and consensus on general functions in [14]. They focus on a plethora of multi-agent coordination problems such as vehicular formations in [47], attitude (namely, orientation) alignment in [82], multi-agent rendezvous in [85], flocking in [95], and coupled oscillators in [40], see survey paper [84]. Most of these problems have also been investigated under the scenarios where

- the nature of agent dynamics is either linear or nonlinear, see [51,70,116],
- the networks are either undirected, directed, or switching, see [71, 116], and
- in the cases where the systems are prone to imperfections such as quantizations, delays, input saturation and others, see [8, 33, 48, 50, 71].

A number of problems in multi-agent coordination can also be posed as distributed optimization problems (DOPs), for instance, a simple multi-agent rendezvous problem can be posed as:

$$\min \sum_i |x_i - x_i(0)|^2 \text{ subject to } x_i = x_j, \forall i, j, \tag{1.1}$$

where x_i denotes the global position of agent i and $x_i(0)$ denotes the agent's initial position. More generally, a DOP is given as follows:

$$\min \sum_i f_i(x_i) \text{ subject to } x_i = x_j, \forall i, j, \tag{1.2}$$

where $f_i(\cdot)$ corresponds to a convex and private local objective function at agent i and the agents across the network eventually agree upon the decision

variable x_i. The DOP in (1.2) can be further generalized to include set and/or inequality constraints.

Algorithms addressing DOPs can be loosely classified based on the techniques they adopt: a) gradient-based approaches in [65, 80], b) alternating direction method of multipliers (ADMM) in [5], c) primal-dual approaches in [126], d) gradient- and Hessian-based approaches in [102], and others, see the survey article in [109]. Most of these algorithms (namely, the ones in [65, 80, 102, 126]) adopt consensus-based approaches and address the DOPs through the discrete-time framework, i.e., the agents in the network run the algorithms iteratively and, often, synchronously.

Over the last decade, motivated by applications involving physical systems, researchers have studied (some of) the aforementioned algorithms in the CT framework. Among these, the gradient-based ones have received considerable attention owing to their low computational costs (which stem from computing gradients) and, more importantly, their flexibility in readily adapting to CT frameworks, see [29, 41, 45, 108, 110].

1.1.2 Networked Control Systems (NCSs)

With the advancements in communication technologies, it may be convenient, and, in some cases necessary (for e.g., in remote implementation of protocols or in applications involving distributed data compilations), to implement algorithms over wireless networks. In such cases, the data transmissions over the network must happen intermittently, owing to finite communication resources, contrary to the case of continuous availability of information in traditional control systems. This notion is pursued under the umbrella of NCSs (see, [39,121]) and sampled-data control (SDC) systems (see, [28]). The methods under these studies can be broadly classified into two categories, namely, time-triggered/sampled-data approaches and event-triggered approaches, see Fig. 1.1 for an illustration. These approaches are often prone to network related issues commonly referred to as network-induced imperfections (NIPs)

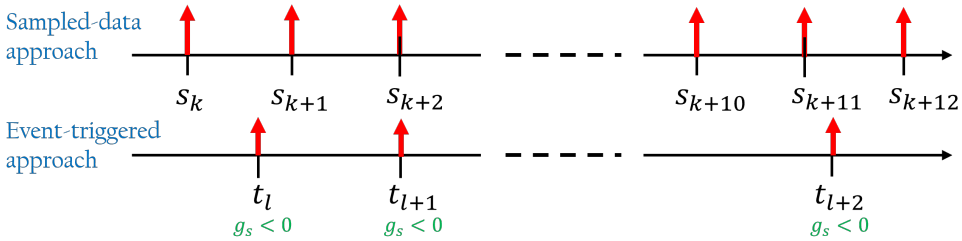

Figure 1.1: An illustration showing broadcasts (depicted in red arrows) across timeline for both sampled-data approaches and event-triggered approaches.

in the literature.

Time-Triggered/Sampled-Data Approaches

In this approach, the broadcasts and/or the controller updates are scheduled to happen at pre-defined sampling instants that could either be periodic or aperiodic and synchronous or asynchronous (in the context of distributed systems or multi-channel networks). Often, the main objective is to compute the upper bounds on sampling intervals such that the closed-loop system meets appropriate notions of stability. This approach is traditionally studied under the title of SDC systems, see the survey article in [28] and the references therein.

Event-Triggered Approaches

Contrary to the time-triggered approach, in this approach the broadcasting and/or the controller updates take place upon occurrence of an *event*[1]. The challenge in this approach is, often, two fold: a) to design the appropriate ETCs, and b) to ensure that the system is not prone to Zeno behavior[2], while simultaneously guaranteeing that the closed-loop system meets appropriate notions of stability, see [94], the survey article in [21] and the references therein. These approaches are naturally aperiodic.

[1]An event is said to have occurred when a mathematical condition involving system variables (known as event-triggering condition (ETC)) is satisfied. This ETC could be monitored either continuously or intermittently.

[2]In the context of event-triggered systems, Zeno behavior is defined as the occurrence of infinite events in a finite interval of time, see [42].

Network-Induced Imperfections

While networked implementation of control and optimization algorithms can be advantageous, often, it comes along with several NIPs such as: a) varying sampling/broadcasting intervals that govern the periodicity of data broadcasts and/or controller updates, b) transmission delays which account for processing times and the time interval between broadcast instants and corresponding arrival instants, c) quantized broadcasts which are essential to communication owing to finite resources/bandwidth, d) data/packet dropouts in cases where receivers fail to pick up broadcasted data, and others, see [38]. A comprehensive study concerning these aspects can be found in survey articles such as [21, 120].

1.2 Literature Review

In this thesis, we focus on developing a framework for networked implementation of CT distributed algorithms. In this section, we present a literature review on the recent developments in networked control and optimization.

1.2.1 Distributed Control

In this subsection, we present literature review associated with the following aspects of networked implementation of distributed control protocols studied in this thesis:

- sampled-data and/or event-triggered implementation,
  - periodic event-triggered control
- NIPs, namely,
  - quantized broadcasts, and
  - transmission delays.

Sampled-Data and/or Event-Triggered Implementation

One way to digitally implement control systems is to employ an emulation-based technique, namely, to first design a CT controller for a CT system and subsequently discretize the controller such that the sampling period (namely, the time interval between two consecutive samplings/broadcasts/updates) is sufficiently small. The design of these sampling instants (or the choice of sampling period) is central to the study of SDC systems where the existence of an upper-bound of allowable sampling periods, called the maximum allowable sampling period (MASP), has been shown for linear systems in [10] and for nonlinear systems in [43,69]. In the context of distributed systems, this notion often translates to how frequently broadcasts must occur in order to ensure appropriate notions of stability, for instance, see consensus algorithms via sampled-data broadcasts in [86].

A possible drawback of SDC systems is that the controllers/transmitters could provide needless inputs/broadcasts to the system even when the system performance is satisfactory. In most cases, this results in unnecessary energy consumption and actuator wear. Compared to the traditional approach, event-triggered control has shown potential in significantly reducing the number of samplings and/or controller updates (only in the cases where Zeno behavior is avoided, see [42]), see [23, 30, 59].

The central aspect of event-triggered control is designing the ETC (or, more generally, the event-triggering mechanism (ETM)) that makes decisions on sampling instants, signal transmissions and controller updates. In the literature, the ETC is broadly classified into two categories depending on how *frequently* it is evaluated, i.e., whether it is monitored continuously or checked periodically (or intermittently) at pre-defined sampling instants; the former notion is referred to as continuous event-triggered control (or, simply, event-triggered control), see, for instance, [1, 30, 94, 101], whereas the later is termed as periodic event-triggered control, see [4, 17, 37, 100], even when the ETC is checked intermittently (and not necessarily periodically). By its construction,

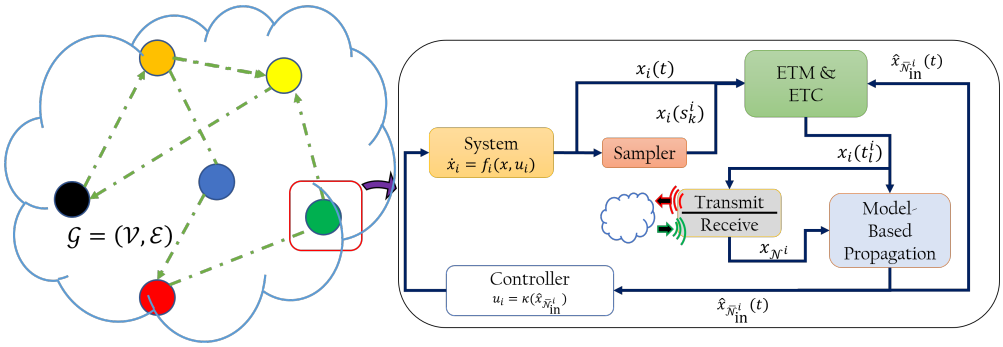

Figure 1.2: An illustration of the model-based control system adopted by agents operating over a communication network $\mathcal{G}$.

a periodic event-triggered controller avoids the problem of Zeno behavior and, to a certain degree, offers freedom in choosing sampling instants at which the ETC is evaluated. In the context of distributed systems, this notion facilitates both synchronous and asynchronous broadcasts alike, thereby helping in reducing network congestion even when the ETM is rendered redundant. In this thesis, we focus our attention on systems that employ either sampled-data approaches and/or periodic event-triggered approaches.

Periodic Event-Triggered Control in Systems and MASs

For linear systems, periodic event-triggered control has been studied via the following three approaches: 1) impulsive system approach, 2) perturbed linear systems approach, and 3) piece-wise linear systems approach, see [35], and dynamic periodic event-triggered controllers were also discussed in [4]. For nonlinear systems, one way to construct such controller schemes is to start from an existing CT event-triggered controller that stabilizes the system, see [76]. Alternatively, an emulation-based technique is employed to design a periodic event-triggered controller in [99]. For the case of nonlinear systems, both [76, 99] employ static ETMs.

For MASs with linear agent dynamics, reference [60] evaluates the ETCs periodically; however, the agents in the network also broadcast their state information at these instants whereas the local controllers are updated only upon event occurrences. Unlike [60], studies in [16, 32, 61, 125] make decisions

on broadcasting information based on the ETCs which are evaluated periodically. For MASs with nonlinear agent dynamics, there are few results which evaluate the ETCs periodically, see [18,90,115]. Reference [90] employed zero-order-hold (ZOH) on the incoming broadcasts; while this may work for systems with bounded nonlinearities (as remarked in [90]), it may not work for systems with Lipschitz or one-sided Lipschitz nonlinearities. Such a concern can be handled by employing model-based propagation of the broadcasted states, see reference in [115] where the authors studied the consensus problem in the case of Lipschitz nonlinear agent dynamics. Our work in [18] (included in Chapter 4 of this thesis) also employed model-based propagation of broadcasts but offered a more general framework for distributed control; an illustration of this framework is depicted in Fig. 1.2. Consequently, we addressed the consensus problems over nonlinear agents (with Lipschitz and one-sided Lipschitz dynamics) as case studies of the proposed framework.

NIP: Quantized Broadcasts

Information exchange in NCSs, in practice, necessitates that the data, prior to broadcasting, undergoes some sort of quantization to accommodate for the limited (or finite) network bandwidth available. NCSs with quantized transmissions have been studied using both static and dynamic quantizers, for instance, see [36, 79, 81, 105, 127] and the references therein. Solely employing static uniform quantizers in NCSs for transmission offers (some) control over the size of transmitted data (namely, by adjusting the quantization gain); however, it often leads to bounded convergence, see [2]. Dynamic quantizers, on the other hand, utilize a zoom parameter to dynamically adjust the quantization gain; in such cases, the precision of data transmitted may not be adjusted but asymptotic convergence can be achieved, see [6, 36, 105].

In the context of MASs, early studies that adopted quantized information in CT consensus problems employed tools from the theory of discontinuous differential equations and nonsmooth analysis for linear agents in [8, 19] and, more recently, for nonlinear agents in [103]. Subsequently, problems involving

quantized information exchange were studied both in the context of sampled-data approaches and event-triggered approaches where the information was, typically, quantized prior to broadcasting; in such cases, researchers could circumvent the difficulties associated with the discontinuous nature of quantizers, see [27, 49, 57, 115, 123] and the references therein. Studies which solely employed static quantizers prior to broadcasting achieved practical consensus, see [123, 124]. On the other hand, studies such as [49, 115] employed static (uniform) quantizers along with encoding and decoding schemes; together, these mechanisms ensured asymptotic convergence. In the last few years, there have also been studies on event-triggered consensus algorithms that employ dynamic quantizers, see [57] for linear agent dynamics and [92] for nonlinear agent dynamics.

With the exception of [115], studies such as [27, 49, 57, 92, 123] on event-triggered distributed control either involved continuous monitoring of ETCs or addressed problems involving agents with linear dynamics.

NIP: Transmission Delays

In practice, data broadcasts suffer from transmission delays; often these delay estimates can also account for processing times taken up by the system's receiver/transmitter hardware. In this context, a large pool of literature in NCSs primarily focuses on systems with linear dynamics, see survey articles [39] and [121]. For CT linear systems, studies have modeled the NCSs in terms of impulsive delay-differential equations, see [25, 64]. For CT nonlinear systems, studies such as [114] and [7] extended the approach of delay-differential equations to handle nonlinearities, and studies such as [74] and [66] employed the concept of approximate discrete-time models. Reference [38] comprehensively expanded the seminal work in [69] to address NCSs that suffer from some of the aforementioned NIPs.

In the case of MASs, early studies such as [71, 72] addressed the problem of transmission delays in consensus of single-integrator systems. Studies employing sampled-data approaches addressed consensus problems for linear agent

dynamics in [22, 93, 107] and for nonlinear agent dynamics in [9, 20, 34]. Most of these studies (namely, [9, 20, 22, 34, 93, 107]) employ the ZOH approach, i.e., they utilize the broadcasted states directly in their control protocols. However, early studies on model-based control have shown potential in stretching the upper bound on the sampling period, see [63, 73]. For linear NCSs, the authors in [63] studied model-based control of systems prone to transmission delays. For nonlinear NCSs prone to transmission delays, approximate discrete-time models were employed to construct a model-based scheme for SDC of the system, see [55]. Recently, in [112], this problem for nonlinear NCSs was studied employing tools from hybrid dynamical systems.

For MASs with nonlinear agent dynamics, studies in [18, 58, 104, 106, 115] have employed model-based propagation of the broadcasted information for SDC of linear and nonlinear agent dynamics. The distinguishing feature in studies such as [18, 115] (and [54]), apart from employing model-based controllers, is that the MASP of the MAS can be computed explicitly unlike in studies such as [58, 104, 106] where it is numerically solved using linear matrix inequalities (LMIs). In [54], the authors discussed the problem of interconnected systems where the (linear) dynamics of a subsystem depends on its fellow subsystems whereas the model-based control protocol depends, solely, on the state of the concerned subsystem. As a result, the transmission delay between the subsystem and the controller only affected the modeling on the concerned subsystem and not its neighboring subsystems. In general, the same is not true for MASs where the delays associated with an agent's broadcast affects models at all of its neighbors. The authors in [115] addressed the case of quantized information exchange among Lipschitz nonlinear agents, but did not discuss the aspect of transmission delays that might affect these exchanges. On the other hand, [90] studied nonlinear MASs in the presence of transmission delays; however, the study employed the ZOH approach on the incoming broadcasts. Furthermore, as remarked in [90], the dynamics of the agents are restricted to bounded nonlinearities. Contrary to [90], our work

in [18] (included in this thesis) offered a general framework for distributed control using model-based propagation of state broadcasts; however, it did not study MASs that may be prone to transmission delays.

1.2.2 Event-Triggered Distributed Optimization

In this thesis, we address the DOP described in (1.2) by designing a CT distributed accelerated gradient algorithm (AGA); we adopt the term accelerated gradient flows (AGFs) to refer to CT AGAs. In this section, we briefly present a literature review associated with AGAs, AGFs, and event-triggered optimization.

AGAs (also referred to as heavy-ball algorithms), first introduced by Polyak in the seminal paper in [75], injects the concept of acceleration, via a momentum term, in traditional gradient descent algorithms. A similar algorithm was later introduced by Nesterov in [67]. These algorithms have been shown to achieve global optimal convergence rates for quadratic cost functions and convex (and strongly convex) functions, respectively. Most of the algorithms (and their variations) are studied in the discrete-time framework. Over the last decade, authors in [91] studied Nesterov algorithms from the eye of dynamical systems providing a CT limit, a differential equation, to the discrete-time Nesterov method. This work has rekindled interest in studying CT accelerated gradient methods in the search of faster and robust algorithms as well as their extensions in a distributed architecture, see [119], [110].

In the recent past, several papers have studied AGFs in the distributed framework, see [110, 117, 122]. In [122], the authors extended the approach in [29] to second-order MASs. However, [122] required the nodes to communicate both states and their derivatives. In [110], exponential convergence with an upper bound on decay rates was established that relied on system parameters through several intermediate coefficients. This makes it difficult to attain arbitrary (fast) convergence rates that can be achieved for AGFs as shown in [117]. This property can be quite useful, particularly, in multi-agent coor-

dination problems. Furthermore, all these studies (namely, [110,117,119,122]) consider the underlying communication topology to be a connected (undirected) graph. Very recently, the case of AGFs for directed networks was studied, see [108]. However, the authors in [108] used a push-pull approach which required exchange of several intermediate states; this is not necessary if the digraph is weight-balanced as shown in [45, 113]. In other words, if a digraph is weight-balanced, then one can save on communication resources by broadcasting (relatively) smaller data vectors.

Similar to the case of distributed control algorithms, for networked implementation of CT optimization algorithms, almost all existing studies employed sampled-data broadcast protocols or continuous event-triggered broadcast protocols, see [45,97,110] and the references therein. For sampled-data broadcast protocols in [45,97], the MASP that separates two consecutive broadcasts was established; and for event-triggered broadcast protocols in [45, 97, 110], the absence of Zeno behavior was demonstrated. To the best of our knowledge, intermittent monitoring of the ETCs has not been studied yet in the context of distributed optimization.

1.3 Thesis Contributions

The contributions of this thesis that distinguish it from related literature are summarized as follows:

- First, we study the problem of designing dynamic periodic ETMs for CT nonlinear systems which can be stabilized via CT state-feedback controllers. We model the closed-loop system as a hybrid dynamical system and, as a consequence of the stability analysis, obtain the MASP.

- Second, we extend the study on nonlinear systems to nonlinear MASs and develop a framework for distributed control via dynamic ETMs that make decisions on state broadcasting. In this study, we utilize model-based propagations of the broadcasted states and design two dynamic

ETMs based on an agent's ability (or inability) to sense states of fellow agents in the network. Furthermore, we discuss two case studies on the problem of consensus amongst (Lipschitz and one-sided Lipschitz) nonlinear agents that interact over both undirected and directed communication networks.

- Third, we investigate a case of distributed control under a specific type of NIP, namely, quantized broadcasts. We address the problem of consensus among nonlinear agents that communicate via quantized broadcasts. For this, we adopt the framework developed for distributed control via dynamic ETMs. Additionally, we consider that each agent employs an encoder scheme (prior to broadcasting information) and decoder schemes (to process received information) in order to achieve asymptotic consensus.

- Fourth, we consider the problem of distributed control subject to yet another NIP, namely, transmission delays. In this study, we propose a methodology for SDC of nonlinear MASs which employ model-based propagation of the broadcasted states. We demonstrate the effectiveness of the proposed framework by addressing the consensus problem on Lipschitz nonlinear agents.

- Finally, we consider a DOP over a weight-balanced directed network where the agents employ AGF. In this study, we first establish sufficient conditions on gains in the AGF to ensure the convergence of the CT algorithm. Subsequently, we design a dynamic ETM that checks for events intermittently and makes decision on broadcast instants.

1.4 Thesis Outline

The remainder of this thesis is organized as follows. Chapter 2 presents concepts from hybrid dynamical systems that are employed throughout this thesis. In Chapter 3, the problem of dynamic event-triggered control of a

nonlinear system is studied. Chapter 4 extends the work on single-agent systems to MASs and offers a framework for distributed control via event-triggered broadcasts. Furthermore, the chapter also presents two case studies on consensus problems that demonstrate the effectiveness of the proposed framework. In Chapter 5, an event-triggered consensus of nonlinear agents broadcasting quantized information is studied. Chapter 6 investigates the problem of sampled-data distributed control in the presence of transmission delays when model-based propagation of broadcasts is employed. In Chapter 7, the proposed distributed control framework is employed to study event-triggered implementation of CT AGAs. Finally, Chapter 8 makes concluding remarks on the thesis and offers some potential directions for future research.

Chapter 2

Preliminaries on Hybrid Dynamical Systems

In this thesis, we employ sampled-data based approach to design broadcast protocols (either time-triggered or event-triggered) for implementing CT algorithms over a network. Activities such as sampling and broadcasting take place at discrete-time instants (namely, sampling and/or event-triggering instants) and allow for instantaneous changes in control (or event mechanism) protocols. These instantaneous changes are referred to as *jumps* and can be described by difference equations. On the other hand, between any two consecutive sampling instants, the algorithms operate in CT and are typically characterized by differential equations; this behavior is termed as *flow*. This *hybrid* nature (namely, combination of flows and jumps across time) of NCSs falls innately under the umbrella of hybrid dynamical systems (or simply referred to as hybrid systems).

One of the consequences of employing hybrid systems approach to model NCSs is that the system's behavior is diligently analyzed, both, during flow and at jumps. This is in contrast to traditional approaches where, for CT systems, one is largely concerned about its behavior during flow (in other words, often, it is adequate if one ensures that the changes caused by jumps do not disrupt the system's stability or, alternatively, result in rise in its Lyapunov function). However, unlike traditional approaches, a close examination of the system's behavior at jumps offers an opportunity to potentially improve the

design of various dynamic ETMs employed throughout this thesis, see Section 3.2 in Chapter 3 for a remark on this. Another instance demonstrating the advantage of adopting hybrid systems approach compared to its traditional counterpart is highlighted in Remark 5.1 which comments on the conservativeness of MASP estimates computed in [115] (using traditional approach) compared to our work in Chapter 5.

Since we adopt hybrid systems framework throughout this thesis, in this chapter, we briefly present some mathematical preliminaries and concepts on hybrid dynamical systems from the textbook in [31] and the articles in [68,69]. The rest of this chapter is organized as follows. Section 2.1 introduces the idea of hybrid dynamical systems followed by Section 2.2 which discusses a class of systems that offer special properties on solutions to these systems. Section 2.3 presents the concept of solutions for hybrid systems and Section 2.4 defines some of the stability notions used in this thesis.

2.1 Introduction

A hybrid system, denoted by the quartet $\mathcal{H} = (C, F, D, G)$, consists of two aspects of dynamical systems, namely, *flows* and *jumps*, and is expressed by the following set of inclusions:

$$\dot{x}(t,j) \in F(x(t,j)), \quad x \in C, \tag{2.1a}$$

$$x(t,j+1) \in G(x(t,j)), \quad x \in D. \tag{2.1b}$$

Here, the differential inclusion in (2.1a) describes the set of vector fields (given by flow map $F(x)$) that the state x can flow along when it is part of the flow set C. Likewise, the difference inclusion in (2.1b) describes the set of states (given by jump map $G(x)$) that x could, instantaneously, take when it is in the jump set D. As a result, the trajectory of x complying with (2.1) is typically parameterized by the pair (t, j) where t denotes the time (during flow) and j denotes the jump instant. From (2.1b) one can infer that the jump phenomenon takes place instantaneously, i.e., time t remains unchanged

before and after a jump. In this context, we use the shorthand notation x^+ to describe jump state $x(t, j+1)$ in (2.1b).

2.2 Nominal Well-Posedness

Throughout this thesis, we study various hybrid dynamical systems that are nominally well-posed. This notion for a hybrid system, vaguely speaking, offers properties such as local boundedness of sets of solutions, the dependence of these solutions on initial conditions, and also offers numerous consequences on asymptotic stability and robustness of the hybrid system. Therefore, in this subsection, we first present (easily verifiable) conditions that ensure that the hybrid system $\mathcal{H}$ is nominally well-posed. For reasons of brevity, we refrain from presenting involved technical definitions of nominal well-posedness and refer the interested reader to Chapter 6 in [31].

Definition 2.1. *(Outer semicontinuous) A set-valued mapping $M : \mathbb{R}^m \rightrightarrows \mathbb{R}^n$ is outer semicontinuous at $x \in \mathbb{R}^m$ if for every sequence of points x_i convergent to x and any convergent sequence of points $y_i \in M(x_i)$, one has $y \in M(x)$, where $\lim_{i\to\infty} y_i = y$. The mapping M is outer semicontinuous if it is outer semicontinuous at each $x \in \mathbb{R}^m$.*

Let $\texttt{dom}A$ denote the domain of mapping A. The following conditions are sufficient (as stated in Lemma 2.1) to ensure that $\mathcal{H}$ is nominally well-posed.

Assumption 2.1. *(Hybrid basic conditions)*

1. *flow domain C and jump domain D are closed subsets of $\mathbb{R}^n$;*
2. *flow map $F : \mathbb{R}^n \rightrightarrows \mathbb{R}^n$ is outer semicontinuous and locally bounded relative to C, $C \subset \texttt{dom}F$, and $F(x)$ is convex for every $x \in C$;*
3. *jump map $G : \mathbb{R}^n \rightrightarrows \mathbb{R}^n$ is outer semicontinuous and locally bounded relative to D and $D \subset \texttt{dom}G$.*

Lemma 2.1. *(Nominal well-posedness) If the hybrid system $\mathcal{H}$ satisfies Assumption 2.1, then it is nominally well-posed.*

2.3 Concept of Solutions

In this section, we formally define the concept of solution for hybrid systems that are nominally well-posed (and refer the interested reader to Proposition 6.10 in [31] for existence of solutions). We also provide a short note on the types of solutions restricting ourselves to those which are relevant to the context of this thesis.

Definition 2.2. *(Hybrid time domain) A compact hybrid time domain is defined by the subset* $\mathfrak{T} = \cup_{j=0}^{J-1}([t_j, t_{j+1}], j) \subset \mathbb{R}_{\geq 0} \times \mathbb{Z}_{\geq 0}$ *where* $j \in \mathbb{Z}_{\geq 0}$ *and* $0 = t_0 \leq t_1 \cdots \leq t_J$. *The set* $\mathfrak{T}$ *is a hybrid time domain if* $\forall (T, J) \in \mathfrak{T}$, $\mathfrak{T} \cap ([0, T] \times \{0, \cdots, J\})$ *is a compact hybrid domain.*

Definition 2.3. *(Hybrid arc) A hybrid arc is defined as a function* $\mathfrak{S} : \mathfrak{T} \to \mathbb{R}^n$ *if* $\mathfrak{T}$ *is a hybrid time domain and if* $\forall j \in \mathbb{Z}_{\geq 0}$, *the function* $t \to \mathfrak{S}(t, j)$ *is locally absolutely continuous on the interval* $I^j = \{t | (t, j) \in \mathfrak{T}\}$.

Definition 2.4. *(Solution of* $\mathcal{H}$*) A hybrid arc* $\mathfrak{S}$, *whose domain is denoted by* $\texttt{dom}\mathfrak{S}$, *is a solution to the hybrid system* $\mathcal{H}$ *if* $\mathfrak{S}(0, 0) \in C \cup D$, *and*

- $\forall j \in \mathbb{Z}_{\geq 0}$ *such that* $I^j := \{t | (t, j) \in \texttt{dom}\mathfrak{S}\}$,

$$\begin{cases} \mathfrak{S}(t, j) \in C, \\ \dot{\mathfrak{S}}(t, j) = F(\mathfrak{S}(t, j)) \end{cases} \qquad \text{for almost all } t \in I^j$$

- $\forall (t, j) \in \texttt{dom}\mathfrak{S}$ *such that* $(t, j + 1) \in \texttt{dom}\mathfrak{S}$,

$$\begin{cases} \mathfrak{S}(t, j) \in D, \\ \mathfrak{S}(t, j + 1) \in G(\mathfrak{S}(t, j)) \end{cases}$$

The solutions to $\mathcal{H}$ are classified based on its hybrid time domain. A solution $\mathfrak{S}$ is

- *complete* if $\texttt{dom}\mathfrak{S}$ is unbounded, i.e., if $\sup_t \mathfrak{T} + \sup_j \mathfrak{T} = \infty$, where $\mathfrak{T}$ is the hybrid time domain defined above;

- *maximal* if there does not exist another solution $\bar{\mathfrak{S}}$ to $\mathcal{H}$ such that $\texttt{dom}\mathfrak{S} \subset \texttt{dom}\bar{\mathfrak{S}}$ and $\mathfrak{S}(t, j) = \bar{\mathfrak{S}}(t, j)$ for all $(t, j) \in \texttt{dom}\mathfrak{S}$;

- *eventually discrete* if $T = \sup_t \mathtt{dom}\mathfrak{S} < \infty$ and $\mathtt{dom}\mathfrak{S} \cap (\{T\} \times \mathbb{Z}_{\geq 0})$ contains at least two points;
- *instantaneously Zeno* if it is complete and eventually discrete;
- *genuinely Zeno* if it is complete but not eventually discrete.

In this thesis, we implicitly assume that are no finite escape times during flow of the constructed hybrid system model $\mathcal{H}$; this along with Assumption 2.1 ensures complete solutions of $\mathcal{H}$, see Proposition 6.10 in [31].

2.4 Stability

In this section, we present definitions of input-to-state stability and asymptotic stability that are borrowed from [68]. Consider the following hybrid system:

$$\begin{cases} \dot{x} = f(t, x, w), & t \in [s_k, s_{k+1}] \\ x^+ = h(x(s_k)), & t \in \{s_k\} \end{cases} \tag{2.2}$$

where $\{s_k | k \in \mathbb{N}\}$ is monotonically increasing sequence of time such that $s_0 = 0$, $x \in \mathbb{R}^n$ and $w \in \mathbb{R}^m$ are the state and external input, respectively, of the system. Assume that functions f, h are such that the hybrid system in (2.2) is nominally well-posed.

Definition 2.5. *(Input-to-state stable) Let $\gamma \in \mathcal{K}$ and $\beta \in \mathcal{KL}$ be given. The system (2.2) is input-to-state stable (ISS) from w to x if for all $t_0 \geq 0$, $x_0 \in \mathbb{R}^n$, $w \in \mathcal{L}_\infty$ and each corresponding solution $x(\cdot)$, we have that*

$$|x(t)| \leq \beta(|x_0|, t - t_0) + \gamma(\|w\|_{\mathcal{L}_\infty}), \quad \forall t \in [t_0, t_0 + T) \tag{2.3}$$

where $[t_0, t_0 + T)$ is the maximal interval of definition of $x(\cdot)$.

Definition 2.6. *(Uniform global asymptotic stability) Let $\beta \in \mathcal{KL}$ be given. The system in (2.2), with $w \equiv 0$, is uniformly globally asymptotically stable is for all $x_0 \in \mathbb{R}^n$ and all corresponding solutions $x(\cdot)$, we have*

$$|x(t, t_0, x_0)| \leq \beta(|x_0|, t - t_0), \quad \forall t \geq t_0 \geq 0. \tag{2.4}$$

Chapter 3

Dynamic Event-Triggered Control of Nonlinear Systems[1]

In this chapter, we present two methods for the design of dynamic periodic event-triggered control of nonlinear systems via state feedback. These methods differ in their construction of the dynamic ETMs; one requires continuous availability of states of the system and the other relaxes this assumption. As a part of the design methodology, we adopt an emulation-based technique, i.e., we assume the knowledge of an existing CT static state-feedback controller that stabilizes the nonlinear system. Subsequently, an auxiliary variable is defined that facilitates the formulation of dynamic ETM which is evaluated at specific sampling instants. Considering the event-based controller updation, the resultant closed-loop system is modeled as a hybrid system. The dynamic ETM and an upper bound on the sampling period, called a maximum allowable sampling period (MASP), are both obtained as a consequence of stability analysis.

The rest of this chapter is organized as follows. Section 3.1 presents preliminaries and notations that are used throughout this thesis. The description and formulation of the problem are addressed in Section 3.2. Section 3.3 discusses two methods of dynamic PETC schemes providing stability analysis in each case. An illustrative example discussing the two methods is provided in

[1]The material in this chapter has been published as: Mani H. Dhullipalla, Hao Yu and Tongwen Chen. Dynamic periodic event-triggered control for nonlinear plants with state feedback. *IFAC PapersOnLine*, 53(2):2814-2819, 2020.

Section 3.4 followed by concluding remarks in Section 3.5.

3.1 Preliminaries

Denote $\mathbb{R}$ to be set of real numbers, $\mathbb{Z}$ to be the set of integers then $\mathbb{R}_{\geq 0} = [0, \infty)$ and $\mathbb{Z}_{\geq 0} = \{0, 1, 2, \dots\}$. Let $|x|$ be the Euclidean norm of an n-dimensional vector $x \in \mathbb{R}^n$. A continuous function $\alpha : [0, a) \to \mathbb{R}_{\geq 0}$ is said to be of class $\mathcal{K}$ if it is strictly increasing and $\alpha(0) = 0$. Further, α is said to be of class $\mathcal{K}_\infty$ if $\alpha(r) \to \infty$ as $r \to \infty$. A continuous function $\beta : [0, a) \times \mathbb{R}_{\geq 0} \to \mathbb{R}_{\geq 0}$ is said to be of class $\mathcal{KL}$ if for a fixed $r \in \mathbb{R}_{\geq 0}$, $\beta(\cdot, r)$ belongs to class $\mathcal{K}$ and for a fixed $s \in [0, a)$, $\beta(s, \cdot)$ decreases to zero. A function f is locally Lipschitz if it satisfies the Lipschitz condition: $|f(x) - f(y)| \leq \mathcal{L}|x - y|$ for some scalar $\mathcal{L}$ in the neighborhood of every point in the domain $\mathcal{X} \subset \mathbb{R}^n$. A function f is locally one-sided Lipschitz if it satisfies the condition: $(x - y)^{\mathrm{T}}(f(x) - f(y)) \leq \mathcal{L}_{os}|x - y|^2$ for some scalar $\mathcal{L}_{os} \in \mathbb{R}$ in the neighborhood of every point in the domain $\mathcal{X}$. The function is globally Lipschitz (or one-sided Lipschitz) if the domain $\mathcal{X} = \mathbb{R}^n$. The Clarke derivative, in [12], is defined as follows: for a locally Lipschitz function $U : \mathbb{R}^n \to \mathbb{R}$ and a vector $v \in \mathbb{R}^n$, $U^\circ(x, v) := \limsup_{h \to 0^+, y \to x} \frac{U(y+hv) - U(y)}{h}$. Furthermore, we have $U^\circ(x, v) \leq \limsup_{y \to x} \langle \nabla U(y), v \rangle$ where $\langle \cdot, \cdot \rangle$ is the inner product and $\nabla U(\cdot)$ is the classical gradient, see [68, 96]. For a C^1 function $U(\cdot)$, the Clarke derivative $U^\circ(x, v)$ reduces to the standard directional derivative $\langle \nabla U(x), v \rangle$. This definition is useful to treat locally Lipschitz functions which may not differentiable everywhere.

The following lemma is used to show asymptotic stability via Lyapunov analysis that is discussed in Section 3.3.

Lemma 3.1 ([12,53]). *Consider two functions $U_1 : \mathbb{R}^n \to \mathbb{R}$ and $U_2 : \mathbb{R}^n \to \mathbb{R}$ that have well-defined Clarke derivatives for $x \in \mathbb{R}^n$ and $v \in \mathbb{R}^n$. Introduce three sets $\mathcal{A} := \{x : U_1(x) > U_2(x)\}$,$\mathcal{B} := \{x : U_1(x) < U_2(x)\}$, $\Omega := \{x : U_1(x) = U_2(x)\}$. Then for any $v \in \mathbb{R}^n$, the function $U(x) := \max\{U_1(x), U_2(x)\}$ satisfies $U^\circ(x; v) = U_1^\circ(x; v)$ for $x \in \mathcal{A}$, $U^\circ(x; v) = U_2^\circ(x; v)$*

for $x \in \mathcal{B}$*, and* $U^\circ(x;v) \leq \max\{U_1^\circ(x;v), U_2^\circ(x;v)\}$ *for* $x \in \Omega$.

3.2 Problem Formulation

Consider the following nonlinear system model

$$\dot{x} = f(x,u), \tag{3.1}$$

where $x \in \mathbb{R}^n$ is the state and $u \in \mathbb{R}^m$ is the control input. The function $f : \mathbb{R}^n \times \mathbb{R}^m \to \mathbb{R}^n$ is assumed to be continuous. It is assumed that the full state vector x is measured, and there exists a static state-feedback controller stabilizing the system in (3.1):

$$u = \kappa(x), \tag{3.2}$$

where $\kappa : \mathbb{R}^m \to \mathbb{R}^n$ is the controller gain function. Due to the limited communication resources, we intend to implement the controller in (3.2) (over a network) in an event-triggered manner. To facilitate this, we define two time instants, namely, sampling instants and event-triggering instants.

First, we define a time sequence $\{s_k\}_{k=0}^{\infty}$, used to check for event occurrences, such that

$$\varepsilon \leq s_{k+1} - s_k \leq T, \tag{3.3}$$

for all $k \in \mathbb{Z}_{\geq 0}$. The upper bound $T > 0$ is to be designed, and the lower bound $\varepsilon \in (0, T]$ between the two consecutive sampling instants, s_k and s_{k+1}, is decided by the hardware constraints and ensures instantaneous Zeno solutions of the hybrid system (defined in (3.7)) are avoided. Note that the condition on sampling instants in (3.3) facilitates both periodic and aperiodic monitoring of event occurrences (namely, evaluating ETC); however, we continue to call this approach *periodic* ETM to keep in line with the terminology used in articles such as [98,99]. Furthermore, let $\{t_l\}_{l=0}^{\infty} \subset \{s_k\}_{k=0}^{\infty}$ be a subsequence denoting the event-triggering instants whose construction is discussed shortly in (3.6).

When an event occurs at time t_l according to some pre-designed ETC, the state $x(t_l)$ will be broadcasted to the controller node that updates the control

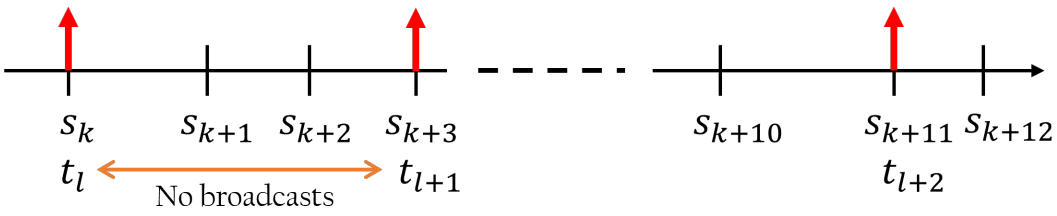

Figure 3.1: Sequence of sampling instants $\{s_k\}$ and event-triggering instants $\{t_l\}$ (where red arrows at $\{t_l\}$ depict broadcasting). Note that the sampling sequence $\{s_k\}$ is not necessarily periodic and that $\{t_l\} \subseteq \{s_k\}$.

signal. Denote $\hat{x}(t) := x(t_l),\ t \in [t_l, t_{l+1})$, as the latest broadcasted state. The periodic event-triggered state-feedback controller is then given by

$$u = \kappa(\hat{x}). \tag{3.4}$$

In this work, we will implement a dynamic periodic ETM, which involves the following piecewise continuous auxiliary variable $\eta \in \mathbb{R}_{\geq 0}$ governed by

$$\begin{cases} \dot{\eta} = f_\eta(\eta, x, e), & t \in [s_k, s_{k+1}); \\ \eta(t^+) = g_s(\eta, x, e), & t \in \{s_k\} \setminus \{t_l\}; \\ \eta(t^+) = g_t(\eta, x, e), & t \in \{t_l\}; \end{cases} \tag{3.5}$$

where $e = \hat{x} - x$ is the broadcast error with $e(t_l) = \mathbf{0}, \forall l \in \mathbb{Z}_{\geq 0}$ upon event occurrence. The function f_η is continuous on $\mathbb{R}_{\geq 0} \times \mathbb{R}^n \times \mathbb{R}^n$ and is such that $f_\eta(0, x, e) \geq 0$ for all $x, e \in \mathbb{R}^n$. The functions g_s and g_t, defined on $\mathbb{R}_{\geq 0} \times \mathbb{R}^n \times \mathbb{R}^n$, are continuous and continuous non-negative, respectively. The considered ETC, evaluated at every sampling instant $\{s_k\}$, is as follows:

$$t_{l+1} = \min\{t > t_l \mid t \in \{s_k\}_{k=0}^{\infty},\ g_s(\eta, x, e) < 0\} \tag{3.6}$$

which generates the subsequence $\{t_k\}_{k=0}^{\infty}$ of event-triggering instants, see Fig. 3.1 for an illustration. Fig. 3.2 depicts the trajectory of auxiliary variable $\eta(t)$ described by the dynamics in (3.5). The occurrence of event at s_{k+1} is also shown in Fig. 3.2 and the value of η^+ at s_{k+1} after the jump can be designed such that $\eta^+ = g_t \geq \eta$; this notion can be observed from the ETMs designed in both Theorems 3.1 and 3.2. Without loss of generality, we assume that the event is triggered at the initial instant, i.e., $e(0) = \mathbf{0}$ and $t_0 = s_0 = 0$.

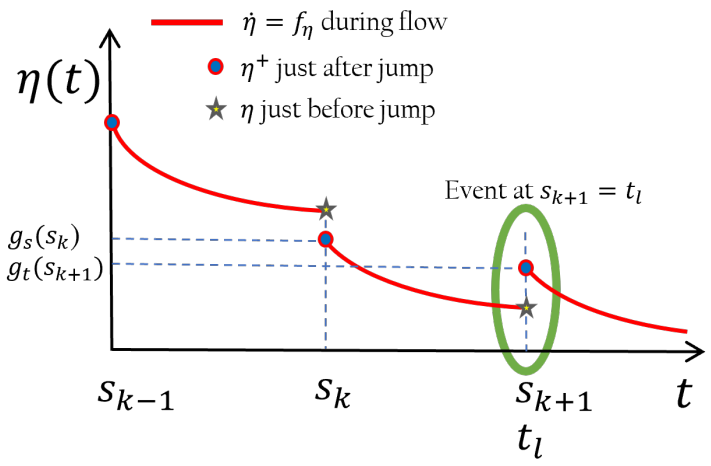

Figure 3.2: Hybrid dynamics of η and event occurrence at s_{k+1}.

Let $\tau \in \mathbb{R}_{\geq 0}$ keep track of the time elapsed since the last sampling instant with the dynamics:

$$\begin{cases} \dot{\tau} = 1, & \text{when } \tau \in [0, T]; \\ \tau^+ = 0, & \text{when } \tau \in [\varepsilon, T]. \end{cases}$$

We thus model the closed-loop system as the following hybrid system:

$$\begin{cases} \dot{q} = F(q), & q \in C, \\ q^+ \in G(q), & q \in D, \end{cases} \tag{3.7}$$

where the augmented state $q := (x, e, \tau, \eta)$, the sets

$$\begin{aligned} C &:= \{q \in \mathbb{R}^{2n+2} \mid \tau \in [0, T],\ \eta \in \mathbb{R}_{\geq 0}\}, \\ D &:= \{q \in \mathbb{R}^{2n+2} \mid \tau \in [\varepsilon, T],\ \eta \in \mathbb{R}_{\geq 0}\}, \end{aligned} \tag{3.8}$$

and the function $F(q)$ and the set-valued mapping $G(q)$ are given by

$$\begin{aligned} F(q) &= \begin{bmatrix} f(x, \kappa(x+e)) \\ -f(x, \kappa(x+e)) \\ 1 \\ f_c(\eta, x, e) \end{bmatrix}, \quad \text{and} \\ G(q) &= \begin{cases} G^1, & g_s(\cdot) > 0; \\ G^2, & g_s(\cdot) < 0; \\ \{G^1, G^2\}, & g_s(\cdot) = 0, \end{cases} \end{aligned} \tag{3.9}$$

respectively, where

$$G^1 = \begin{bmatrix} x \\ e \\ 0 \\ g_s(\eta, x, e) \end{bmatrix}, \quad G^2 = \begin{bmatrix} x \\ \mathbf{0} \\ 0 \\ g_t(\eta, x, e) \end{bmatrix}.$$

Here, the flow set C is such that the system flows between any two sampling instants, say during the interval $[s_k, s_{k+1}]$, and jumps at the sampling instants, i.e., at both $\{s_k, s_{k+1}\}$. It is important to note that the flow map $F(q)$ and the jump map $G(q)$ in (3.9), are continuous and outer semi-continuous respectively. This construction in addition to C and D being closed subsets ensures nominal well-posedness of the hybrid system in (3.7), see Chapter 2 or the textbook in [31].

The main objective in this chapter is to design the upper bound T and the functions f_η, g_s, g_t in (3.5) such that the closed-loop system in (3.7) is asymptotically stable (see Chapter 2 for the definition), i.e., there exists a $\mathcal{KL}$-class function β such that for any initial state $x(0,0)$,

$$|\varphi(t,j)| \leq \beta(|x(0,0)|, t+j),$$

for all $t \in \mathbb{R}_{\geq 0}$ and $j \in \mathbb{Z}_{\geq 0}$ with $\varphi := (x, e)$.

3.3 Main Results

In this section, we will provide two kinds of dynamic periodic ETMs based on different assumptions on the system. In the first one, the ETM is supposed to read the state continuously (while the event is still checked for at discrete sampling instants, s_k). For the second kind, an ISS-Lyapunov function with a linear decay rate will be used explicitly in the event-triggering condition.

3.3.1 Method I

To design the upper bound T and dynamics of η, we start by introducing two assumptions, similar to those in [99], made on the hybrid system in (3.7).

Assumption 3.1. *For the closed-loop system in (3.7), there exist locally Lipschitz functions $W : \mathbb{R}^n \to \mathbb{R}_{\geq 0}$ and $V : \mathbb{R}^n \to \mathbb{R}_{\geq 0}$, $\underline{\alpha}_W, \bar{\alpha}_W, \underline{\alpha}_V, \bar{\alpha}_V, \alpha_V \in \mathcal{K}_\infty$, a non-negative function $H : \mathbb{R} \to \mathbb{R}_{\geq 0}$, scalars $L \geq 0$ and $\gamma > 0$ such that the following holds:*

1. *For any $e \in \mathbb{R}^n$, $\underline{\alpha}_W(|e|) \leq W(e) \leq \bar{\alpha}_W(|e|)$,*

2. *For any $x \in \mathbb{R}^n$ and almost all $e \in \mathbb{R}^n$,*

$$\langle \nabla W(e), -f(x, \kappa(x+e)) \rangle \leq LW(e) + H(x);$$

3. *For any $x \in \mathbb{R}^n$, $\underline{\alpha}_V(|x|) \leq V(x) \leq \bar{\alpha}_V(|x|)$,*

4. *For almost all $x \in \mathbb{R}^n$ and any $e \in \mathbb{R}^n$,*

$$\langle \nabla V(x), f(x, \kappa(x+e)) \rangle \leq -\alpha_V(|x|) + \gamma^2 W^2(|e|) - H^2(x).$$

Assumption 3.2. *There exists a constant $l_\alpha > 0$ such that $\bar{\alpha}_V(|s|) \leq l_\alpha H^2(s)$ for all $s \in \mathbb{R}^n$.*

Items 3 and 4 in Assumption 3.1 imply that the system $\dot{x} = f(x, \kappa(x+e))$ is input-to-state stable (ISS) with respect to $W(e)$, and $V(x)$ is the corresponding ISS-Lyapunov function.

Subsequently, to design the upper bound T, we introduce the following concept of maximum allowable sampling period (MASP). For a given $\lambda \in (0, 1)$, define $T_0(\lambda)$ as

$$T_0(\lambda) = \begin{cases} \frac{1}{L_\mu r} \arctan \frac{r(1-\lambda)}{\frac{2\gamma\lambda}{L_\mu(1+\lambda)} + \frac{\lambda^2+1}{\lambda+1}}, & \gamma > L_\mu, \\ \frac{1-\lambda}{L_\mu(1+\lambda)}, & \gamma = L_\mu, \\ \frac{1}{L_\mu r} \operatorname{arctanh} \frac{r(1-\lambda)}{2\frac{\gamma\lambda}{L_\mu(1+\lambda)} + \frac{\lambda^2+1}{\lambda+1}}, & \gamma < L_\mu, \end{cases} \tag{3.10}$$

where $r := \sqrt{\left|(\frac{\gamma}{L_\mu})^2 - 1\right|}$ and $L_\mu := L + \mu$ with an arbitrarily small constant $\mu > 0$. When λ and μ go to zero, $T_0(\lambda)$ would become the MASP, see [69]. By choosing an appropriate value for the design parameter λ, the upper bound $T = T_0(\lambda)$ is determined. Furthermore, we have the following lemma of $T_0(\lambda)$.

Lemma 3.2 ([69]). *Let $\theta : \mathbb{R}_{\geq 0} \to \mathbb{R}$ be the solution to*

$$\dot{\theta}(s) = \begin{cases} -2L_\mu \theta(s) - \gamma(\theta^2(s) + 1), & s \in [0, T_0(\lambda)]; \\ 0, & s > T_0(\lambda), \end{cases}$$

with $\theta(0) = \frac{1}{\lambda}$. Then $\theta(s)$ is monotonically decreasing and $\theta(s) = \lambda$ for $s \geq T_0(\lambda)$.

The following theorem provides a method to design the ETM in (3.5-3.6).

Theorem 3.1. *Under Assumptions 3.1–3.2, if the functions in (3.5) are given as*

$$\begin{aligned} f_\eta(\eta, x, e) =& -\beta_\eta \eta + \sigma \alpha_V(|x|), \\ g_s(\eta, x, e) =& \eta + \max\{\rho V(x), \gamma\lambda W^2(e)\} - \max\{\rho V(x), \frac{1}{\lambda}\gamma W^2(e)\}, \\ g_t(\eta, x, e) =& \eta + \max\{\rho V(x), \gamma\lambda W^2(e)\} - \rho V(x), \end{aligned} \tag{3.11}$$

where $\beta_\eta > 0,\ \sigma \in (0, 1)$, and ρ satisfies $\rho\gamma l_\alpha \leq \lambda$, then the closed-loop system in (3.7) is asymptotically stable.

Proof. Consider the following Lyapunov function

$$U(q) = V(x) + \max\{\gamma\theta(\tau)W^2(e), \rho V(x)\} + \eta, \tag{3.12}$$

where $\theta(\cdot)$ is defined in Lemma 3.2.

Analysis during flow:

We start by considering stability properties on the flow set, i.e., between two sampling instants, and divide the analysis into three sub-cases depending on the resultant Lyapunov function $U(q)$.

Case I: When $\rho V(x) > \gamma\theta W^2(e)$, one has

$$\gamma^2 W^2(e) < \frac{\gamma\rho V(x)}{\theta} \leq \frac{\gamma\rho V(x)}{\lambda} \leq \frac{V(x)}{l_\alpha},$$

which leads to

$$\begin{aligned} U^\circ &= \dot{V} + \rho\dot{V} + f_\eta(\eta, x, e) \\ &\leq (1 + \rho)\Big(-\alpha_V(|x|) + \frac{V(x)}{l_\alpha} - H^2(x)\Big) + f_\eta(\eta, x, e) \\ &\leq -(1 + \rho - \sigma)\alpha_V(|x|) - \beta_\eta \eta, \end{aligned} \tag{3.13}$$

where the first inequality uses Assumptions 3.1 and 3.2.

Case II: When $\rho V(x) < \gamma\theta W^2(e)$ then

$$\begin{aligned} U^\circ &= \dot{V} + 2\gamma\theta W(e)\dot{W}(e) + \gamma\dot{\theta}W^2(e) + f_\eta(\eta, x, e) \\ &\leq -\alpha_V(|x|) + \gamma^2 W^2(e) - H^2(e) + f_\eta(\eta, x, e) \\ &\quad + 2\gamma\theta W(e)(LW(e) + H(x)) - \gamma W^2(e)[2L_\mu\theta + \gamma(\theta^2+1)] \\ &\leq -2\mu\lambda\gamma W^2(e) - (1-\sigma)\alpha_V(|x|) - \beta_\eta\eta. \end{aligned} \tag{3.14}$$

Case III: Finally, if $\rho V(x) = \gamma\theta W^2(e)$, then from Lemma 3.1 it follows that

$$U^\circ \leq \max\{-\rho\alpha_V(|x|), -2\mu\lambda\gamma W^2(e)\} - (1-\sigma)\alpha_V(|x|) - \beta_\eta\eta. \tag{3.15}$$

Then, based on the definition of U and Lemma 3.1, (3.13-3.14) imply that there exists a positive function $\Gamma : \mathbb{R} \to \mathbb{R}_{\geq 0}$ such that

$$\langle \nabla U(q), F(q) \rangle \leq -\Gamma(U(q)), q \in C, \tag{3.16}$$

where $\Gamma(s)$ is decided by $\rho\alpha_V(s)$, $\beta_\eta s$ and $\max\{2\mu\lambda\gamma s, (1-\sigma)\alpha_V(s)\}$.

Analysis at jumps:

Next, we examine stability of the system on jump sets, i.e., at sampling instants. The analysis here is divided into two cases depending on the triggering of an event which is decided by the sign of $g_s(\eta, x, e)$, as defined in (3.9).

Case I: When $g_s(\eta, x, e) \geq 0$, we have

$$\begin{aligned} U(G(q)) - U(q) &= V(x) + \max\{\rho V(x), \gamma\frac{1}{\lambda}W^2(e)\} \\ &\quad - V(x) - \max\{\rho V(x), \gamma\theta W^2(e)\} + g_s(\eta, x, e) - \eta \\ &= \max\{\rho V(x), \gamma\lambda W^2(e)\} - \max\{\rho V(x), \gamma\theta W^2(e)\} \\ &\leq 0, \end{aligned} \tag{3.17}$$

where the last inequality is due to $\theta(\tau) \geq \lambda$ when $\tau \leq T_0(\lambda)$.

Case II: When $g_s(\eta, x, e) < 0$, then we have

$$\begin{aligned} U(G(q)) - U(q) &= (1+\rho)V(x) + g_t(\eta, x, e) - V(x) \\ &\quad - \max\{\rho V(x), \gamma\theta W^2(e)\} - \eta \\ &\leq 0. \end{aligned} \tag{3.18}$$

Combining (3.17-3.18) leads to

$$U(G(q)) - U(q) \leq 0, \tag{3.19}$$

for all $q \in D$. Therefore, the proof is completed following a similar line in [69] based on (3.16) and (3.19). □

Remark 3.1. *(Trade-off between sampling period and event occurrence) A static version of the triggering condition in Theorem 3.1 can be given as*

$$t_{k+1} = \min\{t \in \{s_i\}, t > t_k | \gamma W^2(e) > \lambda \rho V(x)\}, \tag{3.20}$$

which has the similar form of that in [99]. By selecting $\rho = \frac{\lambda}{\gamma l_\alpha}$*, one can see that there is a tradeoff between the sampling periods and the inter-event steps (the number of sampling instants between two consecutive events), that is, a smaller* λ *would increase* $T_0(\lambda)$ *but would make it easier for the ETC in Theorem 3.1 (or the static ETC in (3.20)) to be satisfied.*

Remark 3.2. *(On dynamic ETM) By introducing the nonnegative variable* η*, the dynamic triggering condition in Theorem 3.1 can discard some transmissions even when* $\gamma W^2(e) > \lambda \rho V(x)$*. Thus, the capacity of dynamic triggering condition to increase* η *plays a key role in prolonging the inter-event times. From (3.11),* $f_\eta(\eta, x, e)$ *can provide some increment when* x *is large, while* $g_t(\eta, x, e)$ *deals with the case of large* e*. Note that* η *cannot increase by the jump with* $g_s(\eta, x, e)$*.*

The main drawback of (3.11) is requiring the ETM to continuously read the state measurement and conduct the integral operation. A direct solution is to modify $f_c(\eta, x, e)$ as

$$f_\eta(\eta, x, e) = -\beta_\eta \eta, \tag{3.21}$$

where σ is set to 0. However, such an f_η would impair the capacity to increase η. The main problem of Method I is that the x-related part of U in (3.12) cannot offer any decrease when the system jumps. Thus, to solve this problem, some new Lyapunov function could be studied.

3.3.2 Method II

In this subsection, we will provide another method to design the dynamic ETM which only needs to read the state x at the discrete sampling instants. To this end, we revise Assumption 3.1 into the following form.

Assumption 3.3. *Suppose that Assumption 3.1 holds with* $\alpha_V(|x|) = \alpha_v V(x)$.

Assumption 3.3 means that the Lyapunov function V converges exponentially in the absence of measurement error e. Then based on this assumption, we introduce the following theorem.

Theorem 3.2. *Under Assumptions 3.2 and 3.3, if the functions in (3.5) are given as*

$$\begin{aligned} f_\eta(\eta, x, e) =& -\beta_\eta \eta, \\ g_s(\eta, x, e) =& \eta + \max\{e^{a\tau}\rho V(x), \gamma\lambda W^2(e)\} - \max\{\rho V(x), \frac{1}{\lambda}\gamma W^2(e)\}, \\ g_t(\eta, x, e) =& \eta + \max\{e^{a\tau}\rho V(x), \gamma\lambda W^2(e)\} - \rho V(x), \end{aligned} \tag{3.22}$$

where $\beta_\eta > 0$ *and design parameters* ρ, a, b *satisfy*

$$a = \frac{\alpha_v \gamma l_\alpha}{\lambda}, \quad b = e^{aT_0}, \quad \rho = \frac{\lambda}{\gamma l_\alpha b}, \tag{3.23}$$

then the closed-loop system in (3.7) is asymptotically stable.

Proof. Consider the following Lyapunov function:

$$O(q) = V(x) + \max\{\gamma\theta(\tau)W^2(e), e^{a\tau}\rho V(x)\} + \eta, \tag{3.24}$$

where $\theta(\tau)$ is governed by Lemma 3.2. Similar to the analysis in Method I, we first study the behavior of O in flow and jump domains separately.

Analysis during flow:

Case I: When $e^{a\tau}\rho V(x) > \gamma\theta W^2(e)$, it follows that

$$\gamma^2 W^2(e) < \frac{e^{a\tau}\gamma\rho V(x)}{\theta} \leq \frac{e^{a\tau}V(x)}{l_\alpha b}$$

where $b = \frac{\lambda}{\gamma l_\alpha \rho}$. Furthermore, we have

$$\begin{aligned} O^\circ =& \dot{V} + ae^{a\tau}\rho V + e^{a\tau}\rho\dot{V} + f_\eta(\eta, x, e) \\ \leq& -\alpha_v V(x) + \gamma^2 W^2(e) - H^2(x) + ae^{a\tau}\rho V - \beta_\eta \eta \\ &+ e^{a\tau}\rho(-\alpha_v V(x) + \gamma^2 W^2(e) - H^2(x)). \end{aligned} \tag{3.25}$$

According to (3.23), a is designed so that $\alpha_v \geq ae^{a\tau}\rho$ and $e^{a\tau} \leq b$ since $\tau \leq T_0(\lambda)$. Then, (3.25) implies

$$\begin{aligned} O^\circ =& -\alpha_v \rho e^{a\tau} V(x) + (1 + e^{a\tau}\rho)(\gamma^2 W^2(e) - H^2(x)) - \beta_\eta \eta \\ \leq& -\alpha_v \rho e^{a\tau} V(x) - \beta_\eta \eta + (1 + e^{a\tau}\rho)(\frac{e^{a\tau}}{b} - 1)H^2(x) \\ \leq& -\alpha_v \rho e^{a\tau} V(x) - \beta_\eta \eta. \end{aligned} \tag{3.26}$$

Case II: When $e^{a\tau}\rho V(x) < \gamma\theta W^2(e)$, the derivation is similar to (3.14) and results in

$$O^\circ \leq -2\mu\lambda\gamma W^2(e) - \alpha_v V(x) - \beta_\eta \eta. \tag{3.27}$$

Case III: When $e^{a\tau}\rho V(x) = \gamma\theta W^2(e)$ from Lemma 3.1 it follows

$$O^\circ \leq \max\{-\alpha_v \rho e^{a\tau} V(x), -2\mu\lambda\gamma W^2(e) - \alpha_v V(x)\} - \beta_\eta \eta. \tag{3.28}$$

Analysis at jumps:

Next, consider analysis at jumps that occur at sampling instants. Again, similar to Method I, we have the following two cases depending on event occurrence.

Case I: When $g_s(\eta, x, e) \geq 0$, we have

$$\begin{aligned} O(G(q)) - O(q) =& V(x) + \max\{\rho V(x), \gamma\frac{1}{\lambda}W^2(e)\} \\ &- V(x) - \max\{e^{a\tau}\rho V(x), \gamma\theta W^2(e)\} \\ &+ g_s(\eta, x, e) - \eta \\ \leq& 0. \end{aligned} \tag{3.29}$$

Case II: When $g_s(\eta, x, e) < 0$, it follows that

$$\begin{aligned} O(G(q)) - O(q) =& (1 + \rho)V(x) + g_t(\eta, x, e) - V(x) \\ &- \max\{e^{a\tau}\rho V(x), \gamma\theta W^2(e)\} - \eta \\ \leq& 0. \end{aligned} \tag{3.30}$$

Therefore, the proof is completed by combining (3.26-3.30). □

Remark 3.3. *To implement the dynamic triggering condition in Theorem 3.2, at each sampling instant $s_k, k \in \mathbb{Z}_{\geq 1}$, the event trigger needs to record the time $s_k - s_{k-1}$ and calculate $e^{a(s_k - s_{k-1})}$. In the special case that the event is detected periodically, both of them are constants that can be determined offline.*

Remark 3.4. *Compared to Theorem 3.1, the method in this subsection (namely, Method II) can offer some extra capacity to increase η at the jump. Before the static condition $\gamma W^2(e) > \lambda\rho V(x)$ is violated, both $g_s(\eta, x, e)$ and $g_t(\eta, x, e)$ must enlarge the value of η. This feature assists in improving the inter-event time and avoids continuous reading of state measurements between two successive sampling instants.*

Remark 3.5. *(On shortcomings of Method II) The main drawback of Method II is using the linear decay rate α_v and its corresponding ISS-Lyapunov function explicitly. Although [78] showed that it is not restrictive to modify the ISS-Lyapunov function in Assumption 3.1 to satisfy Assumption 3.3, note that if the ISS-Lyapunov function $V(x)$ for Method II is derived by relaxing $H(x)$ used in Assumption 3.1 for Method I then this directly affects the gain γ associated with the error e. This increased γ shrinks ρ in* (3.23) *and so the event-triggering condition is easily violated compared to that of Method I. This is demonstrated by the difference in average numbers of triggers between Table 3.1 and Table 3.2 in the numerical example in Section 3.4.*

Remark 3.6. *(For linear systems) If the system in* (3.1) *is linear, then Assumption 3.3 is not necessary, since it is trivial to find a quadratic ISS-Lyapunov function with a linear decay rate in Assumption 3.1. In this case, Method II might generate less events than Method I with f_η in* (3.21)*. Thus, one may prefer to use Method II when the nonlinearity of the system is weak and no state information is available to the ETM continuously.*

3.4 Numerical Example

As an illustrative example, the following scalar nonlinear control system is considered

$$\dot{x} = -x^3 + 0.5x^2 + u,\ u = -2x. \tag{3.31}$$

The corresponding event-triggered controller takes the form $u = -2\hat{x}$. For the system in (3.31), the corresponding Lyapunov functions and relevant quantities for each method are as follows:

Method I (M.I):

Assumption 3.1 is satisfied with Lyapunov functions $V = \frac{x^4}{2} + 2x^2$ and $W = |e|$, and quantities $H(x) = |x^3 - 0.5x^2 + 2x|,\ L = 2,\ \alpha_v(|x|) = 0.047x^6 - 0.061x^4 + 0.1892x^2$, $\gamma = 2.049$. Assumption 3.2 is satisfied by choosing $l_\alpha = 1$. The ETM evaluates the sign of

$$\begin{aligned} g_s(\eta, x, e) = \eta &+ \max\{0.34V(x), 1.73|e|^2\} \\ &- \max\{0.34V(x), 2.62|e|^2\}. \end{aligned} \tag{3.32}$$

Method II (M.II):

In order to satisfy Assumption 3.3, $H(x)$ in Assumption 3.1 is considered to be of the form $H(x) = |px^3 - 0.5x^2 + rx|,\ p > 1, r > 2$. The resultant Lyapunov function satisfying the assumption is $V = \frac{px^4}{2} + rx^2$ with $p = 1.97,\ r = 3.87$ and α_v is 0.08. Additionally for Assumption 3.1, we also have $W = |e|$, $L = 2$, and $\gamma = 26.79$. l_α in Assumption 3.2 is chosen to be 1. The ETM that evaluates the sign of $g_s(\eta, x, e)$, given by

$$\begin{aligned} g_s(\eta, x, e) = \eta &+ \max\{0.003V(x), 2.12|e|^2\} \\ &- \max\{7.7 \cdot 10^{-4}V(x), 337.3|e|^2\}. \end{aligned} \tag{3.33}$$

In Fig. 3.3a, the upper bound $T = T_0(\lambda)$ is plotted as a function of design parameter λ for each method. Stabilization of the system using both methods is depicted through the state trajectories in Fig. 3.3b. As stated in Remark 3.5 of Section 3.3, the increase in γ directly affects the performance

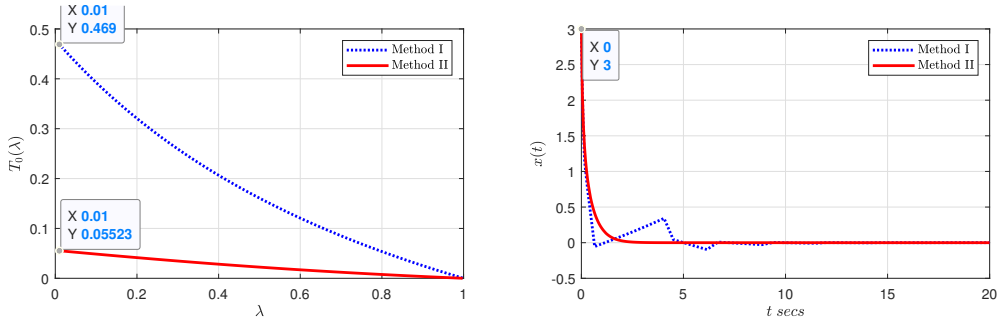

(a) MASP as a function of parameter λ (b) Convergence of state trajectories

Figure 3.3: Plots depicting MASP curves and state trajectories of Method I and Method II.

(namely, the average number of triggers) of the method, as seen in (3.32), (3.33). Notice that the gain γ in M.II is substantially higher than that in M.I and the difference in no. of triggers of M.I in Table 3.1 and those of M.II in Table 3.2 demonstrate its effect. We compare M.I and its variant M.I ($\sigma = 0$) with those of [99] and [77] in Table 3.1. The performance measure is computed over 100 simulations of 20 secs each with a sampling period $\tau = T_0(\lambda) = 0.05$; the initial condition $x(0)$ for each simulation is randomly picked from an interval $[-3, 3]$. The primary focus here is to evaluate and compare the ETMs, so the ETMs in [99] and [77] are adapted so as to fit the specific example in (3.31). From Table 3.1 it can be inferred that a dynamic periodic event-triggered controller can perform better than a static periodic event-triggered controller (namely, [99]) and a continuous event-triggered controller (namely, [77]) for nonlinear systems.

Subsequently, to make a fair comparison amongst the two methods discussed in this chapter, we first remove the effect of gain γ. This is done by adopting the Lyapunov functions and related quantities of M.II to M.I as mod. M.I ($\sigma \neq 0$) and mod. M.I ($\sigma = 0$). Table 3.2 provides performance comparison of the ETMs of the two methods.

M.I	M.I ($\sigma = 0$)	[99]	[77]
14.9	13.0	66.52	15.79

Table 3.1: Average no. of triggers over 100 simulations in 20 secs

M.II	mod. M.I ($\sigma \neq 0$)	mod. M.I ($\sigma = 0$)
360.58	343.04	348.22

Table 3.2: Average no. of triggers over 100 simulations in 20 secs

3.5 Conclusion

We proposed two methods to design dynamic periodic ETM for nonlinear systems using state feedback and provide an upper bound on the sampling period that is dependent on a user defined parameter. For each of the methods, the design results in a closed-loop hybrid system which is asymptotically stable. Since the ETC is evaluated only at sampling instants, the scheme is easily implementable on digital platforms compared to its continuous-time counterparts. A comparative study on an illustrative example supports the view that the dynamic ETM is capable of reducing the average number of events triggered compared to its static counterparts.

Chapter 4

Dynamic Event-Triggered Control of Nonlinear MASs[1]

Dynamic ETMs have shown potential in further reducing the number of events in comparison to their static counterparts while delivering similar system performance. In this chapter, we provide a framework to design dynamic periodic event-triggered controllers for MASs with nonlinear dynamics. A preliminary version of this work on single-agent systems was studied in the previous chapter, also in [17]. The design methodology adopts an emulation-based technique that assumes the existence of a continuous-time state feedback controller that stabilizes the MAS. The dynamic ETMs are constructed based on an agent's ability or inability to sense states (or relative states) of fellow agents in the network. To illustrate the design methodologies, two case studies on nonlinear MASs (with Lipschitz and one-sided Lipschitz), interacting over undirected and directed communication networks, are presented. Finally, the results of the case studies are demonstrated via numerical examples.

The rest of this chapter is organized as follows. Section 4.1 presents preliminaries on algebraic graph theory. The problem is formulated in Section 4.2 followed by the main results which are discussed in Section 4.3. Section 4.4 presents case studies on consensus amongst nonlinear MASs. An illustrative example is simulated in Section 4.5 followed by concluding remarks in Section

[1]The material in this chapter has been published as: Mani H. Dhullipalla, Hao Yu and Tongwen Chen. A framework for distributed control via dynamic periodic event-triggering mechanisms. *Automatica*, 146:110548, 2022.

4.6.

4.1 Preliminaries

In addition to preliminaries introduced in Section 3.1 of Chapter 3, in this section we introduce concepts from algebraic graph theory, see [62] for more information.

A graph (often also referred to as network) is an ordered pair $\mathcal{G} = (\mathcal{V}, \mathcal{E})$ where index set $\mathcal{V} = \{1, 2, \ldots, N\}$ denotes the set of vertices (agents) and $\mathcal{E} \subseteq \mathcal{V} \times \mathcal{V}$ denotes the set of edges (communication links) connecting the vertices (agents). If the set of edges are directed, then $\mathcal{G}$ is a directed graph. A directed edge is an ordered pair $(i, j) \in \mathcal{E}$ where the vertex i is the tail of the edge, while vertex j is its head. If the set of edges are such that $(i, j) \in \mathcal{E} \implies (j, i) \in \mathcal{E},\ \forall i, j \in \mathcal{V}$, then $\mathcal{G}$ is an undirected graph. Let $\mathcal{N}_{\text{in}}^i$ denote the in-neighbor set of vertex i consisting of all vertices $j \in \mathcal{V}$ such that $(j, i) \in \mathcal{E}$ and $\bar{\mathcal{N}}_{\text{in}}^i = \{i\} \bigcup \mathcal{N}_{\text{in}}^i$ denote the set containing indices of agent i and its in-neighbors. Define a nonnegative matrix $\mathsf{A} = [\mathsf{a}_{ij}]_{N \times N}$ called the weighted adjacency matrix where $\mathsf{a}_{ij} > 0 \iff (i, j) \in \mathcal{E}$; otherwise $\mathsf{a}_{ij} = 0$. For undirected graph, the weighted adjacency matrix A is symmetrical. The weighted in-degree of a vertex is $\mathsf{d}_i = \sum_{j=1}^{N} \mathsf{a}_{ji}$ and degree matrix of $\mathcal{G}$ denoted by $\mathsf{D} = \mathtt{diag}([\mathsf{d}_i, \ldots, \mathsf{d}_N])$. The graph Laplacian is then defined as $\mathsf{L} = \mathsf{D} - \mathsf{A}$. For a connected undirected graph, L has exactly one eigenvalue equal to zero and corresponding eigenvector to be $\mathbf{1}$, i.e., $\mathsf{L}\mathbf{1} = \mathbf{0}$ where $\mathbf{1}$ is a vector of appropriate dimension with all entries being equal to 1. All the other eigenvalues are positive and can be arranged as follows: $0 < \Lambda_2 \leq \ldots \Lambda_M$, where Λ_M denotes the largest eigenvalue of L. Here, Λ_2 is known as the algebraic connectivity of $\mathcal{G}$. For a strongly connected directed graph, the general algebraic connectivity is defined as:

$$a_\xi(\mathsf{L}) = \min_{x^{\mathrm{T}}\xi = 0, x \neq 0} \frac{x^{\mathrm{T}} \hat{\mathsf{L}} x}{x^{\mathrm{T}} \Xi x}$$

where $\hat{\mathsf{L}} = (\Xi\mathsf{L} + \mathsf{L}^{\mathrm{T}}\Xi)/2$, $\Xi = \mathrm{diag}(\xi)$, $\xi = [\xi_1, \ldots, \xi_N]^{\mathrm{T}}$ such that $\xi_i > 0, \forall i$

and $\sum_{i\in\mathcal{V}}\xi_i = 1$, see [116].

4.2 Problem Formulation

Consider a MAS with N agents interacting over an established broadcasting network $\mathcal{G} = (\mathcal{V}, \mathcal{E})$. Let each agent in the network have the following dynamics:

$$\dot{x}_i = f_i(x, u_i), \forall i \in \mathcal{V}, \tag{4.1}$$

where i denotes the agent index, $x_i \in \mathbb{R}^n$ is the local state of agent i, $x = [x_1^{\mathrm{T}} \ \cdots \ x_N^{\mathrm{T}}]^{\mathrm{T}} \in \mathbb{R}^{nN}$ is the state vector consisting of all agent states and $u_i \in \mathbb{R}^m$ is the control input. It is assumed that functions $f_i : \mathbb{R}^{nN} \times \mathbb{R}^m \to \mathbb{R}^n, \forall i \in \mathcal{V}$, are continuous and that each agent can broadcast its full state x_i to its neighbors in $\mathcal{G}$. With the availability of neighbor states, it is assumed that a static, distributed state-feedback controller u_i, given by

$$u_i = \kappa(x_{\bar{\mathcal{N}}_{\mathrm{in}}^i}), \ \forall i \in \mathcal{V},$$

stabilizes the MAS in (4.1). Here, $x_{\bar{\mathcal{N}}_{\mathrm{in}}^i} := (\bar{\mathsf{A}}_i \otimes \mathbb{I}_n)x$ where diagonal matrix $\bar{\mathsf{A}}_i = \mathtt{diag}(\{\mathsf{a}_j | \mathsf{a}_j = 1, \forall j \in \bar{\mathcal{N}}_{\mathrm{in}}^i; \mathsf{a}_j = 0, \forall j \notin \bar{\mathcal{N}}_{\mathrm{in}}^i\})$.

In an effort to reduce the consumption of communication and energy resources of the overall MAS, a periodic event-triggered broadcasting strategy is implemented. For this, we define an event-verifying (sampling) time sequence $\{s_k^i\}_{k=0}^{\infty}$ for each agent i such that

$$\varepsilon^i \leq s_{k+1}^i - s_k^i \leq T^i, \ \forall k \in \mathbb{Z}_{\geq 0}, \forall i \in \mathcal{V}, \tag{4.2}$$

where positive constant ε^i is such that $\varepsilon^i \leq T^i$ and T^i is the upper bound that is to be designed. Note that positive $\varepsilon^i, \forall i \in \mathcal{V}$, ensure: i) that instantaneous Zeno solutions[2] of the hybrid system, defined shortly in (4.8), are avoided (see [69] for a remark on this), and ii) in the context of event-triggered systems,

[2]A solution x of (2.1) is instantaneous Zeno if it is complete (namely, $\mathtt{dom}x$ is unbounded) and eventually discrete (namely, $\mathbb{T} = \sup_t \mathtt{dom}x < \infty$ and $\mathtt{dom}x \cap (\{\mathbb{T}\} \times \mathbb{Z}_{\geq 0})$ contains at least two points), see Chapter 2 of this thesis or textbook in [31] for details.

this implies that Zeno behavior[3] is avoided. Furthermore, ε^i, in practice, reflects the smallest interval between two consecutive broadcasts that hardware devices can achieve. Here, the largest value that T^i can take while ensuring closed-loop stability of a dynamical system is known as the MASP, see [69] and [43] for more on MASP of sampled-data nonlinear systems. However, for the overall network, we are interested in $\min_i T^i$ which would be the MASP of the MAS; this suggests that any choice of $\mathsf{T} \in (0, \min_i T^i]$, amongst the agents, would result in asymptotic stability of the MAS.

Next, we define the event-triggering sequence for agent i, denoted by $\{t_l^i\}_{l=0}^{\infty}$, to be a subsequence of $\{s_k^i\}_{k=0}^{\infty}$. The construction of this subsequence depends on the event-triggering condition which will be discussed shortly.

When an event is triggered on agent i, it broadcasts its current state to its neighbors over $\mathcal{G}$. Let $\hat{x}_i(t_l^i)$ denote the broadcasted state at triggering instant t_l^i. Each agent $i \in \mathcal{V}$, adopts a model-based approach, like discussed in [26], to evaluate $\hat{x}_j(t),\ \forall j \in \bar{\mathcal{N}}_{\text{in}}^i$, as follows:

$$\dot{\hat{x}}_j = \Upsilon(\hat{x}_j),\ t \in [t_l^j, t_{l+1}^j), \tag{4.3}$$

with $\hat{x}_j(t_l^j) = x_j(t_l^j)$ as its initial state, where $\Upsilon : \mathbb{R}^n \to \mathbb{R}^n$ is considered to be continuous function. For notational convenience, we use the same model $\Upsilon(\cdot)$ across all agents to propagate broadcast states in the network. For instance, $\Upsilon(\cdot) = \mathbf{0}$ yields a ZOH model in all the agents. However, the methodologies, discussed in Section 4.3, can adopt agent specific models (i.e., $\dot{\hat{x}}_j^i = \Upsilon_i(\hat{x}_j^i)$) and agent-and-neighbor specific models (i.e., $\dot{\hat{x}}_j^i = \Upsilon_{ij}(\hat{x}_j^i)$). Since every agent in the network uses the same mapping to model the evolution of broadcasted states, they all have the same model-based estimate of neighbors' states. Let $\hat{x}(t) = [\hat{x}_1^{\mathrm{T}}(t)\ \cdots\ \hat{x}_N^{\mathrm{T}}(t)]^{\mathrm{T}} \in \mathbb{R}^{nN}$ denote the broadcasted state vector at any time t and $\hat{x}_{\bar{\mathcal{N}}_{\text{in}}^i} := (\bar{\mathsf{A}}_i \otimes \mathbb{I}_n)\hat{x}$ denote all the model-based estimates available to agent i at time t. Then, the periodic event-triggered controller at any time

[3]Occurrence of infinite events in finite time is called Zeno behavior. This phenomenon in systems is undesirable because it is not physically realizable and does not aid in saving resources.

t is given by

$$u_i = \kappa(\hat{x}_{\bar{\mathcal{N}}_{\text{in}}^i}),\ \forall i \in \mathcal{V}. \tag{4.4}$$

Agents in $\mathcal{G}$, in addition to broadcast channels, *may* have active sensing capabilities; i.e., when agents can, intermittently, sense states (or relative states) of their fellow agents using onboard sensors. If available, using this (additional) information aids in improving the performance of the ETM. In this context, we define the index set $\underline{\mathcal{N}}_k^i$ as the set of indices of agents in $\mathcal{G}$ whose states (or relative states) are accessible to i at s_k^i and the state $x_{\underline{\mathcal{N}}_k^i} = (\underline{\mathsf{A}}_{i,k} \otimes \mathbb{I}_n)x$ where diagonal matrix $\underline{\mathsf{A}}_{i,k} = \mathtt{diag}(\{\mathsf{a}_j | \mathsf{a}_j = 1, \forall j \in \underline{\mathcal{N}}_k^i; \mathsf{a}_j = 0, \forall j \notin \underline{\mathcal{N}}_k^i\})$.

In this chapter, a dynamic periodic ETM is implemented by introducing a non-negative auxiliary variable $\eta_i \in \mathbb{R}_{\geq 0}, \forall i \in \mathcal{V}$. The dynamics of η_i is described using hybrid system framework as follows:

$$\dot{\eta}_i = f_\eta^i(\eta_i, \hat{x}_{\bar{\mathcal{N}}_{\text{in}}^i}), \quad t \in [s_k^i, s_{k+1}^i), \tag{4.5a}$$

$$\eta_i^+ = g_s^i(\eta_i, e_i, x_{\underline{\mathcal{N}}_k^i}), \quad t \in \{s_k^i\} \setminus \{t_l^i\}, \tag{4.5b}$$

$$\eta_i^+ = g_t^i(\eta_i, e_i, x_{\underline{\mathcal{N}}_k^i}), \quad t \in \{t_l^i\}, \tag{4.5c}$$

where $e_i = \hat{x}_i - x_i$ is the broadcast error. For all $i \in \mathcal{V}$, the initial condition $\eta_{i,0} = \eta_i(s_0^i)$ is a design parameter that is chosen to be a non-negative scalar. The function f_η^i is continuous on $\mathbb{R}_{\geq 0} \times \mathbb{R}^{nN}$, is such that $f_\eta^i(0, \cdot) \geq 0$, and that any solution (say $\mathsf{S}_{\eta_i}(t, \eta_{i,0}, \hat{x}_{\bar{\mathcal{N}}_{\text{in}}^i})$) to the differential equation $\dot{\eta}_i = f_\eta^i(\eta_i, \hat{x}_{\bar{\mathcal{N}}_{\text{in}}^i})$, for any given bounded $\hat{x}_{\bar{\mathcal{N}}_{\text{in}}^i}$ and for any given non-negative initial state $\eta_{i,0}$, is complete (i.e., $\mathsf{S}_{\eta_i}(t, \eta_{i,0}, \hat{x}_{\bar{\mathcal{N}}_{\text{in}}^i})$ is defined for all time $t \in [0, \infty)$). Furthermore, $g_s^i : \mathbb{R}_{\geq 0} \times \mathbb{R}^n \times \mathbb{R}^{nN} \to \mathbb{R}$ is a continuous function and $g_t^i : \mathbb{R}_{\geq 0} \times \mathbb{R}^n \times \mathbb{R}^{nN} \to \mathbb{R}_{\geq 0}$ is a continuous non-negative function. The dynamic periodic event-triggering condition is then defined as

$$t_{k+1}^i = \{t > t_k^i | t \in \{s_k^i\}_{k=0}^\infty,\ g_s^i(\cdot) < 0\}, \forall i \in \mathcal{V}. \tag{4.6}$$

Intuitively, η_i in (5.10a) accumulates the effect of $\hat{x}_{\bar{\mathcal{N}}_{\text{in}}^i}$ over the interval $[s_k^i, s_{k+1}^i)$. Following this, at s_{k+1}^i, the condition in (4.6) is evaluated which, essentially,

compares the effect of η_i and $x_{\underline{\mathcal{N}}_k^i}$, when available, against that of rising e_i. This comparison is judged by the sign of g_s^i. If $g_s^i > 0$, then the η_i takes up this value, i.e., $\eta_i = g_s^i$; else, $\eta_i = g_t^i$ and the agent state is broadcasted resetting $e_i = 0$. In this context, we also note that the case when $g_s^i = 0$ is handled, slightly, differently when the hybrid dynamics of MAS is defined in (4.8) (see discussion following (4.10)). Furthermore, in Appendix A.1.1, we present an argument to show that $\eta_i \geq 0, \forall i \in \mathcal{V}$, under (mild) conditions imposed on to-be-designed functions f_η^i, g_s^i, and g_t^i.

To aid in the design of event-triggering condition, each agent i tracks the time elapsed since the last event-verifying instant using the variable τ_i. Its dynamics is given as:

$$\begin{cases} \dot{\tau}_i = 1, \text{ when } \tau_i \in [0, T^i] \\ \tau_i^+ = 0, \text{ when } \tau_i \in [\varepsilon^i, T^i]. \end{cases} \tag{4.7}$$

At every s_k^i, the subsequent event-verifying instant s_{k+1}^i is pre-determined such that the inequalities in (4.2) hold. Say $\Delta_k^i = s_{k+1}^i - s_k^i$. When τ_i reaches Δ_k^i, a jump takes place on agent i, i.e., the event-triggering condition in (4.6) is evaluated. Here, we note that at time $t = s_{k+1}^i$, fellow agents (namely, $\{j | j \neq i, j \in \mathcal{V}\}$), in the network may (if $t \in \{s_k^j\}_{k=0}^\infty$) or may not (if $t \notin \{s_k^j\}_{k=0}^\infty$) experience jumps. This notion is reflected in the definition of jump set D, corresponding to the overall MAS defined shortly in (4.9), as a union of subsets.

By combining the MAS dynamics in (4.1), the dynamics of broadcasted state in (4.3), the periodic event-triggered controller in (4.4), the dynamics of ETM in (4.6) and the dynamics of elapsed time in (4.7), the closed-loop system of the MAS can be modeled using the hybrid systems framework as follows:

$$\begin{cases} \dot{q} = F(q), \quad q \in C; \\ q^+ \in G(q), \quad q \in D, \end{cases} \tag{4.8}$$

where $q := (x, e, \hat{x}, \tau, \eta)$ is the augmented state, $e := [e_1^\mathrm{T} \ \cdots \ e_N^\mathrm{T}]^\mathrm{T} \in \mathbb{R}^{nN}$, $\tau := [\tau_1 \ \cdots \ \tau_N]^\mathrm{T} \in [0, T^1] \times \cdots \times [0, T^N]$, $\eta := [\eta_1 \ \cdots \ \eta_N]^\mathrm{T} \in \mathbb{R}_{\geq 0}^N$, the flow set C

and the jump set D are defined as

$$C = \mathbb{R}^{3nN} \times [0, T^1] \times \cdots \times [0, T^N] \times \mathbb{R}^N_{\geq 0},$$
$$D = \bigcup_{i=1}^{N} \Big\{ \mathbb{R}^{3nN} \times [0, T^1] \times \cdots \times \underbrace{[\varepsilon^i, T^i]}_{\text{jump interval for } i} \times \cdots \times [0, T^N] \times \mathbb{R}^N_{\geq 0} \Big\}, \quad (4.9)$$

respectively. $F(q)$ and $G(q)$ in (4.8) are as follows:

$$F(q) = \begin{bmatrix} f^{\mathrm{T}} & (\mathbf{1} \otimes \Upsilon - f)^{\mathrm{T}} & (\mathbf{1} \otimes \Upsilon)^{\mathrm{T}} & \mathbf{1} & f_\eta^{\mathrm{T}} \end{bmatrix}^{\mathrm{T}},$$
$$G(q) = \bigcup_{i=1}^{N} G_i(q) \text{ such that}$$
$$G_i(q) := \begin{cases} \begin{cases} \{G_i^1\}, & g_s^i > 0, \\ \{G_i^2\}, & g_s^i < 0, \\ \{G_i^1,\ G_i^2\}, & g_s^i = 0, \end{cases} & \tau_i \in [\varepsilon^i, T^i], \\ \phi & \tau_i \notin [\varepsilon^i, T^i], \end{cases} \quad (4.10)$$

where ϕ is a null set,

$$G_i^1 := \begin{bmatrix} x^{\mathrm{T}} & e^{\mathrm{T}} & \hat{x}^{\mathrm{T}} & (\mathcal{I}_i \mathbf{1})^{\mathrm{T}} & (\mathcal{I}_i \eta + \bar{g}_s^i)^{\mathrm{T}} \end{bmatrix}^{\mathrm{T}},$$
$$G_i^2 := \begin{bmatrix} x^{\mathrm{T}} & ((\mathcal{I}_i \otimes \mathbb{I}_n)e)^{\mathrm{T}} & (\hat{x} - ((\mathbb{I}_N - \mathcal{I}_i) \otimes \mathbb{I}_n)e)^{\mathrm{T}} & (\mathcal{I}_i \mathbf{1})^{\mathrm{T}} & (\mathcal{I}_i \eta + \bar{g}_t^i)^{\mathrm{T}} \end{bmatrix}^{\mathrm{T}},$$

$f := [f_1^{\mathrm{T}} \ \cdots \ f_N^{\mathrm{T}}]^{\mathrm{T}} \in \mathbb{R}^{nN}$, $f_\eta := [f_\eta^1 \ \cdots \ f_\eta^N]^{\mathrm{T}} \in \mathbb{R}^N$, $\mathcal{I}_i := \mathtt{diag}(\{1, .., 0, .., 1\})$ with 0 at the i-th place, $\bar{g}_s^i := [0 \cdots g_s^i \cdots 0]^{\mathrm{T}}$, $\bar{g}_t^i := [0 \cdots g_t^i \cdots 0]^{\mathrm{T}}$, and $\mathbf{1}$, and $\mathbf{0}$ are vectors of ones and zeros of appropriate dimensions, respectively. Here, we note that although $\hat{x}$ is determined by the pair (x, e), its dynamics has been included in (4.8) because it is used to construct the ETMs.

It can be inferred from the definition of flow and jump sets in (4.9) that the augmented state q flows along $F(q)$ when every agent in the network flows and jumps if at least one agent in the network jumps. We also note that when $g_s^i = 0$, agent i can either choose to broadcast state (i.e., opt for G_i^2) or avoid it (i.e., opt for G_i^1). This construction makes the set-valued mapping $G(q)$ outer semi-continuous. Additionally, the function $F(q)$ is continuous and the sets $C,\ D$ in (4.9) are constructed to be closed subsets; together, these properties on (C, F, D, G) ensure nominal well-posedness of the hybrid system in (4.8), see [31].

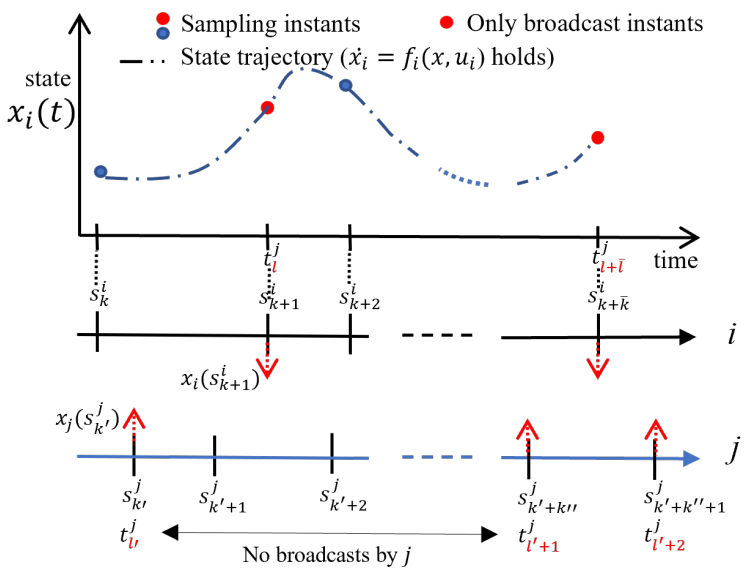

Figure 4.1: Nature of broadcasts between agent i and agent j which employ ETMs. On the two timelines, the black vertical ticks show sampling instants $\{s_k^i\}$ or $\{s_{k'}^j\}$ and the red arrows highlight the broadcast/triggered instants $\{t_l^i\}$ or $\{t_{l'}^j\}$.

Remark 4.1. *(On sampling sequences) First, we note that although the ETM discussed is called periodic ETM, the sampling sequences, as in* (4.2)*, can be both aperiodic and asynchronous thus broadening the scope of this approach. Next, once the upper bound* T^i *in* (4.2) *is determined, each agent in the network, at every sampling instant* s_k^i*, has the flexibility to independently and arbitrarily choose* $\tau^i = s_{k+1}^i - s_k^i$ *within the range* $[\varepsilon^i, T^i]$*. In other words, this choice of* τ^i *at every* s_k^i *determines the subsequent duration of flow and jump instant for the agents. Assuming all agents are triggered, simultaneously, at the start (namely,* $s_0^i = s_0^j, \forall i, j \in \mathcal{V}$*), if* τ^i *across all agents at every sampling instant is the same, then this results in a synchronous protocol (namely,* $s_k^i = s_k^j = s_k, \forall i, j \in \mathcal{V}, \forall k \in \mathbb{Z}_{\geq 0}$*). In other words, in a synchronous protocol the ETM on every agent in the network is evaluated at the same instant, namely,* s_k*. Further, if* $s_k = k \cdot T$ *where positive constant* $T < \min_{\forall i} T^i$*, then the protocol would also be periodic. On the contrary, if* τ^i *for an agent differs from others in the network, which can sometimes be caused due to drifting of local clocks, then this results in an asynchronous protocol (i.e, the ETM*

is evaluated asynchronously). The hybrid systems framework adopted in this work can address both the scenarios described, see the illustration in Fig. 4.1.

The main objective in this work is to design dynamic ETMs, governed by the functions $f_\eta^i,\ g_s^i,\ g_t^i$ in (4.5), and establish MASP of the MAS, namely, $\min_i T^i$ such that the closed-loop hybrid systems model in (4.8) is asymptotically stable.

4.3 Main Results

In this section, we design two dynamic ETMs on the basis of agent's capability in sensing state (or relative state) information of other agents in the network. We consider the following two scenarios.

1. Broadcasting: agents solely depend on broadcast states and communicate over established network $\mathcal{G}$, e.g., power networks.

2. Active sensing: in addition to broadcasting, agents can also obtain states (or relative states) of fellow agents in the network through onboard sensors, e.g., sensing relative distances of nearest neighbors amongst a platoon of vehicles.

4.3.1 Broadcasting

In this subsection, we consider that the agents in $\mathcal{G}$ can only broadcast state information, which implies that the signal $x_{\underline{\mathcal{N}}_k^i}$ in (4.5) is *not* accessible at each event-verifying instant $\{s_k^i\}$. The focus is to design the ETM with the intention that only local information is used during the event-verifying instants $\{s_k^i\}$. For this, we begin by introducing the following assumptions.

Assumption 4.1. *For the hybrid system in* (4.8)*, and* $\forall i \in \mathcal{V}$*, there exist a locally Lipschitz function* $W_i(e_i) : \mathbb{R}^n \to \mathbb{R}_{\geq 0}$*, functions* $\underline{\alpha}_W^i,\ \bar{\alpha}_W^i \in \mathcal{K}_\infty$*, a scalar function* $H_i(x, e) : \mathbb{R}^{2nN} \to \mathbb{R}_{\geq 0}$*, and a non-negative scalar* L_i *such that:*

(a) $\underline{\alpha}^i_W(|e_i|) \leq W_i(e_i) \leq \bar{\alpha}^i_W(|e_i|),\ \forall e_i \in \mathbb{R}^n$;

(b) $\langle W_i(e_i), \Upsilon - f_i \rangle \leq L_i W_i(e_i) + H_i(x, e)$, *for all* $x \in \mathbb{R}^{nN}$ *and almost all* $e_i \in \mathbb{R}^n, \forall i \in \mathcal{V}$.

In Assumption 4.1(b), we assume that growth rate of $W_i(e_i)$ can be linearly upper bounded; this is facilitated by the use of model-based broadcast estimates in (4.3).

Assumption 4.2. *Suppose Assumption 4.1 holds. For the hybrid system in* (4.8)*, there exist a locally Lipschitz function* $V(x) : \mathbb{R}^{nN} \to \mathbb{R}_{\geq 0}$*, continuous functions* $\hat{V}_i(\hat{x}_{\bar{\mathcal{N}}^i_{in}}) : \mathbb{R}^{nN} \to \mathbb{R}_{\geq 0},\ \forall i \in \mathcal{V}$*, functions* $\underline{\alpha}_V,\ \bar{\alpha}_V \in \mathcal{K}_\infty$*, a continuous function* $\Theta(x) : \mathbb{R}^{nN} \to \mathbb{R}^{nN}$*, a positive scalars* α_V *and* $\gamma_i, \forall i \in \mathcal{V}$*, and non-negative scalars* $\omega_i,\ \forall i \in \mathcal{V}$*, such that:*

(a) $\underline{\alpha}_V(|\Theta(x)|) \leq V(x) \leq \bar{\alpha}_V(|\Theta(x)|),\ \forall x \in \mathbb{R}^{nN}$,

(b) $\langle V(x), f \rangle \leq -\alpha_V V(x) + \sum_{i \in \mathcal{V}} \left[\gamma_i^2 W_i^2(e_i) - \omega_i \hat{V}_i(\hat{x}_{\bar{\mathcal{N}}^i_{in}}) - H_i^2(x, e)\right]$*, for almost all* $x \in \mathbb{R}^{nN}$ *and* $\forall e_i \in \mathbb{R}^n, \forall i \in \mathcal{V}$.

Here, the mapping $\Theta(\cdot) : \mathbb{R}^{nN} \to \mathbb{R}^{nN}$ in Assumption 4.2(a) represents a state transformation and it provides additional freedom to address problems involving MASs that do not necessarily converge to the origin with the available control protocol, for e.g., consensus protocols. For such systems, the idea is that $\Theta(x) = \mathbf{0}$ forms the equilibrium set.

Remark 4.2. *(On Assumption 4.2(b)) Assumption 4.2(b) conveys that the MAS* $\dot{x} = f(x, e)$*, where* $x,\ e,\ f(\cdot)$ *are as defined in* (4.8)*, is input-to-state stable (ISS) with respect to* $e_i, \forall i \in \mathcal{V}$*, and correspondingly* V *is the ISS-Lyapunov function of the MAS. Since* V *is ISS-Lyapunov, we have* $\dot{V} \leq -\acute{\alpha}_V V + \sum \acute{\gamma}_i^2 W_i^2$*, where* $\acute{\alpha}_V > 0$*, and* $\acute{\gamma}_i \geq 0, \forall i \in \mathcal{V}$*; to this inequality we can add and subtract terms* $\sum \omega_i \hat{V}_i$ *(and* $\sum H_i^2$*). Here, introducing the term* $\omega_i \hat{V}_i$ *in Assumption 4.2(b) enables slower decay of the auxiliary variable* η_i *(for instance, see* (4.11) *or* (4.18)*), thus facilitating fewer events, and as a consequence fewer broadcasts and, perhaps, fewer controller updates. The*

idea (behind Assumption 4.2(b)) is that the added terms (non-negative terms) $\sum \omega_i \hat{V}_i(\hat{x}_{\bar{\mathcal{N}}_{in}^i})$ *(and* $\sum H_i^2$*) can be absorbed into* $-\acute{\alpha}_V V$ *and* $\sum \acute{\gamma}_j^2 W_j^2$*, since* $\hat{x}_{\bar{\mathcal{N}}_{in}^i} = (\bar{\mathsf{A}}_i \otimes \mathbb{I}_n)(x+e)$*. Consequently,* $\acute{\alpha}_V$ *depreciates to* $\alpha_V > 0$ *and* $\acute{\gamma}_i$*, likely, increases to* γ_i*, ultimately resulting in Assumption 4.2(b). The design constant* $\omega_i, \forall i \in \mathcal{V}$*, can be increased upwards of zero (to a certain extent) while simultaneously ensuring that* $\alpha_V > 0$*.*

Next, in order to compensate for exponential rise of $W_i(e_i)$ and ensure stability, we define a weighing parameter $\theta_i(s),\ s \in \mathbb{R}_{\geq 0}$, that dampens the rise in $W_i(e_i)$, using the following lemma.

Lemma 4.1 ([69])**.** *Let* $\theta_i : \mathbb{R}_{\geq 0} \to \mathbb{R}$ *be the solution to the differential equation*

$$\dot{\theta}_i(s, \hat{\gamma}_i) = \begin{cases} -2L_\mu^i \theta_i(s) - \hat{\gamma}_i(\theta_i^2(s) + 1), & s \in [0, T_0^i(\lambda)] \\ 0, & s > T_0^i(\lambda) \end{cases},$$

with the initial condition $\theta_i(0) = \frac{1}{\lambda_i}$*, where* $L_\mu^i = L_i + \mu_i$ *for sufficiently small* $\mu_i > 0$ *and design parameter* $\hat{\gamma}_i \geq \gamma_i$*. Then* $\theta_i(s, \hat{\gamma}_i)$ *is monotonically decreasing and* $\theta_i(s, \cdot) = \lambda_i$ *for* $s \geq T_0^i(\lambda_i)$*.*

Here, $\lambda_i \in (0, 1)$ is a design parameter that influences both MASP and the event-triggering condition (namely, (4.11) in Theorem 4.1 below). By choosing appropriate parameters such as $\lambda_i,\ \mu_i$ for each agent i, the upper bound $T^i = T_0^i(\lambda_i)$ can be determined using (28) in [69]. Note that, in Lemma 4.1, we also introduce the design parameter $\hat{\gamma}_i \geq \gamma_i$ which differs, slightly, from the definition of $\dot{\theta}_i$ in [69] where $\hat{\gamma}_i = \gamma_i$ was used.

The following theorem presents the main result of this subsection.

Theorem 4.1. *Under Assumption 4.2, if the ETM governed by functions in* (4.5) *is given by*

$$\begin{aligned} f_i^\eta &= -\beta_i \eta_i + \omega_i \hat{V}_i(\hat{x}_{\bar{\mathcal{N}}_{in}^i}), \\ g_s^i &= \eta_i + \hat{\gamma}_i \Big(\lambda_i - \frac{1}{\lambda_i}\Big) W_i^2(e_i), \\ g_t^i &= \eta_i + \hat{\gamma}_i \bar{\lambda}_i W_i^2(e_i), \end{aligned} \tag{4.11}$$

where $\beta_i > 0$ and $\bar{\lambda}_i \in [0, \lambda_i]$, then the closed-loop system in (4.8) *is asymptotically stable with respect to the following set* $\{x \in \mathbb{R}^{nN} \mid \Theta(x) = \mathbf{0}\}$.

Proof. For the closed-loop hybrid system in (4.8), consider the Lyapunov candidate

$$U_1(q) = V(x) + \sum_{i \in \mathcal{V}} \Big[\hat{\gamma}_i \theta_i(\tau_i, \hat{\gamma}_i) W_i^2(e_i) + \eta_i(t) \Big],$$

where W_i and V satisfy Assumptions 4.1 and 4.2, respectively. For notational brevity, we drop arguments of all the functions involved in this proof. We begin the analysis by studying stability aspects over the flow domain C and then address the same over the jump domain D.

Analysis during flow:

Evaluating the Clarke derivative of U_1 at any instant results in:

$$\begin{aligned} U_1^\circ \leq & -\alpha_V V + \sum_{i \in \mathcal{V}} \Big[\gamma_i^2 W_i^2 - \omega_i \hat{V}_i - H_i^2 + \dot{\eta}_i + \hat{\gamma}_i \dot{\theta}_i W_i^2 + 2 \hat{\gamma}_i \theta_i W_i \dot{W}_i \Big] \\ \leq & -\alpha_V V + \sum_{i \in \mathcal{V}} \Big[\gamma_i^2 W_i^2 - H_i^2 - \beta_i \eta_i + \hat{\gamma}_i \big(-2 L_i^\mu \theta_i - \hat{\gamma}_i (\theta_i^2 + 1) \big) W_i^2 \\ & + 2 \hat{\gamma}_i \theta_i W_i \big(L_i W_i + H_i \big) \Big]. \end{aligned} \tag{4.12}$$

Through Young's inequality, we have $2 \hat{\gamma}_i \theta_i W_i H_i \leq (\hat{\gamma}_i \theta_i W_i)^2 + H_i^2$. Using this in (4.12) results in:

$$U_1^\circ \leq -\alpha_V V + \sum_{i \in \mathcal{V}} \Big[-(\hat{\gamma}_i^2 - \gamma_i^2) W_i^2 - \beta_i \eta_i - 2 \gamma_i \mu_i \theta_i W_i^2 \Big]. \tag{4.13}$$

Since, $\alpha_V > 0$ and design parameters $\hat{\gamma}_i \geq \gamma_i$ and $\beta_i > 0$, there exists a positive function $\zeta_1 : \mathbb{R} \to \mathbb{R}_{\geq 0}$ such that $U_1^\circ(q)$ in (4.13) satisfies:

$$U_1^\circ(q) \leq -\zeta_1(U_1(q)), \ \forall q \in C. \tag{4.14}$$

Analysis at jumps:

Evaluating U_1^+ at jumps depends on the occurrence (or non-occurrence) of events on the agents in $\mathcal{G}$. Let time $\mathtt{t}$ denote an instant at which jumps (across the network) occur and let $\mathfrak{I} \subseteq \mathcal{V}$ denote the index set such that

$\mathfrak{I} := \{i | \mathtt{t} \in \{s_k^i\}_{k=0}^{\infty}, \forall i \in \mathcal{V}\}$. $\mathfrak{I}$ represents the set of all agents that experience jump at time $\mathtt{t}$; this means, $\mathfrak{I} = \mathcal{V}$ for synchronous protocols and $\mathfrak{I} \subseteq \mathcal{V}$ for asynchronous protocols. Note that the agents in the complementary set $\mathcal{V} \setminus \mathfrak{I}$ do not, actively, take part in the jump; their states, instantaneously, before and after the jump remain unchanged and as a result their contribution towards convergence analysis at instant $\mathtt{t}$ is zero.

Since the agents in $\mathfrak{I}$ are triggered depending on the sign of $g_s^i(\cdot)$, we define the following three index subsets: $\mathcal{P} = \{i : g_s^i > 0\}$, $\mathcal{Q} = \{i : g_s^i < 0\}$ and $\mathcal{R} = \{i : g_s^i = 0\}$ to distinguish between the agents depending on their jumps described in (4.10). Here, $\mathcal{P} \cup \mathcal{Q} \cup \mathcal{R} = \mathfrak{I}$. Accordingly, each agent in $\mathfrak{I}$ takes one of the following augmented states at the jump instant:

$$\begin{cases} \forall i \in \mathcal{P}, \ \left[x_i^{\mathrm{T}} \ e_i^{\mathrm{T}} \ \hat{x}_i^{\mathrm{T}} \ \tau_i \ \eta_i\right]^+ = \left[x_i^{\mathrm{T}} \ e_i^{\mathrm{T}} \ \hat{x}_i^{\mathrm{T}} \ 0 \ g_s^i\right], \\ \forall i \in \mathcal{Q}, \ \left[x_i^{\mathrm{T}} \ e_i^{\mathrm{T}} \ \hat{x}_i^{\mathrm{T}} \ \tau_i \ \eta_i\right]^+ = \left[x_i^{\mathrm{T}} \ \mathbf{0}^{\mathrm{T}} \ x_i^{\mathrm{T}} \ 0 \ g_t^i\right], \\ \begin{cases} \forall i \in \mathcal{R}_1, \ \left[x_i^{\mathrm{T}} \ e_i^{\mathrm{T}} \ \hat{x}_i^{\mathrm{T}} \ \tau_i \ \eta_i\right]^+ = \left[x_i^{\mathrm{T}} \ e_i^{\mathrm{T}} \ \hat{x}_i^{\mathrm{T}} \ 0 \ g_s^i\right], \\ \forall i \in \mathcal{R}_2, \ \left[x_i^{\mathrm{T}} \ e_i^{\mathrm{T}} \ \hat{x}_i^{\mathrm{T}} \ \tau_i \ \eta_i\right]^+ = \left[x_i^{\mathrm{T}} \ \mathbf{0}^{\mathrm{T}} \ x_i^{\mathrm{T}} \ 0 \ g_t^i\right], \end{cases} \end{cases} \tag{4.15}$$

where $\mathcal{R}_1$ and $\mathcal{R}_2$ are subsets of $\mathcal{R}$ (such that $\mathcal{R}_1 \cup \mathcal{R}_2 = \mathcal{R}$, $\mathcal{R}_1 \cap \mathcal{R}_2 = \phi$) segregated on the basis of jump maps G_i^1 and G_i^2, respectively, that they choose in (4.10) when $g_s^i = 0$. So, at any jump instant, U_1 jumps as follows:

$$\begin{aligned} U_1^+ - U_1 = V(x^+) - V(x) + \sum_{i \in \mathcal{V}} \left[\eta_i^+ - \eta_i\right] \\ + \sum_{i \in \mathcal{V}} \Big[\hat{\gamma}_i \theta_i(0, \hat{\gamma}_i) W_i^2(e_i^+) - \hat{\gamma}_i \theta_i(\tau_i, \hat{\gamma}_i) W_i^2(e_i)\Big]. \end{aligned} \tag{4.16}$$

Note that: a) from (4.10), we have $x_i^+ = x_i, \forall i \in \mathcal{V}$, which implies $V(x^+) = V(x)$; and b) from (4.15), we have $e_i^+ = e_i, \forall i \in \mathcal{P} \cup \mathcal{R}_1$, and $e_i^+ = \mathbf{0}, \forall i \in \mathcal{Q} \cup \mathcal{R}_2$, which implies $W_i(e_i^+) = W_i(e_i)$ and $W_i(e_i^+) = W_i(\mathbf{0}) = 0$, respectively. Using these equalities and (4.11) in (4.16) results in:

$$\begin{aligned} U_1^+ - U_1 = \sum_{i \in \mathcal{Q} \cup \mathcal{R}_2} \Big[g_t^i - \eta_i - \hat{\gamma}_i \theta_i(\tau_i, \hat{\gamma}_i) W_i^2(e_i)\Big] \\ + \sum_{i \in \mathcal{P} \cup \mathcal{R}_1} \Big[g_s^i - \eta_i + \Big(\frac{\hat{\gamma}_i}{\lambda_i} - \hat{\gamma}_i \theta_i(\tau_i)\Big) W_i^2(e_i)\Big] \end{aligned}$$

$$U_1^+ - U_1 \leq -\sum_{i\in\mathcal{Q}\cup\mathcal{R}_2} \hat{\gamma}_i\big[\theta_i(\tau_i,\hat{\gamma}_i) - \bar{\lambda}_i\big]W_i^2(e_i) - \sum_{i\in\mathcal{P}\cup\mathcal{R}_1} \hat{\gamma}_i\Big[\theta_i(\tau_i,\hat{\gamma}_i) - \lambda_i\Big]W_i^2(e_i).$$

Since, $\theta_i(\tau_i,\cdot) \geq \lambda_i \geq \bar{\lambda}_i$ from Lemma 4.1, this implies that at the jump instants we have

$$U_1(G(q)) \leq U_1(q),\ q \in D. \tag{4.17}$$

Using (4.14) and (4.17), the proof is completed by following an argument that is similar to the proof of Theorem 1 in [69]. □

4.3.2 Active Sensing

In this subsection, in addition to broadcasting capabilities, we consider the situation where agents have the capability to infer states (or relative states) of agents in the network via onboard sensors, which enables $x_{\underline{\mathcal{N}}_k^i}$ in (4.5). The focus is then to design an ETM that utilizes these relative state measurements in order to *further* reduce the number of broadcasts and controller updates at each agent. To facilitate this, in addition to Assumption 4.1 in Subsection 4.3.1, we make the following assumptions.

Assumption 4.3. *Suppose Assumption 4.1 holds. For the hybrid system in* (4.8)*, there exist a locally Lipschitz function* $V(x) : \mathbb{R}^{nN} \to \mathbb{R}_{\geq 0}$*, continuous functions* $\hat{V}_i(\hat{x}_{\bar{\mathcal{N}}_{in}^i}) : \mathbb{R}^{nN} \to \mathbb{R}_{\geq 0}, \forall i \in \mathcal{V}$*, scalar functions* $J_i(x,e) : \mathbb{R}^{2nN} \to \mathbb{R}_{\geq 0}, \forall i \in \mathcal{V}$*, functions* $\underline{\alpha}_V,\ \bar{\alpha}_V \in \mathcal{K}_\infty$*, a continuous function* $\Theta(x) : \mathbb{R}^{nN} \to \mathbb{R}^{nN}$*, a positive scalars* $\alpha_V,\ \gamma_i, \forall i \in \mathcal{V}$*, and non-negative scalars* $\omega_i, \forall i \in \mathcal{V}$*, such that:*

(a) $\underline{\alpha}_V(|\Theta(x)|) \leq V(x) \leq \bar{\alpha}_V(|\Theta(x)|),\ \forall x \in \mathbb{R}^{nN}$*;*

(b) $\langle V(x), f\rangle \leq -\alpha_V V(x) + \sum_{i\in\mathcal{V}}\big[\gamma_i^2 W_i^2(e_i) - \omega_i\hat{V}_i(\hat{x}_{\bar{\mathcal{N}}_{in}^i}) - H_i^2(x,e) - J_i(x,e)\big]$*, for almost all* $x \in \mathbb{R}^{nN}$ *and* $\forall e_i \in \mathbb{R}^n, \forall i \in \mathcal{V}$*.*

Furthermore, $\forall i \in \mathcal{V}$*, there also exists a locally Lipschitz function* $V_i(x) : \mathbb{R}^{nN} \to \mathbb{R}_{\geq 0}$*, scalar functions* $\hat{H}_i(x,e)$*,* $\hat{J}_i(x,e) : \mathbb{R}^{2nN} \to \mathbb{R}_{\geq 0}$*, positive scalars* α_i *and* c_i *such that:*

(c) $\sum_{i\in\mathcal{V}} V_i(x) = V(x)$,

(d) $\langle V_i(x), f\rangle \leq -\alpha_i V_i(x) + c_i\big(\hat{H}_i^2(x,e) + \hat{J}_i(x,e)\big)$, *for almost all* $x \in \mathbb{R}^{nN}$ *and* $\forall e_i \in \mathbb{R}^n, \forall i \in \mathcal{V}$,

(e) $\sum_{i\in\mathcal{V}} \hat{H}_i^2 \leq \sum_{i\in\mathcal{V}} H_i^2$ *and* $\sum_{i\in\mathcal{V}} \hat{J}_i \leq \sum_{i\in\mathcal{V}} J_i$.

Assumption 4.4. *For each agent* $i \in \mathcal{V}$, *there exists a positive semi-definite function* $\tilde{V}_i(x_{\underline{\mathcal{N}}_k^i})$ *such that:*

$$\tilde{V}_i(x_{\underline{\mathcal{N}}_k^i}) \leq V_i(x)$$

where recall that $\underline{\mathcal{N}}_k^i$ *is the set of agents whose states (or relative states) can be actively sensed by agent* i *at* s_k^i.

Remark 4.3. *(On* V_i, J_i *and* $\tilde{V}_i$*) Items (a) and (b) in Assumption 4.3, similar to Assumption 4.2, convey input-to-state stability of the closed-loop system in* (4.8) *with respect to* $e_i, \forall i \in \mathcal{V}$. *In the case that* $J_i = 0$, *Assumption 4.3(a)–(b) is identical to Assumption 4.2. However, introducing* J_i *in Assumption 4.3(b) provides for additional freedom while choosing the function* V_i *which captures local (namely, agent-wise) effect of event-triggered controller* u_i *on agent dynamic* $\dot{x}_i = f_i(x, u_i)$. *Depending on the specific problem that is being addressed, the choice of* V_i *may not be unique; furthermore, it may not be dependent, solely, on neighbors' information. To address this and generalize the approach, we introduce* $\tilde{V}_i(x_{\underline{\mathcal{N}}_k^i})$ *in Assumption 4.4 which only depends on the set* $\underline{\mathcal{N}}_k^i$. *Choice of functions* V_i, J_i *and* $\tilde{V}_i$ *in two different settings is demonstrated in Section 4.4.*

Remark 4.4. *(On Assumption 4.3(d)–(e)) Assumption 4.3(d) conveys that the decay of the local function* V_i *can be exponentially bounded and the term, say* $\mathfrak{R}_i$, *accounts for the effect that neighbors, local dynamics and the event-triggered controller have on* $\dot{V}_i$. *The idea behind Assumption 4.3(d) is that* $\mathfrak{R}_i$ *can be upper bounded using terms* $\hat{H}_i^2$ *which is similar to* H_i^2, *and* $\hat{J}_i$ *which collects remaining residuals. Here, the scaling factor* c_i *provides for additional*

design freedom. Assumption 4.3(e) ensures that the cumulative effect of $\hat{H}_i^2$ is smaller than the cumulative effect of H_i^2. The same holds true for $\sum \hat{J}_i$ and $\sum J_i$. Furthermore, we also note that in Assumption 4.3(b), one can replace J_i with $\hat{J}_i$ for all agents $i \in \mathcal{V}$ but the same is not true for $\hat{H}_i^2$ as shown in the case of Subsection 4.4.2.

Remark 4.5. *(On Assumptions 4.3 – 4.4) Assumptions 4.3 – 4.4 are moderate considering Assumption 4.2 and active sensing capabilities. In fact, they have the following trivial choices if we abandon the active sensing capability and forgo Assumption 4: $\hat{J}_i = J_i = 0$, $\hat{H}_i = H_i$ and $\tilde{V}_i(x_{\underline{\mathcal{N}}_k^i}) = 0$; however, these selections would not lead to any performance improvement in the ETM.*

The following theorem provides the main result of this subsection.

Theorem 4.2. *Under Assumptions 4.3 and 4.4, if the ETM governed by functions in* (4.5) *is given by*

$$\begin{aligned} f_i^\eta &= -\beta_i\eta_i + \omega_i\hat{V}_i(\hat{x}_{\bar{\mathcal{N}}_{in}^i}), \\ g_s^i &= \eta_i + \tilde{\gamma}_i\Big(\theta_i(\tau_i) - \frac{1}{\lambda_i}\Big)W_i^2(e_i) + \rho_i\big(e^{a_i\tau_i} - 1\big)\tilde{V}_i(x_{\underline{\mathcal{N}}_k^i}), \\ g_t^i &= \eta_i + \tilde{\gamma}_i\theta_i(\tau_i)W_i^2(e_i) + \rho_i\big(e^{a_i\tau_i} - 1\big)\tilde{V}_i(x_{\underline{\mathcal{N}}_k^i}), \end{aligned} \tag{4.18}$$

where $\beta_i > 0$ and the design parameters $(a_i, \rho_i, \tilde{\gamma}_i)$ are such that, $\forall i \in \mathcal{V}$,

$$\begin{aligned} &e^{a_i\tau_i}\rho_i a_i - \alpha_V \leq 0, \\ &e^{a_i\tau_i}\rho_i c_i + \epsilon_{U_2} \leq 1, \\ &\frac{\tilde{\gamma}_i}{\hat{\gamma}_i} < \epsilon_{U_2} < 1 \text{ and } \gamma_i^2 < \tilde{\gamma}_i\hat{\gamma}_i, \end{aligned} \tag{4.19}$$

then the closed-loop system in (4.8) *is asymptotically stable with respect to the following set $\{x \in \mathbb{R}^{nN} \mid \Theta(x) = \mathbf{0}\}$.*

Proof. Consider the Lyapunov function

$$U_2(q) = V(x) + \sum_{i\in\mathcal{V}}\Big[\tilde{\gamma}_i\theta_i(\tau_i, \hat{\gamma}_i)W_i^2(e_i) + e^{a_i\tau_i}\rho_i V_i(x) + \eta_i(t)\Big],$$

where $W_i,\ V_i,\ V$ satisfy Assumptions 4.1 and 4.3 and triplet $(a_i, \rho_i, \tilde{\gamma}_i), \forall i \in \mathcal{V}$, are scalars that are to be determined. Similar to the proof of Theorem 4.1, we drop arguments of all the functions involved in this proof. We begin the analysis with the flow domain C and then address the same over the jump domain D.

Analysis during flow:

At any instant in C, the Clarke derivative of U_2 is

$$\begin{aligned}
U_2^\circ \leq & \sum \Big[-\alpha_V V_i + \gamma_i^2 W_i^2 - \omega_i \hat{V}_i - H_i^2 - J_i + \dot{\eta}_i + \big(\tilde{\gamma}_i \dot{\theta}_i W_i^2 + 2\tilde{\gamma}_i \theta_i W_i \dot{W}_i\big) \\
& + \big(e^{a_i \tau_i} \rho_i \dot{V}_i + a_i e^{a_i \tau_i} \rho_i V_i \dot{\tau}_i\big) \Big] \\
\leq & \sum \Big[-\alpha_V V_i + \gamma_i^2 W_i^2 - H_i^2 - J_i + a_i e^{a_i \tau_i} \rho_i V_i + e^{a_i \tau_i} \rho_i \big(-\alpha_i V_i \\
& + c_i \hat{H}_i^2 + c_i \hat{J}_i \big) + 2\tilde{\gamma}_i \theta_i \big(L_i W_i^2 + H_i W_i\big) \\
& + \tilde{\gamma}_i \big(-2L_\mu^i \theta_i - \hat{\gamma}_i \theta_i^2 - \hat{\gamma}_i \big) W_i^2 - \beta_i \eta_i \Big] \\
\leq & \sum \Big[-\big(\alpha_V - e^{a_i \tau_i} \rho_i a_i\big) V_i - e^{a_i \tau_i} \rho_i \alpha_i V_i - \big(\tilde{\gamma}_i \hat{\gamma}_i - \gamma_i^2\big) W_i^2 \\
& - \big(1 - e^{a_i \tau_i} \rho_i c_i\big) \hat{H}_i^2 - \big(1 - e^{a_i \tau_i} \rho_i c_i\big) \hat{J}_i - \tilde{\gamma}_i \hat{\gamma}_i \theta_i^2 W_i^2 \\
& + 2\tilde{\gamma}_i \theta_i H_i W_i - 2\gamma_i \theta_i W_i^2 \mu - \beta_i \eta_i \Big]. \qquad (4.20)
\end{aligned}$$

Using Young's inequality on $2\tilde{\gamma}_i \theta_i H_i W_i$ in (4.20) yields:

$$\begin{aligned}
U_2^\circ \leq & \sum_{i \in \mathcal{V}} \Big[-\big(\alpha_V - e^{a_i \tau_i} \rho_i a_i\big) V_i - e^{a_i \tau_i} \rho_i \alpha_i V_i - \big(\tilde{\gamma}_i \hat{\gamma}_i - \gamma_i^2\big) W_i^2 \\
& - \big(1 - e^{a_i \tau_i} \rho_i c_i - \epsilon_{U_2}\big) \hat{H}_i^2 - \big(1 - e^{a_i \tau_i} \rho_i c_i\big) \hat{J}_i - \big(\tilde{\gamma}_i \hat{\gamma}_i - \frac{\tilde{\gamma}_i^2}{\epsilon_{U_2}}\big) \theta_i^2 W_i^2 \\
& - 2\gamma_i \theta_i W_i^2 \mu - \beta_i \eta_i \Big]. \qquad (4.21)
\end{aligned}$$

Considering that the design parameters satisfy conditions in (4.19) and Assumption 4.3, there exists a positive function $\zeta_2 : \mathbb{R} \to \mathbb{R}_{\geq 0}$ such that $U_2^\circ(q)$ in (4.21) satisfies:

$$U_2^\circ(q) \leq -\zeta_2(U_2(q)),\ \forall q \in C. \qquad (4.22)$$

Analysis at jumps:

For the analysis here, we borrow the index sets $\mathfrak{I}$, $\mathcal{P}$, $\mathcal{Q}$, $\mathcal{R}$, $\mathcal{R}_1$, and $\mathcal{R}_2$ (see (4.15)) which are defined in the proof of Theorem 4.1. Recall that $\mathfrak{I} =$

$\mathcal{P} \cup \mathcal{Q} \cup \mathcal{R}$. At every jump instant in D, we have the following:

$$\begin{aligned} U_2^+ - U_2 =& V(x^+) - V(x) + \sum_{i \in \mathcal{V}} \Big[\eta_i^+ - \eta_i \\ &+ \tilde{\gamma}_i \theta_i(\tau_i^+, \hat{\gamma}_i) W_i^2(e_i^+) - \tilde{\gamma}_i \theta_i(\tau_i, \hat{\gamma}_i) W_i^2(e_i) \\ &+ e^{a_i \tau_i^+} \rho_i V_i(x^+) - e^{a_i \tau_i} \rho_i V_i(x) \Big]. \end{aligned}$$

Using the jumps outlined in (4.15) yields the following:

$$\begin{aligned} U_2^+ - U_2 =& \sum_{i \in \mathcal{Q} \cup \mathcal{R}_2} \Big[g_t^i - \eta_i - \tilde{\gamma}_i \theta_i(\tau_i) W_i^2(e_i) - \big(e^{a_i \tau_i} - 1\big) \rho_i V_i(x) \Big] \\ &+ \sum_{i \in \mathcal{P} \cup \mathcal{R}_1} \Big[g_s^i - \eta_i + \tilde{\gamma}_i \Big(\frac{1}{\lambda_i} - \theta_i(\tau_i) \Big) W_i^2(e_i) - \big(e^{a_i \tau_i} - 1\big) \rho_i V_i(x) \Big] \\ \leq& - \sum_{i \in \mathfrak{I}} \rho_i \big(e^{a_i \tau_i} - 1\big) \big(V_i(x) - \tilde{V}_i(x_{\underline{\mathcal{N}}_k^i}) \big). \end{aligned}$$

Subsequently, employing Assumption 4.4, we have

$$U_2(G(q)) \leq U_2(q), \ q \in D. \tag{4.23}$$

Again, using (4.22) and (4.23), the proof is completed via the argument in the proof of Theorem 1 in [69]. □

Remark 4.6. *(On sensing network) In Theorem 4.4, $\tilde{V}_i(x_{\underline{\mathcal{N}}_k^i})$ in (4.18) utilizes the states (or relative states) that are sensed by i at s_k^i. The network formed as a consequence of sensing across all agents, called the sensing network, will likely be directed and it need not be the same as the broadcast network $\mathcal{G}$. Agents, depending on their onboard sensors, may have different criteria on selecting neighbors for active sensing, for example, choosing nearest neighbors or choosing neighbors based on the sensor's range. These criteria could make the sensing network time-varying. Furthermore, in the case of a directed broadcast network $\mathcal{G}$ it is well-known that consensus is achieved if and only if $\mathcal{G}$ is strongly connected; such a property is not necessary for the sensing network. Lastly, it is plausible that at a certain event-verifying instant s_k^i some or all agents have no neighbors to sense, e.g., if the fellow agents are beyond the sensor's range. In such cases, the agents adopt a trivial choice, i.e. $\tilde{V}_i = 0$, as*

stated in Remark 4.5. This is also a reason why $\hat{V}_i$, affecting the flow of η_i in (4.18) *(and in* (4.11)*), is independent of $x_{\underline{\mathcal{N}}_k^i}$ and relies on only (model-based) broadcast states $\hat{x}_{\bar{\mathcal{N}}_{in}^i}$ as stated in Assumptions 4.2 and 4.3.*

4.4 Consensus in Control-Affine MASs

In this section, we analyze two case studies on the consensus problem of nonlinear MASs in order to demonstrate the use of the two ETMs presented in Section 4.3. First, we introduce the agent dynamics as follows:

$$\dot{x}_i = \bar{f}(x_i) + u_i,\ \forall i \in \mathcal{V}, \tag{4.24}$$

where, for brevity of notation, we consider the scalar case, namely $x_i, u_i \in \mathbb{R}$. To achieve consensus of the MAS in (4.24), the distributed control protocol employed by each agent is $u_i = -\kappa \mathsf{L}_i x$ where L_i is the $i-$th row of the Laplacian matrix L. Further, conditions on control gain κ that ensure consensus are presented, shortly, in Subsections 4.4.1 and 4.4.2. A periodic event-triggered implementation of the control protocol, as per (4.4), takes the form

$$u_i = -\kappa \mathsf{L}_i \hat{x},\ \kappa > 0, \tag{4.25}$$

where $\hat{x}$ is the augmented vector of the broadcasted agent states. Each agent i, adopts $\dot{\hat{x}}_i = \Upsilon(\hat{x}_i) = \bar{f}(\hat{x}_i)$ as the dynamics of their model-based broadcast estimates. Defining the auxiliary variables η_i, τ_i as in (4.5) and (4.7), respectively, and the augmented vectors as defined in Section 4.2, the hybrid systems model of the MAS in (4.24) with (4.25) is:

$$\begin{cases} \dot{q} = \begin{bmatrix} [\bar{f}](x) - \kappa \mathsf{L}(x+e) \\ [\bar{f}](\hat{x}) - [\bar{f}](x) + \kappa \mathsf{L}(x+e) \\ [\bar{f}](\hat{x}) \\ \mathbf{1} \\ f_\eta \end{bmatrix}, & q \in C, \\ q^+ \in \bigcup_{i=1}^N G_i(q), & q \in D, \end{cases} \tag{4.26}$$

where $[\bar{f}](x) = [\bar{f}(x_1) \dots \bar{f}(x_N)]^{\mathrm{T}}$ denotes the augmented vector of nonlinear function $\bar{f}$, $G_i(q)$ is the same as in (4.10).

For the MAS in (4.26), we consider the following two cases based on the associated broadcast network and agent dynamics. For each of these cases, we demonstrate that the two dynamic ETMs designed in Subsection 4.3.1 and Subsection 4.3.2 asymptotically stabilize the closed-loop system in (4.26) w.r.t. their respective stability sets.

4.4.1 Undirected Networks, Lipschitz Dynamics

In this subsection, we consider an undirected network $\mathcal{G}$ and assume that the dynamics $\bar{f}(\cdot)$ of the agent is globally Lipschitz with a Lipschitz constant $\mathcal{L}$. Prior to presenting the main result in this subsection, we note that the continuous-time controller, $u_i = -\kappa \mathsf{L}_i x$, achieves consensus when the control gain κ is such that

$$\kappa > \frac{\mathcal{L}}{\Lambda_2}\sqrt{\frac{2\mathsf{d}_M}{\Lambda_2}} = \kappa_0, \tag{4.27}$$

where $\mathsf{d}_M = \max_i \mathsf{d}_i$.

The main result is as follows.

Theorem 4.3. *Let the MAS in* (4.24) *operate over a connected undirected network $\mathcal{G}$ with Laplacian L and let $\mathcal{L}$ denote a Lipschitz constant associated with dynamics $\bar{f}(\cdot)$. Further, let control gain $\kappa = \mathfrak{p}\kappa_0$, where $\mathfrak{p} > 1$ and κ_0 is defined in* (4.27).

1. ***Broadcasting**: Let $W_i = |e_i|, \forall i \in \mathcal{V}$, $V = \frac{K}{2}|z|^2$ where $z = \mathsf{L}x$ and $\hat{V}_i = |\mathsf{L}_i\hat{x}|^2, \forall i \in \mathcal{V}$. Under Assumption 4.2, $\forall i \in \mathcal{V}$, if the dynamic ETM governed by* (4.11) *is such that: $\beta_i > 0$,*

$$\begin{aligned} \omega_i &= \Big(\Lambda_2 - \frac{\Lambda_M^2}{2\epsilon_2}\Big)(1-\pi_1)(1-\xi_1)\kappa K, \\ \hat{\gamma}_i^2 &\geq \gamma_i^2 = K\kappa\Xi_3 + 2\kappa^2 \mathrm{Tr}(\mathsf{A}^T\mathsf{A}), \end{aligned} \tag{4.28}$$

where $\Xi_3 = \big[\frac{\epsilon_2}{2} + \Big(\Lambda_2 - \frac{\Lambda_M^2}{2\epsilon_2}\Big)(1-\pi_1)(\frac{1}{\xi_1}-1)\big]\Lambda_M^2$, design parameters are

such that $\xi_1 \in (0, 1]$,

$$\epsilon_2 \in \Big(\frac{\Lambda_M^2}{2\Lambda_2}\frac{\mathfrak{p}}{\mathfrak{p}-1}, \infty\Big), \tag{4.29a}$$

$$\pi_1 \in \Big(\frac{\Lambda_2}{\mathfrak{p}}\big(\Lambda_2 - \frac{\Lambda_M^2}{2\epsilon_2}\big)^{-1}, 1\Big), \tag{4.29b}$$

$$K > 2\kappa^2 / \Big[\big(\Lambda_2 - \frac{\Lambda_M^2}{2\epsilon_2}\big)\pi_1\kappa - \Lambda_2\kappa_0\Big], \tag{4.29c}$$

then the closed-loop system in (4.26) *is asymptotically stable w.r.t. the set*

$$\{x \in \mathbb{R}^N \mid \mathsf{L}x = \mathbf{0}\}. \tag{4.30}$$

2. ***Active Sensing****: Let* $V_i = \tilde{V}_i = \frac{K}{2}|\mathsf{L}_i x|^2, \forall i \in \mathcal{V}$. *Under Assumptions 4.3 - 4.4,* $\forall i \in \mathcal{V}$, *if the dynamic ETM governed by* (4.18) *is such that:* a_i, ρ_i, $\tilde{\gamma}_i$ *satisfy conditions in* (4.19), $\beta_i > 0$, ω_i *is as in* (4.28),

$$\hat{\gamma}_i^2 \geq \; K\kappa\Xi_3 + 2\kappa^2\frac{\Lambda_M^2}{\epsilon_4}\sum_{j\in\mathcal{V}}|\mathsf{L}_j| \tag{4.31}$$

where Ξ_3 *is the same as in item (1), scalars* π_1, ξ_1, ϵ_2 *are the same as in* (4.29), $\epsilon_3 = \frac{\sqrt{2}}{\sqrt{\Lambda_2 \mathsf{d}_M}}$,

$$\epsilon_4 \in \Big(0, \min\Big\{1, \min_i \frac{\mathsf{d}_i(2 - \frac{\mathcal{L}_{\epsilon_3}}{\kappa})}{|\mathsf{A}_i|^2 + |\mathsf{L}_i|}, \min_i \frac{|\mathsf{L}_i|\Lambda_M^2}{|\mathsf{A}_i|^2}\Big\}\Big), \tag{4.32a}$$

$$K > 2\kappa^2\Big(\frac{N}{\epsilon_4} + \frac{2}{\epsilon_3}\frac{\mathcal{L}}{\Lambda_2\kappa}\Big) / \Big[\big(\Lambda_2 - \frac{\Lambda_M^2}{2\epsilon_2}\big)\pi_1\kappa - \Lambda_2\kappa_0\Big], \tag{4.32b}$$

then the closed-loop system in (4.26) *is asymptotically stable w.r.t.* (4.30).

The proof of Theorem 4.3 is presented in Appendix A.1.2.

4.4.2 Directed Networks, One-Sided Lipschitz Dynamics

In this subsection, we consider the case of a directed network $\mathcal{G}$ and we assume that the dynamics $\bar{f}(\cdot)$ of the agent is globally one-sided Lipschitz with a one-sided Lipschitz constant $\mathcal{L}_{\text{os}}$. Similar to Section 4.4.1, we first note

that the continuous-time controller achieves consensus when the control gain κ satisfies:

$$\kappa > \frac{\mathcal{L}_{\text{os}}}{a_\xi(\mathsf{L})} = \bar{\kappa}_0, \tag{4.33}$$

where $a_\xi(\mathsf{L})$ is the general algebraic connectivity of $\mathcal{G}$ introduced in Section 4.1.

Note that the result that follows is more general than the case study considered in Section 4.4.1 and is also beyond the case of local Lipschitz continuity.

Theorem 4.4. *Let the MAS in* (4.24) *operate over a strongly connected directed network $\mathcal{G}$ with Laplacian L and let $\mathcal{L}_{os}$ be a global one-sided Lipschitz constant associated with $\bar{f}(\cdot)$. ξ is such that $a_\xi(\mathsf{L}) > 0$. Further, let the control gain $\kappa = \bar{\mathfrak{p}}\bar{\kappa}_0$, $\bar{\mathfrak{p}} > 1$, where $\bar{\kappa}_0$ is defined in* (4.33).

1. ***Broadcasting:*** *Let $W_i = |e_i|, \forall i \in \mathcal{V}$, $V = \sum_{i\in\mathcal{V}} \frac{K}{2}\xi_i|x_i - \bar{x}|^2$ and $\hat{V}_i(\hat{x}_{\bar{\mathcal{N}}_{in}^i}) = |\mathsf{L}_i\hat{x}|^2, \forall i \in \mathcal{V}$. Under Assumption 4.2, $\forall i \in \mathcal{V}$, if the dynamic ETM governed by* (4.11) *is such that: $\beta_i > 0$, $\omega_i = \frac{\vartheta}{2} \geq 0$,*

$$\hat{\gamma}_i^2 \geq \; K\kappa\frac{\epsilon_1\bar{\Lambda}_M^2}{2} + 2\kappa^2\text{Tr}(\mathsf{A}^T\mathsf{A}) + \vartheta\text{Tr}(\mathsf{L}^T\mathsf{L})$$

where, $\epsilon_1 \in \left(\frac{1}{2a_\xi(\mathsf{L})}\frac{\bar{\mathfrak{p}}}{\bar{\mathfrak{p}}-1}, \infty\right)$ and K is such that

$$K > \frac{2\gamma + 4\kappa^2}{\xi_{min}}\text{Tr}(\mathsf{L}^T\mathsf{L})/\Big[2(a_\xi(\mathsf{L})\kappa - \mathcal{L}_{os}) - \frac{\kappa}{\epsilon_1}\Big], \tag{4.34}$$

then the closed-loop system in (4.24) *is asymptotically stable w.r.t.*

$$\{x \in \mathbb{R}^N \mid \big(\mathbb{I}_N - \mathbf{1}_N\xi^T\big)x = \mathbf{0}\}. \tag{4.35}$$

2. ***Active Sensing:*** *For every $i \in \mathcal{V}$, let $V_i = \frac{K}{2}\xi_i|x_i - \bar{x}|^2$, and $\tilde{V}_i = \frac{K\xi_{min}}{2N|\mathsf{L}_{i,k}^s|^2}|\mathsf{L}_{i,k}^s x|^2$, where $\mathsf{L}_{i,k}^s$ is the i-th row of Laplacian matrix L_t^s associated with the sensing network at time $t \in \{s_k^i\}_{k=0}^\infty$. Under Assumptions 4.3 – 4.4, $\forall i \in \mathcal{V}$, if the dynamic ETM governed by* (4.18) *is such that a_i, ρ_i, $\tilde{\gamma}_i$ satisfy conditions in* (4.19) *and $\beta_i > 0$, ω_i, $\hat{\gamma}_i$ and K are the same as in item (1) above, then the closed-loop system in* (4.26) *is asymptotically stable.*

The proof of Theorem 4.4 is presented in Appendix A.1.3.

In addition to Remark 4.6, through the following remarks: 1) we establish the reasoning behind considering separate case studies for undirected and directed broadcast networks; and 2) we also present the motivation behind Assumptions 4.3 – 4.4 considered in Section 4.3.

Remark 4.7. *(On V_i) The case study in Subsection 4.4.1 on undirected networks could be considered as a special case of the 2^{nd} case study in Subsection 4.4.2 on directed networks. However, the two case studies have been provided in this work to demonstrate the construction of the functions V_i and $\tilde{V}_i$. Note that in the proof of Theorem 4.4 in Appendix A.3, V_i in Assumption 4.3(c)–(d) has been constructed entirely from the ISS stability of the global function V in* (A.13)*; as a result we have $\hat{J}_i = 0, \forall i \in \mathcal{V}$. However, the same is not true in the case of V_i in Theorem 4.3 for the undirected case which satisfies Assumption 4.3 with non-zero $\hat{J}_i = J_i$. For this reason, as stated in Remark 3, we provide additional flexibility in the design by including the term J_i in Assumption 4.3.*

Remark 4.8. *(On , $\tilde{V}_i$) For the case of undirected networks, in Part 2 of Theorem 4.3, the function $\tilde{V}_i(x_{\underline{\mathcal{N}}_k^i}) = \frac{K}{2}|\mathsf{L}_i x|^2$ can be constructed from the choice of Lyapunov function V and the function V_i which were used in the proof of Theorem 4.3. Here, the sensing network is the same as the established broadcasted network, i.e. $\underline{\mathcal{N}}_k^i = \bar{\mathcal{N}}_{in}^i, \forall i \in \mathcal{V}, \forall k \in \mathbb{Z}_{\geq 0}$. However, such a selection of $\tilde{V}_i$ may not be feasible (or perhaps desirable) in the case of directed networks, which motivates the differences in V_i and $\tilde{V}_i$. Hence, Assumption 4.4 somewhat decouples the selections of these functions in analysis and implementation; although, note that $\tilde{V}_i < V_i$ could lead to more events. This is another reason on why we do not simply present the scenario in Subsection 4.4.1 as a special case of that in Subsection 4.4.2.*

4.5 Numerical Example

As an illustration of the two case studies, we consider that the following agent dynamics and control protocol:

$$\forall i \in \mathcal{V}, \quad \begin{cases} \dot{x}_i = -x_i^3 + 0.1\sin(x_i) + u_i, \\ u_i = -\kappa \mathsf{L}_i x, \kappa = 0.5. \end{cases} \tag{4.36}$$

It is straightforward to see that the system in (4.36) is one-sided Lipschitz with one-sided Lipschitz constant $\mathcal{L}_{\text{os}} = 0.1$. Here, κ in (4.36) satisfies both (4.27) and (4.33), simultaneously, for the broadcast networks considered below. The periodic event-triggered protocol is $u_i = -\kappa \mathsf{L}_i \hat{x}$. For the MAS in (4.36), we set the lower bound of sampling period, ε^i in (4.2), to be 1 ms, the time step to be 0.1 ms and simulation time to be 5 s.

Network Topology	$\lambda_i, \forall i$	$\bar{T}_{\text{m}}$	ETMs	Metrics	
				M1	M2
Undirected	0.66	1 ms	(4.37)	9.51	9
			(4.38)	2.39	39
	0.44	2 ms	(4.37)	19.18	8
			(4.38)	4.97	38
	0.23	3 ms	(4.37)	32.71	6
			(4.38)	8.94	30
Directed	0.69	1 ms	(4.39)	12.73	6
			(4.40)	10.44	8
	0.46	2 ms	(4.39)	27.54	6
			(4.40)	21.31	6
	0.26	3 ms	(4.39)	44.88	3
			(4.40)	38.89	6

Table 4.1: Comparison between the two dynamic ETMs proposed in (4.11) and (4.18).

Undirected networks: Consider $\lambda_i = 0.66, \ \forall i \in \mathcal{V}$.

Part 1: Broadcasting. Some of the design parameters referred to in Theorem 4.3(1) are as follows: $K = 55$, $\xi_1 = 0.5$, $\epsilon_2 = 10$, $\pi_1 = 0.75$. The dynamic ETM

adopted is (4.11) and is described by the following triplet $\forall i \in \mathcal{V},\ (f_\eta^i, g_s^i, g_t^i)$:

$$\begin{cases} f_\eta^i = & -0.1\eta_i + 1.64|\mathsf{L}_i\hat{x}|^2, \\ g_s^i = & \eta_i - 314.07|e_i|^2, \\ g_t^i = & \eta_i + 242.40|e_i|^2. \end{cases} \tag{4.37}$$

Assumptions 4.1 and 4.2 are satisfied through scalars $L_i = 0.1 + 0.5\mathsf{d}_i$, $\alpha_V = 7.73 \times 10^{-4}$, $\omega_i = \{1.64\}$, $\gamma_i = \{71.15\}$.

Part 2: Active Sensing. Some of the design parameters referred to in Theorem 4.3(2) are as follows: $K = 441,\ \epsilon_3 = 0.51,\ \epsilon_4 = 0.5$. In this case, the dynamic ETM adopted is (4.18) and the triplet (f_η^i, g_s^i, g_t^i) is as follows:

$$\begin{cases} f_\eta^i = -0.1\eta_i + 13.21|\mathsf{L}_i\hat{x}|^2, \\ g_s^i = \eta_i + 133.5(\theta_i - 1.51)|e_i|^2 + \frac{9.19}{10^6}|\mathsf{L}_i x|^2, \\ g_t^i = \eta_i + 133.5\theta_i|e_i|^2 + \frac{9.19}{10^6}|\mathsf{L}_i x|^2. \end{cases} \tag{4.38}$$

Assumption 3 is satisfied through $\alpha_V = 4.16\times10^{-5}$, $\alpha_i = \{0.34, 0.39, 0.32, 0.38\}$, $\gamma_i = \{201.34\}$, $\omega_i = \{13.21\}$, $c_i = \{220.5\}$.

Further, $H_i = 0.5(|\mathsf{A}_i|^2|e|^2 + |z_i|^2)$ and $J_i = \frac{1}{2}(2|z|^2 - |z_i|^2) + \frac{1}{2}(71.79|\mathsf{L}_i| - |\mathsf{A}_i|^2)|e|^2 + 0.19\sum_{j\in\mathcal{V}} \mathsf{a}_{ij}|x_i - x_j|^2$. Figure 4.2 depicts the underlying communication network and state trajectories of agents achieving consensus and Fig. 4.4 shows the corresponding inter-event times for the case of active sensing.

Directed networks: Consider $\lambda_i = 0.69,\ \forall i \in \mathcal{V}$.

Part 1: Broadcasting. Design parameters referred to in Theorem 4.4(1) are as follows: $K = 1.27 \times 10^4,\ \omega_i = \{0.5\},\ \gamma_i = \{250.40\},\ \epsilon_1 = 1.1$. Here, the dynamic ETM adopted is (4.11) and is described by the following triplet (f_η^i, g_s^i, g_t^i):

$$\begin{cases} f_\eta^i = & -0.1\eta_i + \frac{1}{2}|\mathsf{L}_i\hat{x}|^2, \\ g_s^i = & \eta_i - 272.0|e_i|^2, \\ g_t^i = & \eta_i + 247.2|e_i|^2. \end{cases} \tag{4.39}$$

Assumptions 4.1 and 4.2 are satisfied through scalars $L_i = 0.1 + 0.5\mathsf{d}_i$, $\alpha_V = 4.48 \times 10^{-4}$, $\omega_i = \{0.5\}$, $\gamma_i = \{250.40\}$.

Part 2: Active Sensing. Design parameters referred to in Theorem 4.4(2) are

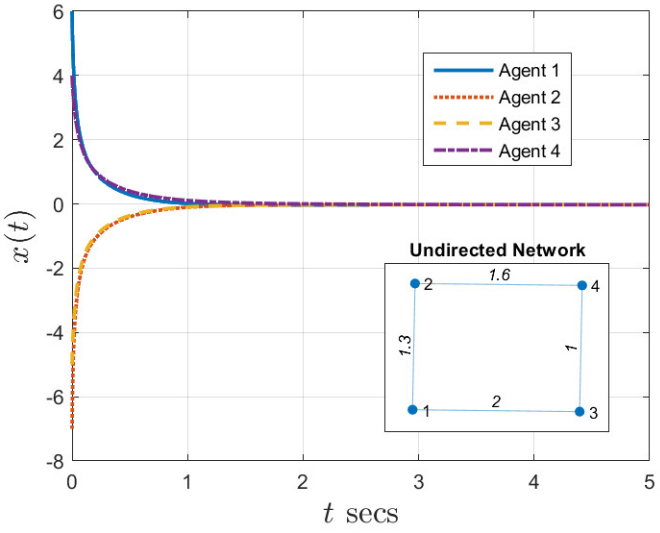

Figure 4.2: Consensus in undirected network

the same as those in Theorem 4.4(1). In this case, the dynamic ETM adopted is (4.18) and the triplet (f_η^i, g_s^i, g_t^i) is as follows:

$$\begin{cases} f_\eta^i = -0.1\eta_i + |\mathsf{L}_i\hat{x}|^2, \\ g_s^i = \eta_i + 211.7(\theta_i - 1.44)|e_i|^2 + \frac{1.7}{10^5}|\mathsf{L}_i x|^2, \\ g_t^i = \eta_i + 211.7\theta_i|e_i|^2 + \frac{1.7}{10^5}|\mathsf{L}_i x|^2. \end{cases} \tag{4.40}$$

Assumption 3 is satisfied through α_V, ω_i, the same as in Part 1 of Directed networks, and $\alpha_i = \{0.03\}$, $c_i = \{7.91 \times 10^3\}$.

Further, $H_i = 0.5(|\mathsf{A}_i|^2|e|^2 + |\mathsf{L}_i(x - \bar{x}\mathbf{1})|^2)$ and $J_i = 0$. Figure 4.3 depicts the underlying communication network and state trajectories of agents achieving consensus and Fig. 4.5 shows the corresponding inter-event times for the case of active sensing.

4.5.1 Analysis

First, we compare the two dynamic ETMs discussed in this work, namely, (4.11) and (4.18). For this, we use two metrics, denoted by M1 and M2, which are defined as follows:

M1 $\frac{\langle \mathsf{n}(\{t_l^i\})\rangle}{\langle \mathsf{n}(\{s_k^i\})\rangle}\%$: the percentage of events triggered over the total number of event-verifying instants involved where $\langle \mathsf{n}(\mathcal{T})\rangle$ represents the cardinality

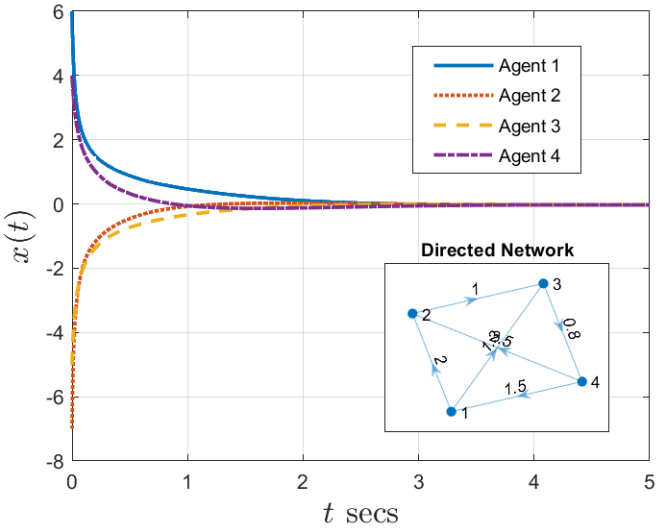

Figure 4.3: Consensus in directed network

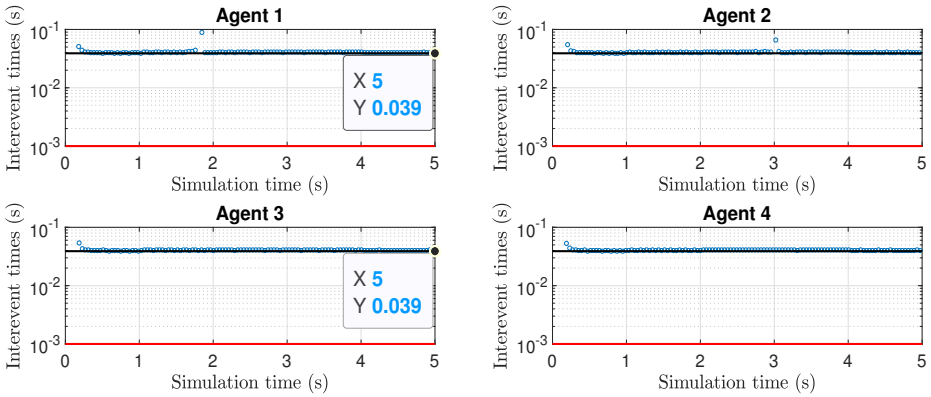

Figure 4.4: Inter-event times of agents in undirected networks

of set $\mathcal{T}$ averaged across all agents;

M2 $t_{\text{lb-IET}}$: the lower-bound of inter-event time, measured in ms, across all agents over the simulation time, namely, $t_{\text{lb-IET}} = \min_{i,l}(t^i_{l+1} - t^i_l)$.

Table 4.1 provides a comparison between the two ETMs described in Section 4.3. For each network topology (undirected or directed) the comparison is made over three different sampling periods denoted by $\bar{T}_{\text{m}} = \min_i T^i_0(\lambda_i)$. It can be inferred from Table 4.1 that for each $\bar{T}_{\text{m}}$, the percentage of events, M1, is fewer in the case where agents can actively sense neighbors' (relative)

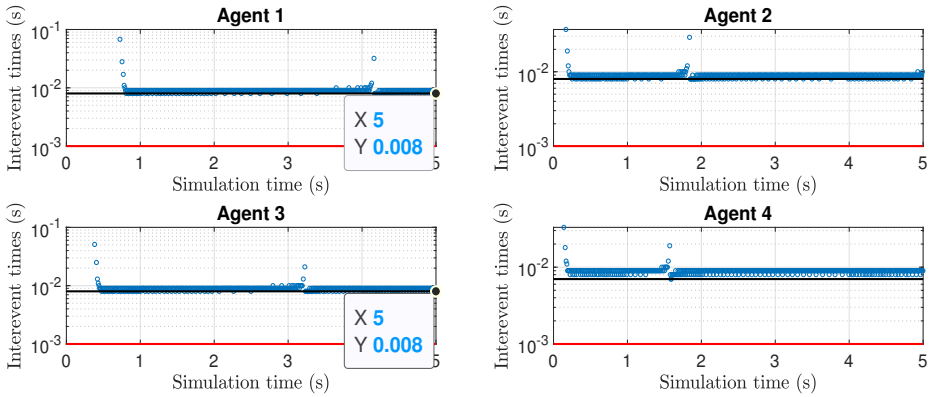

Figure 4.5: Inter-event times of agents in directed networks

information. This implies that the percentage of broadcasts, and as a result, the no. of controller updates an agent requires is considerably lower (particularly in the case of directed networks, see Table 4.1) than in the scenario where it solely relies on broadcasted information. Alongside M1, the metric M2 describing lower-bound of inter-event times is also of considerable importance, particularly for implementation, because this governs the frequency at which broadcasts and controller updates take place. From Table 4.1 it can also be inferred that when agents have access to more information (referring to ETMs in (4.38), (4.40)), the frequency of broadcasts/controller updates is lowered significantly.

Next, we evaluate the dynamic ETM in (4.11) and (4.18) against the static ETM (similar to the one in [100]). Note that the static ETM in [100] is designed for networked control systems and cannot be used directly in our context. However, for comparative purposes we adopt the following two static ETMs, one for each broadcast topology: (i) for undirected networks

$$\begin{aligned} t_{k+1}^i = &\{t > t_k^i | t \in \{s_k^i\}_{k=0}^{\infty},\ 133.5(\theta_i(\tau_i) - 1.51)|e_i|^2 \\ &+ 9.19 \times 10^{-6}|\mathsf{L}_i x|^2 < 0\},\ \forall i \in \mathcal{V}; \end{aligned} \tag{4.41}$$

Network Topology	$\bar{T}_m$	ETMs	Metrics	
			M1	M2
Undirected	1 ms	(4.37)	9.51	9
		(4.38)	2.39	39
		(4.41)	97.0	1
Directed	1 ms	(4.39)	12.73	6
		(4.40)	10.44	8
		(4.42)	92.4	1

Table 4.2: Comparison between static and dynamic ETMs.

and (ii) for directed networks

$$t_{k+1}^i = \{t > t_k^i | t \in \{s_k^i\}_{k=0}^{\infty},\ 211.7(\theta_i(\tau_i) - 1.44)|e_i|^2 + 1.7 \times 10^{-5}|\mathsf{L}_i x|^2 < 0\},\ \forall i \in \mathcal{V}. \tag{4.42}$$

Table 4.2 provides a comparison between static and dynamic ETMs for both network topologies. It can be inferred from Table 4.2 that the dynamic ETMs perform considerably better than their static counterparts, both in undirected and directed network topologies.

4.6 Conclusion

In this work, we proposed two design methodologies, based on the agent's ability (or inability) to actively sense the states or relative states of agents, for periodic event-triggered control of nonlinear multi-agent systems via dynamic event-triggering mechanisms. The general MAS was modeled using a hybrid systems framework after assuming the knowledge of a state-feedback controller that stabilizes the continuous-time MAS. Maximum allowable sampling periods and dynamics of the ETMs were obtained as a consequence of the stability results provided. To demonstrate the utility of the design procedures, two case studies of consensus in nonlinear control-affine MASs with both undirected and directed communication topologies were studied. Subsequently, an illustrative example was considered to convey the effectiveness of

the two dynamic ETMs. Future work would aim at extending the research to systems with different broadcasting capabilities.

Chapter 5

Dynamic Event-Triggered Consensus of Nonlinear MASs with Quantized Broadcasts[1]

Information exchange among agents operating over a network, in practice, is restrained by limited communication bandwidth; this concern is often addressed by employing quantized broadcasts. In this chapter, we study the problem of consensus of nonlinear MASs over a directed network where the agents employ: a) encoders that quantize relevant information prior to broadcasting, and b) decoders that process this information upon arrival. The decision on the broadcast instant itself is made with the help of a dynamic ETM in that the agents evaluate their respective event-triggering conditions intermittently at pre-designed sampling instants (which may be both aperiodic and asynchronous). Subsequently, the agents utilize model-based propagates of the decoded neighbor states in their control protocols to achieve consensus. The overall MAS is modeled using the hybrid systems framework and the results are demonstrated through an illustrative example.

The rest of this chapter is organized as follows. Section 5.1 presents preliminaries specific to this chapter. Section 5.2 discusses the problem and introduces some intermediate variables such as encoded and decoded states.

[1]The material in this chapter has been accepted for publication as: Mani H. Dhullipalla, Hao Yu and Tongwen Chen. Event-triggered consensus of nonlinear agents with quantized broadcasts: A hybrid systems approach. *22nd IFAC World Congress*, Japan, July 2023.

Subsequently, the hybrid dynamics of the overall system is formulated and the main results are presented in Section 5.3. Finally, a numerical example is simulated in Section 5.4 followed by concluding remarks made in Section 5.5.

5.1 Preliminaries

In addition to preliminaries introduced in Section 4.1 of Chapter 4, in this section, we introduce the concept of uniform quantizer. A uniform quantizer $\mathfrak{q} : \mathbb{R} \to \mathbb{R}$ is defined as:

$$\mathfrak{q}(x) = \Delta \Big\lfloor \frac{x}{\Delta} + \frac{1}{2} \Big\rfloor,$$

where $\Delta > 0$ is called the quantizer gain. The quantization error $\mathfrak{q}(x) - x$ is such that $|\mathfrak{q}(x) - x| \leq \frac{\Delta}{2}$ for all $x \in \mathbb{R}$. In this work, we use the quantizer to establish the hybrid dynamics of the overall system; therefore, we define a set-valued (outer semicontinuous) quantizer mapping $\mathfrak{q}_{\text{osc}}(x) : \mathbb{R} \to \mathbb{R}$ as follows:

$$\mathfrak{q}_{\text{osc}}(x) = \begin{cases} m\Delta, & m - \frac{1}{2} < \frac{x}{\Delta} < m + \frac{1}{2}, \\ \Big\{ m\Delta, (m+1)\Delta \Big\}, & x = \Big(m + \frac{1}{2} \Big)\Delta, \end{cases} \tag{5.1}$$

where $m \in \mathbb{Z}$. For $x \in \mathbb{R}^n$, the quantizer $\mathfrak{q}_{\text{osc}}(x)$ operates element-wise and the quantization error is upper-bounded as $|\mathfrak{q}_{\text{osc}}(x) - x| \leq \frac{\Delta}{2}\sqrt{n}$.

5.2 Problem Formulation

5.2.1 The Problem

Consider that each agent in a directed network $\mathcal{G} := (\mathcal{V}, \mathcal{E})$ has the following agent dynamics:

$$\dot{x}_i = f(x_i) + u_i, \ \forall i \in \mathcal{V}, \tag{5.2}$$

where $x_i \in \mathbb{R}^n$ is the agent state and $u_i \in \mathbb{R}^n$ is the control protocol. Assume that the unforced dynamics, namely, $f(\cdot) : \mathbb{R}^n \to \mathbb{R}^n$ in (5.2), is a globally one-sided Lipschitz continuous function with a one-sided Lipschitz constant

$\mathcal{L}_{os} \in \mathbb{R}$. The distributed control protocol employed by the MAS in (5.2) is given by

$$u_i = -\kappa \sum_{j \in \mathcal{N}_{\text{in}}^i} \mathsf{a}_{ij}(x_i - x_j),\ \forall i \in \mathcal{V}. \tag{5.3}$$

Since we adopt an emulation-based approach in this chapter, we assume that the control gain κ in (5.3) is large enough to achieve consensus. The following lemma is a result from [116] which addresses this aspect.

Lemma 5.1. *([116]) The MAS in* (5.2) *with the control input in* (5.3) *can achieve global consensus if*

$$a_\xi(\mathsf{L})\kappa > \mathcal{L}_{os}, \tag{5.4}$$

where $a_\xi(\mathsf{L})$ *is the general algebraic connectivity of* L.

Note that $a_\xi(\mathsf{L})$ and ξ are described in Section 4.1 of Chapter 4.

5.2.2 Intermediate Variables

In order to implement an event-based controller that is inherently Zeno-free, we formulate the consensus problem in Section 5.2.1 using the hybrid systems framework. To facilitate this, in this subsection, we define several intermediate variables and, with their aid, present hybrid dynamics of the MAS in Section 5.3.1.

First, we define two time sequences, namely, sampling sequence and event-triggering sequence. For each agent $i \in \mathcal{V}$, let $\{s_k^i\}_{k=0}^\infty$ denote the sampling sequence such that

$$\varepsilon^i \leq s_{k+1}^i - s_k^i \leq T^i, \forall k \in \mathbb{Z}_{\geq 0}, \tag{5.5}$$

where ε^i is an arbitrarily small positive constant and T^i is the to-be-designed upper bound on the sampling interval $s_{k+1}^i - s_k^i$. The event-triggering sequence $\{t_l^i\}_{l=0}^\infty$ is a subsequence of $\{s_k^i\}_{k=0}^\infty$ whose construction is determined by the event-triggering condition which is discussed shortly. The idea is that each agent evaluates the event-triggering condition at $\{s_k^i\}$ and a subset of these instants, that satisfy the event-triggering condition, are referred to as

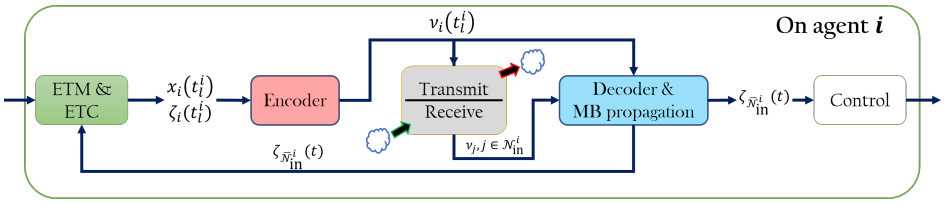

Figure 5.1: An illustration of the encoder and decoder modules on every agent $i \in \mathcal{V}$.

event-triggered instants, namely, $\{t_l^i\}$. In the scenario that $\{t_l^i\} = \{s_k^i\}, \forall i \in \mathcal{V}$, and $\forall l, k \in \mathbb{Z}_{\geq 0}$, the event-triggered protocol reduces to a sampled-data protocol.

To have control over the size of packets (i.e., the number of bits per broadcast) that are broadcasted over the network, we assume that each agent broadcasts information via a uniform quantizer. To accomplish this and achieve asymptotic stability, each agent employs: i) an encoder that manipulates local state and quantizes information, ii) decoders that process information received from $j \in \mathcal{N}_{\text{in}}^i$, and iii) a global multiplier $\mathfrak{m}$ that operates with the knowledge of global time, see Fig. 5.1 for an illustration. The definition and hybrid dynamics of the variables involved is as follows. First, each agent $i \in \mathcal{V}$ employs an encoder and broadcasts the encoded state $\nu_i \in \mathbb{R}^n$ to its out-neighbors. The hybrid dynamics of the ν_i is as follows:

$$\begin{cases} \dot{\nu}_i = \mathbf{0}, & t \in [t_l^i, t_{l+1}^i), \\ \nu_i^+ = \nu_i, & t \in \{s_k^i\} \setminus \{t_l^i\}, \\ \nu_i^+ = \mathfrak{q}_{\text{osc}}\left(\frac{x_i - \zeta_i}{\mathfrak{m}}\right), & t \in \{t_l^i\}. \end{cases} \tag{5.6}$$

Second, upon receiving ν_i, agent i and its out-neighbors employ decoders and propagate the decoded state $\zeta_i \in \mathbb{R}^n$ via the following hybrid dynamics:

$$\begin{cases} \dot{\zeta}_i = f(\zeta_i), & t \in [t_l^i, t_{l+1}^i), \\ \zeta_i^+ = \zeta_i, & t \in \{s_k^i\} \setminus \{t_l^i\}, \\ \zeta_i^+ = \zeta_i + \mathfrak{m}\mathfrak{q}_{\text{osc}}\left(\frac{x_i - \zeta_i}{\mathfrak{m}}\right), & t \in \{t_l^i\}. \end{cases} \tag{5.7}$$

where $\zeta_i(0) = \mathbf{0}$. For notational convenience, in (5.6) and (5.7), we implicitly assume that all agents in $\mathcal{V}$ employ the uniform quantizer defined in (5.1); however, the approach in this chapter readily extends to the case where each

agent employs a different uniform quantizer (i.e., with quantization gain Δ_i) for encoding and decoding operations. As a consequence, since each out-neighbor of i employs the same hybrid dynamics for the decoded state, ζ_i is identical across its out-neighbors. Let $\zeta \in \mathbb{R}^{nN}$ denote the concatenation of the decoded states. Finally, the dynamics of the multiplier $\mathfrak{m} \in \mathbb{R}_{\geq 0}$ is as follows:

$$\begin{cases} \dot{\mathfrak{m}} = -\alpha_{\mathfrak{m}} \mathfrak{m}, \quad \forall t \in [0, \infty) \end{cases} \tag{5.8}$$

where the decay rate $\alpha_{\mathfrak{m}}$ and the initial condition $\mathfrak{m}(t = 0)$ are both positive and identical across all agents (global information). To evaluate $\mathfrak{m}$, the agents must be aware of the global time elapsed which is captured by t.

Using the model-based decoded state ζ, each agent in $\mathcal{V}$ employs an event-triggered implementation of the control protocol in (5.3) given by

$$u_i = -\kappa \sum_{j \in \mathcal{N}_{\text{in}}^i} \mathsf{a}_{ij}(\zeta_i - \zeta_j) = -\kappa(\mathsf{L}_i \otimes \mathbb{I}_n)\zeta. \tag{5.9}$$

Prior to designing the event-triggering condition, we define a non-negative auxiliary variable $\eta_i \in \mathbb{R}_{\geq 0}, \forall i \in \mathcal{V}$. The dynamics of η_i is described using hybrid system framework as follows:

$$\dot{\eta}_i = f_\eta^i(\eta_i, \zeta_{\bar{\mathcal{N}}^i}), \quad t \in [s_k^i, s_{k+1}^i), \tag{5.10a}$$

$$\eta_i^+ = g_s^i(\eta_i, e_i), \quad t \in \{s_k^i\} \setminus \{t_l^i\}, \tag{5.10b}$$

$$\eta_i^+ = g_t^i(\eta_i, e_i), \quad t \in \{t_l^i\}, \tag{5.10c}$$

where $e_i = \zeta_i - x_i$ is the network-induced quantized error, $\zeta_{\bar{\mathcal{N}}^i} := (\bar{\mathsf{A}}_i \otimes \mathbb{I}_n)\zeta$, $\bar{\mathsf{A}}_i = \mathtt{diag}(\{\mathsf{a}_j | \mathsf{a}_j = 1, \forall j \in \mathcal{N}_{\text{in}}^i \cup \{i\}; \text{otherwise, } \mathsf{a}_j = 0\})$. In (5.10), for each agent $i \in \mathcal{V}$, we assume that $f_\eta^i : \mathbb{R}_{\geq 0} \times \mathbb{R}^{nN} \to \mathbb{R}$ is a continuous function such that $f_\eta^i(0, \cdot) \geq 0$ and, for any initial state $\eta_{i,0}$ and for any bounded $\zeta_{\bar{\mathcal{N}}^i}$, the solution to $\dot{\eta}_i = f_\eta^i(\eta_i, \zeta_{\bar{\mathcal{N}}^i})$ is complete. Furthermore, the functions $g_s^i : \mathbb{R}_{\geq 0} \times \mathbb{R}^n \to \mathbb{R}$ and $g_t^i : \mathbb{R}_{\geq 0} \times \mathbb{R}^n \to \mathbb{R}_{\geq 0}$ are continuous and continuous non-negative, respectively. An argument to show non-negativeness of η_i under the (aforementioned) mild assumptions made on functions f_η^i, g_s^i, g_t^i is provided

in [18]. With the help of hybrid dynamics of η_i, for each agent $i \in \mathcal{V}$, the event-triggering condition (consequently, event-triggering instant) is defined as follows:

$$t_{k+1}^i = \{t > t_k^i | t \in \{s_k^i\}_{k=0}^{\infty},\ g_s^i(\cdot,\cdot) < 0\}. \tag{5.11}$$

For completeness of the exposition, we state the hybrid dynamics of the network-induced quantized error e_i as follows:

$$\begin{cases} \dot{e}_i = f(\zeta_i) - f(x_i) + \kappa(\mathsf{L}_i \otimes \mathbb{I}_n)\zeta, & \\ e_i^+ = e_i, & t \in \{s_k^i\} \setminus \{t_l^i\}, \\ e_i^+ = e_i - \mathfrak{m}\mathfrak{q}_{\text{osc}}\big(\frac{e_i}{\mathfrak{m}}\big), & t \in \{t_l^i\}. \end{cases} \tag{5.12}$$

Let $e \in \mathbb{R}^{nN}$ denote the concatenation of errors e_i. Furthermore, each agent in $\mathcal{V}$ also needs to keep track of time elapsed since the last sampling instant in order to check for inequalities in (5.5). For this, we define the timer variable $\tau_i, \forall i \in \mathcal{V}$. Its dynamics is governed by:

$$\begin{cases} \dot{\tau}_i \quad = 1 \ \text{ when } \ \tau_i \in [0, T^i], \\ \tau_i^+ \quad = 0 \ \text{ when } \ \tau \in [\varepsilon^i, T^i]. \end{cases} \tag{5.13}$$

Let τ be a concatenation of all the timer variables.

5.3 Consensus via Quantized Broadcasts

In this section, we present the hybrid dynamics of the MAS using variables defined in Section 5.2.2 and subsequently present the result on event-triggered consensus.

5.3.1 Hybrid Dynamics

Let $q = (x, e, \zeta, \tau, \eta, \mathfrak{m}, t)$ denote the augmented state that represents the overall MAS which operates with quantized communication and event-based broadcast protocol. The hybrid dynamics of q is expressed as follows:

$$\begin{cases} \dot{q} = F(q), & q \in C, \\ q^+ \in \bigcup_{i=1}^N G_i(q), & q \in D, \end{cases} \tag{5.14}$$

where the flow set C and jump set D are defined as:

$$C = \mathbb{R}^{3nN} \times [0, T^1] \times \cdots \times [0, T^N] \times \mathbb{R}^N_{\geq 0} \times \mathbb{R}^2_{\geq 0},$$
$$D = \bigcup_{i=1}^{N} \Big\{ \mathbb{R}^{3nN} \times [\varepsilon^1, T^1] \times \cdots \times [\varepsilon^N, T^N] \times \mathbb{R}^N_{\geq 0} \times \mathbb{R}^2_{\geq 0} \Big\}.$$

The function $F(q)$ in (5.14) is as follows:

$$F(q) = \begin{bmatrix} [f](x) - \kappa(\mathsf{L} \otimes \mathbb{I}_n)(x+e) \\ [f](\zeta) - [\bar{f}](x) + \kappa(\mathsf{L} \otimes \mathbb{I}_n)(x+e) \\ [f](\zeta) \\ \mathbf{1} \\ f_\eta \\ -\alpha_{\mathfrak{m}} \mathfrak{m} \\ 1 \end{bmatrix}, \tag{5.15}$$

where $[f](x) = [(f(x_1))^{\mathrm{T}} \cdots (f(x_N))^{\mathrm{T}}]^{\mathrm{T}}$ denotes the augmented vector of functions f operating on x, and the set-valued jump mapping $G_i(q)$ is

$$G_i(q) := \begin{cases} \begin{cases} \{G_i^1\}, & g_s^i > 0, \\ \{G_i^2\}, & g_s^i < 0, \\ \{G_i^1,\ G_i^2\}, & g_s^i = 0, \end{cases} & \tau_i \in [\varepsilon^i, T^i], \\ \phi & \tau_i \notin [\varepsilon^i, T^i], \end{cases} \tag{5.16}$$

where ϕ is a null set,

$$G_i^1 := \begin{bmatrix} x^{\mathrm{T}} & e^{\mathrm{T}} & \zeta^{\mathrm{T}} & (\mathcal{I}_i \mathbf{1})^{\mathrm{T}} & (\mathcal{I}_i \eta + \bar{g}_s^i)^{\mathrm{T}} & \mathfrak{m} & t \end{bmatrix}^{\mathrm{T}},$$
$$G_i^2 := \begin{bmatrix} x^{\mathrm{T}} & (\bar{e}_i)^{\mathrm{T}} & (\bar{\zeta}_i)^{\mathrm{T}} & (\mathcal{I}_i \mathbf{1})^{\mathrm{T}} & (\mathcal{I}_i \eta + \bar{g}_t^i)^{\mathrm{T}} & \mathfrak{m} & t \end{bmatrix}^{\mathrm{T}},$$

$\bar{e}_i = e - \mathfrak{m}(\bar{\mathcal{I}}_i \otimes \mathbb{I}_n)\mathfrak{q}_{\mathrm{osc}}(\frac{e}{\mathfrak{m}})$, $\bar{\zeta}_i = \zeta + \mathfrak{m}(\bar{\mathcal{I}}_i \otimes \mathbb{I}_n)\mathfrak{q}_{\mathrm{osc}}(\frac{e}{\mathfrak{m}})$, $\mathcal{I}_i := \mathtt{diag}(\{1, .., 0, .., 1\}_{N \times 1})$ with 0 at the i-th place, $\bar{\mathcal{I}}_i := \mathbb{I}_N - \mathcal{I}_i$ with 1 at the i-th place, $\bar{g}_s^i := [0 \cdots g_s^i \cdots 0]^{\mathrm{T}}$ and $\bar{g}_t^i := [0 \cdots g_t^i \cdots 0]^{\mathrm{T}}$.

From the definition of flow and jump maps in (5.14), it is straightforward to verify that they are both outer semi-continuous mappings. We also note that the sets C and D in (5.14) are closed subsets. These properties of the hybrid system in (5.14) ensure that it is nominally well-posed, see Chapter 6 in [31] for details.

5.3.2 Consensus

In this subsection, we first define a decaying parameter θ_i through which MASP can be computed for each agent in $\mathcal{V}$ and subsequently present the theorem for event-triggered consensus which describes the dynamics of the ETM.

θ_i is defined using the following lemma from [69].

Lemma 5.2 ([69]). *Let $\theta_i : \mathbb{R}_{\geq 0} \to \mathbb{R}$ be the solution to the differential equation*

$$\dot{\theta}_i(s) = \begin{cases} -2L_\mu^i \theta_i(s) - \gamma_i(\theta_i^2(s)+1), & s \in [0, T_0^i(\lambda_i)] \\ 0, & s > T_0^i(\lambda_i) \end{cases},$$

with the initial condition $\theta_i(0) = \frac{1}{\lambda_i}$, where $L_\mu^i = L_i + \mu_i$, $\mu_i > 0$ is arbitrarily small constant, and γ_i is the error gain. Then, $\theta_i(s)$ is monotonically decreasing and $T_0^i(\lambda_i)$ is such that $\theta_i(s) = \lambda_i$ for $s \geq T_0^i(\lambda_i)$.

Here, $\lambda_i \in (0,1)$ is a design parameter that influences both the MASP and the ETM (namely, hybrid dynamics in (5.17)). By choosing appropriate parameters such as λ_i, μ_i for each agent i, the upper bound $T^i \leq T_0^i(\lambda_i)$ can be determined using (28) in [69]. Furthermore, L_i in Lemma 5.2 is defined in (A.14) and depends on $\mathcal{L}_{os}$, control gain κ, and in-degree d_i.

The main result of this chapter is stated as below and the proof is presented in Appendix A.2.1.

Theorem 5.1. *For the MAS in* (5.14)*, if the upper bound on sampling interval (defined in* (5.5)*) is given by $T_0^i(\lambda_i)$ stated in Lemma 5.2, and if the dynamic ETM governed by* (5.10) *is such that $\forall i \in \mathcal{V}$ we have:*

$$\begin{aligned} f_\eta^i &= -\beta_i \eta_i + \frac{\vartheta}{2}|\mathsf{L}_i \zeta|^2, \\ g_s^i &= \eta_i + \gamma_i\Big(\lambda_i - \frac{1}{\lambda_i}\Big)|e_i|^2, \\ g_t^i &= \eta_i + \gamma_i \lambda_i |e_i|^2, \end{aligned} \tag{5.17}$$

where $\beta_i > 0$, $\vartheta \geq 0$, $\lambda_i \in (0,1)$,

$$\begin{aligned}
\gamma_i^2 \geq\ & K\kappa\frac{\epsilon_1\bar{\Lambda}_M^2}{2} + 2\kappa^2\mathrm{Tr}(\mathsf{A}^T\mathsf{A}) + \vartheta\mathrm{Tr}(\mathsf{L}^T\mathsf{L}),\\
K >\ & \frac{2\gamma + 4\kappa^2}{\xi_{min}}\mathrm{Tr}(\mathsf{L}^T\mathsf{L})/\Big[2(a_\xi(\mathsf{L})\kappa - \mathcal{L}_{os}) - \frac{\kappa}{\epsilon_1}\Big],\\
\epsilon_1 \in\ & \Big(\frac{1}{2a_\xi(\mathsf{L})}\frac{\bar{\mathfrak{p}}}{\bar{\mathfrak{p}}-1}, \infty\Big),
\end{aligned} \tag{5.18}$$

and the control gain $\kappa = \bar{\mathfrak{p}}\frac{\mathcal{L}_{os}}{a_\xi(\mathsf{L})}$, $\bar{\mathfrak{p}} > 1$, *then, the closed-loop system in* (5.14) *is asymptotically stable w.r.t. the consensus set*

$$\{x \in \mathbb{R}^{nN} \mid \big(\big(I_N - \mathbf{1}_N\xi^T\big) \otimes I_n\big)x = \mathbf{0}\}. \tag{5.19}$$

Through the following remarks we discuss our results in comparison with the results in [115].

Remark 5.1. *By adopting the framework discussed in [18], in this chapter, we show that the computation of MASP (via Lemma 5.2) can be made independent of the nature of broadcasts (namely, exact state broadcasts in [18] or quantized information broadcasts in this chapter). However, the study in [115] differs in this respect; in [115], the computation of MASP was dependent on the nature of broadcasts and appeared to be more conservative for the case of quantized broadcasts, see (23) and (35) in [115]. In this context, see Table 5.1 in Section 5.4.*

Remark 5.2. *Second, we note that [115] presented results associated with consensus of Lipschitz nonlinear dynamics over undirected graphs with periodic sampling. It is worth mentioning that [115] did remark that their work could be extended to the case of aperiodic sampling but offered no further analysis in this context. On the contrary, in this work we present results for agents with continuous one-sided Lipschitz dynamics over directed graphs with aperiodic sampling by adopting the framework discussed in [18].*

Remark 5.3. *Next, the ETM in [115] is dependent on the difference between model-based propagation of the true state* x_i, *say* $\hat{x}_i$, *and the true state* x_i.

This implies that in addition to the agent modeling the decoded states of itself and its neighbors, it must also evaluate $\hat{x}_i$ to evaluate the event-triggering condition, see (25) in [115]. Unlike [115], the ETM in this work is governed by the functions in (5.17) *in Theorem 5.1 which are solely dependent on the error $e_i = \zeta_i - x_i$, eliminating the need to model $\hat{x}_i$.*

5.4 Numerical Example

In this section, we present an illustration of our results by borrowing the numerical example from [18]. We consider that each agent in the network adopts the following dynamics:

$$\forall i \in \mathcal{V}, \quad \begin{cases} \dot{x}_i = -x_i^3 + 0.1\sin(x_i) + u_i, \\ u_i = -\kappa \mathsf{L}_i x, \kappa = 0.5, \end{cases} \tag{5.20}$$

over a directed network whose graph Laplacian L is given by:

$$\mathsf{L} = \begin{bmatrix} 2 & 0 & 0 & -2 \\ -1.3 & 2.3 & 0 & -1 \\ -0.8 & -1.5 & 2.3 & 0 \\ 0 & 0 & -2.5 & 2.5 \end{bmatrix}. \tag{5.21}$$

Notice that $f(x_i) = -x_i^3 + 0.1\sin(x_i)$ in (5.20) is not globally Lipschitz but is globally one-sided Lipschitz with one-sided Lipschitz constant $\mathcal{L}_{os} = 0.1$. Here, $\kappa = 0.5$ in (5.20) satisfies the inequality in Lemma 5.1. The event-triggered control protocol that uses the broadcast information is $u_i = -\kappa \mathsf{L}_i \zeta$. For the MAS in (5.20), we set the lower bound of sampling period, ε^i in (5.5), to be 1 ms, the time step for flow computation to be 0.1 ms and the total simulation time to be 20 s. Figure 5.2 depicts the consensus of agent states when the quantizer gain $\Delta = 0.5$ and $\alpha_{\mathtt{m}} = \beta_i = 0.1$.

Next, we compare our approach in this work (and its predecessor in [18]) against the work in [115] in terms of the following two aspects: a) the MASP $:= \max_{\lambda_i \in (0,1)} T_0^i(\lambda_i)$, and b) the performance of ETM in the case of quantized broadcasting. For brevity, we label [115] as R_1, [18] as R_2 and the work in this chapter as R_3 in Tables 5.1 and 5.2. We observed that the MASP computation in [115] may result in slightly conservative bounds compared to this work

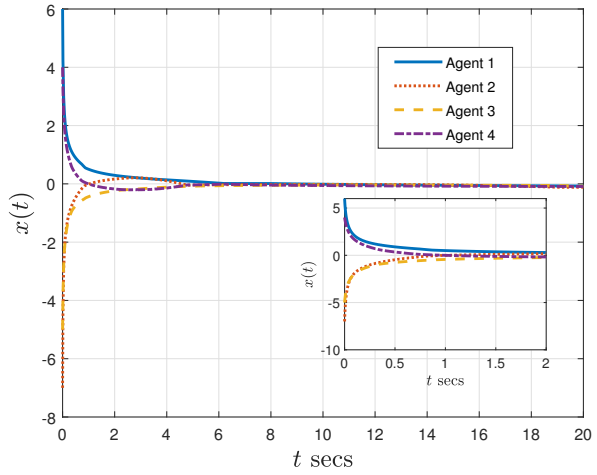

Figure 5.2: Consensus with $\Delta = 0.5$ and $\alpha_{\mathfrak{m}} = 0.1$.

(or [18]); this is due to the way the error gain γ in [115] was computed, see Table 5.1. Table 5.1 also offers a comparison between the two ETMs, namely, the one in [115] and the one governed by (5.17) in this chapter.

Table 5.2 depicts the comparison in terms of percentage of events (averaged across all agents over simulation time of 20 s) for various λ_i which affect the choice of the chosen sampling period $\bar{T}_{\mathrm{m}}$ as follows $\bar{T}_{\mathrm{m}} \leq \min_i T_0^i(\lambda_i)$. Here, we compare the performance of [18] against this work by varying design parameters $(\alpha_{\mathfrak{m}}, \Delta)$ associated with the global multiplier $\mathfrak{m}$ and the quantizer $\mathfrak{q}_{\mathrm{osc}}$. It can be seen that for a given $\alpha_{\mathfrak{m}}$, smaller Δ results in fewer events. For this simulation example, we have also observed that as long as $\alpha_{\mathfrak{m}} \leq \beta_i$, the quantization levels, determined by the values of $\mathfrak{q}(e_i/\mathfrak{m})$, were bounded below 1; however, unlike [115], in this chapter no theoretical bounds on the quantization range are presented.

5.5 Conclusion

In this chapter, we studied the event-triggered consensus of nonlinear agents (with one-sided Lipschitz dynamics) that interact over static directed networks through quantized broadcasts. We addressed this problem by modeling the MAS using the hybrid systems framework wherein the sampling and

	MASP	Chosen $\bar{T}_m$	Percentage of events $(\alpha_{\mathtt{m}}, \Delta)$	
	(in ms)		$(0.1, 0.01)$	$(0.05, 0.01)$
R_1	1.6	1 ms	11.11	11.11
R_2	4.4		–	–
R_3	4.4		15.88	19.19

Table 5.1: Performance comparison between R_1: [115], R_2: [18] and R_3: this work.

λ_i	$\bar{T}_{\mathrm{m}}$ (ms)	Percentage of events			
		R_2	R_3 with $(\alpha_{\mathtt{m}}, \Delta)$		
			$(0.1, 0.1)$	$(0.1, 0.01)$	$(0.05, 0.01)$
0.69	1	13.37	46.32	15.88	19.19
0.45	2	28.60	71.14	24.66	30.14
0.25	3	46.25	85.09	30.55	39.25

Table 5.2: Performance comparison of the ETM with and without quantized broadcasts.

events instants are characterized as jumps in the overall system. As a consequence of establishing stability of the overall hybrid system, we obtained the MASP and the dynamics of the ETM. Through an illustrative example we convey the effectiveness of the ETM and provide a comparative study against existing research. Our future work in this direction would focus on estimating the quantization range necessary to avoid saturation.

Chapter 6

Sampled-Data Control of Nonlinear MASs prone to Transmission Delays[1]

In this chapter, we consider the problem of distributed control of nonlinear MASs where the information broadcasts over a network are susceptible to one type of imperfection, namely, transmission delays. The design methodology employed is such that the sampling instants (at which agents broadcast information) could be both aperiodic and asynchronous in nature. The broadcasts, upon arrival, are propagated by the agents through dynamical models and these propagates are used in their control protocols. The overall MAS is formulated as a hybrid dynamical system whose stability governs the upper bounds on: a) the sampling interval, namely, the duration between two consecutive broadcasts, and b) the transmission delays that the broadcasts might be prone to. Finally, through a case study on the consensus of Lipschitz nonlinear agents we demonstrate the effectiveness of the proposed methodology.

The chapter is organized as follows. The problem is formulated in Section 6.1 followed by its hybrid systems model which is presented in Section 6.2. The main results are discussed in Section 6.3 and its effectiveness is demonstrated via a case study in 6.4. Finally, concluding remarks are stated in Section 6.5.

[1]The material in this chapter was submitted for publication as: Mani H. Dhullipalla, Hao Yu and Tongwen Chen. Distributed control under transmission delays: a model-based hybrid systems approach. *IEEE Transactions on Automatic Control.*

6.1 Problem Formulation

Consider a MAS of N agents interacting over a network $\mathcal{G} = (\mathcal{V}, \mathcal{E})$. Let each agent in $\mathcal{G}$ have the following nonlinear dynamics:

$$\dot{x}_i = f_i(x, u_i), \forall i \in \mathcal{V}, \tag{6.1}$$

where $x_i \in \mathbb{R}^n$ is the agent state, $u_i \in \mathbb{R}^m$ is the control input and x is the concatenation of agent states. Here, the function $f_i : \mathbb{R}^{nN} \times \mathbb{R}^m \to \mathbb{R}^n$ is assumed to be a continuous function. For the MAS in (6.1), we assume that there exists a distributed static state feedback controller, given by

$$u_i = \kappa(x_{\bar{\mathcal{N}}^i_{\text{in}}}), \forall i \in \mathcal{V}, \tag{6.2}$$

that stabilizes it. Here $x_{\bar{\mathcal{N}}^i_{\text{in}}} := (\bar{\mathsf{A}}_i \otimes \mathbb{I}_n)x$ where the diagonal matrix $\bar{\mathsf{A}}_i = \mathtt{diag}(\{\mathsf{a}_j | \mathsf{a}_j = 1, \forall j \in \bar{\mathcal{N}}^i_{\text{in}}; \mathsf{a}_j = 0, \forall j \notin \bar{\mathcal{N}}^i_{\text{in}}\})$ and $\bar{\mathcal{N}}^i_{\text{in}}$ is the index set defined in Section 4.1.

To implement the control protocol in (6.2), agents in the network require continuous access to their neighbor states which is seldom possible in scenarios where a wireless network is employed to accomplish this task. Therefore, in this work, we consider a networked systems approach to implement the aforementioned control protocol u_i over a broadcast network $\mathcal{G}$. For this, it is desired that each agent i broadcasts its full state information x_i at discrete sampling instants s^i_k where $\{s^i_k | s^i_k < s^i_{k+1}\}^\infty_{k=0}$. For every agent $i \in \mathcal{V}$, the sampling interval $s^i_{k+1} - s^i_k$ must satisfy the following two inequalities:

$$\varepsilon^i \leq s^i_{k+1} - s^i_k \leq T^i. \tag{6.3}$$

The lower bound ε^i in (6.3) is an arbitrarily small positive constant that ensures instantaneous Zeno solutions[2] are avoided and, in practice, reflects the physical constraints of hardware devices employed. The upper bound $T^i \geq \varepsilon^i$ in (6.3) is a parameter that is to be designed and, in this work, is referred to as the MASP associated with agent i.

[2]A solution x of hybrid system $\mathcal{H}$ is instantaneous Zeno if it is complete and eventually discrete, see Chapter 2 of this thesis or [31] for technical definitions.

The states, as mentioned earlier, are broadcasted over $\mathcal{G}$ and are likely to suffer from transmission delays. Let $\delta_j^{i,k}$ denote the time interval between when state broadcast is initiated by agent i (say, at s_k^i) and when the state is received by agent $j \in \mathcal{N}_{\text{out}}^i$ (namely, at time $s_k^i + \delta_j^{i,k}$). We consider that the delay, for all agents $i \in \mathcal{V}$, is bounded as follows: $0 \leq \delta_j^{i,k} \leq T_{\text{MAD}}^i, \forall j \in \bar{\mathcal{N}}_{\text{out}}^i$, where $T_{\text{MAD}}^i \leq T^i$ denotes the maximum allowable delay (MAD) associated with broadcasts originating from agent i. Here, note that $\delta_i^{i,k} = 0, \forall i \in \mathcal{V}$, i.e., we assume that any agent $i \in \mathcal{V}$ is immediately aware of its own latest broadcast.

Assumption 6.1. *(Small-delay condition) At every $k \in \mathbb{Z}_{\geq 0}$, each agent $i \in \mathcal{V}$ satisfies*

$$\delta_j^{i,k} \in [0, \min\{T_{MAD}^i, s_{k+1}^i - s_k^i\}], \forall j \in \mathcal{N}_{out}^i.$$

Assumption 6.1 is the so-called small-delay condition. This assumption ensures that any broadcast from agent, say, i, arrives at their out-neighbors: a) in the order that it was broadcasted, and b) it arrives before i initiates its subsequent broadcast.

Subsequently, we consider a model-based approach to propagate the broadcasts that are available to an agent. In this chapter, we assume that the agent, say, j, broadcasts both the state $x_j(s_l^j)$ and the corresponding broadcast instant s_l^j. Let $\hat{x}_j^i$ denote the propagated state of in-neighbor $j \in \mathcal{N}_{\text{in}}^i$ as perceived by i and let $r_i^{j,l} = s_l^j + \delta_i^{j,l}$ denote the arrival time of this state at i. The hybrid dynamics of $\hat{x}_j^i$ is given by:

$$\begin{cases} \dot{\hat{x}}_j^i = \Upsilon_j^i(\hat{x}_j^i), & t \in [r_i^{j,l}, r_i^{j,l+1}), \\ \hat{x}_j^i((r_i^{j,l})^+) = \tilde{x}_j^i(r_i^{j,l}), & t = \{r_i^{j,l}\}, \end{cases} \tag{6.4}$$

where $\Upsilon_j^i : \mathbb{R}^n \to \mathbb{R}^n$ is a continuous function. Here, $\tilde{x}_j^i(r_i^{j,l})$ is assumed to be, instantaneously, computable using the solution $\mathfrak{S}_{\Upsilon_j^i}(\tilde{x}_j^i(0), t_{\text{flow}})$ to the following system:

$$\begin{cases} \dot{\tilde{x}}_j^i = \Upsilon_j^i(\tilde{x}_j^i), & t \in [s_l^j, s_{l+1}^j), \\ \tilde{x}_j^i((s_l^j)^+) = x_j(s_l^j), & t \in \{s_l^j\}. \end{cases} \tag{6.5}$$

In other words, $\tilde{x}_j^i(r_i^{j,l}) = \mathfrak{S}_{\Upsilon_j^i}(x_j(s_l^j), \delta_i^{j,l})$. Let $\hat{x}^i = [(\hat{x}_1^i)^{\mathrm{T}} \cdots (\hat{x}_N^i)^{\mathrm{T}}]^{\mathrm{T}} \in \mathbb{R}^{nN}$ and $\tilde{x}^i = [(\tilde{x}_1^i)^{\mathrm{T}} \cdots (\tilde{x}_N^i)^{\mathrm{T}}]^{\mathrm{T}} \in \mathbb{R}^{nN}$. For the protocols utilizing the available broadcasts directly (i.e., employing ZOH), $\Upsilon_j^i(\cdot) = \mathbf{0}, \forall i, j \in \mathcal{V}$, and $\hat{x}_j^i = \hat{x}_j^k$ where j is the in-neighbor of agents i and k.

Remark 6.1. *(On model-based dynamics) Here, we considered that each agent $j \in \mathcal{V}$ broadcasts both its sampling instant s_l^j and its sampled state $x_j(s_l^j)$; this is often referred to as the time-stamp technique, see [26]. Using this data, the receiving agent $i \in \mathcal{N}_{out}^j$ computes the initial condition of the model-based state $\hat{x}_j^i$ at $r_i^{j,l}$. With the mild assumption that Υ_j^i is continuous, this approach is applicable in the case where the solution to the differential equation: $\dot{\mathsf{x}} = \Upsilon_j^i(\mathsf{x}), \mathsf{x}(t_0) = \mathsf{x}_0$, is easily computable for $t \geq t_0$, for instance, in the case of linear systems as in [54] or, as an example, in the case of single-link robots as in Section 6.4.2.*

Owing to the communication network, each agent i employs the following control protocol:

$$u_i = \kappa(\hat{x}^i_{\bar{\mathcal{N}}_{\mathrm{in}}^i}), \tag{6.6}$$

where $\hat{x}^i_{\bar{\mathcal{N}}_{\mathrm{in}}^i} := (\bar{\mathsf{A}}_i \otimes \mathbb{I}_n)\hat{x}^i$. The primary objective of this work is to determine the pair $(T^i_{\mathrm{MAD}}, T^i), \forall i \in \mathcal{V}$, such that the revised control protocol in (6.6) stabilizes the MAS in (6.1).

6.2 Hybrid Systems Modeling

In this section, we model the MAS in (6.1) using the hybrid systems framework. For this, we define variables both w.r.t. in-neighbors (because u_i in (6.6) is a function of $\hat{x}^i_{\bar{\mathcal{N}}_{\mathrm{in}}^i}$) and out-neighbors (because it facilitates convergence analysis in Section 6.3).

Let $e_i^j(t) = \hat{x}_i^j(t) - x_i(t) \in \mathbb{R}^n, \forall j \in \mathcal{N}_{\mathrm{out}}^i$, denote the network-induced error of agent i as perceived by agent j and let $\tilde{e}_i^j = \tilde{x}_i^j - \hat{x}_i^j \in \mathbb{R}^n, \forall j \in \mathcal{N}_{\mathrm{out}}^i$. Let $e_i^j, \tilde{e}_i^j = \mathbf{0}, \forall j \notin \mathcal{N}_{\mathrm{out}}^i$. Depending on the context, we perceive the quantity e_i^j

as the out-neighbor error for agent i (for some $j \in \mathcal{N}^i_{\text{out}}$) or as the in-neighbor error for agent j (for some $i \in \mathcal{N}^j_{\text{in}}$). Using the model-based estimates in (6.4), the flow dynamics of $e^j_i, \forall j \in \mathcal{N}^i_{\text{out}}$, is

$$\dot{e}^j_i = \Upsilon^j_i(\hat{x}^j_i) - f_i(x_i),\ t \in [r^{i,k}_j, r^{i,k+1}_j), \tag{6.7}$$

where the boundary condition, namely, $e^j_i(r^{i,k}_j)$, is revised via jump dynamics at the arrival instants $r^{i,k}_j$ is as follows:

$$\begin{aligned} e^j_i((r^{i,k}_j)^+) &= \hat{x}^j_i((r^{i,k}_j)^+) - x_i((r^{i,k}_j)^+) \\ &= \tilde{x}^j_i(r^{i,k}_j) - x_i(r^{i,k}_j) \\ &= \tilde{x}^j_i(r^{i,k}_j) - \hat{x}^j_i(r^{i,k}_j) + \hat{x}^j_i(r^{i,k}_j) - x_i(r^{i,k}_j) \\ &= \tilde{e}^j_i(r^{i,k}_j) + e^j_i(r^{i,k}_j). \end{aligned} \tag{6.8}$$

Next, we examine the hybrid dynamics of $\tilde{e}^j_i$. The flow dynamics of $\tilde{e}^j_i$ is as follows:

$$\dot{\tilde{e}}^j_i = \Upsilon^j_i(\tilde{x}^j_i) - \Upsilon^j_i(\hat{x}^j_i). \tag{6.9}$$

Because $\tilde{x}^j_i$ and $\hat{x}^j_i$ jump at instants s^i_k and $r^{i,k}_l$, respectively, we examine jump dynamics at both these instants. First, jump at a broadcast instant on i, namely, at s^i_k:

$$\begin{aligned} \tilde{e}^j_i((s^i_k)^+) &= \tilde{x}^j_i((s^i_k)^+) - \hat{x}^j_i((s^i_k)^+) \\ &= x_i(s^i_k) - \hat{x}^j_i(s^i_k) \\ &= -e^j_i(s^i_k). \end{aligned} \tag{6.10}$$

Subsequently, jump at an arrival instant of $(x_i(s^i_k), s^i_k)$ on $j \in \mathcal{N}^i_{\text{out}}$, namely, at $r^{i,k}_j$:

$$\begin{aligned} \tilde{e}^j_i((r^{i,k}_j)^+) &= \tilde{x}^j_i((r^{i,k}_j)^+) - \hat{x}^j_i((r^{i,k}_j)^+) \\ &= \tilde{x}^j_i(r^{i,k}_j) - \tilde{x}^j_i(r^{i,k}_j) \\ &= \mathbf{0}. \end{aligned} \tag{6.11}$$

Next, let $l_i^j \in \{0,1\}$ denote an indicator variable associated with agent i and its out-neighbor $j \in \mathcal{N}_{\text{out}}^i$. If $j \notin \mathcal{N}_{\text{out}}^i$, then $l_i^j = 0$. At s_k^i, when agent i broadcasts data it sets $l_i^j = 1, \forall j \in \mathcal{N}_{\text{out}}^i$. When neighbor j receives this data, the indicator l_i^j is reset to 0. At the next sampling instant s_{k+1}^i, owing to Assumption 6.1, $l_i^j = 0, \forall j \in \mathcal{N}_{\text{out}}^i$; consequently, upon broadcast, the indicator $l_i^j, \forall j \in \mathcal{N}_{\text{out}}^i$, is reset to 1. Without loss of generality, we set $l_i^i = 1, \forall t \in [0, \infty), \forall i \in \mathcal{V}$. In Section 6.3, we will use l_i to construct jumps associated with broadcasted state $x_i(s_k^i)$.

Finally, prior to introducing the hybrid systems model, we define the timer variable τ_i to track the time elapsed since the last sampling instant on agent i. Its dynamics is governed by:

$$\begin{cases} \dot{\tau}_i & = 1 \ \text{ when } \ \tau_i \in [0, T^i], \\ \tau_i^+ & = 0 \ \text{ when } \ \tau \in [\varepsilon^i, T^i]. \end{cases} \tag{6.12}$$

Let τ be the concatenation of all the timer variables.

We present the hybrid dynamics of the overall MAS. Each agent $i \in \mathcal{V}$ is affected by its in-neighbors $j \in \mathcal{N}_{\text{in}}^i$; therefore, the hybrid dynamics of the overall MAS involves the following concatenated variables: for every $i \in \mathcal{V}$, let in-neighbor errors be $e^i = [(e_1^i)^{\mathrm{T}} \cdots (e_N^i)^{\mathrm{T}}]^{\mathrm{T}} \in \mathbb{R}^{nN}$, $\tilde{e}^i = [(\tilde{e}_1^i)^{\mathrm{T}} \cdots (\tilde{e}_N^i)^{\mathrm{T}}]^{\mathrm{T}} \in \mathbb{R}^{nN}$ and in-neighbor indicators be $l^i = [l_1^i, \ldots, l_N^i]^{\mathrm{T}} \in \{0,1\}^N$. Furthermore, let $x = [x_1^{\mathrm{T}} \cdots x_N^{\mathrm{T}}]^{\mathrm{T}} \in \mathbb{R}^{nN}$, $e = [(e^1)^{\mathrm{T}} \cdots (e^N)^{\mathrm{T}}]^{\mathrm{T}} \in \mathbb{R}^{nN^2}$, $\tilde{e} = [(\tilde{e}^1)^{\mathrm{T}} \cdots (\tilde{e}^N)^{\mathrm{T}}]^{\mathrm{T}} \in \mathbb{R}^{nN^2}$, $l_{\text{in}} = [(l^1)^{\mathrm{T}} \cdots (l^N)^{\mathrm{T}}]^{\mathrm{T}} \in \{0,1\}^{N^2}$, $\tau = [\tau_1 \cdots \tau_N]^{\mathrm{T}}$. Then, the hybrid dynamics of $q = (x, e, \tilde{e}, l, \tau)$ is given by:

$$\begin{cases} \dot{q} = F(q), & q \in C \\ q^+ \in G(q), & q \in D \end{cases} \tag{6.13}$$

where flow and jump sets are defined as follows:

$$\begin{aligned} C = & \Big\{ \mathbb{R}^{nN+2nN^2} \times \{0,1\}^{N^2} \times [0, T^1] \times \cdots \times [0, T^N] \\ & \quad | \{ l_i^{\mathrm{T}} \mathbf{1} > 1 \wedge \tau_i \leq T_{\text{MAD}}^i \} \vee \{ l_i^{\mathrm{T}} \mathbf{1} = 1 \wedge \tau_i \leq T^i \}, \forall i \in \mathcal{V} \Big\}, \\ D = & \bigcup_{i \in \mathcal{V}} D_i, \ D_i = \big\{ q \in C | \ \{ l_i^{\mathrm{T}} \mathbf{1} > 1 \wedge \tau_i \leq T_{\text{MAD}}^i \} \\ & \quad \vee \{ l_i^{\mathrm{T}} \mathbf{1} = 1 \wedge \{ \varepsilon^i \leq \tau_i \leq T^i \} \} \big\}, \end{aligned} \tag{6.14}$$

where out-neighbor indicators are concatenated in $l_i = [l_i^1 \cdots l_i^N]^{\mathrm{T}}$. In (6.13), the continuous function $F(q)$ is given by

$$F(q) = \left[f^{\mathrm{T}} \ (\Upsilon_{\hat{x}} - \mathbf{1}_N \otimes f)^{\mathrm{T}} \ (\Upsilon_{\tilde{x}} - \Upsilon_{\hat{x}})^{\mathrm{T}} \ \mathbf{0}^{\mathrm{T}} \ \mathbf{1}^{\mathrm{T}}\right]^{\mathrm{T}}, \tag{6.15}$$

and the set-valued mapping $G(q) = \bigcup_{i \in \mathcal{V}} G_i(q)$,

$$G_i(q) = \begin{cases} & \overbrace{\qquad\qquad}^{i \text{ waiting to broadcast}} \\ G_i^{\mathrm{b}}(q), & \overbrace{l_i^{\mathrm{T}}\mathbf{1} = 1,} \\ G_i^{\mathrm{u}}(q), & \underbrace{l_i^{\mathrm{T}}\mathbf{1} > 1,}_{j \in \mathcal{N}_{\mathrm{out}}^i \text{ awaiting updates}} \end{cases} . \tag{6.16}$$

Note that, in (6.16), the set-valued maps $G_i(q)$ are based $l_i^{\mathrm{T}}\mathbf{1}$ which identifies agents in $\mathcal{N}_{\mathrm{out}}^i$ that are yet to receive broadcasts from i. Here,

$$\begin{aligned}
f &= [f_1^{\mathrm{T}} \cdots f_N^{\mathrm{T}}]^{\mathrm{T}} \in \mathbb{R}^{nN} \\
\Upsilon_{\hat{x}} &= [(\Upsilon_{\hat{x}}^1)^{\mathrm{T}} \cdots (\Upsilon_{\hat{x}}^N)^{\mathrm{T}}]^{\mathrm{T}} \in \mathbb{R}^{nN^2} \\
\Upsilon_{\tilde{x}} &= [(\Upsilon_{\tilde{x}}^1)^{\mathrm{T}} \cdots (\Upsilon_{\tilde{x}}^N)^{\mathrm{T}}]^{\mathrm{T}} \in \mathbb{R}^{nN^2} \\
\Upsilon_{\hat{x}}^i &= [(\Upsilon_1^i(x_1 + e_1^i))^{\mathrm{T}} \cdots (\Upsilon_N^i(x_N + e_N^i))^{\mathrm{T}}]^{\mathrm{T}}, \\
\Upsilon_{\tilde{x}}^i &= [(\Upsilon_1^i(x_1 + e_1^i + \tilde{e}_1^i))^{\mathrm{T}} \cdots (\Upsilon_N^i(x_N + e_N^i + \tilde{e}_N^i))^{\mathrm{T}}]^{\mathrm{T}}, \\
G_i^{\mathrm{b}} &= \left[x^{\mathrm{T}} \ (e - \Gamma_i^e e)^{\mathrm{T}} \ (\tilde{e} - \Gamma_i^{\tilde{e}}(\tilde{e} + e))^{\mathrm{T}} \ (l + \Gamma_i^l \mathbf{1})^{\mathrm{T}} \ (\Gamma_i^\tau \tau)^{\mathrm{T}}\right]^{\mathrm{T}}, \\
G_i^{\mathrm{u}} &= \bigcup_{j \in \mathcal{N}_{\mathrm{out}}^i} G_{ij}^{\mathrm{u}}, \\
G_{ij}^{\mathrm{u}} &= \left[x^{\mathrm{T}} \ (e + \Gamma_{ij}^e \tilde{e})^{\mathrm{T}} \ (\tilde{e} - \Gamma_{ij}^e \tilde{e})^{\mathrm{T}} \ (l - \Gamma_{ij}^l \mathbf{1})^{\mathrm{T}} \ \tau^{\mathrm{T}}\right]^{\mathrm{T}},
\end{aligned} \tag{6.17}$$

where $\Gamma_{\{\}}^{\{\}}$ matrices associated with broadcast jump maps G_i^{b} and update jump maps G_{ij}^{u} are: $\left\{\Gamma_i^e = \Gamma_i \otimes \Gamma_i \otimes \mathbb{I}_n, \Gamma_i^{\tilde{e}} = \hat{\mathsf{A}}_i^{\mathrm{dia}} \otimes \Gamma_i \otimes \mathbb{I}_n, \Gamma_i^l = \hat{\mathsf{A}}_i^{\mathrm{dia}} \otimes \Gamma_i, \Gamma_i^\tau = \mathbb{I}_N - \Gamma_i\right\}$, and $\left\{\Gamma_{ij}^e = \Gamma_j \otimes \Gamma_i \otimes \mathbb{I}_n, \Gamma_{ij}^h = \Gamma_{ij}^e, \Gamma_{ij}^l = \Gamma_j \otimes \Gamma_i\right\}$, respectively. $\Gamma_i \in \mathbb{R}^{N \times N}$ is a diagonal matrix with the i-th diagonal entry 1 and others 0, $\mathbb{I}_n \in \mathbb{R}^{n \times n}$ is identity matrix of dimension n, $l_{\mathrm{in}}^{\mathrm{dia}}$ is the diagonalized matrix of vector l_{in} and $\hat{\mathsf{A}}_i^{\mathrm{dia}} = \bar{\mathsf{A}}_i - \Gamma_i$ ($\bar{\mathsf{A}}_i$ is defined in Section 6.1). We note that the assumptions on continuity of f and Υ, and the construction of $G(q)$, to ensure that the set-valued mapping is outer semicontinuous, allow the hybrid dynamics in (6.13) to be nominally well-posed, see Chapter 6 in [31].

6.3 Main Results

In this section, we make some assumptions on functions associated with the hybrid system and subsequently establish upper-bounds on transmission delays, namely, T^i_{MAD}, and on sampling intervals, namely, T^i, while also ensuring stability.

In this work, jumps in the hybrid system in (6.13) are characterized by observing the changes that are caused by a broadcasted state, say, $x_i(s^i_k)$, on its out-neighbors in $\mathcal{N}^i_{\text{out}}$ rather than observing the changes that are caused by various broadcasted states, sent by the in-neighbors in $\mathcal{N}^i_{\text{in}}$, on i. In other words, the focus is on changes caused by a packet $(s^i_k, x_i(s^i_k))$ and is not on the changes that occur at agent i. Adopting this perspective allows us to, neatly, distinguish between the broadcast instants and update instants (caused by data arrival on out-neighbors). To facilitate this distinction, we define d_i based on l_i:

$$d_i = \begin{cases} 0, & l_i^{\mathrm{T}} \mathbf{1}_i = 1, \\ 1, & l_i^{\mathrm{T}} \mathbf{1}_i > 1. \end{cases} \tag{6.18}$$

When $d_i = 0$, the subsequent jump affecting $(e_i, \tilde{e}_i)$ is because of broadcasting by i; otherwise, the subsequent jump affecting $(e_i, \tilde{e}_i)$ is caused by the arrival of state $x_i(s^i_k)$ at some $j \in \mathcal{N}^i_{\text{out}}$.

In what follows, we make technical assumptions about the hybrid system in (6.13).

Assumption 6.2. *(On agent dynamics f_i and models Υ^j_i) For every $i \in \mathcal{V}$, there exists scalar functions $\hat{H}^j_i, \hat{H}^{max}_i : \mathbb{R}^{nN} \times \mathbb{R}^{nN} \to \mathbb{R}_{\geq 0}$, non-negative scalars $\tilde{L}^j_i$ and $\hat{L}^j_i$ such that, $\forall j \in \bar{\mathcal{N}}^i_{out}$, we have*

a) $|\dot{\tilde{e}}^j_i| \leq \tilde{L}^j_i |\tilde{e}^j_i|$;

b) $|\dot{e}^j_i| \leq \hat{L}^j_i |e^j_i| + \hat{H}^j_i(x, e^i)$;

c) $\hat{H}^j_i(x, e^i) \leq \hat{H}^{max}_i(x, e^i)$.

Remark 6.2. *Assumptions 6.2a) and 6.2b) essentially governs the nature of the growth of error variables $\tilde{e}_i^j$ and e_i^j, respectively. We note that Assumption 6.2a) holds for Lipschitz Υ_i^j but can also hold true for one-sided Lipschitz Υ_i^j with $\tilde{L}_i^j = \max\{0, \mathcal{L}_i^j\}$ where $\mathcal{L}_i^j$ denotes the one-sided Lipschitz constant of Υ_i^j. Assumption 6.2c) establishes a bound on the residual terms in $\hat{H}_i^j(x, e^i)$ that are used to bound the growth rate of $e_i^j, \forall j \in \mathcal{N}_{out}^i$.*

Assumption 6.3. *For the hybrid system in* (6.13)*, and $\forall i \in \mathcal{V}$, there exist a locally Lipschitz function $W_i(e_i, \tilde{e}_i) : \mathbb{R}^{nN} \times \mathbb{R}^{nN} \to \mathbb{R}_{\geq 0}$, functions $\underline{\alpha}_W^i$, $\bar{\alpha}_W^i \in \mathcal{K}_\infty$, scalar function $H_i^{d_i} : \mathbb{R}^{nN} \times \mathbb{R}^{nN} \to \mathbb{R}_{\geq 0}$, non-negative constant $L_i^{d_i}$ and scalar $\lambda_i \in (0, 1)$ such that*

a) $\underline{\alpha}_W^i(|e_i|) \leq W_i \leq \bar{\alpha}_W^i(|(e_i, \tilde{e}_i)|),\ \forall e_i, \tilde{e}_i \in \mathbb{R}^{nN}$,

b) let $\dot{e}_i = \bar{F}_{e_i}$, $\dot{\tilde{e}}_i = \bar{F}_{\tilde{e}_i}$ *and let* $\bar{F} \in \{\bar{F}_{\tilde{e}_i}, \bar{F}_{e_i} + \bar{F}_{\tilde{e}_i}\}$, *then*

$$\langle \nabla W_i, \bar{F} \rangle \leq L_i^{d_i} W_i + H_i^{d_i}(x, e^i),$$

$\forall x \in \mathbb{R}^{nN}$ *and almost all* $e_i, \tilde{e}_i \in \mathbb{R}^{nN}, \forall i \in \mathcal{V}$,

c) $W_i(e_i^+, \tilde{e}_i^+) \leq W_i(e_i, \tilde{e}_i)$ *when* $d_i = 1$ *and* $d_i^+ \in \{0, 1\}$,

d) $W_i(e_i^+, \tilde{e}_i^+) \leq \lambda_i W_i(e_i, \tilde{e}_i)$ *when* $d_i = 0$ *and* $d_i^+ = 1$.

Assumption 6.4. *Suppose Assumptions 6.3a) and 6.3b) hold. For the hybrid system in* (6.13)*, there exist a locally Lipschitz function $V(x) : \mathbb{R}^{nN} \to \mathbb{R}_{\geq 0}$, functions $\underline{\alpha}_V$, $\bar{\alpha}_V$, $\alpha_V \in \mathcal{K}_\infty$, a continuous function $\Theta(x) : \mathbb{R}^{nN} \to \mathbb{R}^{nN}$ and positive error gains $\gamma_i^{d_i}, d_i \in \{0, 1\}$, such that*

a) $\underline{\alpha}_V(|\Theta(x)|) \leq V(x) \leq \bar{\alpha}_V(|\Theta(x)|),\ \forall x \in \mathbb{R}^{nN}$,

b) $\langle \nabla V(x), f(x, e) \rangle \leq -\alpha_V(|\Theta(x)|) + \sum_{i \in \mathcal{V}} \left[(\gamma_i^{d_i})^2 |e^i|^2 - (H_i^{d_i}(x, e^i))^2\right]$, *for almost all* $x \in \mathbb{R}^{nN}$ *and* $\forall e^i \in \mathbb{R}^n, \forall i \in \mathcal{V}$.

Remark 6.3. *Note that $\Theta(x)$ in Assumption 6.4 represents a state transformation and aids in addressing problems involving MASs that do not necessarily converge to the origin, see [18]. Assumption 6.4b) conveys that the MAS*

$\dot{x} = f(x, e)$ is input-to-state stable (ISS) with respect to $e^i, \forall i \in \mathcal{V}$, where the error gain $\gamma_i^{d_i}$ may be dependent on d_i if the residual $H_i^{d_i}$ is dependent on d_i.

Prior to stating the result on stability of the closed-loop system in (6.13), we need to ensure that the conditions laid out in Assumption 6.3 are met. This notion is addressed through the following lemma whose proof is given in Appendix A.3.1.

Lemma 6.1. *(On W_i) Suppose Assumption 6.2 holds. If $W_i(e_i, \tilde{e}_i)$ is defined as:*

$$W_i(e_i, \tilde{e}_i) := \max\{\lambda_i|\tilde{e}_i|, |e_i + \tilde{e}_i|\}, \forall i \in \mathcal{V}, \tag{6.19}$$

then Assumption 6.3 is satisfied with $L_i^{d_i} = {\lambda_i}^{-1}\Big(d_i\tilde{L}_i^{max} + 2\sqrt{|\bar{\mathcal{N}}^i_{out}|}\hat{L}_i^{max}\Big)$, $H_i^{d_i}(x, e^i) = \sqrt{|\bar{\mathcal{N}}^i_{out}|}\hat{H}_i^{max}(x, e^i)$, where $\lambda_i \in (0, 1)$ is a design parameter.

For each agent $i \in \mathcal{V}$, we define two weight parameters $\theta_i^{d_i}(s), s \in \mathbb{R}_{\geq 0}$, one for each $d_i \in \{0, 1\}$, using the following two differential equations:

$$\dot{\theta}_i^{d_i} = -2L_i^{d_i}\theta_i^{d_i} - \breve{\gamma}_i((\theta_i^{d_i})^2 + 1), \tag{6.20}$$

where constants $L_i^{d_i}$ are defined in Assumption 6.3, $\breve{\gamma}_i = 2\gamma_{\max}/\lambda_i$, $\gamma_{\max} = \max_{i,d_i}\gamma_i^{d_i}$ and $\gamma_i^{d_i}, d_i \in \{0, 1\}$, are defined in Assumption 6.4. Note that $\theta_i^{d_i}(\cdot), d_i \in \{0, 1\}$, for each agent $i \in \mathcal{V}$, are monotonically decreasing parameters that are used to compensate for the growth of error measure $W_i(e_i, \tilde{e}_i)$ and aid in determining T^i_{MAD} and T^i as shown in the following result whose proof is presented in Appendix A.3.2.

Theorem 6.1. *(Asymptotic stability in the presence of small-delays) Suppose $T^i_{MAD}, T^i, \forall i \in \mathcal{V}$, are such that Assumption 6.1 holds and, additionally, the solutions $\theta_i^0(\cdot)$ and $\theta_i^1(\cdot)$ of (6.20) satisfy the inequalities:*

$$\begin{cases} \theta_i^0(\tau_i) \geq (\lambda_i)^2\theta_i^1(0), & \tau_i \in [0, T^i], \\ \theta_i^1(\tau_i) \geq \theta_i^0(\tau_i), & \tau_i \in [0, T^i_{MAD}], \end{cases} \tag{6.21}$$

for some positive initial conditions $\theta_i^{\{0,1\}}(0)$. Then, under Assumptions 6.2, 6.3 and 6.4, the closed-loop system in (6.13) is asymptotically stable with respect to the set $\{x \in \mathbb{R}^{nN} \mid \Theta(x) = \mathbf{0}\}$.

Remark 6.4. *We note that for the specific choice of W_i constructed in Lemma 6.1, $H_i^{d_i}$ is independent of d_i. As a consequence, the error gain $\gamma_i^{d_i}$ in Assumption 6.4b) could also be independent of d_i. Therefore, using Lemma 6.1, the bound in Assumption 6.4b) can be rephrased in terms of W_i as follows: $\langle \nabla V(x), f(x,e)\rangle \leq -\alpha_V(|\Theta(x)|) + \sum_{i\in\mathcal{V}} \left[\breve{\gamma}_i^2 W_i^2 - (H_i^{d_i})^2\right]$ where we use the fact that $\sum_{i\in\mathcal{V}} |e^i|^2 = \sum_{i\in\mathcal{V}} |e_i|^2$. Subsequently, this notion is also reflected in the design of $\theta_i^{d_i}$ in (6.20) where $\breve{\gamma}_i$ is adopted instead of $\gamma_i^{d_i}$.*

Remark 6.5. *The methodology discussed in this chapter relies on the assumption (specifically, Assumption 6.4) that the considered MASs is, to a certain extent, robust to external input. This notion can be exploited, perhaps with suitable modifications, in order to ensure that the methodology is applicable to several real-world applications involving multi-agent coordination problems such as attitude (namely, orientation) alignment, multi-agent rendezvous, flocking, coupled oscillators, consensus in power generators, see articles [84, 88] and the references therein for further description over these problems.*

6.4 Consensus of Nonlinear MASs

In this section, we consider a case study on consensus of Lipschitz nonlinear agents and, subsequently, offer a numerical example to illustrate our results.

6.4.1 Lipschitz Dynamics

Let the agent dynamics be given by

$$\dot{x}_i = f(x_i) - \kappa(\mathsf{L}_i \otimes \mathbb{I}_n)\hat{x}^i, \forall i \in \mathcal{V}, \tag{6.22}$$

where the unforced dynamics $f(x_i) : \mathbb{R}^n \to \mathbb{R}^n$ is globally Lipschitz with a Lipschitz constant $\mathcal{L}$, L is the graph Laplacian of connected undirected network $\mathcal{G}$ (see [62] for its properties) and the control gain κ is such that

$$\kappa > \frac{\mathcal{L}}{\Lambda_2}\sqrt{\frac{2\mathsf{d}_M}{\Lambda_2}} = \kappa_0, \quad \mathsf{d}_M = \max_i \mathsf{d}_i, \tag{6.23}$$

where d_i is the degree of agent i. Note that the condition in (6.23) can ensure consensus of the MAS in (6.22) with a CT controller $u_i = \kappa(\mathsf{L}_i \otimes \mathbb{I}_n)x$.

The following result, whose proof is given in Appendix A.3.3, addresses the consensus of Lipschitz nonlinear MASs.

Theorem 6.2. *(Consensus in the presence of small-delays) Consider the MAS in* (6.22)*, with a given control gain* $\kappa = \mathfrak{p}\kappa_0$ *satisfying* (6.23)*, where* $\hat{x}^i \in \mathbb{R}^{nN}$ *is the concatenation of model-based neighbor states propagated via the model* $\Upsilon^i_j(\cdot) = f(\cdot),\ \forall j \in \mathcal{N}^i_{out}$*. Under Assumptions 6.2, 6.3 and 6.4, if* $\tilde{L}^j_i = \hat{L}^j_i = \mathcal{L}, \forall i, j \in \mathcal{V}$*,* $(\hat{H}^j_i)^2 = 2\kappa^2(|(\mathsf{L}_i \otimes \mathbb{I}_n)x|^2 + |(\mathsf{L}_i \otimes \mathbb{I}_n)e^i|^2), \forall j \in \mathcal{N}^i_{out}$*,* $V(x) = \frac{K}{2}|(\mathsf{L} \otimes \mathbb{I}_n)x|^2$*,*

$$\breve{\gamma}_i^2 = 4\frac{|\mathsf{L}_i^{max}|^2}{\lambda_i^2}\Big(K\kappa\frac{\epsilon_2}{2} + 2\kappa^2|\bar{\mathcal{N}}^i_{out}|\Big),\ \epsilon_2 > \frac{\Lambda_M^2}{2\Lambda_2}\frac{\mathfrak{p}}{\mathfrak{p}-1},$$
$$K > 2\kappa^2|\bar{\mathcal{N}}^i_{out}|/\Big[\big(\Lambda_2 - \frac{\Lambda_M^2}{2\epsilon_2}\big)\kappa - \Lambda_2\kappa_0\Big],$$

where Λ_2 *and* Λ_M *are the smallest and the largest non-zero eigenvalues of* L*, respectively, then the closed-loop system in* (6.22) *is asymptotically stable w.r.t. the set* $\{x \in \mathbb{R}^{nN} | (\mathsf{L} \otimes \mathbb{I}_n)x = \mathbf{0}\}$*.*

6.4.2 Numerical Example

In this section, we present an illustrative example to demonstrate the results in Section 6.4.1. Consider a network of single-link robots with the following dynamics:

$$\dot{x}_i = \begin{bmatrix} x_{i,2} \\ -\sin(x_{i,1}) \end{bmatrix} - \kappa(\mathsf{L}_i \otimes \mathbb{I}_2)\hat{x}^i, \quad \kappa = 2, \tag{6.24}$$

where $x_i = [x_{i,1}\ x_{i,2}]^{\mathrm{T}}$, $f(x_i)$ is globally Lipschitz with a Lipschitz constant $\mathcal{L} = 1$ and the control gain κ satisfies (6.23). For the simulation, we set the time step for flow computation to be 0.1 ms and the total time to be 5 s. When $\lambda_i = 0.3$, $T^i = T^i_{\mathrm{MAD}} = 1$ ms, $\forall i \in \mathcal{V}$, is chosen by examining the trajectories of weight parameters $\theta^0_i(s)$ and $\theta^1_i(s)$ that satisfy conditions in (6.21); these trajectories are depicted in Fig. 6.1. Using this, let $\bar{\delta} =$

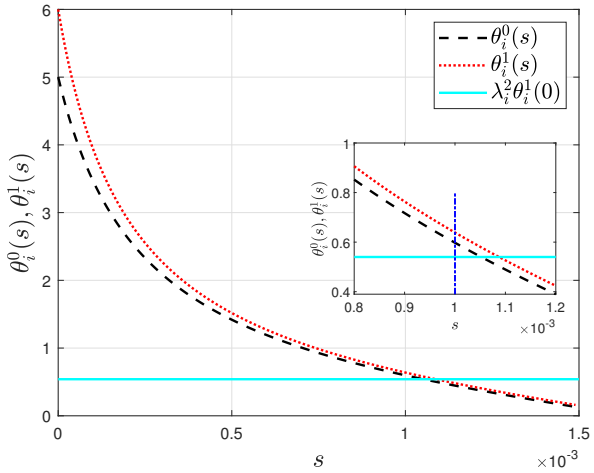

Figure 6.1: Trajectory of weights $\theta_i^0(\cdot)$ and $\theta_i^1(\cdot)$ for $\lambda_i = 0.3$.

$[0.2\ 0.3\ 0.4\ 0.6]T^i_{\text{MAD}} \leq T^i$ ms denote the delays associated with broadcasts from agents indexed $\{1, 2, 3, 4\}$, respectively. Figure 6.2 depicts the state trajectories of the nonlinear MAS in (6.24) in the presence of transmission delays given by $\bar{\delta}$.

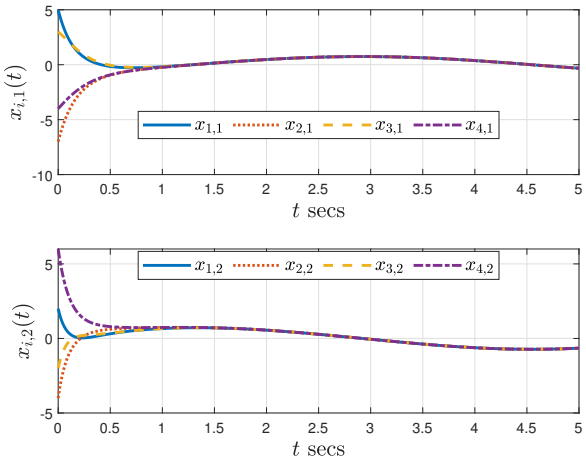

Figure 6.2: Consensus of state trajectories.

6.5 Conclusion

In this chapter, we studied the problem of distributed control of nonlinear MASs that are prone to small transmission delays. First, we offer a general approach to address this problem by employing model-based propagates of the neighbors' states and subsequently model the overall MAS using the hybrid systems framework. As a consequence of the stability analysis, we determine the bounds on delay (namely, MAD) and sampling interval (namely, MASP) for each agent. Furthermore, to demonstrate the effectiveness of the proposed framework, we present a case study on the consensus of agents with Lipschitz nonlinear dynamics interacting over an undirected network. Finally, a numerical example is simulated to illustrative the results of the case study.

Chapter 7

Dynamic Event-Triggered AGFs for Weight-Balanced Networks[1]

Accelerated gradients algorithms are currently at the receiving end of widespread interest in optimization theory, both under discrete- and continuous-time frameworks. In light of recent developments, in the first part of our work, we study the problem of designing a CT AGA for weight-balanced directed networks unlike the existing references that only address this problem for the case of undirected networks. We show that the convergence is exponential and the convergence rate is proportional to the gain, associated with the gradient term, which can be arbitrarily chosen. Subsequently, in the second part of our work, to facilitate digital implementation of the discussed algorithm, we employ an event-based broadcasting protocol on each node of the digraph that *intermittently* checks for events by evaluating an ETC and accordingly making decision on broadcasting. The distributed system is reformulated using the hybrid systems framework and is Zeno-free by design; this formulation allows us to improve the performance of the ETM and, as a consequence, the broadcast protocol. We provide a numerical example to demonstrate our results.

The rest of this chapter is organized as follows. In Section 7.1, some notations and preliminaries specific to this chapter are presented. The problem

[1]The material in this chapter has been submitted for publication as: Mani H. Dhullipalla, Hao Yu and Tongwen Chen. Accelerated gradient flows for weight-balanced digraphs with event-based broadcasting. *IEEE Transactions on Control of Network Systems.*

statement and algorithm are described Section 7.2. Convergence results for the distributed algorithm are described in Section 7.3. The algorithm is reformulated through the hybrid systems framework and a periodic event-based broadcast protocol is designed in Section 7.4. Numerical simulations demonstrate the effectiveness of CT algorithm and the performance of event-based broadcasts in Section 7.5. Concluding remarks are made in Section 7.6.

7.1 Notation and Preliminaries

In addition to the preliminaries on algebraic graph theory described in Section 4.1 of Chapter 4, in this section we introduce some notation specific to this chapter and provide some useful properties of weight-balanced directed networks.

7.1.1 Notation

First, let Z_a, Z_b, Z_{sym} be three coefficients (or parameters) then they are often referred together as $Z_{\{\}}$; for instance, $Z_{\{\}} > 0$ implies that each of the three coefficients Z_a, Z_b, Z_{sym} are positive. Let A be a square matrix, then Λ_M^A corresponds to the maximum eigenvalue of A.

7.1.2 Preliminaries

A digraph is weight-balanced if $\mathsf{d}_i = \sum_{j\in\mathcal{V}} \mathsf{a}_{ij} = \sum_{j\in\mathcal{V}} \mathsf{a}_{ji} = \mathsf{d}_i^{\text{out}}$, $\forall i \in \mathcal{V}$, i.e., in-degree at every node equals its out-degree. Let $\mathsf{L}_s \coloneqq (\mathsf{L} + \mathsf{L}^{\mathrm{T}})/2$ and $\mathsf{L}_{ss} \coloneqq (\mathsf{L} - \mathsf{L}^{\mathrm{T}})/2$ denote the symmetric and skew symmetric decompositions of Laplacian L, respectively. The following lemma, from [11, 52], is used to show convergence of dynamics in Section 7.3.

Lemma 7.1. *(On weight-balanced networks) Let $\mathcal{G}$ be a strongly connected and weight-balanced digraph with Laplacian L. Then, it follows that:*

1. $\mathsf{L}_s \succeq 0$ *and* 0 *is its simple eigenvalue;*

2. *there exists* $\Gamma \in \mathbb{R}^{N\times N} \succ 0$ *such that*

$$\mathsf{L}_s\Gamma = \Gamma\mathsf{L}_s = \mathbb{I}_N - \frac{1}{N}\mathbf{1}\mathbf{1}^T;$$

3. *there exists non-negative scalar* ϵ_{L} *such that*

$$\epsilon_{\mathsf{L}}\mathsf{L}_s - \mathsf{L}_{ss}^T\mathsf{L}_{ss} \succeq 0.$$

7.2 Problem Formulation

Let $\mathcal{G} = (\mathcal{V}, \mathcal{E})$ be the digraph over which N computing nodes interact. Each node $i \in \mathcal{V}$ is provided with local cost function $f_i : \mathbb{R}^n \to \mathbb{R}$ which is private (namely, known only to i). Consider the following DOP:

$$\min \sum_{i\in\mathcal{V}} f_i(x_i) \text{ subject to } \; x_i = x_j, \; \forall i, j \in \mathcal{V}, \tag{7.1}$$

where $x_i \in \mathbb{R}^n$ is the local optimization variable. Next, we make some assumptions on local cost functions.

Assumption 7.1. *On local cost:*

1. $f_i(\cdot)$, $\forall i \in \mathcal{V}$, *is convex and continuously differentiable everywhere;*

2. *gradient* $\nabla f_i(\cdot)$ *is* $\mathfrak{L}_i$*-Lipschitz, i.e.,*

$$|\nabla f_i(x) - \nabla f_i(y)| \leq \mathfrak{L}_i|x - y|;$$

3. f_i *is* μ_i*-strongly convex, i.e.,*

$$f_i(y) \geq f_i(x) + \nabla f_i(x)^T(y - x) + \frac{\mu_i}{2}|y - x|^2.$$

Assumption 7.1 ensures that the DOP in (7.1) has a unique minimum, denoted $x^\star$. Here, we note that the assumption on strong convexity of f_i is similar to the assumptions made in existing literature such as [45, 111], [108, 110, 113, 117, 122]. This assumption can be (slightly) relaxed to ensure that only the global function $\sum_i f_i$ is either strongly convex, like in [113], or it is restricted strongly convex as defined in [110]. The analysis in Section 7.3, with small changes, extends to these relaxations.

Assumption 7.2. *The communication network $\mathcal{G}$ is a static, strongly connected and weight-balanced directed graph.*

In this chapter, we consider that each node $i \in \mathcal{V}$ has the following dynamics:

$$\begin{aligned} \dot{x}_i &= \mathfrak{a}_1 v_i - \mathfrak{a}_2 \sum_{j\in\mathcal{V}} \mathsf{a}_{ij}\big(x_i - x_j\big), \\ \dot{v}_i &= -\mathfrak{b}_1 \nabla f_i(x_i) - \mathfrak{b}_2 v_i - \mathfrak{b}_3 q_i, \\ \dot{q}_i &= \sum_{j\in\mathcal{V}} \mathsf{a}_{ij}\big(x_i - x_j\big),\ \sum_{i\in\mathcal{V}} q_i(0) = 0, \end{aligned} \tag{7.2}$$

where state variables $x_i,\ v_i,\ q_i \in \mathbb{R}^n$ and gains $\mathfrak{a}_{\{1,2\}}, \mathfrak{b}_{\{1,2,3\}}$ are positive scalars.

Remark 7.1. *(On motivation) The dynamics in* (7.2) *is motivated by the CT algorithm in [117] which provides an accelerated gradient method for undirected networks. The algorithm in [117] can be obtained by making the substitutions:* $\mathfrak{a}_{\{1,2\}} = 1$*, and* $\mathfrak{b}_2 = \mathfrak{b}_3$*, in* (7.2)*. However, the resultant algorithm may not necessarily address the case of weight-balanced directed networks; this is, perhaps, because of the specific choice of gains considered in [117]. In Appendix A.4.1, we offer a counter-example to demonstrate that the algorithm in [117] fails to converge over a weight-balanced digraph whereas the algorithm in* (7.2) *(designed via Theorem 7.1) converges. Similar counter-examples can be constructed for [110] and [122]. Therefore, we begin with the most general case, namely,* (7.2)*.*

The objective of the chapter is: 1) to show that the system, with node dynamics (7.2), ensures that $x_i, \forall i \in \mathcal{V}$, approaches $x^\star$ asymptotically for weight-balanced directed networks; and 2) to develop an event-based broadcast strategy (which is defined in Section 7.4) so that the objective in item 1) can be achieved through intermittent broadcasts as opposed to continuous transmission in (7.2).

7.3 Main Results: Convergence

In this section, we address the first objective of this work, i.e., to prove that each node with dynamics (7.2) asymptotically reaches the global minima $x^\star$ over a weight-balanced digraph. For this, let $x = [x_1^{\mathrm{T}},\ ,\cdots,\ x_N^{\mathrm{T}}]^{\mathrm{T}} \in \mathbb{R}^{nN}$; similarly, $v \in \mathbb{R}^{nN}$ and $q \in \mathbb{R}^{nN}$ are concatenated vectors of v_i's and q_i's, respectively. Then, in compact form, the dynamics of the distributed system can be expressed as

$$\begin{cases} \dot{x} &= \mathfrak{a}_1 v - \mathfrak{a}_2 \mathsf{L}^n x \\ \dot{v} &= -\mathfrak{b}_1[\nabla f(x)] - \mathfrak{b}_2 v - \mathfrak{b}_3 q\ , \\ \dot{q} &= \mathsf{L}^n x,\ \mathbf{1}^{\mathrm{T}} q(0) = \mathbf{0} \end{cases} \tag{7.3}$$

where $\mathsf{L}^n = \mathsf{L} \otimes \mathbb{I}_n$. Here, $\big[\nabla f(\cdot)\big]$ is defined as $[\nabla f(y)] \coloneqq [\nabla f_1(y_1)^{\mathrm{T}}, \cdots, \nabla f_N(y_N)^{\mathrm{T}}]^{\mathrm{T}}$, $\forall y = [y_1^{\mathrm{T}},\ ,\cdots,\ y_N^{\mathrm{T}}]^{\mathrm{T}} \in \mathbb{R}^{nN}$.

The following lemma establishes the equilibrium of (7.3).

Lemma 7.2. *(On equilibrium) Let* E *denote the equilibrium of the overall system in* (7.3) *and let* $x^\star$ *denote the minimum of DOP in* (7.1)*. Then,* $\mathsf{E} = (\bar{x}^\star, \mathbf{0}, -\frac{\mathfrak{b}_1}{\mathfrak{b}_3}\big[\nabla f(\bar{x}^\star)\big])$ *where* $\bar{x}^\star = \mathbf{1}_N \otimes x^\star$.

Proof. Let $\mathsf{E} \coloneqq (\bar{x}, \bar{v}, \bar{q})$ and let $(\bar{x}_i, \bar{v}_i, \bar{q}_i)$ denote the node-wise triplet of E. From (7.2), the conditions for equilibrium, $\forall i \in \mathcal{V}$, are as follows:

$$\sum_{j\in\mathcal{V}} \mathsf{a}_{ij}\big(\bar{x}_i - \bar{x}_j\big) = 0, \tag{7.4a}$$

$$\mathfrak{a}_1 \bar{v}_i - \mathfrak{a}_2 \sum_{j\in\mathcal{V}} \mathsf{a}_{ij}\big(\bar{x}_i - \bar{x}_j\big) = 0, \tag{7.4b}$$

$$-\mathfrak{b}_1 \nabla f_i(\bar{x}_i) - \mathfrak{b}_2 \bar{v}_i - \mathfrak{b}_3 \bar{q}_i = 0. \tag{7.4c}$$

From (7.4a), $\bar{x}_i = \bar{x}_j = x_c, \forall i, j \in \mathcal{V}$, where $x_c \in \mathbb{R}^n$ denotes the consensus state; employing this into (7.4b) establishes $\bar{v}_i = 0, \forall i \in \mathcal{V}$. This results in $\mathfrak{b}_1 \nabla f_i(\bar{x}_i) + \mathfrak{b}_3 \bar{q}_i = 0$ from (7.4c). From (7.2), we see that $\sum_{i\in\mathcal{V}} \dot{q}_i = 0$, which implies that if $q_i(0)$ is chosen such that $\sum_{i\in\mathcal{V}} q_i(t) = \sum_{i\in\mathcal{V}} q_i(0) = 0$, then $\mathfrak{b}_1 \sum_{i\in\mathcal{V}} \nabla f_i(x_c) = -\mathfrak{b}_3 \sum_{i\in\mathcal{V}} \bar{q}_i = 0$. Under Assumption 7.1, the condition $\sum_{i\in\mathcal{V}} \nabla f_i(x_c) = 0$ implies that $x_c = x^\star \in \mathbb{R}^n$, where $x^\star$ denotes the global minimum. This completes the proof. □

Next, in order to translate the equilibrium E to the origin we define transformation variables as follows: $\big(a_i, b_i, c_i\big) \coloneqq \big(x_i - x^\star, v_i, q_i + \frac{\mathfrak{b}_1}{\mathfrak{b}_3}\nabla f_i(x^\star)\big)$. The system dynamics in the transformed variables is given as:

$$\begin{cases} \dot{a} &= \mathfrak{a}_1 b - \mathfrak{a}_2 \mathsf{L}^n a, \\ \dot{b} &= \mathfrak{b}_1 \nabla_f - \mathfrak{b}_2 b - \mathfrak{b}_3 c, \\ \dot{c} &= \mathsf{L}^n a,\ \mathbf{1}^{\mathrm{T}} c(0) = \mathbf{0}, \end{cases} \tag{7.5}$$

where $\nabla_f = \big[\nabla f(\bar{x}^\star)\big] - \big[\nabla f(x)\big]$ and state variables $(a,\ b,\ c)$ are appropriate concatenations of transformed states $(a_i,\ b_i,\ c_i)$, respectively.

Now we present the main result of this Section and provide its proof in Appendix A.4.2.

Theorem 7.1. *Suppose Assumptions 7.1 and 7.2 hold. If the system gains* $\mathfrak{a}_{\{\}}$, $\mathfrak{b}_{\{\}}$ *satisfy the following inequality:*

$$\begin{aligned} \min\Big\{\mathfrak{S}_{\frac{\Delta}{\phi}}\frac{\mu}{4}, \frac{\mathfrak{b}_2}{\mathfrak{b}_1}\mathfrak{X}_b - \big(\mathfrak{X}_b+1\big)\frac{1}{2\mathfrak{S}_{\frac{\Delta}{\phi}}}\frac{\mathfrak{L}^2}{\mu}\Big\} - \mathfrak{R}(\mathfrak{S}_{\frac{\Delta}{\phi}}\mathfrak{p})\frac{\mathfrak{b}_2}{2\mathfrak{a}_2} \\ -\big(\mathfrak{X}_b+1\big)\mathfrak{L}\Big(\frac{\mathfrak{L}}{4\mu}+\frac{1}{2}\Big)\max\{\varepsilon, \frac{1}{\varepsilon}\} > 0, \end{aligned} \tag{7.6}$$

where $\mu = \min_{i\in\mathcal{V}}\{\mu_i\}$, $\mathfrak{L} = \max_{i\in\mathcal{V}}\{\mathfrak{L}_i\}$, $\mathfrak{R} > \frac{(\Lambda_M^\Gamma \mathfrak{L})^2 \epsilon_{\mathsf{L}}}{2\mu}$, Λ_M^Γ *is the max. eigenvalue of* Γ, $\mathfrak{X}_b > 0$, $\varepsilon > 0$, $\mathfrak{p} = \frac{\mathfrak{a}_1}{\mathfrak{b}_2}$, *and*

$$\mathfrak{S}_{\frac{\Delta}{\phi}} = \frac{1+\sqrt{1+4\frac{\mathfrak{p}}{\mathfrak{J}}}}{2\mathfrak{p}}, \quad \mathfrak{J} = \frac{2\mu}{\mathfrak{L}^2}\frac{1}{\mathfrak{X}_b+1}\frac{\mathfrak{b}_2}{\mathfrak{b}_1}, \tag{7.7}$$

then the dynamical system in (7.3) *converges to the equilibrium* E *exponentially fast with a decay rate that is proportional to the gradient gain* $\mathfrak{b}_1$.

Remark 7.2. *(On sufficiency conditions) Theorem 7.1 establishes sufficiency conditions on the gains* $\mathfrak{a}_{\{\}}$, $\mathfrak{b}_{\{\}}$. *In the case of undirected networks, these conditions can be expressed, relatively, easily (see [29], [117]); however, for directed networks, conditions on gains may not be straight forward (see [45]). The problem on existence of gains translates to ensuring simultaneous feasibility of conditions (such as positivity of* $\mathfrak{C}_{\{\}}$ *in* (A.46) *and satisfying* (A.43)

which, together, narrows down to inequality in (7.6)*) that ensure the algorithm's convergence. A detailed analysis on this is presented in the proof of Theorem 7.1 in Appendix A.4.2.*

Remark 7.3. *(On arbitrary fast convergence) The decay rate* α_V *in* (A.47)*, associated with the exponential convergence of the Lyapunov function* V*, is proportional to gain* $\mathfrak{b}_1$ *that is attached to* $\nabla f_i(x_i)$ *in* (7.2)*. This is in line with conclusions about arbitrary fast convergence made in [117]. Note that the gains* $\mathfrak{a}_{\{1,2\}}$*,* $\mathfrak{b}_{\{2,3\}}$ *can be designed relative to* $\mathfrak{b}_1$*; this relationship is described in* (A.53) *of Appendix A.4.2. From a design perspective, this implies that the design parameters (namely,* $\mathfrak{p}, \mathfrak{r}_{\{1,2\}}$ *in* (A.53)*) need to be designed only once after which the gradient gain* $\mathfrak{b}_1$ *can be arbitrarily varied to achieve fast convergence rates.*

7.4 Main Results: Event-Based Broadcasting

In this section, we address the second objective of this work, i.e., to enable intermittent broadcasts of state information. Implementing (7.2) for distributed optimization requires continuous knowledge of neighbors' states which is not always feasible, particularly, if the nodes are interacting over wireless communication networks. To address this, we utilize a periodic event-based broadcast protocol where the idea is to *check* for an event occurrence at specific sampling instants and make decision on state broadcasting, see illustration in Fig. 7.1. To facilitate this, we adopt hybrid systems approach inspired from studies such as [4,17,37,99,100], [69]; the advantage of this framework is, mainly, twofold: a) to an extent, it can handle both synchronous and asynchronous protocols alike, and b) it offers flexibility in designing sampling sequences (defined in Subsection 7.4.1) at which the ETC is evaluated and, some, broadcasts occur. The later could help reduce network congestion.

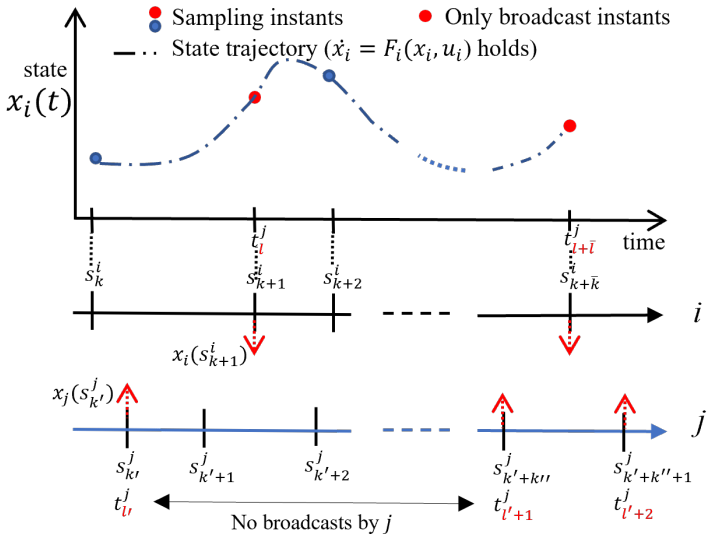

Figure 7.1: Illustration of the nature of broadcasts between two agents that employ periodic event-based broadcasting protocols. Note that neither sampling instants nor broadcast instants are necessarily synchronous or periodic unlike commonly employed discrete-time algorithms.

7.4.1 Problem Formulation in Hybrid Systems' Framework

Briefly, each node *flows* along the dynamics in (7.9) for a certain interval and at its sampling instants the agent checks for event occurrence, makes a *jump*, and, if deemed necessary, it also broadcasts its local state to neighbors.

First, we define sampling and event-triggering instants. For each node $i \in \mathcal{V}$, let the sequence $\{s^i_k\}_{k=0}^{\infty}$ denote instants at which the ETC is evaluated. The interval between two sampling instants is bounded as follows:

$$s^i_{k+1} - s^i_k \in \left[\varepsilon^i, T^i\right], \ \forall k \in \mathbb{Z}_{\geq 0}, \forall i \in \mathcal{V}, \tag{7.8}$$

where the lower bound ε^i is a positive quantity such that $\varepsilon^i < T^i$ and the upper bound T^i is to be designed as a consequence of asymptotic convergence. Note that arbitrarily small and positive ε^i ensures both instantaneous Zeno

solutions[2] and occurrence of Zeno behavior[3] (in event-triggered systems) are avoided.

Remark 7.4. *(On 'periodic' event-based protocol) Here, we note that the sampling sequences $\{s_k^i\}$ (and as a consequence, the protocol), governed by its interval constraint in* (7.8)*, are not necessarily periodic or synchronous; however, to keep in line with the terminology used in [17, 99, 100], we continue to call the approach discussed in this section as periodic event-based broadcasting. This notion is illustrated in Fig. 7.1.*

The event-triggering instants are instants at which the ETC is satisfied; these are denoted by sequence $\{t_l^i\}_{l=0}^{\infty}$. Since the ETC on each node is evaluated at sampling instants $\{s_k^i\}$, the event-triggering instants $\{t_l^i\}$ must form a subsequence of $\{s_k^i\}$. This can be inferred from the update rule for t_l^i in (7.13).

Next, we discuss system dynamics with intermittent broadcasts. Let $\hat{x}_i(t) = x_i(t_l^i),\ t \in [t_l^i, t_{l+1}^i)$, denote the broadcast state of node i and let $e_i = \hat{x}_i - x_i$ be the broadcast error. Let $\hat{x} = [\hat{x}_1^{\mathrm{T}},\ \cdots,\ \hat{x}_N^{\mathrm{T}}]^{\mathrm{T}}$ and $e = [e_1^{\mathrm{T}},\ \cdots,\ e_N^{\mathrm{T}}]^{\mathrm{T}}$ be concatenated states. The broadcast state in node dynamics enters through the consensus terms as follows:

$$\begin{aligned}
\dot{x}_i &= \mathfrak{a}_1 v_i - \mathfrak{a}_2 \sum_{j\in\mathcal{V}} \mathsf{a}_{ij}\big(\hat{x}_i - \hat{x}_j\big),\\
\dot{v}_i &= -\mathfrak{b}_1 \nabla f_i(x_i) - \mathfrak{b}_2 v_i - \mathfrak{b}_3 q_i,\\
\dot{q}_i &= \sum_{j\in\mathcal{V}} \mathsf{a}_{ij}\big(\hat{x}_i - \hat{x}_j\big).
\end{aligned} \tag{7.9}$$

The dynamics of q still stays on the manifold $\sum_{i\in\mathcal{V}} q_i = 0$, like in Section 7.3, which is ensured by choosing initial condition such that $\sum_{i\in\mathcal{V}} q_i(0) = \mathbf{0}$. This is essential to enforce convergence to equilibrium E and, as a consequence,

[2]Hybrid systems can adopt complete solutions that become eventually discrete, i.e., in essence, after a certain time the solution only uses the jump map without ever flowing again. Such solutions are called instantaneous Zeno solutions. For further details on hybrid systems, see Chapter 2 in [31].

[3]Zeno behavior, or, occurrence of infinite events in finite time, is undesirable because realizing such a notion in physical systems is impractical. This phenomenon also leads to Zeno solutions of the hybrid systems.

the minima $x^\star$. Using the state translation $(x, v, q) \to (a, b, c)$ from Section 7.3, the dynamics of the system can be expressed as:

$$\begin{aligned}\dot{a} &= \mathfrak{a}_1 b - \mathfrak{a}_2 \mathsf{L}^n (a + e),\\ \dot{b} &= \mathfrak{b}_1 \nabla_f - \mathfrak{b}_2 b - \mathfrak{b}_3 c,\\ \dot{c} &= \mathsf{L}^n (a + e).\end{aligned} \tag{7.10}$$

Since we considered the case of ZOH for the broadcast state, the error dynamics, $\dot{e}_i = -\dot{x}_i = -\dot{a}_i$, is given by:

$$\begin{cases} \dot{e}_i = -\mathfrak{a}_1 b_i + \mathfrak{a}_2 \sum_{j\in\mathcal{V}} \mathsf{a}_{ij}\big(\hat{x}_i - \hat{x}_j\big), & t \in [s_k^i, s_{k+1}^i) \\ e_i^+ = e_i & t \in \{s_k^i\} \setminus \{t_l^i\} \\ e_i^+ = \mathbf{0}, & t \in \{t_l^i\} \end{cases} \tag{7.11}$$

where $\hat{x}_i - \hat{x}_j = a_i - a_j + e_i - e_j$. In (7.11), when an event occurs, i.e., when $t \in \{t_l^i\}$, the state $\hat{x}_i^+ = \hat{x}_i(t_l^i) = x_i(t_l^i)$ is broadcasted and the error e_i, instantaneously after jump (or broadcast), is set to $\mathbf{0}$; for other sampling instants, i.e., $t \in \{s_k^i\} \setminus \{t_l^i\}$, e_i stays unchanged instantaneously after the jump. Note that for the broadcast dynamics in (7.10), the flow domain has not yet been rigorously defined; this will be addressed shortly in (7.16).

Prior to introducing the ETC, we introduce the auxiliary variable $\eta_i \in \mathbb{R}_{\geq 0}$ which captures dynamics of the ETM as follows:

$$\begin{cases} \dot{\eta}_i = f_\eta^i(\eta_i, \mathcal{X}), & t \in [s_k^i, s_{k+1}^i), \\ \eta_i^+ = g_s^i(\eta_i, \mathcal{X}), & t \in \{s_k^i\} \setminus \{t_l^i\}, \\ \eta_i^+ = g_t^i(\eta_i, \mathcal{X}), & t \in \{t_l^i\}. \end{cases} \tag{7.12}$$

Here, the positivity of η_i is ensured by the design of its dynamics (i.e., functions f_η^i, g_s^i, and g_t^i) and the initial condition $\eta_i(0) \geq 0$. Note that η_i in (7.12) jumps to different values, namely, g_s^i or g_t^i, depending on the occurrence or non-occurrence of an event. Using (7.12), the ETC (and the update rule for $\{t_l^i\}$) is as follows:

$$t_{l+1}^i = \{t > t_l^i \mid t \in \{s_k^i\}_{k=0}^\infty,\ g_s^i < 0\}, \forall i \in \mathcal{V}. \tag{7.13}$$

Finally, to monitor the bounds on sampling period defined in (7.8), each node $i \in \mathcal{V}$ also keeps track of the time elapsed since the last (namely, most

recent) sampling instant using non-negative scalar τ_i. For any $k \in \mathbb{Z}_{\geq 0}$, it is straightforward to see that τ_i is governed by:

$$\begin{cases} \dot{\tau}_i = 1, & t \in [s_k^i, s_{k+1}^i), \\ \tau_i^+ = 0, & t \in \{s_{k+1}^i\}. \end{cases} \tag{7.14}$$

Note that τ_i in (7.14) resets at every sampling instant independent of event-occurrence.

Now, we are prepared to discuss hybrid dynamics[4] of the augmented state $\mathcal{X} \coloneqq [a^{\mathrm{T}}\ b^{\mathrm{T}}\ c^{\mathrm{T}}\ e^{\mathrm{T}}\ \eta^{\mathrm{T}}\ \tau^{\mathrm{T}}]^{\mathrm{T}}$ which is expressed as follows:

$$\begin{cases} \dot{\mathcal{X}} = F(\mathcal{X}), & \mathcal{X} \in C, \\ \mathcal{X}^+ \in G(\mathcal{X}), & \mathcal{X} \in D, \end{cases} \tag{7.15}$$

where the flow and jump domains, i.e., C and D, respectively, are defined as:

$$\begin{aligned} C &= \mathbb{R}^{4nN} \times \mathbb{R}_{\geq 0}^{N} \times [0, T^1] \times \cdots \times [0, T^N], \\ D &= \bigcup_{i=1}^{N} \Big\{ \mathbb{R}^{4nN} \times \mathbb{R}_{\geq 0}^{N} \times [0, T^1] \times \cdots \times \underbrace{[\varepsilon^i, T^i]}_{\text{sampling instant on } i} \times \cdots \times [0, T^N] \Big\}. \end{aligned} \tag{7.16}$$

The function F and set-valued mapping G in (7.15) are

$$\begin{aligned} F(\mathcal{X}) &= \begin{bmatrix} \mathfrak{a}_1 b - \mathfrak{a}_2 \mathsf{L}^n (a+e) \\ \mathfrak{b}_1 \nabla_f - \mathfrak{b}_2 b - \mathfrak{b}_3 c \\ \mathsf{L}^n (a+e) \\ -\mathfrak{a}_1 b + \mathfrak{a}_2 \mathsf{L}^n (a+e) \\ f_\eta \\ \mathbf{1} \end{bmatrix}, \ G(\mathcal{X}) = \bigcup_{i=1}^{N} G_i(\mathcal{X}), \\ G_i(\mathcal{X}) &:= \begin{cases} \begin{cases} \{G_i^1\}, & g_s^i > 0; \\ \{G_i^2\}, & g_s^i < 0; \\ \{G_i^1,\ G_i^2\}, & g_s^i = 0; \end{cases} & \tau_i \in [\varepsilon^i, T^i] \\ \phi & \tau_i \notin [\varepsilon^i, T^i] \end{cases} \end{aligned} \tag{7.17}$$

where ϕ is a null set,

$$\begin{aligned} G_i^1 &:= \big[\, a^{\mathrm{T}}\ b^{\mathrm{T}}\ c^{\mathrm{T}}\ e^{\mathrm{T}}\ (\mathcal{I}_i \eta + \bar{g}_s^i)^{\mathrm{T}}\ (\mathcal{I}_i \mathbf{1})^{\mathrm{T}} \,\big]^{\mathrm{T}}, \\ G_i^2 &:= \big[\, a^{\mathrm{T}}\ b^{\mathrm{T}}\ c^{\mathrm{T}}\ (\mathcal{I}_i^n e)^{\mathrm{T}}\ (\mathcal{I}_i \eta + \bar{g}_t^i)^{\mathrm{T}}\ (\mathcal{I}_i \mathbf{1})^{\mathrm{T}} \,\big]^{\mathrm{T}}, \end{aligned}$$

[4]For hybrid dynamics, we follow the formulation in [31]. To save space, we omit mathematical definitions on concepts and notations used in Section 7.4. In this regard, we refer the interested reader to Chapter 2 or textbook [31] for details.

$f_\eta := [f_\eta^1 \ \cdots \ f_\eta^N]^{\mathrm{T}}$, $\mathcal{I}_i := \mathtt{diag}(\{1, \cdots, 0, \cdots, 1\}) \in \mathbb{R}^{N\times N}$ with 0 at the i-th place on the diagonal, $\mathcal{I}_i^n = \mathcal{I}_i \otimes \mathbb{I}_n$, $\bar{g}_s^i := [0 \cdots g_s^i \cdots 0]^{\mathrm{T}} \in \mathbb{R}^N$ and $\bar{g}_t^i := [0 \cdots g_t^i \cdots 0]^{\mathrm{T}} \in \mathbb{R}^N$.

For the hybrid system in (7.15), the domain C, defined in (7.16), is such that all the nodes in the network could flow when $\mathcal{X} \in C$. The domain D, defined as a union of subsets, is such that the system in (7.15) jumps if *at least* one node jumps (i.e., when τ_i equals the pre-decided sampling interval). Note that at a jump instant, say $\mathfrak{t}$, only the nodes in the index set $\mathfrak{Y} = \{j | \mathfrak{t} \in \{s_k^j\}, \forall j \in \mathcal{V}\}$ actively participate in the jump. Consequently, the states of nodes in $\mathcal{V} \setminus \mathfrak{Y}$ remain unaffected, instantaneously, after jump. When the system jumps, the states (a, b, c), instantaneously after jump, do not change for all agents in $\mathcal{V}$; however, depending on the sign of g_s^i, the error e_i for node i could change as described in (7.17). Furthermore, the function F and set-valued mapping G are continuous and outer semi-continuous, respectively, and the domains C and D are closed sets; these ensure the property of nominal well-posedness of the hybrid system in (7.15), see [31].

7.4.2 ETC and Sampling Period

To determine the appropriate ETC and sampling sequence for asymptotic convergence, we first examine the effect that broadcast error e has over the Lyapunov function V (defined in (A.41)) used to prove Theorem 7.1 in Section 7.3. Since the broadcast error e enters the system in (7.2) through consensus terms, only derivative of functions V_a and V_c, defined in Appendix A.4.2, are affected, see Appendix A.4.3). This is assuming that $\pi = \mathfrak{a}_2\Delta$, in the definition of Q, is upheld to arrive at (A.40). Considering the function V defined in (A.41), its derivative along the broadcast dynamics in (7.10) is upper-bounded as follows:

$$\dot{V} \leq -\hat{\mathfrak{C}}_a|a|^2 - \mathfrak{C}_b|b|^2 - \hat{\mathfrak{C}}_c|c|^2 - \mathfrak{C}_{\mathrm{sym}} a^{\mathrm{T}} \mathsf{L}_s a + \mathfrak{C}_e|e|^2, \tag{7.18}$$

where the expressions for coefficients $\hat{\mathfrak{C}}_{\{\}}$, $\mathfrak{C}_e$ are provided in Appendix A.4.4).

Noticing the last term in (7.18), we define $W_i \coloneqq |e_i|, \forall i \in \mathcal{V}$, to keep track of the error growth; its derivative along (7.11), defined for almost all $e_i, \forall i \in \mathcal{V}$, is upper-bounded by:

$$\langle \nabla W_i, \dot{e}_i \rangle \leq \ (\mathfrak{a}_2 \mathsf{d}_i) W_i + | - \mathfrak{a}_1 b_i + \mathfrak{a}_2 \mathsf{L}^n a - \mathfrak{a}_2 \mathsf{A}^n e|. \tag{7.19}$$

Since the coefficients $\mathfrak{a}_{\{1,2\}}$ in (7.19) are proportional to $\mathfrak{b}_1$ (see (A.53)), the bound on the error growth rate also increases with increasing $\mathfrak{b}_1$.

Next, in order to contain the growth of W_i and facilitate the design of the sampling interval, motivated by [69], we define a decaying weight $\theta_i(\mathsf{t}),\ \mathsf{t} \in \mathbb{R}_{\geq 0}$, using the following lemma.

Lemma 7.3. *Let $\theta_i : \mathbb{R}_{\geq 0} \to \mathbb{R}$ be the solution to the differential equation*

$$\dot{\theta}_i(\mathsf{t}) = \begin{cases} -\left(\frac{\mathfrak{b}_1}{\delta_1}\gamma_i \theta_i^2(\mathsf{t}) + 2L_\nu^i \theta_i(\mathsf{t}) + \gamma_i\right), & \mathsf{t} \in [0, T_0^i(\lambda_i)] \\ 0, & \mathsf{t} > T_0^i(\lambda_i) \end{cases} \tag{7.20}$$

with the initial condition $\theta_i(0) = {\lambda_i}^{-1}$, where $\lambda_i \in (0,1)$, $\gamma_i > 0$, $L_\nu^i = \mathfrak{a}_2 \mathsf{d}_i + \nu_i$ for sufficiently small $\nu_i > 0$. Then, $\theta_i(\mathsf{t})$ is monotonically decreasing and $\theta_i(\mathsf{t}) = \lambda_i, \forall \mathsf{t} \geq T_0^i(\lambda_i)$.

From Lemma 7.3, it is straightforward to see that $T_0^i(\lambda_i)$ is the time that θ_i takes to traverse from the initial condition $\theta_i(0) = \lambda_i^{-1}$ to $\theta_i(T_0^i) = \lambda_i$ along (7.20). Here, $\lambda_i \in (0,1)$ is a local design parameter that influences both $T_0^i(\lambda_i)$ and the event-triggering condition governed by g_s^i (see (7.21b) in Theorem 7.2). $\nu_i > 0$ is also a local design parameter that is introduced to achieve asymptotic stability of the broadcast system (see proof of Theorem 7.2 in Appendix A.4.4)); an arbitrarily small choice of ν_i is adequate. By choosing appropriate parameters such as $\lambda_i,\ \nu_i$, for each node $i \in \mathcal{V}$, $T_0^i(\lambda_i)$ can be determined by slightly altering expressions in [69]. In the remarks that follow Theorem 7.2, we will address aspects concerning parameters γ_i, δ_1 and $\mathfrak{b}_1$ in (7.20).

In the theorem that follows, we design the dynamics of η_i that governs the ETC in (7.13). The sketch of the proof is presented here.

Theorem 7.2. *Suppose Assumptions 7.1 and 7.2 hold. For all $i \in \mathcal{V}$, let $\hat{V}_i = \mathfrak{c}_{\mathsf{L}}|\mathsf{L}_i^n \hat{x}|^2$, $W_i = |e_i|$, and $\beta_i > 0$. If the functions associated with dynamics of η_i in* (7.12) *are as follows:*

$$f_\eta^i = -\beta_i \eta_i + \mathfrak{b}_1 \hat{V}_i, \tag{7.21a}$$

$$g_s^i = \eta_i + \gamma_i \Big(\theta_i - \frac{1}{\lambda_i}\Big) W_i^2, \tag{7.21b}$$

$$g_t^i = \eta_i + \gamma_i \lambda_i W_i^2, \tag{7.21c}$$

where γ_i is the error gain, θ_i, λ_i are as defined in Lemma 7.1, then the ETC in (7.13) *ensures that the hybrid system in* (7.15) *is asymptotically stable with respect to the origin.*

Sketch of Proof: The proof progresses by showing convergence of Lyapunov function U, which is defined as:

$$U \coloneqq V + \sum_{i \in \mathcal{V}} \big\{ \gamma_i \theta_i W_i^2 + \eta_i \big\},$$

along (7.15), in both flow and jump domains, C and D, respectively. Here, γ_i is the error gain in the upper-bound for $\dot{V}$

$$\begin{aligned} \dot{V} \leq & -\hat{\mathfrak{C}}_a |a|^2 - \mathfrak{C}_b |b|^2 - \hat{\mathfrak{C}}_c |c|^2 - \mathfrak{C}_{\text{sym}} a^{\mathrm{T}} \mathsf{L}_s a \\ & + \sum_{\forall i \in \mathcal{V}} \big\{ \gamma_i^2 |e_i|^2 - \frac{\delta_1}{\mathfrak{b}_1} H_i^2 - \mathfrak{b}_1 \hat{V}_i \big\}, \end{aligned} \tag{7.22}$$

which in turn stems from (7.18). The scalar function H_i stems from upper-bounding the growth rate of W_i in (7.19) and $\hat{V}_i$ is included to improve the performance of ETC in (7.13) by slowing down decay of η_i in (7.21). The details of the proof are presented in Appendix A.4.4. □

The following remarks explain the effect that the gradient gain $\mathfrak{b}_1$ has over the design of ETC.

Remark 7.5. *(On ETC design relative to $\mathfrak{b}_1$) In Section 7.3, we showed that the algorithm in* (7.5) *can achieve arbitrary fast convergence by varying $\mathfrak{b}_1$. In addition to designing the dynamics of η_i-s and sampling periods T_0^i-s, in this subsection, we are also interested in making the design of aforementioned*

attributes relative to $\mathfrak{b}_1$*. This provides us with freedom to arbitrarily choose* $\mathfrak{b}_1$*, like in Section 7.3, and still ensure the stability of hybrid system in* (7.15) *with* η_i *governed by* (7.21)*. In order to achieve this goal, we explicitly introduced the gradient gain* $\mathfrak{b}_1$ *in the dynamics of* θ_i *in Lemma 7.3. Appendix A.4.4) that presents the proof of Theorem 7.2 shows the steps taken to make the design relative to* $\mathfrak{b}_1$*.*

Remark 7.6. *(On fast convergence and broadcasts) From* (7.20) *in Lemma 7.3, it can be seen that with increase in* $\mathfrak{b}_1$ *(implying faster convergence), for a fixed* λ_i*, the sampling period* T_0^i *shrinks. In other words, faster convergence necessitates frequent event checks and, perhaps, frequent broadcasts. This is attributed to the coefficients of the quadratic expression in* θ_i *which are all dependent on* $\mathfrak{b}_1$*. This includes the error gain* γ_i *in* (7.22) *which is also affected by both* $\mathfrak{b}_1$ *and* δ_1 *as follows:*

$$\begin{aligned}\gamma_i^2 =&\frac{\mathfrak{S}_{\frac{\Delta}{\phi}}\phi^2}{2\mathfrak{b}_1}\Big(\Re\frac{\mathfrak{r}_2}{\mathfrak{r}_1}\sigma_{\mathsf{L}}\varrho_1+\frac{\mathfrak{r}_1}{\mathfrak{r}_2}\frac{\mathfrak{L}^2}{2\mu}\mathfrak{b}_1^2(\iota_1+\lambda_M^{\Gamma}\lambda_M^{\mathsf{L}_s}\epsilon_{\mathsf{L}}\iota_2)\Big)\\&+\mathfrak{b}_1\Big(2\delta_1\frac{\mathfrak{r}_1^2}{\mathfrak{r}_2^2}Tr(\mathsf{A}^T\mathsf{A})+\mathfrak{c}_{\mathsf{L}}Tr(\mathsf{L}^T\mathsf{L})\Big).\end{aligned}\tag{7.23}$$

Remark 7.7. *(On performance of the ETM) When* $\mathfrak{b}_1$ *is increased, from* (7.21a)*, we see that* η_i *decays slower; this could suggest that* g_s^i *becomes negative less frequently. However, this is not the case since increased* $\mathfrak{b}_1$ *also fastens the error growth in* (7.19)*. The result is a combined effect of these two notions, often, resulting in a higher number of events considering that* g_s^i *in* (7.21b) *involves* W_i^2 *and not* W_i*.*

Remark 7.8. *(On convergence rate* $\propto \mathfrak{b}_1$*) The convergence rate of the broadcast dynamics in* (7.10) *depends on the slowest term in* (A.61)*. Note that the coefficients* $\bar{\mathfrak{C}}_{\{a,b\}}$*,* $\hat{\mathfrak{C}}_{\mathrm{c}}$ *in* (A.61) *are shown to be proportional to* $\mathfrak{b}_1$ *in Appendix A.4.4); then, we could construct* β_i *and* λ_i *(*$\theta_i \geq \lambda_i$*) as linear functions of* $\mathfrak{b}_1$ *in order to make the overall convergence rate* $\propto \mathfrak{b}_1$*. Although, this can show arbitrary fast convergence for* (7.10)*, it is, further, detrimental to the performance of the ETC (which is affected by* $\mathfrak{b}_1$ *as noted in Remark 7.7) governed*

by (7.21). *So, in this chapter, we do not pursue arbitrary fast convergence for the case of system in* (7.10) *with intermittent broadcasts.*

7.5 Numerical Example

In this section, we consider the following local objective functions for the unconstrained problem in (7.1):

$$f_1(x) = \frac{3}{4}x^2 + \frac{1}{2}x\log(x^2+2), \quad f_2(x) = \frac{1}{2}x^2 + \frac{1}{2}\frac{x^2}{\sqrt{x^2+1}},$$
$$f_3(x) = (x-4)^2, \quad f_4(x) = x^2 + \frac{x^2}{\log(x^2+3)}. \tag{7.24}$$

The global objective function $\sum_{i\in\mathcal{V}} f_i$, is solved by nodes interacting over a weight-balanced digraph $\mathcal{G}$ whose Laplacian is given by:

$$\mathsf{L} = \begin{bmatrix} 1 & -1 & 0 & 0 \\ 0 & 1 & -1 & 0 \\ 0 & 0 & 1 & -1 \\ -1 & 0 & 0 & 1 \end{bmatrix}.$$

The initial states are $x(0) = [5\ 0\ 7\ \ -1]^{\mathrm{T}}$. The minimum of $\sum f_i$ occurs at $x^\star = 0.85$ and its value at $x^\star$ is $\sum f_i(x^\star) = 12.79$. For $\mathfrak{b}_1 = 1$, the dynamics of each node is as follows:

$$\begin{cases} \dot{x}_i = \frac{0.1}{4}v_i - 1\sum_{j\in\mathcal{V}} \mathsf{a}_{ij}\big(x_i - x_j\big), \\ \dot{v}_i = -\nabla f_i(x_i) - 15v_i - 3.65q_i, \\ \dot{q}_i = \sum_{j\in\mathcal{V}} \mathsf{a}_{ij}\big(x_i - x_j\big),\ q_i(0) = 0. \end{cases} \tag{7.25}$$

The simulation results are discussed in two parts: 1) demonstrating that the convergence rate of dynamics discussed in Section 7.3 is proportional to $\mathfrak{b}_1$; and 2) examining the performance of the event-based broadcast strategy discussed in Section 7.4.

First, the risk-ratio of DOP in (7.1) is given by the quantity $\sum\{f_i(x_i) - f_i(x^\star)\}/\sum f_i(x^\star)$ and the figures Fig. 7.2 and Fig. 7.3 depict risk-ratio in a semi-log plot against simulation time of 100 secs. Here, we show that the convergence of the algorithm in (7.5) can be achieved arbitrarily fast by increasing the gradient gain $\mathfrak{b}_1$. In Fig. 7.2, we also make a comparison against an existing CT algorithm which is a modified Lagrangian-based approach (denoted

$\lambda_i, \forall i \in \mathcal{V}$		0.09	0.27	0.7
$\mathfrak{b}_1 = 1,\ \delta_1 = 1$	MASP (in ms)	4	3	1
	% Broadcasts	48.43	27.47	7.54
$\mathfrak{b}_1 = 1,\ \delta_1 = 0.5$	MASP (in ms)	2.8	2	0.6
	% Broadcasts	44.02	23.19	6.01
$\mathfrak{b}_1 = 3,\ \delta_1 = 0.5$	MASP (in ms)	1.9	1.2	0.3
	% Broadcasts	65.65	33.53	7.50

Table 7.1: MASP and broadcast percentages

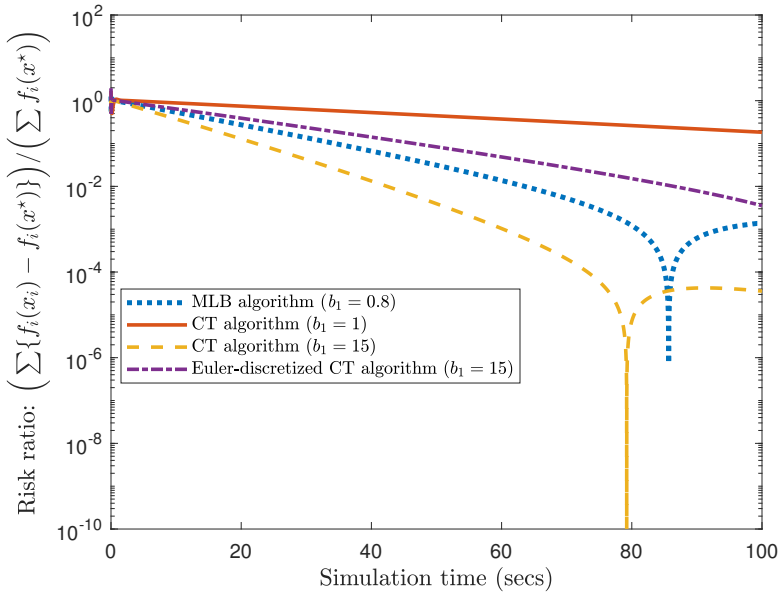

Figure 7.2: Performance comparison by varying $\mathfrak{b}_1$.

MLB in Fig. 7.2) for weight-balanced directed networks described in [45]. The dynamics in (7.5) can be expressed as:

$$\ddot{x} = -\mathfrak{a}_1\mathfrak{b}_1\nabla f - \mathfrak{b}_2\dot{x} - \underbrace{\mathfrak{a}_2\mathfrak{b}_2\mathsf{L}x}_{\text{proportional}} - \underbrace{\mathfrak{a}_1\mathfrak{b}_3\int \mathsf{L}x dx}_{\text{integral}} - \underbrace{\mathfrak{a}_2\mathsf{L}\dot{x}}_{\text{derivative}}; \tag{7.26}$$

and for a fair comparison, we adopt the following dynamics for the MLB approach:

$$\dot{x} = -\mathfrak{a}_1\mathfrak{b}_1\nabla f - \mathfrak{a}_2\mathfrak{b}_2\mathsf{L}x - \mathfrak{a}_1\mathfrak{b}_3\int \mathsf{L}x dx. \tag{7.27}$$

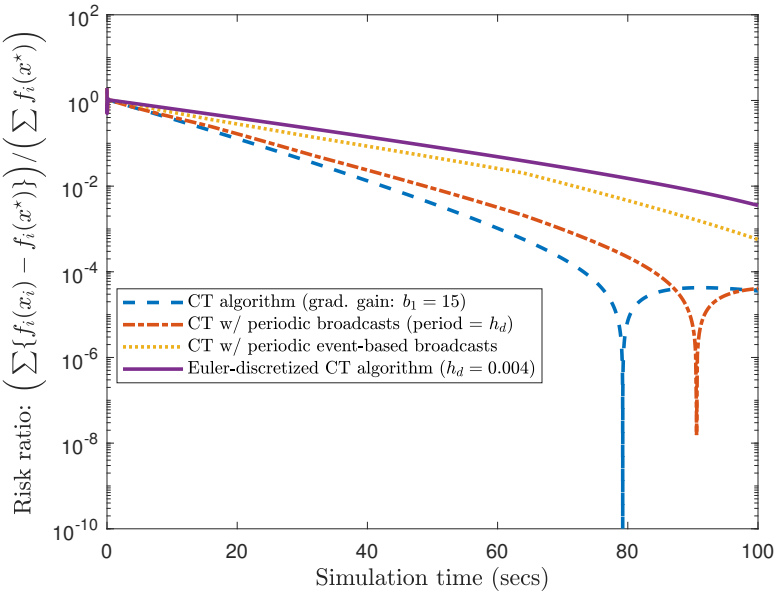

Figure 7.3: Performance comparison of Euler-discretized algorithm and CT algorithm with continuous and discrete broadcasts.

It is worth mentioning that as $\mathfrak{b}_1$ is increased beyond $\mathfrak{b}_1 = 0.8$, the state trajectory of (7.27) diverges from the equilibrium. Figure 7.2 supports the argument that accelerated gradient methods can, potentially, achieve higher convergence rates using gradient information in comparison to the MLB approach.

Next, to evaluate the performance of the event-based broadcast protocol we begin with the node dynamics in (7.25). The flow dynamics of $\eta_i, \forall i \in \mathcal{V}$, is given by:

$$\dot{\eta}_i = -0.1\eta_i + \frac{3}{2}\mathfrak{b}_1|\mathsf{L}_i^n\hat{x}|^2, \ t \in [s_k^i, s_{k+1}^i),$$

where $\eta_i(0) = 1, \forall i \in \mathcal{V}$, and the jump dynamics is governed by (7.21). The simulation time considered is 100 s and the time step for flow computations is chosen to be 0.1 ms. By setting $\lambda_i = 0.27, \ \forall i \in \mathcal{V}$, in Lemma 7.3, the MASP, i.e., $\min\{T^i\}$, is around 3 ms as shown in Table 7.1; this implies that the ETC in (7.13) is checked every 3 ms contrary to being evaluated at every time step, i.e. 0.1 ms, in (implementation of) continuous-time ETC. Further, Table 7.1 shows the influence of design parameter $\lambda_i, \forall i \in \mathcal{V}$, on: a) the MASP of the overall system (7.10); and b) the ETC (7.13) through

the overall percentage of broadcasts, i.e., averaging over all the nodes in $\mathcal{G}$. From (7.21), it can be inferred that a higher λ_i could result in fewer events but would need more frequent monitoring of the ETC; Table 7.1 supports this argument. It also shows the effect of changing $\mathfrak{b}_1$ and δ_1 on the MASP and percentage of broadcasts; these results substantiate the comments made in Remarks 7.6 and 7.7. Figure 7.3 shows the performance of the CT algorithms, when $\mathfrak{b}_1 = 15$, with periodic broadcasts and periodic event-based broadcasts. Notice that the performance of CT algorithm with event-based broadcasting lies between the two bounding curves, namely, the (purely) CT algorithm and its Euler-discretized counterpart.

7.6 Conclusion

In this chapter, we first studied the convergence of a distributed accelerated gradient flow over weight-balanced directed networks. We showed that the algorithm converges exponentially and arbitrarily fast based, solely, on the choice of the gradient gain. Next, to facilitate digital implementation, we designed an event-based broadcast protocol which intermittently checks for events and makes broadcast decisions. In this regard, the methodology adopted also aids in designing the sampling instants for each node at which the events are checked (a subset of these instants are broadcast instants); this helps in mitigating network congestion. Finally, we demonstrate the results using a numerical example.

Chapter 8

Conclusions and Future Work

In this chapter, we make some concluding remarks on the studies in this thesis and, subsequently, offer some potential research directions and interesting problems for future work.

8.1 Conclusions

This thesis focuses on developing methodologies for implementing distributed algorithms over networks using tools from the theory of hybrid dynamical systems. The outcomes of the work in the thesis are summarized as follows:

1. First, we considered a single CT nonlinear system that can be stabilized by a static state feedback controller. Using an emulation-based technique, we designed two dynamic ETMs that govern the instants at which the system can broadcast its state to the controller and achieve asymptotic stability. The design methodologies adopted are Zeno-free and are such that the ETCs are evaluated intermittently at pre-defined sampling instants (either periodic or aperiodic); a subset of these sampling instants qualify as event-triggering/broadcast instants.

2. Second, we extended the study from single systems to MASs interacting over networks. We developed a general framework for distributed control of agents that employed the designed dynamic ETMs to make decisions

on the broadcast instants; these mechanisms are based on an agent's ability or inability to sense states (or relative states) of fellow agents in the network at its own sampling instants. The ETC on the agents can be evaluated both aperiodically and asynchronously; this notion helps reduce network congestion even in cases where the ETMs are rendered redundant and the agents are forced to broadcast at every sampling instant. Furthermore, to broaden the scope of application, we considered that each agent employs a model-based controller that propagates the broadcasted state upon arrival. We demonstrated the effectiveness of the developed framework through two case studies on consensus of nonlinear MASs (with Lipschitz and one-sided Lipschitz dynamics), interacting over both undirected and directed networks.

3. Third, we adopted the framework developed for distributed control via dynamic ETMs to handle a particular kind of NIP, namely, quantized broadcasts. In this case, we studied the consensus problem involving one-sided Lipschitz nonlinear agents interacting over a directed network. In addition to ETMs, we considered that the agents employed: a) encoders that quantized relevant information prior to broadcasting, and b) decoders that processed this information upon arrival. Subsequently, the agents utilized model-based propagates of the decoded neighbor states in their control protocols to achieve consensus asymptotically.

4. Fourth, we developed a framework for sampled-data distributed control of MASs to handle yet another important NIP, namely, transmission delays. The framework employed time-stamp techniques, i.e., each agent broadcasts both state and the time associated with it, and is designed for the general case where the agents employ model-based controllers. The methodology is such that the pre-defined sampling instants (at which agents broadcast information) can be both aperiodic and asynchronous in nature. As a consequence of the stability analysis, the upper bounds on: a) the sampling interval, and b) the transmission delays are estab-

lished without LMIs. We demonstrated the effectiveness of the methodology through a case study on consensus of Lipschitz nonlinear agents.

5. Finally, we considered a convex DOP where the agents: i) are assigned private local cost functions; ii) communicate over a weight-balanced directed network; and iii) employ AGFs to converge to the global minima. First, we proved that the CT algorithm converges asymptotically with a convergence rate that is proportional to the gradient gain which can be chosen arbitrarily. Subsequently, to facilitate networked implementation, each agent employed an ETM that intermittently evaluates the ETC and makes decision on broadcasting the local optimization variable.

8.2 Future Work

The future directions on the distributed control framework discussed in this thesis are summarized as follows:

1. **Robust to modeling errors:**

   The framework of distributed control discussed in Chapters 4, 5 and 6 employs a model-based framework for propagating broadcasted states. This approach generalizes the existing work which largely employs ZOH approach on these propagated states and, as a consequence, expands the scope of the framework. For instance, in the case of consensus problems involving (homogeneous) Lipschitz nonlinear agents, consensus is achieved under the assumption that the agents are *precisely* aware of their own dynamics. However, such an assumption may not always hold. Therefore, a challenging and promising research direction for the future would be to extend the framework, discussed (in Chapters 4 and 6) in this thesis, to handle modeling uncertainties and, consequently, make the framework more robust.

2. **Other NIPs:**

   In this thesis, we addressed two important imperfections, namely, quan-

tized broadcasts and transmission delays. In the case of quantized broadcasts considered in Chapter 5, the problem of determining saturation ranges is yet to be addressed. In addition to this there are several other imperfections, for instance, deterministic/random packet losses, inclusion of transmission protocols (such as round-robin (RR) or try-once-discard (TOD)) in the case of model-based networked controls, and others. These problems are yet to be addressed and could result in fruitful future work.

3. **Necessary conditions on gains in distributed optimization:**
For networked implementation of algorithms, throughout this thesis we employ emulation-based techniques. In this regard, it was first essential to establish sufficiency conditions on the gains in the proposed CT accelerated algorithm in Chapter 7 similar to most of the existing literature in this context with the exception of [29]. In order to determine necessary conditions on gains $(\mathfrak{a}_{\{\}}, \mathfrak{b}_{\{\}})$ for distributed optimization algorithms taking the following forms (or their variations):

Generalization of algorithm in [45]:
- Second order (x, q)

$$\begin{bmatrix} \dot{x} \\ \dot{q} \end{bmatrix} = \underbrace{\begin{bmatrix} -\mathfrak{a}_2 \mathsf{L} & \mathfrak{a}_1 \mathbb{I} \\ \mathsf{L} & \mathbf{0} \end{bmatrix}}_{\bar{A}} \begin{bmatrix} x \\ q \end{bmatrix} + \underbrace{\begin{bmatrix} -\mathfrak{b}_1 \nabla f \\ \mathbf{0} \end{bmatrix}}_{\text{ext. input}}.$$

Algorithm in Chapter 7:
- Third order (x, v, q)

$$\begin{bmatrix} \dot{x} \\ \dot{v} \\ \dot{q} \end{bmatrix} = \underbrace{\begin{bmatrix} -\mathfrak{a}_2 \mathsf{L} & \mathfrak{a}_1 \mathbb{I} & \mathbf{0} \\ \mathbf{0} & -\mathfrak{b}_2 \mathbb{I} & -\mathfrak{b}_3 \mathbb{I} \\ \mathsf{L} & \mathbf{0} & \mathbf{0} \end{bmatrix}}_{\bar{A}} \begin{bmatrix} x \\ v \\ q \end{bmatrix} + \underbrace{\begin{bmatrix} \mathbf{0} \\ -\mathfrak{b}_1 \nabla f \\ \mathbf{0} \end{bmatrix}}_{\text{ext. input}},$$

we must ensure that the state matrix $\bar{A}$ in the above equations is Hurwitz and study the system's properties around the equilibrium. Currently, with the exception of [29], this problem is largely unanswered. Addressing this problem also allows for relaxation of the assumption on strong convexity of the local objective functions that was used in Chapter 7.

Bibliography

[1] K. J. Åström and B. Bernhardsson. Comparison of periodic and event based sampling for first-order stochastic systems. *IFAC Proceedings Volumes*, 32(2):5006–5011, 1999.

[2] J. Baillieul and P. J. Antsaklis. Control and communication challenges in networked real-time systems. *Proceedings of the IEEE*, 95(1):9–28, 2007.

[3] D. Bertsekas and J. Tsitsiklis. *Parallel and distributed computation: numerical methods*. Athena Scientific, 2015.

[4] D. P. Borgers, V. S. Dolk, and W. P. M. H. Heemels. Dynamic periodic event-triggered control for linear systems. In *Proceedings of the 20th International Conference on Hybrid Systems: Computation and Control*, pages 179–186, 2017.

[5] S. Boyd, N. Parikh, and E. Chu. *Distributed Optimization and Statistical Learning via the Alternating Direction Method of Multipliers*. Now Publishers Inc, 2011.

[6] R. W. Brockett and D. Liberzon. Quantized feedback stabilization of linear systems. *IEEE Transactions on Automatic Control*, 45(7):1279–1289, 2000.

[7] J. Cao, S. Zhong, and Y. Hu. Novel delay-dependent stability conditions for a class of mimo networked control systems with nonlinear perturbation. *Applied Mathematics and Computation*, 197(2):797–809, 2008.

[8] F. Ceragioli, C. De Persis, and P. Frasca. Discontinuities and hysteresis in quantized average consensus. *Automatica*, 47(9):1916–1928, 2011.

[9] C. P. Chen, G.-X. Wen, Y.-J. Liu, and F.-Y. Wang. Adaptive consensus control for a class of nonlinear multiagent time-delay systems using neural networks. *IEEE Transactions on Neural Networks and Learning Systems*, 25(6):1217–1226, 2014.

[10] T. Chen and B. A. Francis. Input-output stability of sampled-data systems. *IEEE Transactions on Automatic Control*, 36(1):50–58, 1991.

[11] W. Chen and W. Ren. Event-triggered zero-gradient-sum distributed consensus optimization over directed networks. *Automatica*, 65:90–97, 2016.

[12] F. H. Clarke. *Optimization and Nonsmooth Analysis*. New York: Interscience, 1983.

[13] J. Cortés. Finite-time convergent gradient flows with applications to network consensus. *Automatica*, 42(11):1993–2000, 2006.

[14] J. Cortés. Distributed algorithms for reaching consensus on general functions. *Automatica*, 44(3):726–737, 2008.

[15] C. De Persis, E. R. Weitenberg, and F. Dörfler. A power consensus algorithm for dc microgrids. *Automatica*, 89:364–375, 2018.

[16] C. Deng, W.-W. Che, and Z.-G. Wu. A dynamic periodic event-triggered approach to consensus of heterogeneous linear multiagent systems with time-varying communication delays. *IEEE Transactions on Cybernetics*, 51(4):1812–1821, 2020.

[17] M. H. Dhullipalla, H. Yu, and T. Chen. Dynamic periodic event-triggered control for nonlinear plants with state feedback. *IFAC-PapersOnLine*, 53(2):2814–2819, 2020.

[18] M. H. Dhullipalla, H. Yu, and T. Chen. A framework for distributed control via dynamic periodic event-triggering mechanisms. *Automatica*, 146:110548, 2022.

[19] D. V. Dimarogonas and K. H. Johansson. Stability analysis for multi-agent systems using the incidence matrix: Quantized communication and formation control. *Automatica*, 46(4):695–700, 2010.

[20] L. Ding and G. Guo. Sampled-data leader-following consensus for nonlinear multi-agent systems with markovian switching topologies and communication delay. *Journal of the Franklin Institute*, 352(1):369–383, 2015.

[21] L. Ding, Q.-L. Han, X. Ge, and X.-M. Zhang. An overview of recent advances in event-triggered consensus of multiagent systems. *IEEE Transactions on Cybernetics*, 48(4):1110–1123, 2017.

[22] L. Ding, Q.-L. Han, and G. Guo. Network-based leader-following consensus for distributed multi-agent systems. *Automatica*, 49(7):2281–2286, 2013.

[23] V. S. Dolk, D. P. Borgers, and W. P. M. H. Heemels. Output-based and decentralized dynamic event-triggered control with guaranteed $\mathcal{L}_p$-gain performance and Zeno-freeness. *IEEE Transactions on Automatic Control*, 62(1):34–49, 2017.

[24] M. Fiedler. Algebraic connectivity of graphs. *Czechoslovak Mathematical Journal*, 23(2):298–305, 1973.

[25] H. Gao, T. Chen, and J. Lam. A new delay system approach to network-based control. *Automatica*, 44(1):39–52, 2008.

[26] E. Garcia and P. Antsaklis. Model-based event-triggered control for systems with quantization and time-varying network delays. *IEEE Transactions on Automatic Control*, 58(2):422–434, 2012.

[27] E. Garcia, Y. Cao, H. Yu, P. J. Antsaklis, and D. Casbeer. Decentralised event-triggered cooperative control with limited communication. *International Journal of Control*, 86(9):1479–1488, 2013.

[28] X. Ge, Q.-L. Han, D. Ding, X. Zhang, and B. Ning. A survey on recent advances in distributed sampled-data cooperative control of multi-agent systems. *Neurocomputing*, 275:1684–1701, 2018.

[29] B. Gharesifard and J. Cortés. Distributed continuous-time convex optimization on weight-balanced digraphs. *IEEE Transactions on Automatic Control*, 59(3):781–786, 2013.

[30] A. Girard. Dynamic triggering mechanisms for event-triggered control. *IEEE Transactions on Automatic Control*, 60(7):1992–1997, 2015.

[31] R. Goebel, R. G. Sanfelice, and A. R. Teel. *Hybrid Dynamical Systems: Modeling, Stability, and Robustness*. Princeton University Press, 2012.

[32] G. Guo, L. Ding, and Q.-L. Han. A distributed event-triggered transmission strategy for sampled-data consensus of multi-agent systems. *Automatica*, 50(5):1489–1496, 2014.

[33] M. Guo and D. V. Dimarogonas. Consensus with quantized relative state measurements. *Automatica*, 49(8):2531–2537, 2013.

[34] W. He, B. Zhang, Q.-L. Han, F. Qian, J. Kurths, and J. Cao. Leader-following consensus of nonlinear multiagent systems with stochastic sampling. *IEEE Transactions on Cybernetics*, 47(2):327–338, 2016.

[35] W. P. M. H. Heemels, M. C. F. Donkers, and A. R. Teel. Periodic event-triggered control for linear systems. *IEEE Transactions on Automatic Control*, 58(4):847–861, 2012.

[36] W. P. M. H. Heemels, D. Nešić, A. R. Teel, and N. van de Wouw. Networked and quantized control systems with communication delays.

In *Proceedings of the 48th IEEE Conference on Decision and Control (CDC) and 28th Chinese Control Conference (CCC)*, pages 7929–7935, 2009.

[37] W. P. M. H. Heemels, R. Postoyan, M. Donkers, A. R. Teel, A. Anta, P. Tabuada, and D. Nešić. Periodic event-triggered control. *Event-Based Control and Signal Processing*, pages 105–119, 2015.

[38] W. P. M. H. Heemels, A. R. Teel, N. van de Wouw, and D. Nešić. Networked control systems with communication constraints: Tradeoffs between transmission intervals, delays and performance. *IEEE Transactions on Automatic control*, 55(8):1781–1796, 2010.

[39] J. P. Hespanha, P. Naghshtabrizi, and Y. Xu. A survey of recent results in networked control systems. *Proceedings of the IEEE*, 95(1):138–162, 2007.

[40] A. Jadbabaie, N. Motee, and M. Barahona. On the stability of the kuramoto model of coupled nonlinear oscillators. In *Proceedings of the American Control Conference (ACC)*, volume 5, pages 4296–4301, 2004.

[41] M. Ji and M. Egerstedt. Distributed coordination control of multiagent systems while preserving connectedness. *IEEE Transactions on Robotics*, 23(4):693–703, 2007.

[42] K. H. Johansson, M. Egerstedt, J. Lygeros, and S. Sastry. On the regularization of Zeno hybrid automata. *Systems and Control Letters*, 38(3):141–150, 1999.

[43] I. Karafyllis and C. Kravaris. Global stability results for systems under sampled-data control. *International Journal of Robust and Nonlinear Control*, 19(10):1105–1128, 2009.

[44] H. K. Khalil. *Nonlinear Systems*. Prentice Hall, 2002.

[45] S. S. Kia, J. Cortés, and S. Martínez. Distributed convex optimization via continuous-time coordination algorithms with discrete-time communication. *Automatica*, 55:254 – 264, 2015.

[46] H. Kim, H. Shim, and J. H. Seo. Output consensus of heterogeneous uncertain linear multi-agent systems. *IEEE Transactions on Automatic Control*, 56(1):200–206, 2010.

[47] J. R. T. Lawton, R. W. Beard, and B. J. Young. A decentralized approach to formation maneuvers. *IEEE Transactions on Robotics and Automation*, 19(6):933–941, 2003.

[48] L. Li, D. W. Ho, and J. Lu. A unified approach to practical consensus with quantized data and time delay. *IEEE Transactions on Circuits and Systems I: Regular Papers*, 60(10):2668–2678, 2013.

[49] T. Li and L. Xie. Distributed coordination of multi-agent systems with quantized-observer based encoding-decoding. *IEEE Transactions on Automatic Control*, 57(12):3023–3037, 2012.

[50] Y. Li, J. Xiang, and W. Wei. Consensus problems for linear time-invariant multi-agent systems with saturation constraints. *IET Control Theory & Applications*, 5(6):823–829, 2011.

[51] Z. Li, W. Ren, X. Liu, and M. Fu. Consensus of multi-agent systems with general linear and lipschitz nonlinear dynamics using distributed adaptive protocols. *IEEE Transactions on Automatic Control*, 58(7):1786–1791, 2012.

[52] Z. Li, Z. Wu, Z. Li, and Z. Ding. Distributed optimal coordination for heterogeneous linear multiagent systems with event-triggered mechanisms. *IEEE Transactions on Automatic Control*, 65(4):1763–1770, 2019.

[53] D. Liberzon, D. Nesic, and A. R. Teel. Lyapunov-based small-gain theorems for hybrid systems. *IEEE Transactions on Automatic Control*, 59(6):1395–1410, 2014.

[54] K.-Z. Liu, A. R. Teel, X.-M. Sun, and X.-F. Wang. Model-based dynamic event-triggered control for systems with uncertainty: a hybrid system approach. *IEEE Transactions on Automatic Control*, 66(1):444–451, 2020.

[55] X. Liu, H. J. Marquez, K. D. Kumar, and Y. Lin. Sampled-data control of networked nonlinear systems with variable delays and drops. *International Journal of Robust and Nonlinear Control*, 25(1):72–87, 2015.

[56] N. A. Lynch. *Distributed algorithms*. Elsevier, 1996.

[57] J. Ma, L. Liu, H. Ji, and G. Feng. Quantized consensus of multiagent systems by event-triggered control. *IEEE Transactions on Systems, Man, and Cybernetics: Systems*, 50(9):3231–3242, 2018.

[58] Q. Ma, J. Lu, and H. Xu. Consensus for nonlinear multi-agent systems with sampled data. *Transactions of the Institute of Measurement and Control*, 36(5):618–626, 2014.

[59] M. Mazo, A. Anta, and P. Tabuada. An ISS self-triggered implementation of linear controllers. *Automatica*, 46(8):1310 – 1314, 2010.

[60] X. Meng and T. Chen. Event based agreement protocols for multi-agent networks. *Automatica*, 49(7):2125–2132, 2013.

[61] X. Meng, L. Xie, and Y. C. Soh. Asynchronous periodic event-triggered consensus for multi-agent systems. *Automatica*, 84:214–220, 2017.

[62] M. Mesbahi and M. Egerstedt. *Graph Theoretic Methods in Multiagent Networks*. Princeton University Press, 2010.

[63] L. A. Montestruque and P. J. Antsaklis. On the model-based control of networked systems. *Automatica*, 39(10):1837–1843, 2003.

[64] P. Naghshtabrizi, J. P. Hespanha, and A. R. Teel. Stability of delay impulsive systems with application to networked control systems. *Transactions of the Institute of Measurement and Control*, 32(5):511–528, 2010.

[65] A. Nedić and A. Ozdaglar. Distributed subgradient methods for multi-agent optimization. *IEEE Transactions on Automatic Control*, 54(1):48–61, 2009.

[66] D. Nešić, A. R. Teel, and P. V. Kokotović. Sufficient conditions for stabilization of sampled-data nonlinear systems via discrete-time approximations. *Systems & Control Letters*, 38(4-5):259–270, 1999.

[67] Y. E. Nesterov. A method for solving the convex programming problem with convergence rate $o(1/k^2)$. In *Doklady Akademii Nauk SSSR*, volume 269, pages 543–547, 1983.

[68] D. Nešić and A. R. Teel. Input-output stability properties of networked control systems. *IEEE Transactions on Automatic Control*, 49(10):1650–1667, 2004.

[69] D. Nešić, A. R. Teel, and D. Carnevale. Explicit computation of the sampling period in emulation of controllers for nonlinear sampled-data systems. *IEEE Transactions on Automatic Control*, 54(3):619–624, March 2009.

[70] R. Olfati-Saber, J. A. Fax, and R. M. Murray. Consensus and cooperation in networked multi-agent systems. *Proceedings of the IEEE*, 95(1):215–233, 2007.

[71] R. Olfati-Saber and R. M. Murray. Consensus problems in networks of agents with switching topology and time-delays. *IEEE Transactions on Automatic Control*, 49(9):1520–1533, 2004.

[72] A. Papachristodoulou, A. Jadbabaie, and U. Münz. Effects of delay in multi-agent consensus and oscillator synchronization. *IEEE Transactions on Automatic Control*, 55(6):1471–1477, 2010.

[73] I. G. Polushin, P. X. Liu, and C.-H. Lung. On the model-based approach to nonlinear networked control systems. *Automatica*, 44(9):2409–2414, 2008.

[74] I. G. Polushin and H. J. Marquez. Multirate versions of sampled-data stabilization of nonlinear systems. *Automatica*, 40(6):1035–1041, 2004.

[75] B. T. Polyak. Some methods of speeding up the convergence of iteration methods. *USSR Computational Mathematics and Mathematical Physics*, 4(5):1–17, 1964.

[76] R. Postoyan, A. Anta, W. P. M. H. Heemels, P. Tabuada, and D. Nešić. Periodic event-triggered control for nonlinear systems. In *52nd IEEE Conference on Decision and Control (CDC)*, pages 7397–7402, 2013.

[77] R. Postoyan, A. Anta, D. Nešić, and P. Tabuada. A unifying lyapunov-based framework for the event-triggered control of nonlinear systems. In *50th IEEE Conference on Decision and Control and European Control Conference*, pages 2559–2564, Dec 2011.

[78] L. Praly and Y. Wang. Stabilization in spite of matched unmodeled dynamics and an equivalent definition of input-to-state stability. *Mathematics of Control, Signals and Systems*, 9:1–33, 1996.

[79] F.-L. Qu, Z.-H. Guan, D.-X. He, and M. Chi. Event-triggered control for networked control systems with quantization and packet losses. *Journal of the Franklin Institute*, 352(3):974–986, 2015.

[80] M. G. Rabbat and R. Nowak. Distributed optimization in sensor networks. In *Proceedings of the 3rd International Symposium on Information Processing in Sensor Networks*, pages 20–27, 2004.

[81] F. Rasool, D. Huang, and S. K. Nguang. Robust $\mathcal{H}_\infty$ output feedback control of networked control systems with multiple quantizers. *Journal of the Franklin Institute*, 349(3):1153–1173, 2012.

[82] W. Ren and R. W. Beard. Decentralized scheme for spacecraft formation flying via the virtual structure approach. *Journal of Guidance, Control, and Dynamics*, 27(1):73–82, 2004.

[83] W. Ren and R. W. Beard. Consensus seeking in multiagent systems under dynamically changing interaction topologies. *IEEE Transactions on Automatic Control*, 50(5):655–661, 2005.

[84] W. Ren, R. W. Beard, and E. M. Atkins. A survey of consensus problems in multi-agent coordination. In *Proceedings of the American Control Conference (ACC)*, pages 1859–1864, 2005.

[85] W. Ren, R. W. Beard, and T. W. McLain. Coordination variables and consensus building in multiple vehicle systems. In *Cooperative control*, pages 171–188. Springer, 2005.

[86] W. Ren and Y. Cao. Convergence of sampled-data consensus algorithms for double-integrator dynamics. In *47th IEEE Conference on Decision and Control (CDC)*, pages 3965–3970, 2008.

[87] W. Ren and N. Sorensen. Distributed coordination architecture for multi-robot formation control. *Robotics and Autonomous Systems*, 56(4):324–333, 2008.

[88] D. Romeres, F. Dörfler, and F. Bullo. Novel results on slow coherency in consensus and power networks. In *Proceedings of the European Control Conference (ECC)*, pages 742–747, 2013.

[89] R. O. Saber and R. M. Murray. Consensus protocols for networks of dynamic agents. In *Proceedings of the American Control Conference (ACC)*, volume 2, pages 951–956, 2003.

[90] K. J. A. Scheres, V. S. Dolk, M. S. Chong, R. Postoyan, and W. P. M. H. Heemels. Distributed periodic event-triggered control of nonlinear multi-agent systems. *IFAC-PapersOnLine*, 55(13):168–173, 2022.

[91] W. Su, S. Boyd, and E. Candes. A differential equation for modeling nesterov's accelerated gradient method: Theory and insights. *Advances in Neural Information Processing Systems*, 27:2510–2518, 2014.

[92] Y. Sun, L. Li, and D. W. C. Ho. Quantized synchronization control of networked nonlinear systems: Dynamic quantizer design with event-triggered mechanism. *IEEE Transactions on Cybernetics*, 2021.

[93] Y. G. Sun and L. Wang. Consensus of multi-agent systems in directed networks with nonuniform time-varying delays. *IEEE Transactions on Automatic Control*, 54(7):1607–1613, 2009.

[94] P. Tabuada. Event-triggered real-time scheduling of stabilizing control tasks. *IEEE Transactions on Automatic Control*, 52(9):1680–1685, 2007.

[95] H. G. Tanner, A. Jadbabaie, and G. J. Pappas. Flocking in fixed and switching networks. *IEEE Transactions on Automatic control*, 52(5):863–868, 2007.

[96] A. R. Teel and L. Praly. On assigning the derivative of a disturbance attenuation control lyapunov function. *Mathematics of Control, Signals and Systems*, 13(2):95–124, 2000.

[97] N.-T. Tran, Y.-W. Wang, X.-K. Liu, J.-W. Xiao, and Y. Lei. Distributed optimization problem for second-order multi-agent systems with event-triggered and time-triggered communication. *Journal of the Franklin Institute*, 356(17):10196–10215, 2019.

[98] W. Wang, R. Postoyan, D. Nešić, and W. P. M. H. Heemels. Periodic event-triggered control for nonlinear networked control systems. *IEEE Transactions on Automatic Control*, 65(2):620–635, 2019.

[99] W. Wang, R. Postoyan, D. Nešić, and W. P. M. H. Heemels. Stabilization of nonlinear systems using state-feedback periodic event-triggered controllers. In *55th IEEE Conference on Decision and Control (CDC)*, pages 6808–6813, Dec 2016.

[100] W. Wang, R. Postoyan, D. Nešić, and W. P. M. H. Heemels. Periodic event-triggered control for nonlinear networked control systems. *IEEE Transactions on Automatic Control*, 65(2):620–635, 2020.

[101] X. Wang and M. D. Lemmon. Event-triggering in distributed networked control systems. *IEEE Transactions on Automatic Control*, 56(3):586–601, 2010.

[102] E. Wei, A. Ozdaglar, and A. Jadbabaie. A distributed newton method for network utility maximization–i: Algorithm. *IEEE Transactions on Automatic Control*, 58(9):2162–2175, 2013.

[103] J. Wei, X. Yi, H. Sandberg, and K. H. Johansson. Nonlinear consensus protocols with applications to quantized communication and actuation. *IEEE Transactions on Control of Network Systems*, 6(2):598–608, 2018.

[104] G. Wen, Z. Duan, W. Yu, and G. Chen. Consensus of multi-agent systems with nonlinear dynamics and sampled-data information: a delayed-input approach. *International Journal of Robust and Nonlinear Control*, 23(6):602–619, 2013.

[105] C. Wu, X. Zhao, W. Xia, J. Liu, and T. Başar. $\mathcal{L}_2$-gain analysis for dynamic event-triggered networked control systems with packet losses and quantization. *Automatica*, 129:109587, 2021.

[106] Y. Wu, H. Su, P. Shi, Z. Shu, and Z.-G. Wu. Consensus of multiagent systems using aperiodic sampled-data control. *IEEE Transactions on Cybernetics*, 46(9):2132–2143, 2015.

[107] F. Xiao and L. Wang. Asynchronous consensus in continuous-time multi-agent systems with switching topology and time-varying delays. *IEEE Transactions on Automatic Control*, 53(8):1804–1816, 2008.

[108] H.-R. Yang and W. Ni. Continuous-time distributed heavy-ball algorithm for distributed convex optimization over undirected and directed graphs. *Machine Intelligence Research*, 19(1):75–88, 2022.

[109] T. Yang, X. Yi, J. Wu, Y. Yuan, D. Wu, Z. Meng, Y. Hong, H. Wang, Z. Lin, and K. H. Johansson. A survey of distributed optimization. *Annual Reviews in Control*, 47:278 – 305, 2019.

[110] X. Yi, L. Yao, T. Yang, J. George, and K. H. Johansson. Distributed optimization for second-order multi-agent systems with dynamic event-triggered communication. In *IEEE Conference on Decision and Control (CDC)*, pages 3397–3402, 2018.

[111] H. Yu and T. Chen. A new Zeno-free event-triggered scheme for robust distributed optimal coordination. *Automatica*, 129, 109639, 2021.

[112] H. Yu and T. Chen. Model-based networked control for nonlinear systems with transmission delays. In *13th IEEE Asian Control Conference (ASCC)*, pages 1856–1861, 2022.

[113] H. Yu, M. H. Dhullipalla, and T. Chen. A generalized algorithm for continuous-time distributed optimization. In *Proceedings of the American Control Conference (ACC)*, pages 820–825, 2021.

[114] M. Yu, L. Wang, and T. Chu. Sampled-data stabilisation of networked control systems with nonlinearity. *IEE Proceedings-Control Theory and Applications*, 152(6):609–614, 2005.

[115] P. Yu and D. V. Dimarogonas. Explicit computation of sampling period in periodic event-triggered multiagent control under limited data

rate. *IEEE Transactions on Control of Network Systems*, 6(4):1366–1378, 2018.

[116] W. Yu, G. Chen, and M. Cao. Consensus in directed networks of agents with nonlinear dynamics. *IEEE Transactions on Automatic Control*, 56(6):1436–1441, 2011.

[117] W. Yu, P. Yi, and Y. Hong. A gradient-based dissipative continuous-time algorithm for distributed optimization. In *Proceedings of the Chinese Control Conference (CCC)*, pages 7908–7912, 2016.

[118] H. Zhang and J. Chen. Bipartite consensus of general linear multi-agent systems. In *Proceedings of the American Control Conference (ACC)*, pages 808–812, 2014.

[119] J. Zhang, C. A. Uribe, A. Mokhtari, and A. Jadbabaie. Achieving acceleration in distributed optimization via direct discretization of the heavy-ball ode. In *Proceedings of the American Control Conference (ACC)*, pages 3408–3413, 2019.

[120] L. Zhang, H. Gao, and O. Kaynak. Network-induced constraints in networked control systems—a survey. *IEEE Transactions on Industrial Informatics*, 9(1):403–416, 2012.

[121] X.-M. Zhang, Q.-L. Han, X. Ge, D. Ding, L. Ding, D. Yue, and C. Peng. Networked control systems: A survey of trends and techniques. *IEEE/CAA Journal of Automatica Sinica*, 7(1):1–17, 2019.

[122] Y. Zhang and Y. Hong. Distributed optimization design for second-order multi-agent systems. In *Proceedings of the Chinese Control Conference (CCC)*, pages 1755–1760, 2014.

[123] Z. Zhang, L. Zhang, F. Hao, and L. Wang. Periodic event-triggered consensus with quantization. *IEEE Transactions on Circuits and Systems II: Express Briefs*, 63(4):406–410, 2015.

[124] Z. Zhang, L. Zhang, F. Hao, and L. Wang. Leader-following consensus for linear and lipschitz nonlinear multiagent systems with quantized communication. *IEEE Transactions on Cybernetics*, 47(8):1970–1982, 2016.

[125] S. Zheng, P. Shi, R. K. Agarwal, and C. P. Lim. Periodic event-triggered output regulation for linear multi-agent systems. *Automatica*, 122:109223, 2020.

[126] M. Zhu and S. Martínez. On distributed convex optimization under inequality and equality constraints. *IEEE Transactions on Automatic Control*, 57(1):151–164, 2011.

[127] L. Zou, Z. Wang, Q.-L. Han, and D. Zhou. Ultimate boundedness control for networked systems with try-once-discard protocol and uniform quantization effects. *IEEE Transactions on Automatic Control*, 62(12):6582–6588, 2017.

Appendix A

In this appendix, we collect proofs of theorems and lemmas presented in this thesis.

A.1 For Chapter 4

A.1.1 On Non-negativeness of η_i

Lemma A.1. *For all $i \in \mathcal{V}$, let the initial state $\eta_{i,0} \geq 0$. If the functions (f_η^i, g_s^i, g_t^i) in* (4.5) *are as described in Section 4.2, then the ETM in* (4.6) *ensures that η_i stays non-negative.*

Proof. Since the initial condition $\eta_{i,0} \geq 0$, $\forall i \in \mathcal{V}$, without loss of generality, we consider that $\eta_i(s_k^i) \geq 0$ for some $k \in \mathbb{Z}_{\geq 0}$.

First, we discuss the flow of η_i in $t \in [s_k^i, s_{k+1}^i)$. In this case, η_i flows along the continuous function $f_\eta^i(\eta_i, \hat{x}_{\bar{\mathcal{N}}^i})$ until: a) it encounters jumps in the MAS (caused by events among neighboring agents) during (s_k^i, s_{k+1}^i), or b) the next sampling instant s_{k+1}^i. In case a), if agent $j \in \mathcal{N}^i$ broadcasts its state information (broadcasts are assumed to be finite), then at $s_{k'}^j \in (s_k^i, s_{k+1}^i)$, the MAS in (4.8) experiences jump as a result, $\hat{x}_j$ is updated, $\eta_i^+ = \eta_i(t^+ = s_{k'}^j)$, and the function $f_\eta^i(\eta_i, \hat{x}_{\bar{\mathcal{N}}^i}(t^+ = s_{k'}^j))$ may jump to a finite point such that $f_\eta^i(\eta_i, \hat{x}_{\bar{\mathcal{N}}^i}(t^+ = s_{k'}^j)) \neq f_\eta^i(\eta_i, \hat{x}_{\bar{\mathcal{N}}^i}(t))$. However, since the solution S_{η_i} exists for every $\hat{x}_{\bar{\mathcal{N}}^i} \in \mathbb{R}^{nN}$, η_i continues to flow along the revised function f_η^i until it encounters either of the aforementioned cases (i.e., case a) or b)) again. As a result, $\eta_i(t)$ is continuous on $[s_k^i, s_{k+1}^i)$. If $\forall t \in [s_k^i, s_{k+1}^i)$, $f_\eta^i \geq 0$, then

$\eta_i(t) \geq 0$. If there exists $t' \in [s_k^i, s_{k+1}^i)$ such that $\eta_i(t') = 0$, then since $f_\eta^i(0,\cdot) \geq 0$, $\eta_i(t > t') \geq 0$.

Next, we discuss the jumps of η_i at s_{k+1}^i. At s_{k+1}^i, the event-triggering condition in (4.6) is evaluated to decide the jump state of η_i. As seen in (4.5), broadcast states of agents across the network, at s_{k+1}^i, do not affect g_s^i and g_t^i. If $g_s^i < 0$, then $\eta_i^+ = \eta_i(s_{k+1}^i) = g_t^i \geq 0$. On the otherhand, if $g_s^i \geq 0$, then $\eta_i^+ = \eta_i(s_{k+1}^i) = g_s^i \geq 0$. □

A.1.2 Proof of Theorem 4.3

In order to prove that the dynamic ETMs associated with (4.11) and (4.18) ensure asymptotic stability of (4.26), it suffices to determine appropriate functions W_i, V_i, V and $\tilde{V}_i$ that satisfy Assumptions 4.1–4.4 stated in Subsections 4.3.1 and 4.3.2. Therefore, we address the proof in two parts by considering a constant control gain $\kappa = \mathfrak{p}\kappa_0$, $\mathfrak{p} > 1$, that complies with (4.27).

Part 1: Broadcasting. For this, consider $W_i = |e_i|$ and $V = \frac{K}{2}|z|^2$ where $z = \mathsf{L}x$ and $K > 0$.

(**1.1**) Under Assumption 4.1, it is straightforward to see that the candidate function $|e_i|$ satisfies Assumption 4.1(a). For Assumption 4.1(b), we evaluate $\dot{W}_i$ as:

$$\begin{aligned}\dot{W}_i &\leq |\bar{f}(\hat{x}_i) - \bar{f}(x_i) + \kappa\mathsf{L}(x+e)| \\ &= \mathcal{L}|e_i| + \kappa|d_i e_i - \mathsf{A}_i e + \mathsf{L}_i x| \\ &\leq (\mathcal{L} + \kappa d_i)W_i + \kappa|-\mathsf{A}_i e + z_i|, \end{aligned} \tag{A.1}$$

where d_i is the degree of agent i, $z_i = \mathsf{L}_i x$, A_i is the i-th row of adjacency matrix A and H_i is such that:

$$H_i^2(x,e) = 2\kappa^2\big(|\mathsf{A}_i|^2|e|^2 + z_i^2\big).$$

(**1.2**) Consider $V = \frac{K}{2}|z|^2$ and let the stability set be $\Theta(x) = \mathsf{L}x$, then Assumption 4.2(a) holds. To evaluate Assumption 4.2(b), we examine the derivative of V which is given by $\dot{V} = Kz^{\mathrm{T}}\big(\mathsf{L}[\bar{f}] - \kappa\mathsf{L}(z + \mathsf{L}e)\big)$. Here, the 1st term in $\dot{V}$

can be simplified as follows using a design parameter $\epsilon_1 > 0$:

$$\begin{aligned} z^{\mathrm{T}}\mathsf{L}[\bar{f}] &= \sum_{i\in\mathcal{V}} z_i(\mathsf{L}_i[\bar{f}](x)) \le \sum_{i\in\mathcal{V}} |z_i||\sum_{j\in\mathcal{V}} a_{ij}(f(x_i)-f(x_j))| \\ &\le \sum_{i\in\mathcal{V}} \frac{\mathcal{L}\epsilon_1 d_i}{2} z_i^2 + \frac{\mathcal{L}}{2\epsilon_1}\sum_{i,j\in\mathcal{V}} a_{ij}|x_i-x_j|^2 \\ &\le \frac{\mathcal{L}\epsilon_1 d_M}{2}|z|^2 + \frac{\mathcal{L}}{\epsilon_1\Lambda_2}|z|^2 \\ &= \Gamma_1|z|^2, \end{aligned} \tag{A.2}$$

where we used the well-known identity associated with connected undirected graphs:

$$\frac{1}{2}\sum_{i,j=1}^{N} a_{ij}|x_i-x_j|^2 = x^{\mathrm{T}}\mathsf{L}x \le \frac{1}{\Lambda_2}x^{\mathrm{T}}\mathsf{L}^2x.$$

Let $\epsilon_1 = \sqrt{2}(\sqrt{d_M\Lambda_2})^{-1}$, then Γ_1 in (A.2) reduces to $\Gamma_1 = \mathcal{L}\sqrt{\frac{2d_M}{\Lambda_2}}$. Next, the 2^{nd} term in $\dot{V}$ can be upper-bounded as: , i.e.,

$$\begin{aligned} -z^{\mathrm{T}}\mathsf{L}(z+\mathsf{L}e) \le & -\Big(\Lambda_2 - \frac{\Lambda_M^2}{2\epsilon_2}\Big)|z|^2 + \frac{\epsilon_2\Lambda_M^2}{2}|e|^2 \\ = & -\Big(\Lambda_2 - \frac{\Lambda_M^2}{2\epsilon_2}\Big)\Big(\pi_1|z|^2 + (1-\pi_1)|\mathsf{L}\hat{x}-\mathsf{L}e|^2\Big) + \frac{\epsilon_2\Lambda_M^2}{2}|e|^2 \\ \le & -\Xi_1|z|^2 + \sum_{i\in\mathcal{V}}\Big\{\Xi_3|e_i|^2 - \Xi_2|\mathsf{L}_i\hat{x}|^2\Big\}, \end{aligned} \tag{A.3}$$

where

$$\begin{aligned} \Xi_1 &= \Big(\Lambda_2 - \frac{\Lambda_M^2}{2\epsilon_2}\Big)\pi_1, \\ \Xi_2 &= \Big(\Lambda_2 - \frac{\Lambda_M^2}{2\epsilon_2}\Big)(1-\pi_1)(1-\xi_1), \\ \Xi_3 &= \Big[\frac{\epsilon_2}{2} + \Big(\Lambda_2 - \frac{\Lambda_M^2}{2\epsilon_2}\Big)(1-\pi_1)(\frac{1}{\xi_1}-1)\Big]\Lambda_M^2 \end{aligned}$$

and $\xi_1 \in (0,1]$. Using inequalities (A.2) and (A.3), the bound for $\dot{V}$ is given by:

$$\dot{V} \le -\Big(\Xi_1\kappa - \Gamma_1\Big)K|z|^2 + \sum_{i\in\mathcal{V}} K\kappa\Big\{\Xi_3|e_i|^2 - \Xi_2|\mathsf{L}_i\hat{x}|^2\Big\}, \tag{A.4}$$

where the positivity of $\Xi_1\kappa - \Gamma_1$ can be ensured by choosing the design parameters such that $\epsilon_2 \in (\frac{\Lambda_M^2}{2\Lambda_2}\frac{\mathfrak{p}}{\mathfrak{p}-1}, \infty)$ and $\pi_1 \in \big(\frac{\Lambda_2}{\mathfrak{p}}(\Lambda_2 - \frac{\Lambda_M^2}{2\epsilon_2})^{-1}, 1\big)$. Next, we evaluate $\sum_{i\in\mathcal{V}} H_i^2$ as follows:

$$\begin{aligned}\sum_{i\in\mathcal{V}} H_i^2 &= 2\kappa^2|z|^2 + 2\kappa^2\sum_{i\in\mathcal{V}}|\mathsf{A}_i|^2|e|^2 \\ &= \frac{4\kappa^2}{K}V + 2\kappa^2\mathrm{Tr}(\mathsf{A}^{\mathrm{T}}\mathsf{A})|e|^2.\end{aligned}$$

Adding and subtracting $\sum_{i\in\mathcal{V}} H_i^2$ from (A.4) results in:

$$\begin{aligned}\dot{V} \leq\ &-\Big(\Xi_1\kappa - \Gamma_1 - \frac{2\kappa^2}{K}\Big)K|z|^2 + \sum_{i\in\mathcal{V}}\Big\{\Big(K\kappa\Xi_3 + 2\kappa^2\mathrm{Tr}(\mathsf{A}^{\mathrm{T}}\mathsf{A})\Big)|e_i|^2 \\ &- K\kappa\Xi_2|\mathsf{L}_i\hat{x}|^2 - H_i^2\Big\}\end{aligned}$$

which satisfies Assumption 4.2(b) when K is chosen such that (4.32b) holds.

Hence, all the assumptions in Theorem 4.1 have been satisfied which directly concludes asymptotic stability w.r.t. (4.30).

Part 2: Active Sensing. Here, Assumption 4.1 is satisfied via (A.1). Before evaluating $\dot{V}$ to satisfy Assumption 4.3(b), we will ensure Assumption 4.3(d) is satisfied. For this, consider $V_i = \frac{K}{2}|z_i|^2$ where $z_i = \mathsf{L}_i x$; this satisfies Assumption 4.3(c).

(**2.1**) For Assumption 4.3(d), $\dot{V}_i$ takes the form $\dot{V}_i = Kz_i(\mathsf{L}_i[\bar{f}](x)) - K\kappa z_i(\mathsf{L}_i(z + \mathsf{L}e))$. Here, the 1st term can be upper-bounded, similar to (A.2), as:

$$\begin{aligned}z_i(\mathsf{L}_i[\bar{f}](x)) &\leq \mathcal{L}\sum_{j\in\mathcal{V}} a_{ij}\Big(\frac{\epsilon_3 z_i^2}{2} + \frac{|x_i - x_j|^2}{2\epsilon_3}\Big) \\ &= \frac{\mathcal{L}\epsilon_3 d_i}{2}z_i^2 + \frac{\mathcal{L}}{2\epsilon_3}\sum_{j\in\mathcal{V}} a_{ij}|x_i - x_j|^2, \qquad \text{(A.5)}\end{aligned}$$

and the 2nd term can be upper-bounded as:

$$\begin{aligned}-z_i(\mathsf{L}_i(z + \mathsf{L}e)) &= -d_i z_i^2 + z_i(\mathsf{A}_i z + \mathsf{L}_i\mathsf{L}e) \\ &\leq -\Big(d_i - \frac{\epsilon_4|\mathsf{A}_i|^2}{2} - \frac{\epsilon_5|\mathsf{L}_i|}{2}\Big)z_i^2 \\ &\quad + \frac{1}{2\epsilon_4}|z|^2 + \frac{|\mathsf{L}_i|\Lambda_M^2}{2\epsilon_5}|e|^2, \qquad \text{(A.6)}\end{aligned}$$

where $\epsilon_3,\ \epsilon_4,\ \epsilon_5 > 0$ are identical $\forall i \in \mathcal{V}$. Using inequalities (A.5), (A.6) the upper bound for $\dot{V}_i$ can be expressed as:

$$\dot{V}_i \leq -\Big(\Big(d_i - \frac{\epsilon_4|\mathsf{A}_i|^2}{2} - \frac{\epsilon_5|\mathsf{L}_i|}{2}\Big)\kappa - \frac{\mathcal{L}\epsilon_3 d_i}{2}\Big)Kz_i^2 + \frac{K}{4\kappa}\Big(\frac{2\kappa^2}{\epsilon_4}|z|^2 + \frac{2|\mathsf{L}_i|\Lambda_M^2\kappa^2}{\epsilon_5}|e|^2 + \frac{2\mathcal{L}\kappa}{\epsilon_3}\sum_{j\in\mathcal{V}} a_{ij}|x_i - x_j|^2\Big). \tag{A.7}$$

where $c_i = K/(4\kappa), \forall i \in \mathcal{V}$. Let $\epsilon_4 = \epsilon_5$ and let $\epsilon_3 = \epsilon_1$ where ϵ_1 is defined in Part 1 of this proof; then, the positivity of α_i is ensured by the choice of ϵ_4 in (4.32a) and ϵ_3. It is necessary to show that the numerator in the second argument of the min function in (4.32a) is positive; this is demonstrated as follows:

$$\begin{aligned} 2 - \mathcal{L}\frac{\epsilon_3}{\kappa} &= 2 - \mathcal{L}\frac{\sqrt{2}}{\sqrt{\Lambda_2 d_M}}\frac{1}{\mathfrak{p}}\frac{\Lambda_2\sqrt{\Lambda_2}}{\mathcal{L}\sqrt{2d_M}} \\ &= 2 - \frac{1}{\mathfrak{p}}\frac{\Lambda_2}{d_M} \\ &\geq 2 - \frac{1}{\mathfrak{p}}\frac{N}{N-1}\frac{d_m}{d_M} \\ &> 0, \end{aligned}$$

where $d_m = \min_i d_i$. Here, we recall that $\mathfrak{p} > 1$, use the well known upper-bound of $\Lambda_2 \leq \frac{N}{N-1}d_m$ (see [24]), and the fact that $d_m/d_M \leq 1$.

The inequality in (A.7) can be expressed in the form $\dot{V}_i \leq -\alpha_i V_i + c_i\big[\hat{H}_i^2 + \hat{J}_i\big]$ as in Assumption 4.3(d) where

$$\hat{H}_i^2 = H_i^2 = 2\kappa^2\big(|\mathsf{A}_i|^2|e|^2 + z_i^2\big)$$

and as a result $\hat{J}_i$ is

$$\hat{J}_i = 2\kappa^2\Big[\frac{|z|^2}{\epsilon_4} - z_i^2\Big] + 2\kappa^2\Big[\frac{|\mathsf{L}_i|\Lambda_M^2}{\epsilon_4} - |\mathsf{A}_i|^2\Big]|e|^2 + \frac{2\mathcal{L}\kappa}{\epsilon_3}\sum_{j\in\mathcal{V}} a_{ij}|x_i - x_j|^2 > 0.$$

Assumption 4.3(a) is the same as in Part 1 of the proof. For Assumption 4.3(b), we first sum $H_i^2 + \hat{J}_i$ over all agents which results in:

$$\sum_{i\in\mathcal{V}}(H_i^2 + \hat{J}_i) \leq \Big(\frac{2\kappa^2 N}{\epsilon_4 K} + \frac{4\kappa}{\epsilon_3 K}\frac{\mathcal{L}}{\Lambda_2}\Big)K|z|^2 + \Big(\frac{2\Lambda_M^2\kappa^2\sum_{i\in\mathcal{V}}|\mathsf{L}_i|}{\epsilon_4}\Big)|e|^2.$$

By adding and subtracting $\sum_{i\in\mathcal{V}}(H_i^2+\hat{J}_i)$ from the right-hand side of (A.4) gives:

$$\begin{aligned}\dot{V}\leq&-\Big(\Xi_1\kappa-\Gamma_1-\frac{2\kappa^2}{K}\Big(\frac{N}{\epsilon_4}+\frac{2}{\epsilon_3}\frac{\mathcal{L}}{\Lambda_2\kappa}\Big)\Big)K|z|^2\\&+\sum_{i\in\mathcal{V}}\Big\{\Big(K\kappa\Xi_3+\frac{2\Lambda_M^2\kappa^2\sum_{j\in\mathcal{V}}|\mathsf{L}_j|}{\epsilon_4}\Big)|e_i|^2\\&-K\kappa\Xi_2|\mathsf{L}_i\hat{x}|^2-H_i^2-J_i\Big\},\end{aligned}\tag{A.8}$$

where $J_i=\hat{J}_i$. Here, $H_i=\hat{H}_i$, $J_i=\hat{J}_i$ which satisfies Assumption 4.3(e). Finally, (A.8) takes the form $\dot{V}\leq-\alpha_V V+\sum_{i=1}^N\{\gamma_i^2|e_i|^2-\omega_i\hat{V}_i-H_i^2-J_i\}$ satisfying Assumption 4.3(d).

(**2.2**) For Assumption 4.4, we choose $\tilde{V}_i(x_{\underline{\mathcal{N}}_k^i})=V_i(x)$ since

$$V_i(x)=\frac{K}{2}|z_i|^2=\frac{K}{2}|\sum_{j\in\mathcal{V}}a_{ij}(x_j-x_i)|^2$$

depends only on neighbors' states.

Therefore, assumptions in Theorem 4.2 are met which concludes asymptotic stability w.r.t. (4.30). □

A.1.3 Proof of Theorem 4.4

Similar to the proof of Theorem 4.3, it suffices to determine appropriate functions $W_i(e_i)$, $V(x)$, $V_i(x)$, $\hat{V}_i(\hat{x}_{\bar{\mathcal{N}}^i})$ and $\tilde{V}_i(x_{\underline{\mathcal{N}}_k^i})$ that satisfy Assumptions 4.1–4.4 for the system in (4.26). Again, we address the proof in two parts by considering a given control gain $\kappa=\bar{\mathfrak{p}}\bar{\kappa}_0$, $\bar{\mathfrak{p}}>1$, that complies with (4.33).

Part 1: Broadcasting. Consider $W_i=|e_i|,\ \forall i\in\mathcal{V}$, and $V=\sum_{i\in\mathcal{V}}\frac{K}{2}\xi_i|x_i-\bar{x}|^2$, where $\bar{x}=\xi^{\mathrm{T}}x$, $e_i=\hat{x}_i-x_i$ and K is a positive constant.

(**1.1**) Since $W_i=|e_i|$, Assumption 4.1(b) is satisfied as follows:

$$\dot{W}_i\leq\max\{0,\mathcal{L}_{os}+\kappa d_i\}W_i+\kappa|-\mathsf{A}_ie+\mathsf{L}_ix|.\tag{A.9}$$

Similar to proof of Theorem 4.3, H_i is such that:

$$H_i^2=2\kappa^2\big(|\mathsf{A}_i|^2|e|^2+|\mathsf{L}_i(x-\mathbf{1}\bar{x})|^2\big),$$

since $\mathsf{L}_i\mathbf{1} = 0$.

(**1.2**) For Assumption 4.2, let $V(x) = \frac{K}{2}\sum_{i\in\mathcal{V}}\xi_i|x_i - \bar{x}|^2 = \frac{K}{2}x^{\mathrm{T}}M^{\mathrm{T}}\Xi Mx$ where $M = I_N - \mathbf{1}_N\xi^{\mathrm{T}}$ and $\Xi = \mathrm{diag}\{\xi_1, \cdots, \xi_N\}$. The derivative of V is given by $\dot{V} = Kx^{\mathrm{T}}M^{\mathrm{T}}\Xi M\big([\bar{f}](x) - \kappa(\mathsf{L}(x+e))\big)$ where we examine individual terms. First, we note that

$$x^{\mathrm{T}}M^{\mathrm{T}}\Xi M[\bar{f}](x) = x^{\mathrm{T}}M^{\mathrm{T}}\Xi\Big[[\bar{f}](x) - \mathbf{1}\xi^{\mathrm{T}}[\bar{f}](x)\Big] = x^{\mathrm{T}}M^{\mathrm{T}}\Xi[\bar{f}](x) \tag{A.10}$$

since $x^{\mathrm{T}}M^{\mathrm{T}}\Xi\mathbf{1} = \sum_{i=1}^{N}\xi_i(x_i - \bar{x}) = 0$. Subtracting $0 = x^{\mathrm{T}}M^{\mathrm{T}}\Xi\mathbf{1}\bar{f}(\bar{x})$ from (A.10) results in

$$\begin{aligned} x^{\mathrm{T}}M^{\mathrm{T}}\Xi M[\bar{f}](x) &= x^{\mathrm{T}}M^{\mathrm{T}}\Xi\big[[\bar{f}](x) - \mathbf{1}f(\bar{x})\big] \\ &= \sum_{i\in\mathcal{V}}\xi_i(x_i - \bar{x})^{\mathrm{T}}(f(x_i) - f(\bar{x})) \\ &\leq \mathcal{L}_{os}\sum_{i\in\mathcal{V}}\xi_i|x_i - \bar{x}|^2. \end{aligned}$$

Next, we investigate bound for the 2$^{\text{nd}}$ term in $\dot{V}$. Here, we use the property that $M\mathsf{L} = \mathsf{L}M - (\mathbf{1}\xi^{\mathrm{T}})\mathsf{L}$ which is straight forward to derive. Then, the bound for the 2$^{\text{nd}}$ term is as follows:

$$-\kappa x^{\mathrm{T}}M^{\mathrm{T}}\Xi M\mathsf{L}x = -\kappa x^{\mathrm{T}}M^{\mathrm{T}}\Xi\mathsf{L}Mx \leq -a_\xi(\mathsf{L})\kappa x^{\mathrm{T}}M^{\mathrm{T}}\Xi Mx.$$

The 3$^{\text{rd}}$ term, namely, $-\kappa x^{\mathrm{T}}M^{\mathrm{T}}\Xi M\mathsf{L}e$, is bounded as follows:

$$\begin{aligned} \kappa x^{\mathrm{T}}M^{\mathrm{T}}\Xi M\mathsf{L}e &= -\kappa x^{\mathrm{T}}M^{\mathrm{T}}\Xi\mathsf{L}Me = -\kappa x^{\mathrm{T}}M^{\mathrm{T}}\Xi\mathsf{L}e \\ &\leq \frac{\kappa}{2\epsilon_1}|\Xi Mx|^2 + \frac{\kappa\epsilon_1}{2}|\mathsf{L}e|^2 \\ &\leq \frac{\kappa}{\epsilon_1 K}V + \frac{\kappa\epsilon_1}{2}|\mathsf{L}e|^2, \end{aligned}$$

because $\Xi \succ \Xi^2$. Collectively, the bound on $\dot{V}$ can be expressed as:

$$\dot{V} \leq -\Big[\kappa\Big(2a_\xi(\mathsf{L}) - \frac{1}{\epsilon_1}\Big) - 2\mathcal{L}_{os}\Big]V - \frac{\kappa\epsilon_1 K\bar{\Lambda}_M^2}{2}|e|^2, \tag{A.11}$$

where $\bar{\Lambda}_M^2 = \max(\mathrm{eig}(\mathsf{L}^{\mathrm{T}}\mathsf{L}))$. Consider the following two inequalities:

$$\begin{aligned} \omega_i\hat{V}_i(\hat{x}_{\bar{\mathcal{N}}^i}) = \frac{\vartheta}{2}|\mathsf{L}_i\hat{x}|^2 &= \frac{\vartheta}{2}|\mathsf{L}_i(x - \mathbf{1}\bar{x}) + \mathsf{L}_ie|^2 \\ &\leq \frac{2\vartheta}{K\xi_{\min}}|\mathsf{L}_i|^2V + \vartheta|\mathsf{L}_i|^2|e|^2 \end{aligned}$$

and $H_i^2 \leq 2\kappa^2|A_i|^2|e|^2 + \frac{4\kappa^2|\mathsf{L}_i|^2}{K\xi_{\min}}V$. Adding and subtracting $\sum_{i\in\mathcal{V}}\{\omega_i\hat{V}_i(\hat{x}_{\bar{\mathcal{N}}^i}) + H_i^2\}$ to (A.11) results in:

$$\begin{aligned}\dot{V} \leq & -\Big[\kappa\Big(2a_\xi(\mathsf{L}) - \frac{1}{\epsilon_1}\Big) - \frac{(2\vartheta + 4\kappa^2)\mathrm{Tr}(\mathsf{L}^{\mathrm{T}}\mathsf{L})}{K\xi_{\min}} - 2\mathcal{L}_{os}\Big]V \\ & + \sum_{i\in\mathcal{V}}\Big\{\Big(\frac{\kappa\epsilon_1 K\bar{\Lambda}_M^2}{2} + \vartheta\mathrm{Tr}(\mathsf{L}^{\mathrm{T}}\mathsf{L}) + 2\kappa^2\mathrm{Tr}(\mathsf{A}^{\mathrm{T}}\mathsf{A})\Big)|e_i|^2 \\ & - \omega_i\hat{V}_i(\hat{x}_{\bar{\mathcal{N}}^i}) - H_i^2\Big\}. \end{aligned} \tag{A.12}$$

This inequality takes the form of upper-bound in Assumption 4.2(b).

Hence, all the assumptions in Theorem 4.1 have been satisfied which concludes asymptotic stability w.r.t. (4.35).

Part 2: Active Sensing. Here, Assumption 4.1 is satisfied via (A.9). Before examining Assumption 4.3(b), we will ensure Assumption 4.3(d) is met. (**2.1**) For Assumption 4.3, consider $V_i(x) = \frac{1}{N}V(x), \forall i \in \mathcal{V}$. From (A.11), add and subtract H_i^2, this results in:

$$\dot{V} \leq \ -\breve{\alpha}_V V + \sum_{i\in\mathcal{V}}\{\breve{\gamma}_i^2|e_i|^2 - H_i^2\}, \tag{A.13}$$

where

$$\begin{aligned}\breve{\alpha}_V &= \Big[\kappa\Big(2a_\xi(\mathsf{L}) - \frac{1}{\epsilon_1}\Big) - \frac{4\kappa^2\mathrm{Tr}(\mathsf{L}^{\mathrm{T}}\mathsf{L})}{K\xi_{\min}} - 2\mathcal{L}_{os}\Big], \\ \breve{\gamma}_i^2 &= \Big[\frac{\kappa\epsilon_1 K\bar{\Lambda}_M^2}{2} + 2\kappa^2\mathrm{Tr}(\mathsf{A}^{\mathrm{T}}\mathsf{A})\Big], \ \forall i \in \mathcal{V}.\end{aligned}$$

Here, the expression for $\breve{\gamma}_i^2$ is independent of i, therefore we drop i from its notation and use $\breve{\gamma}^2$ instead. From H_i^2 in item (1.1) above, we can infer that: $\sum_{i\in\mathcal{V}}|e_i|^2 \leq \sum_{i\in\mathcal{V}}\frac{1}{2\kappa^2\mathrm{Tr}(\mathsf{A}^{\mathrm{T}}\mathsf{A})}H_i^2$. Using this inequality in (A.13) and dividing the resultant inequality by N results in the following:

$$\dot{V}_i \leq -\breve{\alpha}_V V_i + \Big(\frac{\breve{\gamma}^2}{2\kappa^2\mathrm{Tr}(\mathsf{A}^{\mathrm{T}}\mathsf{A})} - 1\Big)\frac{\sum_{i\in\mathcal{V}}H_i^2}{N},$$

where $\alpha_i = \breve{\alpha}_V$, $c_i = \frac{\breve{\gamma}^2}{2\kappa^2\mathrm{Tr}(\mathsf{A}^{\mathrm{T}}\mathsf{A})} - 1$, $\hat{H}_i = \frac{\sum_{i\in\mathcal{V}}H_i^2}{N}$, $\hat{J}_i = J_i = 0$. As a consequence, Assumptions 4.3(d) and 4.3(e) are realized.

The choice of $\hat{H}_i^2$ and $\hat{J}_i$ in item (2.1) above, implies that Assumption

4.3(b) is identical to Assumption 4.2(b) and is satisfied through (A.12).
(**2.2**) Let $\tilde{V}_i(x_{\underline{\mathcal{N}}_k^i}) = \frac{K\xi_{\min}}{2N|\mathsf{L}_{i,k}^s|^2}|\mathsf{L}_{i,k}^s x|^2$. Then, Assumption 4.4 is satisfied as follows:

$$\begin{aligned}\tilde{V}_i(x_{\underline{\mathcal{N}}_k^i}) = \frac{K\xi_{\min}}{2N|\mathsf{L}_{i,k}^s|^2}|\mathsf{L}_{i,k}^s x|^2 &= \frac{K\xi_{\min}}{2N|\mathsf{L}_{i,k}^s|^2}|\mathsf{L}_{i,k}^s(x-\mathbf{1}\bar{x})|^2\\ &\leq \frac{K\xi_{\min}}{2N}|(x-\mathbf{1}\bar{x})|^2\\ &\leq V_i(x),\end{aligned}$$

where $\mathsf{L}_{i,k}^s$ is the i-th row of Laplacian matrix L_t^s associated with the sensing network at time $t \in \{s_k^i\}_{k=0}^{\infty}, \forall i \in \mathcal{V}$, and is such that $\mathsf{L}_{i,k}^s\mathbf{1} = 0, \forall i \in \mathcal{V}$.

Hence, all the conditions in Theorem 4.2 are satisfied which concludes asymptotic stability w.r.t. (4.35). □

A.2 For Chapter 5

A.2.1 Proof of Theorem 5.1

We address the proof in two parts. In Part 1, we establish upper-bounds for growth rate of $W_i = |e_i|$ and decay rate of V (defined shortly). Subsequently, in Part 2, we use the upper-bounds from Part 1 to demonstrate convergence.

Part 1: We begin by examining two candidate functions, namely, $W_i = |e_i|,\ \forall i \in \mathcal{V}$, and $V = \sum_{i\in\mathcal{V}} \frac{K}{2}\xi_i|x_i - \bar{x}|^2$, where $\bar{x} = \sum_{i\in\mathcal{V}}\xi_i x_i \in \mathbb{R}^n$ and $K > 0$.

First, we determine bound on the growth rate of W_i as follows:

$$\begin{aligned}W_i^{\circ} \leq\ & \max\{0, \mathcal{L}_{os} + \kappa d_i\}W_i + \kappa|(\mathsf{A}_i \otimes \mathbb{I}_n)e|\\ &+ \kappa|(\mathsf{L}_i \otimes \mathbb{I}_n)x|,\\ \leq\ & L_i W_i + H_i \qquad\qquad (A.14)\end{aligned}$$

where $L_i = \max\{0, \mathcal{L}_{os} + \kappa d_i\}$ and H_i is such that: $H_i^2 = 2\kappa^2\big(|\mathsf{A}_i|^2|e|^2 + |(\mathsf{L}_i \otimes \mathbb{I}_n)(x - \mathbf{1}_N \otimes \bar{x})|^2\big)$, since $\mathsf{L}_i\mathbf{1}_N = 0$.

Next, we examine bound on growth rate of $V(x)$ in the presence of errors

$e_i, \forall i \in \mathcal{V}$. We begin by noting that

$$V(x) = \frac{K}{2}\sum_{i\in\mathcal{V}} \xi_i |x_i - \bar{x}|^2 = \frac{K}{2} x^{\mathrm{T}} M^{\mathrm{T}} \Xi M x$$

where $M = (\mathbb{I}_N - \mathbf{1}_N \xi^{\mathrm{T}}) \otimes \mathbb{I}_n = \mathbb{I}_{nN} - \mathbf{1}_N \xi^{\mathrm{T}} \otimes \mathbb{I}_n$ and $\Xi = \mathrm{diag}\{\xi\} \otimes \mathbb{I}_n$. The derivative of V can be upper-bounded as follows:

$$\begin{aligned}
V^\circ &= K x^{\mathrm{T}} M^{\mathrm{T}} \Xi M \Big([f] - \kappa(\mathsf{L} \otimes \mathbb{I}_n)(x+e) \Big) \\
&\leq -\Big[\kappa \Big(2a_\xi(\mathsf{L}) - \frac{1}{\epsilon_1} \Big) - \frac{(2\vartheta + 4\kappa^2)\mathrm{Tr}(\mathsf{L}^{\mathrm{T}}\mathsf{L})}{K\xi_{\min}} - 2\mathcal{L}_{os} \Big] V \\
&\quad + \sum_{i\in\mathcal{V}} \Big\{ \Big(\frac{\kappa\epsilon_1 K \bar{\Lambda}_M^2}{2} + \vartheta \mathrm{Tr}(\mathsf{L}^{\mathrm{T}}\mathsf{L}) + 2\kappa^2 \mathrm{Tr}(\mathsf{A}^{\mathrm{T}}\mathsf{A}) \Big) |e_i|^2 - \omega_i \hat{V}_i(\zeta_{\bar{\mathcal{N}}^i}) - H_i^2 \Big\} \\
&= -\alpha_V V + \sum_{i\in\mathcal{V}} \Big\{ \gamma_i^2 |e_i|^2 - \omega_i \hat{V}_i - H_i^2 \Big\} \qquad \text{(A.15)}
\end{aligned}$$

Complete derivation of the upper-bounds expressed in (A.14) and (A.15) can be found in Appendix A.1.3.

Part 2: The two inequalities, namely, (A.14) and (A.15), from Part 1 aid in demonstrating asymptotic stability. Here, we consider the following Lyapunov candidate function:

$$U_1(q) = \frac{K}{2} x^{\mathrm{T}} M^{\mathrm{T}} \Xi M x + \sum_{i\in\mathcal{V}} \{\gamma_i \theta_i |e_i|^2 + \eta_i\}.$$

• *Analysis during flow:*

We begin the analysis by evaluating the Clarke's derivative of U_1 as follows:

$$\begin{aligned}
(U_1)^\circ \leq\ & -\alpha_V V + \sum_{i\in\mathcal{V}} \Big\{ \gamma_i^2 |e_i|^2 - \omega_i \hat{V}_i - H_i^2 + \gamma_i(-2L_i^\mu \theta_i \\
& - \gamma_i \theta_i^2 - \gamma_i)|e_i|^2 + 2\gamma_i \theta_i (L_i |e_i| + H_i)|e_i| - \beta_i \eta_i + \omega_i \hat{V}_i \Big\} \\
\leq\ & -\alpha_V V - \sum_{i\in\mathcal{V}} \Big\{ 2\mu_i \gamma_i \theta_i |e_i|^2 + \beta_i \eta_i \Big\} \\
\leq\ & -\alpha_{U_1} U_1 \qquad \text{(A.16)}
\end{aligned}$$

where $\alpha_{U_1} = \min\{\alpha_V, \min_i\{2\mu_i\gamma_i\lambda_i\}, \min_i\{\beta_i\}\}$.

• *Analysis at jump instants:*

At any instant $\mathtt{t}$, a subset of agents in $\mathcal{V}$ experience jumps; this is denoted

by the index set $\mathfrak{I}$ defined as $\mathfrak{I} := \{i|\mathtt{t} \in \{s_k^i\}_{k=0}^{\infty}\}$. Furthermore, since these jumps depend on the sign of g_s^i, we define the following index sets: $\mathcal{P} = \{i|i \in \mathfrak{I},\ g_s^i > 0\},\ \mathcal{Q} = \{i|i \in \mathfrak{I},\ g_s^i < 0\}$ and $\mathcal{R} = \{i|i \in \mathfrak{I},\ g_s^i = 0\}$. Agents in $\mathcal{R}$, jump to either of the two states, namely, G_i^1 and G_i^2, as expressed in (5.16); therefore, these agents can be further subdivided into subsets $\mathcal{R}_1 = \{i|i \in \mathcal{R},\ G_i(q) = G_i^1(q)\}$ and $\mathcal{R}_2 = \{i|i \in \mathcal{R},\ G_i(q) = G_i^2(q)\}$.

Here, $e_i^+ = e_i,\ \eta_i^+ = g_s^i, \forall i \in \mathcal{P} \cup \mathcal{R}_1$, and $e_i^+ = e_i - \mathfrak{m}\mathfrak{q}_{\text{osc}}\big(\frac{e_i}{\mathfrak{m}}\big),\ \eta_i^+ = g_t^i, \forall i \in \mathcal{Q} \cup \mathcal{R}_2$. Therefore, at any jump instant $\mathtt{t}$ we have:

$$\begin{aligned}(U_1)^+ - U_1 = &\sum_{i \in \mathcal{P} \cup \mathcal{R}_1} \Big\{ \Big(\frac{\gamma_i}{\lambda_i} - \gamma_i \theta_i \Big) |e_i|^2 + g_s^i - \eta_i \Big\} \\ &+ \sum_{i \in \mathcal{Q} \cup \mathcal{R}_2} \Big\{ \frac{\gamma_i}{\lambda_i} |e_i - \mathfrak{m}_{\mathtt{t}} \mathfrak{q}_{\text{osc}}\Big(\frac{e_i}{\mathfrak{m}_{\mathtt{t}}} \Big)|^2 - \gamma_i \theta_i |e_i|^2 + g_t^i - \eta_i \Big\} \\ \leq &\sum_{i \in \mathcal{Q} \cup \mathcal{R}_2} \frac{\gamma_i}{\lambda_i} \frac{n\Delta^2}{4} \mathfrak{m}_{\mathtt{t}}^2, \end{aligned} \tag{A.17}$$

where recall that $\Delta/2$ is the quantization error associated with $\mathfrak{q}_{\text{osc}}(\cdot)$.

• *Analysis showing that* $\limsup_{l \to \infty} U_1^+(t_l^i) = 0, \forall i \in \mathcal{V}$*:*

From the above analysis, we note that the hybrid dynamics of Lyapunov function U_1 is governed by the following inequalities:

$$\begin{cases} (U_1)^\circ \leq -\alpha_{U_1} U_1, \\ (U_1)^+ \leq U_1 + \sum_{i \in \mathcal{Q} \cup \mathcal{R}_2} \bar{\Delta}_i \mathfrak{m}_{\mathtt{t}}^2. \end{cases} \tag{A.18}$$

where $\bar{\Delta}_i = \frac{\gamma_i}{\lambda_i} \frac{n\Delta^2}{4}$. Here, because the MAS operates in an asynchronous manner, the time interval between two consecutive jumps in the overall system cannot be lower bounded unlike in the case of synchronous (and periodic) protocols studied in [115]. However, from (5.5) we note that each agent in $\mathcal{V}$ flows for at least the duration of ε^i. In other words, if $i \in \mathfrak{I}$ (jump index set) at time instant $\mathtt{t}$, then $i \notin \mathfrak{I}$ during the interval $(\mathtt{t}, \mathtt{t} + \varepsilon^i)$; therefore, it does not participate in any jumps (in the overall system) that might occur during this interval. Using this notion, we construct a bounding trajectory for U_1 and show that the bounding trajectory asymptotically converges to zero.

For each agent $i \in \mathcal{V}$, we define $\bar{U}_{1,i}$ such that its hybrid dynamics is

expressed as:

$$\begin{cases} (\bar{U}_{1,i})^{\circ} = -\alpha_{U_1}\bar{U}_{1,i}, & t \in (t_l^i, t_{l+1}^i), \\ (\bar{U}_{1,i})^{+} = \bar{U}_{1,i}, & t \in \{s_k^i\} \setminus \{t_l^i\}, \\ (\bar{U}_{1,i})^{+} = \bar{U}_{1,i} + \bar{\Delta}_i \mathfrak{m}_t^2, & t \in \{t_l^i\}, \end{cases} \tag{A.19}$$

along with the initial condition $\bar{U}_{1,i}(\mathtt{t}=0) = \frac{1}{N}U_1(\mathtt{t}=0)$. From the comparison lemma in [44], we note that

$$U_1 \leq \sum_{i\in\mathcal{V}} \bar{U}_{1,i}, \forall t \in [0,\infty).$$

To show that $\bar{U}_{1,i}$ converges to zero, we evaluate the expression for $(\bar{U}_{1,i})^+$ at triggering instants $\{t_l^i\}$ and show that as $t_l^i \to \infty$, $(\bar{U}_{1,i})^+ \to 0$.

First, we evaluate the expression for $\bar{U}_{1,i}(t_1^i)^+$ and subsequently for arbitrary event instant t_l^i as follows:

$$\begin{aligned} \bar{U}_{1,i}(t_1^i)^+ &= \bar{U}_{1,i}(0)e^{-\alpha_{U_1}t_1^i} + \bar{\Delta}_i\mathfrak{m}_0^2 e^{-2\alpha_{\mathfrak{m}}t_1^i} \\ \bar{U}_{1,i}(t_2^i)^+ &= \bar{U}_{1,i}(0)e^{-\alpha_{U_1}t_2^i} + \bar{\Delta}_i\mathfrak{m}_0^2 e^{-2\alpha_{\mathfrak{m}}t_1^i}e^{-\alpha_{U_1}(t_2^i - t_1^i)} \\ &\quad + \bar{\Delta}_i\mathfrak{m}_0^2 e^{-2\alpha_{\mathfrak{m}}t_2^i} \\ &\vdots \\ \bar{U}_{1,i}(t_l^i)^+ &= \bar{U}_{1,i}(0)e^{-\alpha_{U_1}t_l^i} + \Big[\sum_{k=1}^{l-1}\Big\{e^{-2\alpha_{\mathfrak{m}}t_k^i}e^{-\alpha_{U_1}(t_l^i - t_k^i)}\Big\} \\ &\quad + e^{-2\alpha_{\mathfrak{m}}t_l^i}\Big]\bar{\Delta}_i\mathfrak{m}_0^2. \end{aligned} \tag{A.20}$$

From (5.5), recall that $s_{k+1}^i - s_k^i > \varepsilon^i$; this, by the definition of event-triggering condition in (5.11), implies that $t_{l+1}^i - t_l^i > \varepsilon^i$. Therefore, we have that $t_{l'}^i - t_{k'}^i > (l'-k')\varepsilon^i, \forall l', k' \in \mathbb{Z}_{\geq 0}$. This implies that $\bar{U}_{1,i}(t_l^i)^+$ can be upper-bounded as follows:

$$\begin{aligned} \bar{U}_{1,i}(t_l^i)^+ &\leq \bar{U}_{1,i}(0)\pi^l + \bar{\Delta}_i\mathfrak{m}_0^2\sum_{k=1}^{l}\varpi^k\pi^{l-k} \\ &= \hat{U}_{1,i}^0\pi^l + \bar{\Delta}_i\mathfrak{m}_0^2\sum_{k=0}^{l}\varpi^k\pi^{l-k} \end{aligned} \tag{A.21}$$

where $\hat{U}_{1,i}^0 = \bar{U}_{1,i}(0) - \bar{\Delta}_i\mathfrak{m}_0^2$, $\pi = e^{-\alpha_{U_1}\varepsilon^i}$ and $\varpi = e^{-2\alpha_{\mathfrak{m}}\varepsilon^i}$. Note that the summation term in (A.21) is symmetric in π and ϖ and is geometric in nature.

Therefore, we have

$$\bar{U}_{1,i}(t_l^i)^+ \leq \begin{cases} \hat{U}_{1,i}^0 \pi^l + \frac{\bar{\Delta}_i \mathfrak{m}_0}{\pi - \varpi} \pi^{l+1}, & 2\alpha_{\mathfrak{m}} > \alpha_{U_1}, \\ \hat{U}_{1,i}^0 \pi^l + \frac{\bar{\Delta}_i \mathfrak{m}_0}{\varpi - \pi} \varpi^{l+1}, & 2\alpha_{\mathfrak{m}} < \alpha_{U_1}, \\ \hat{U}_{1,i}^0 \pi^l + \bar{\Delta}_i \mathfrak{m}_0 (l\pi^l), & 2\alpha_{\mathfrak{m}} = \alpha_{U_1}. \end{cases} \tag{A.22}$$

It is straightforward to see that as $l \to \infty$, the bound on $\bar{U}_{1,i}(t_l^i)^+$ goes to 0 and its rate of decay is governed by $2\alpha_{\mathfrak{m}}$ when $2\alpha_{\mathfrak{m}} < \alpha_{U_1}$ or by α_{U_1}, otherwise. Since, $U_1 \leq \sum_{i \in \mathcal{V}} \bar{U}_{1,i}$; it follows that $\lim_{t \to \infty} U_1$ also reaches zero from above. This concludes the proof. □

A.3 For Chapter 6

A.3.1 Proof of Lemma 6.1

In this proof, we show that the choice of $W_i(e_i, \tilde{e}_i)$ in (6.19) satisfies Assumption 6.3.

• First, Assumption 6.3a) is satisfied as follows:

$$\begin{aligned} \underline{\alpha}_W^i(|e_i|) = \frac{\lambda_i}{2}|e_i| &\leq \frac{\lambda_i}{2}(|\tilde{e}_i| + |e_i + \tilde{e}_i|) \\ &\leq \max\{\lambda_i|\tilde{e}_i|, |e_i + \tilde{e}_i|\} = W_i \\ &\leq |e_i| + |\tilde{e}_i| = \bar{\alpha}_W^i(|(e_i, \tilde{e}_i)|). \end{aligned} \tag{A.23}$$

Here, recall that $\lambda_i \in (0, 1)$.

• Second, we evaluate $\langle \nabla W_i, \bar{F} \rangle$ to show that Assumption 6.3b) holds. Depending on the outcome of the max function in (6.19), we have the following three cases.

Case I: When $W_i = \lambda_i|\tilde{e}_i|$,

$$\begin{aligned} \langle \nabla W_i, \bar{F}_{\tilde{e}_i} \rangle &\leq \lambda_i |(\bar{\mathsf{A}}_i^{\mathrm{dia}} l_i^{\mathrm{dia}} \otimes \mathbb{I}_n)(\Upsilon_i(\tilde{x}_i) - \Upsilon_i(\hat{x}_i))| \\ &\leq \lambda_i \Big(\sum_{j \in \mathcal{N}_{\mathrm{out}}^i} l_i^j (\tilde{L}_i^j |\tilde{e}_i^j|)^2 \Big)^{\frac{1}{2}} \\ &\leq \lambda_i d_i \tilde{L}_i^{\max} |\tilde{e}_i| \leq d_i \tilde{L}_i^{\max} W_i, \end{aligned} \tag{A.24}$$

where $\bar{F}_{\tilde{e}_i} = (\bar{\mathsf{A}}_i^{\mathrm{dia}} l_i^{\mathrm{dia}} \otimes \mathbb{I}_n)(\Upsilon_i(\tilde{x}_i) - \Upsilon_i(\hat{x}_i))$, $\tilde{L}_i^{\max} = \max_{j \in \mathcal{N}_{\mathrm{out}}^i} \tilde{L}_i^j$ and $\lambda_i|\tilde{e}_i| \leq W_i$ (by definition of W_i). Note that if $d_i = 0$ (i.e., when out-neighbors have

received broadcasts from i), then $\tilde{e}_i^j = \mathbf{0}, \forall j \in \mathcal{N}_{\text{out}}^i$, till the next broadcast instant s_{k+1}^i. Therefore, we have $\langle \nabla W_i, \bar{F}_{\tilde{e}_i} \rangle \leq 0$ which is reflected in (A.24) with the inclusion of d_i.

Case II: When $W_i = |e_i + \tilde{e}_i|$,

$$\begin{aligned}
\langle \nabla W_i, \bar{F}_{\tilde{e}_i} + \bar{F}_{e_i} \rangle \leq\ & |\bar{F}_{\tilde{e}_i}| + |\bar{F}_{e_i}| \\
&\leq d_i \tilde{L}_i^{\max} |\tilde{e}_i| + |\Upsilon_i(\hat{x}_i) - (\bar{\mathsf{A}}_i^T \otimes f_i(x_i))| \\
&\leq d_i \tilde{L}_i^{\max} |\tilde{e}_i| + \Big(\sum_{j \in \mathcal{N}_{\text{out}}^{\bar{i}}} (\hat{L}_i^j |e_i^j| + \hat{H}_i^j(x, e^i))^2 \Big)^{\frac{1}{2}} \\
&\leq d_i \tilde{L}_i^{\max} |\tilde{e}_i| + \sqrt{|\mathcal{N}_{\text{out}}^{\bar{i}}|} (\hat{L}_i^{\max} |e_i| + \hat{H}_i^{\max}(x, e^i)) \\
&\leq \frac{1}{\lambda_i} \Big(d_i \tilde{L}_i^{\max} + 2\sqrt{|\mathcal{N}_{\text{out}}^{\bar{i}}|} \hat{L}_i^{\max} \Big) W_i + \sqrt{|\mathcal{N}_{\text{out}}^{\bar{i}}|} \hat{H}_i^{\max}(x, e^i),
\end{aligned}$$

where we use the inequality $\lambda_i |e_i| \leq 2W_i$ from (A.23).

Case III: When $W_i = \lambda_i |\tilde{e}_i| = |e_i + \tilde{e}_i|$, then

$$\begin{aligned}
W_i^\circ \leq & \max \Bigg\{ d_i \tilde{L}_i^{\max} W_i, \frac{1}{\lambda_i} \Big(d_i \tilde{L}_i^{\max} + 2\sqrt{|\mathcal{N}_{\text{out}}^{\bar{i}}|} \hat{L}_i^{\max} \Big) W_i \\
& + \sqrt{|\mathcal{N}_{\text{out}}^{\bar{i}}|} \hat{H}_i^{\max}(x, e^i) \Bigg\} \\
= & \frac{1}{\lambda_i} \Big(d_i \tilde{L}_i^{\max} + 2\sqrt{|\mathcal{N}_{\text{out}}^{\bar{i}}|} \hat{L}_i^{\max} \Big) W_i + \sqrt{|\mathcal{N}_{\text{out}}^{\bar{i}}|} \hat{H}_i^{\max}. \qquad \text{(A.25)}
\end{aligned}$$

• Third, for Assumption 6.3c), we consider the jump at the arrival instant $\mathtt{t}$ when $d_i = 1$. At $\mathtt{t}$, let the index set $\mathcal{N}_{\text{out}}^{i,k} := \{j | \mathtt{t} \in \{r_j^{i,k}\}, \forall j \in \mathcal{N}_{\text{out}}^i\}$ denote the set of all agents that received the state broadcasted by i at s_k^i. At $\mathtt{t}$, $d_i^+ \in \{0, 1\}$, $(e_i^i)^+ = e_i^i$, and, $\forall j \in \mathcal{N}_{\text{out}}^{i,k}$, $(e_i^j)^+ = e_i^j + \tilde{e}_i^j$, $(\tilde{e}_i^j)^+ = \mathbf{0}$. For all $j \notin \mathcal{N}_{\text{out}}^{i,k}$, $(e_i^j)^+ = e_i^j$ and $(\tilde{e}_i^j)^+ = \tilde{e}_i^j$. Using these expressions, we evaluate W_i^+ as follows:

$$\begin{aligned}
W_i^+ =\ & \max\{\lambda_i |\tilde{e}_i^+|, |e_i^+ + \tilde{e}_i^+|\} \\
=\ & \max \Big\{ \lambda_i |\tilde{e}_i - (\sum_{j \in \mathcal{N}_{\text{out}}^{i,k}} \Gamma_j \otimes \mathbb{I}_n) \tilde{e}_i|, \\
& |e_i + (\sum_{j \in \mathcal{N}_{\text{out}}^{i,k}} \Gamma_j \otimes \mathbb{I}_n) \tilde{e}_i + \tilde{e}_i - (\sum_{j \in \mathcal{N}_{\text{out}}^{i,k}} \Gamma_j \otimes \mathbb{I}_n) \tilde{e}_i| \Big\}
\end{aligned}$$

$$
\begin{aligned}
&= \max\{\lambda_i|\tilde{e}_i - (\sum_{j\in\mathcal{N}_{\text{out}}^{i,k}} \Gamma_j \otimes \mathbb{I}_n)\tilde{e}_i|, |e_i + \tilde{e}_i|\} \\
&\leq \max\{\lambda_i|\tilde{e}_i|, |e_i + \tilde{e}_i|\} = W_i. \qquad \text{(A.26)}
\end{aligned}
$$

Here, we note that any arrival instant $\mathtt{t}$ that corresponds to update on agents in $\mathcal{N}_{\text{out}}^{i,k}$, $d_i = 1$; this immediately follows from the definitions of l_i^j and d_i discussed in Sections 6.2 and 6.3, respectively.

• Finally, for Assumption 6.3d), we consider the jump at the sampling instant $\mathtt{t} = s_k^i$ on i when $d_i = 0$ and when i is about to perform its next broadcast. At $\mathtt{t}$, $d_i^+ = 1$, $(e_i^i)^+, (\tilde{e}_i^i)^+ = \mathbf{0}$ and, $\forall j \in \mathcal{N}_{\text{out}}^i$, $(e_i^j)^+ = e_i^j$, $(\tilde{e}_i^j)^+ = -e_i^j$. Using these expressions, we evaluate W_i^+ as follows:

$$
\begin{aligned}
W_i^+ &= \max\{\lambda_i|\tilde{e}_i^+|, |e_i^+ + \tilde{e}_i^+|\} \\
&= \max\{\lambda_i|\tilde{e}_i - (\mathsf{A}_i^{\text{dia}} \otimes \mathbb{I}_n)(\tilde{e}_i + e_i)|, \\
&\quad |e_i - (\Gamma_i \otimes \mathbb{I}_n)e_i + \tilde{e}_i - (\bar{\mathsf{A}}_i^{\text{dia}} \otimes \mathbb{I}_n)(\tilde{e}_i + e_i)|\} \\
&= \max\{\lambda_i| - e_i + (\Gamma_i \otimes \mathbb{I}_n)e_i|, |\mathbf{0}|\} \leq \lambda_i|e_i|. \qquad \text{(A.27)}
\end{aligned}
$$

Here, we note that $\tilde{e}_i - (\mathsf{A}_i^{\text{dia}} \otimes \mathbb{I}_n)(\tilde{e}_i + e_i) = -e_i + (\Gamma_i \otimes \mathbb{I}_n)e_i$. From (6.11), we see that after the broadcasted state is received at the out-neighbors $\mathcal{N}_{\text{out}}^i$, $\tilde{e}_i^j = \mathbf{0}, \forall t \in [r_j^{i,k}, s_{k+1}^i)$. Therefore, $W_i = \max\{\lambda_i|\mathbf{0}|, |e_i|\} = |e_i|$. Consequently, $W_i^+ \leq \lambda_i W_i$, satisfying Assumption 6.3d).

Note that if there is a jump instant $\mathtt{t}$ such that $\mathtt{t} \in \{s_k^i\} \wedge \{r_j^{i,k} | j \in \mathcal{N}_{\text{out}}^{i,k}\}$ (namely, if the broadcast instant on i coincides with the arrival instant on $j \in \mathcal{N}_{\text{out}}^i$), then, first, the jump corresponding to update is evaluated (i.e., $d_i = 1 \to d_i^+ = 0$) and subsequently the jump corresponding to broadcast is evaluated (i.e., $d_i = 0 \to d_i^+ = 1$). Such an occurrence can take place if the transmission delay $\delta_j^{i,k} = s_{k+1}^i - s_k^i$ for some out-neighbor $j \in \mathcal{N}_{\text{out}}^i$. Since the number of agents in the network is finite, the jumps at such a jump instant $\mathtt{t}$ are also finite. □

A.3.2 Proof of Theorem 6.1

For the closed-loop hybrid system in (6.13), consider the Lyapunov candidate

$$U(q) = V(x) + \sum_{i\in\mathcal{V}} \breve{\gamma}_i \theta_i^{d_i}(\tau_i) W_i^2(e_i, \tilde{e}_i).$$

For notational brevity, we drop the arguments of functions involved in U.

• *Analysis during flow:*

At any instant $\mathtt{t}$, let index sets $\mathfrak{M} := \{i | d_i = 0\}$ and $\mathfrak{N} := \{i | d_i = 1\}$ denote agents that are either ready to broadcast (namely, those in $\mathfrak{M}$) or agents whose broadcasted states are yet to be received by, at least some, out-neighbors (namely, those in $\mathfrak{N}$). By definition, $\mathfrak{M} \cap \mathfrak{N} = \phi$ and $\mathfrak{M} \cup \mathfrak{N} = \mathcal{V}$. With the aid of these sets, the Clarke derivative of $U(q)$ can be expressed as follows:

$$\begin{aligned} U^\circ \leq & -\alpha_V(|\Theta(x)|) + \sum_{i\in\mathfrak{M}\cup\mathfrak{N}} \big[(\breve{\gamma}_i W_i)^2 - (H_i^{d_i})^2\big] \\ & + \sum_{i\in\mathfrak{M}} \big[\breve{\gamma}_i\big(- 2L_i^0\theta_i^0 - \breve{\gamma}_i((\theta_i^0)^2 + 1)\big) W_i^2 \\ & + 2\breve{\gamma}_i\theta_i^0 W_i W_i^\circ\big] + \sum_{i\in\mathfrak{N}} \big[\breve{\gamma}_i\big(- 2L_i^1\theta_i^1 - \breve{\gamma}_i((\theta_i^1)^2 \\ & + 1)\big) W_i^2 + 2\breve{\gamma}_i\theta_i^1 W_i W_i^\circ\big] \leq -\alpha_V(|\Theta(x)|). \end{aligned} \tag{A.28}$$

This implies that there exists a positive function $\zeta : \mathbb{R} \to \mathbb{R}_{\geq 0}$ such that $U^\circ(q)$ satisfies

$$U^\circ \leq -\zeta(U). \tag{A.29}$$

• *Analysis at jumps:*

At any jump instant $\mathtt{t}$, let $\mathfrak{I} := \{i | (\mathtt{t} \in \{s_k^i\}_{k=0}^\infty \wedge d_i = 0) \vee (\mathtt{t} \in \{r_j^{i,k}\}_{k=0}^\infty \wedge d_i = 1)\}$ denote the index set of agents that are actively involved in the jump, i.e., they either broadcast at $\mathtt{t}$ or their previously broadcasted state arrived at their respective out-neighbors at $\mathtt{t}$. The remaining agents in $\mathcal{V}$ do not participate in the jump, i.e., $q_i^+ = q_i, \forall i \in \mathcal{V}\backslash\mathfrak{I}$. Based on the above definition of $\mathfrak{I}$, we define index sets $\mathfrak{P} := \{i | \mathtt{t} \in \{s_k^i\}_{k=0}^\infty \wedge d_i = 0\}$ and $\mathfrak{Q} = \{i | \mathtt{t} \in \{r_j^{i,k}\}_{k=0}^\infty \wedge d_i = 1\}$.

This implies that

$$\forall i \in \mathfrak{P}, \begin{cases} W_i^+ & \leq \lambda_i W_i, \\ \tau_i^+ & = 0, \\ d_i^+ & = 1, \\ \theta_i^{d_i^+} & = \theta_i^1(0), \end{cases} \qquad \forall i \in \mathfrak{Q}, \begin{cases} W_i^+ & \leq W_i, \\ \tau_i^+ & = \tau_i, \\ d_i^+ & \in \{0,1\}, \\ \theta_i^{d_i^+} & \in \{\theta_i^0(\tau_i), \\ & \quad \theta_i^1(\tau_i)\}. \end{cases} \tag{A.30}$$

At $\mathtt{t}$, using (A.30), we have:

$$\begin{aligned} U^+ - U = & \sum_{i\in\mathfrak{P}} \breve{\gamma}_i \theta_i^1 (W_i^+)^2 - \sum_{i\in\mathfrak{P}} \breve{\gamma}_i \theta_i^0 W_i^2 \\ & + \sum_{i\in\mathfrak{Q}} \breve{\gamma}_i \theta_i^{\{0,1\}} (W_i^+)^2 - \sum_{i\in\mathfrak{Q}} \breve{\gamma}_i \theta_i^1 W_i^2 \\ \leq & \sum_{i\in\mathfrak{P}} ((\lambda_i)^2 \theta_i^1(0) - \theta_i^0(\tau_i)) \breve{\gamma}_i W_i^2 \\ & + \sum_{i\in\mathfrak{Q}} (\theta_i^{0,1}(\tau_i) - \theta_i^1(\tau_i)) \breve{\gamma}_i W_i^2, \end{aligned} \tag{A.31}$$

where the notation $\theta_i^{\{0,1\}}$ suggests that d_i can take either values 0 or 1. This implies that, at the jump instants, we have

$$U(G(q)) \leq U(q), q \in D. \tag{A.32}$$

Using (A.29) and (A.32), the proof is completed by following an argument similar to the proof of Theorem 1 in [69]. □

A.3.3 Proof of Theorem 6.2

It suffices to show that the dynamics in (6.22), with the functions $V(x) = \frac{K}{2}|(\mathsf{L} \otimes \mathbb{I}_n)x|^2$, $W_i(e_i, \tilde{e}_i)$ as in Lemma 6.1, and $\Theta(x) = (\mathsf{L} \otimes \mathbb{I}_n)x$, satisfies Assumptions 6.2, 6.3 and 6.4. Let $\mathsf{L}^n = \mathsf{L} \otimes \mathbb{I}_n$ and $\mathsf{L}_i^n = \mathsf{L}_i \otimes \mathbb{I}_n$.

• First, for Assumption 6.2, because of the model $\Upsilon_i^j(\cdot) = f(\cdot)$, it is straightforward to see that $\tilde{L}_i^j = \mathcal{L}, \forall i, j \in \mathcal{V}$. Next, the growth of error $e_i^j = \hat{x}_i^j - x_i$ is bounded as follows:

$$\begin{aligned} \dot{e}_i^j &= f(\hat{x}_i^j) - f(x_i) + \kappa \mathsf{L}_i^n \hat{x}^i, \\ &\leq \mathcal{L}|e_i^j| + \kappa|\mathsf{L}_i^n x| + \kappa|\mathsf{L}_i^n e^i|. \end{aligned} \tag{A.33}$$

The quantities $\hat{L}_i^j$ and $\hat{H}_i^j(x, e^i)$, stated in Theorem 6.2, can be inferred from the bound in (A.33). Since, the expression for $\hat{H}_i^j(x, e^i)$ is independent of j, $\hat{H}_i^{\max} = \hat{H}_i^j, \forall j \ \in \ \mathcal{N}_{\text{out}}^i$.

• Second, Assumption 6.3 is directly satisfied by choosing W_i as in Lemma 6.1. Using Assumption 6.2 and Lemma 6.1, the quantities $L_i^{d_i}$ and $H_i^{d_i}(x, e^i)$ are as follows:

$$\begin{aligned} L_i^{d_i} &= \mathcal{L}\Big(d_i + 2\sqrt{|\bar{\mathcal{N}}_{\text{out}}^i|}\Big)\lambda_i{}^{-1}, \\ (H_i^{d_i})^2 &= 2|\bar{\mathcal{N}}_{\text{out}}^i|\kappa^2\big(|\mathsf{L}_i^n x|^2 + |\mathsf{L}_i^n e^i|^2\big). \end{aligned} \tag{A.34}$$

• Finally, for Assumption 6.4, we examine the derivative of $V(x) = \frac{K}{2}|\mathsf{L}^n x|^2$ that is as follows: $\dot{V} = K z^{\mathrm{T}} \mathsf{L}^n([f] - \kappa(z + [e]))$ where $[f] = [f(x_1)^{\mathrm{T}} \cdots f(x_N)^{\mathrm{T}}]^{\mathrm{T}}$ and $[e] = [(\mathsf{L}_1^n e^1)^{\mathrm{T}} \cdots (\mathsf{L}_N^n e^N)^{\mathrm{T}}]^{\mathrm{T}}$. The terms in $\dot{V}$ can be upper-bounded as follows:

$$\dot{V} \leq -2\Big[\Big(\Lambda_2 - \frac{\Lambda_M}{2\epsilon_2}\Big)\kappa - \Gamma_1\Big]V + \sum_{i\in\mathcal{V}} \frac{\epsilon_2 K\kappa}{2}|\mathsf{L}_i^n e^i|^2, \tag{A.35}$$

where $\Gamma_1 = \mathcal{L}\sqrt{\frac{2d_M}{\Lambda_2}}$ (see Appendix A.1.2 for details on the derivation leading up to the bound in (A.35)). Adding and subtracting $\sum_{i\in\mathcal{V}}(H_i^{d_i})^2$ to the bound in (A.35) results in:

$$\begin{aligned} \dot{V} \leq & -2\Big[\Big(\Lambda_2 - \frac{\Lambda_M}{2\epsilon_2}\Big)\kappa - \Gamma_1\Big]V + \sum_{i\in\mathcal{V}}\Big\{\frac{\epsilon_2 K\kappa}{2}|\mathsf{L}_i^n e^i|^2 \\ & + 2|\bar{\mathcal{N}}_{\text{out}}^{\max}|\kappa^2(|\mathsf{L}_i^n e^i|^2 + |\mathsf{L}_i^n x|^2) - (H_i^{d_i})^2\Big\} \\ \leq & -2\Big[\Big(\Lambda_2 - \frac{\Lambda_M}{2\epsilon_2}\Big)\kappa - \Gamma_1 - 2\frac{|\bar{\mathcal{N}}_{\text{out}}^{\max}|\kappa^2}{K}\Big]V \\ & + \sum_{i\in\mathcal{V}}\Big\{\Big(\frac{\epsilon_2 K\kappa}{2} + 2|\bar{\mathcal{N}}_{\text{out}}^{\max}|\kappa^2\Big)|\mathsf{L}_i|^2|e^i|^2 - (H_i^{d_i})^2\Big\} \end{aligned}$$

$$\begin{aligned} \dot{V} \leq & -\alpha_V V + \sum_{i\in\mathcal{V}}\Big\{\Big(\frac{\epsilon_2 K\kappa}{2} + 2|\bar{\mathcal{N}}_{\text{out}}^{\max}|\kappa^2\Big)|\mathsf{L}_i^{\max}|^2|e_i|^2 - (H_i^{d_i})^2\Big\} \\ \leq & -\alpha_V V + \sum_{i\in\mathcal{V}}\Big\{\frac{4\gamma^2}{\lambda_i^2}W_i^2 - (H_i^{d_i})^2\Big\}. \end{aligned} \tag{A.36}$$

Here, in the third inequality we use: $\sum_{i\in\mathcal{V}}|e^i|^2 = \sum_{i\in\mathcal{V}}|e_i|^2$. □

A.4 For Chapter 7

A.4.1 Counter-example

In this subsection, we offer a counter-example to demonstrate that the distributed accelerated algorithm in [117], designed for undirected graphs, may not work for weight-balanced digraphs. Consider the following convex optimization problem: $\min_{x_i\in\mathbb{R}} \sum_{i=1}^{5} \frac{m_i}{2}|x_i - x_i(0)|^2$ where $x(0) = [5\ 0\ 7\ -1\ -4]^{\mathrm{T}}$, and node inertia $m = [14\ 2\ 2.5\ 3\ 2]^{\mathrm{T}}$. This problem has to be solved, in a distributed manner, over a weight-balanced digraph given by the graph Laplacian:

$$\mathsf{L} = \frac{1}{8}\begin{bmatrix} 0.6986 & -0.5326 & -0.1654 & -0.0004 & -0.0002 \\ -0.0595 & 0.9182 & -0.6676 & -0.0681 & -0.1230 \\ -0.0213 & -0.0004 & 0.9207 & -0.5809 & -0.3181 \\ -0.0248 & -0.2458 & 0 & 0.8293 & -0.5587 \\ -0.5930 & -0.1394 & -0.0877 & -0.1799 & 1 \end{bmatrix}. \tag{A.37}$$

The algorithm in [117], is

$$\begin{cases} \dot{x} = v - \mathsf{L}x, \\ \dot{v} = -\beta\nabla f - kv - kq, \\ \dot{q} = \mathsf{L}x, \sum_i q_i(0) = \mathbf{0}, \end{cases} \tag{A.38}$$

where $\beta = 0.55$ and $k = 113.63$ satisfy the sufficiency conditions stated in (15) of [117]. Our algorithm is as follows:

$$\begin{cases} \dot{x} = \frac{0.1}{4}v - 4\mathsf{L}x, \\ \dot{v} = -\nabla f - 2v - 196q, \\ \dot{q} = \mathsf{L}x, \sum_i q_i(0) = \mathbf{0}. \end{cases} \tag{A.39}$$

Fig. A.1(a) and A.1(b) depict the position trajectories when (A.38) (from [117]) and (A.39) (our algorithm) are employed over (A.37), respectively.

Furthermore, we also note that one can generate similar counter-examples, perhaps, using the Laplacian in (A.37) and objective functions used in this subsection, for accelerated gradient algorithms designed for undirected graphs in [110], [122]; therefore, discussion on sufficiency conditions for weight-balanced digraphs in Section 7.3 is necessary.

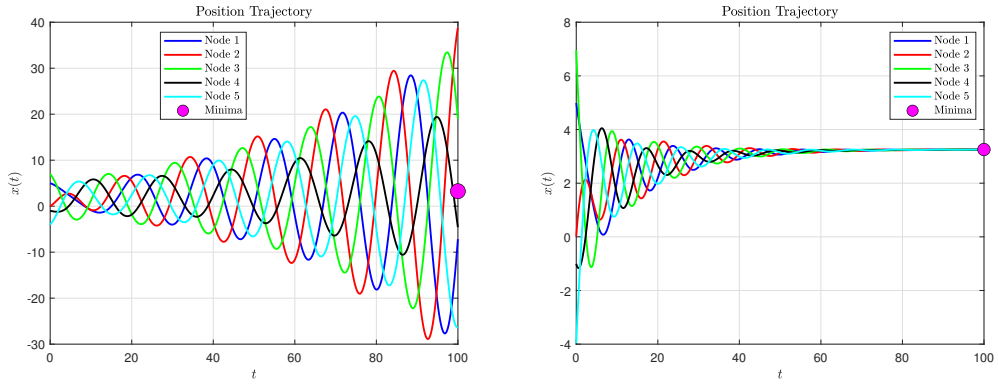

(a) Algorithm in [117] (b) Our algorithm

Figure A.1: Counter-example demonstrating that algorithm designed for undirected graph (such as [117]) may not work for weight-balanced digraphs.

A.4.2 Proof of Theorem 7.1

We present the proof in two parts. In Part 1, we describe the construction of Lyapunov function and establish an upper bound, as a function of gains $a_{\{\}}, b_{\{\}}$, on its decay rate. In Part 2, we analyze the coefficients associated with terms in this upper bound to ensure positivity, and as a consequence, guarantee convergence of (7.3) and existence of gains.

Part 1: First, we define the following terms and their derivatives.

1) Define $Q \coloneqq \Delta a + \phi b + \pi c$ where Δ, ϕ, π are positive scalars. Then, $\dot{Q} = \big(\mathfrak{a}_1\Delta - \mathfrak{b}_2\phi\big)b + \phi\mathfrak{b}_1\nabla_f - \phi\mathfrak{b}_3 c$ if $\pi = \mathfrak{a}_2\Delta$. Evaluating $\frac{d}{dt}(\frac{1}{2}|Q|^2)$ results in:

$$\begin{aligned} Q^{\mathrm{T}}\dot{Q} = \phi\big(\mathfrak{a}_1\Delta - \mathfrak{b}_2\phi\big)|b|^2 - \pi\phi\mathfrak{b}_3|c|^2 \\ + \Delta\big(\mathfrak{a}_1\Delta - \mathfrak{b}_2\phi\big)a^{\mathrm{T}}b - \Delta\phi\mathfrak{b}_3 a^{\mathrm{T}}c + \phi\mathfrak{b}_1 Q^{\mathrm{T}}\nabla_f \\ + \big(\pi\big(\mathfrak{a}_1\Delta - \mathfrak{b}_2\phi\big) - \phi^2\mathfrak{b}_3\big)b^{\mathrm{T}}c. \end{aligned} \tag{A.40}$$

2) Let $V_c \coloneqq \frac{1}{2}c^{\mathrm{T}}\Gamma^n c$ where $\Gamma^n = \Gamma \otimes \mathbb{I}_n$ and Γ satisfies Lemma 7.1, then

$$\begin{aligned} \dot{V}_c = c^{\mathrm{T}}\Gamma^n \mathsf{L}^n a = c^{\mathrm{T}}a + c^{\mathrm{T}}\Gamma^n \mathsf{L}_{ss}^n a \\ \leq c^{\mathrm{T}}a + \frac{\lambda_M^\Gamma}{2\zeta_1}|c|^2 + \frac{\lambda_M^\Gamma\zeta_1}{2}|\mathsf{L}_{ss}^n a|^2 \\ \leq\ c^{\mathrm{T}}a + \frac{\lambda_M^\Gamma}{2\zeta_1}|c|^2 + \frac{\lambda_M^\Gamma\zeta_1\epsilon_{\mathsf{L}}}{2}a^{\mathrm{T}}\mathsf{L}_s^n a, \end{aligned}$$

where $\mathsf{L}_s^n = \mathsf{L}_s \otimes \mathbb{I}_n$, $\mathsf{L}_{ss}^n = \mathsf{L}_{ss} \otimes \mathbb{I}_n$.

3) Let $V_b \coloneqq \frac{1}{2}|b|^2$, then $\dot{V}_b = -\mathfrak{b}_2|b|^2 - \mathfrak{b}_3 b^{\mathrm{T}} c + \mathfrak{b}_1 b^{\mathrm{T}} \nabla_f$.

4) Let $V_a \coloneqq \frac{1}{2}|a|^2$, then $\dot{V}_a = \mathfrak{a}_1 a^{\mathrm{T}} b - \mathfrak{a}_2 a^{\mathrm{T}} \mathsf{L}_s^n a$.

Consider the following Lyapunov function

$$V \coloneqq \frac{1}{2}|Q|^2 + K_a V_a + K_b V_b + \Delta\phi\mathfrak{b}_3 V_c, \tag{A.41}$$

where $K_{\{a,b\}}$ are positive scalars. Using aforementioned items 1)–4), the derivative of V along (7.5) is upper bounded as:

$$\begin{aligned}
\dot{V} \leq\ & \phi\Delta\mathfrak{b}_1 a^{\mathrm{T}} \nabla_f - \big(K_b\mathfrak{b}_2 - \phi\big(\mathfrak{a}_1\Delta - \mathfrak{b}_2\phi\big)\big)|b|^2 \\
& - \big(\phi\Delta\mathfrak{a}_2\mathfrak{b}_3 - \Delta\phi\mathfrak{b}_3\frac{\lambda_M^\Gamma}{2\zeta_1}\big)|c|^2 + \big(\phi^2 + K_b\big)\mathfrak{b}_1 b^{\mathrm{T}}\nabla_f \\
& + \phi\Delta\mathfrak{a}_2\mathfrak{b}_1 c^{\mathrm{T}}\nabla_f + \big(K_a\mathfrak{a}_1 + \Delta\big(\mathfrak{a}_1\Delta - \mathfrak{b}_2\phi\big)\big)a^{\mathrm{T}}b \\
& + \big(\mathfrak{a}_2\Delta\big(\mathfrak{a}_1\Delta - \mathfrak{b}_2\phi\big) - \big(\phi^2 + K_b\big)\mathfrak{b}_3\big)b^{\mathrm{T}}c \\
& - \big(K_a\mathfrak{a}_2 - \Delta\phi\mathfrak{b}_3\frac{\lambda_M^\Gamma\zeta_1\epsilon_{\mathsf{L}}}{2}\big)a^{\mathrm{T}}\mathsf{L}_s^n a.
\end{aligned} \tag{A.42}$$

Here, we disintegrate (and dissolve) the following terms in (A.42) and selectively absorb them into coefficients of $|a|^2$, $|b|^2$, $|c|^2$ and $a^{\mathrm{T}}\mathsf{L}_s^n a$: 1) we note that $a^{\mathrm{T}}\nabla_f \leq -\mu|a|^2$; 2) we set

$$\mathfrak{a}_2\Delta\big(\mathfrak{a}_1\Delta - \mathfrak{b}_2\phi\big) - \big(\phi^2 + K_b\big)\mathfrak{b}_3 = 0, \tag{A.43}$$

which eliminates the cross term $b^{\mathrm{T}}c$; 3) we disintegrate the leftover cross terms through Young's inequality as follows:

$$\begin{cases}
a^{\mathrm{T}}b & \leq \frac{\varepsilon_1}{2}|a|^2 + \frac{1}{2\varepsilon_1}|b|^2, \\
b^{\mathrm{T}}\nabla_f & \leq \mathfrak{L}\Big(\frac{\varepsilon_2}{2}|a|^2 + \frac{1}{2\varepsilon_2}|b|^2\Big), \\
c^{\mathrm{T}}\nabla_f & \leq \mathfrak{L}\Big(\frac{\varepsilon_3}{2}|a|^2 + \frac{1}{2\varepsilon_3}|c|^2\Big).
\end{cases} \tag{A.44}$$

Using the aforementioned items and (A.44) in (A.42) results in the following:

$$\begin{aligned}
\dot{V} &\leq -\mathfrak{C}_a|a|^2 - \mathfrak{C}_b|b|^2 - \mathfrak{C}_c|c|^2 - \mathfrak{C}_{\mathrm{sym}}a^{\mathrm{T}}\mathsf{L}_s^n a \\
&\leq -\min\{\mathfrak{C}_a,\ \mathfrak{C}_b,\ \mathfrak{C}_c\}(|a|^2 + |b|^2 + |c|^2)
\end{aligned} \tag{A.45}$$

where the coefficients $\mathfrak{C}_{\{\cdot\}}$ are given by

$$\begin{aligned}\mathfrak{C}_a &= \phi\Delta\mu\mathfrak{b}_1 - \big(K_a\mathfrak{a}_1 + \Delta\big(\mathfrak{a}_1\Delta - \mathfrak{b}_2\phi\big)\big)\frac{\varepsilon_1}{2} \\ &\quad - \big(\phi^2 + K_b\big)\mathfrak{b}_1\frac{\mathfrak{L}\varepsilon_2}{2} - \phi\Delta\mathfrak{a}_2\mathfrak{b}_1\frac{\mathfrak{L}\varepsilon_3}{2}, \qquad \text{(A.46a)} \\ \mathfrak{C}_b &= \big(K_b\mathfrak{b}_2 - \phi\big(\mathfrak{a}_1\Delta - \mathfrak{b}_2\phi\big)\big) - \big(\phi^2 + K_b\big)\mathfrak{b}_1\frac{\mathfrak{L}}{2\varepsilon_2} \\ &\quad - \big(K_a\mathfrak{a}_1 + \Delta\big(\mathfrak{a}_1\Delta - \mathfrak{b}_2\phi\big)\big)\frac{1}{2\varepsilon_1}, \qquad \text{(A.46b)} \\ \mathfrak{C}_c &= \phi\Delta\big(\mathfrak{a}_2\mathfrak{b}_3 - \mathfrak{b}_3\frac{\lambda_M^\Gamma}{2\zeta_1} - \mathfrak{a}_2\mathfrak{b}_1\frac{\mathfrak{L}}{2\varepsilon_3}\big), \qquad \text{(A.46c)} \\ \mathfrak{C}_{\text{sym}} &= \big(K_a\mathfrak{a}_2 - \phi\Delta\mathfrak{b}_3\frac{\lambda_M^\Gamma\zeta_1\epsilon_{\mathsf{L}}}{2}\big). \qquad \text{(A.46d)}\end{aligned}$$

If we ensure that every $\mathfrak{C}_{\{\cdot\}} > 0$ in (A.46), then from (A.45), it can be seen that the Lyapunov function V has linear decay rate, i.e., $\dot{V} \leq -\alpha_V V$ where

$$\alpha_V \geq \frac{\min\{\mathfrak{C}_a,\ \mathfrak{C}_b,\ \mathfrak{C}_c\}}{\lambda_M^{\mathfrak{P}}} \propto \mathfrak{b}_1\phi^2, \qquad \text{(A.47)}$$

and $\lambda_M^{\mathfrak{P}}$ is the maximum eigenvalue of $\mathfrak{P}$ given by

$$\mathfrak{P} = \frac{1}{2}\begin{bmatrix} (K_a+\Delta^2)\mathbb{I}_N & \Delta\phi\mathbb{I}_N & \pi\Delta\mathbb{I}_N \\ \Delta\phi\mathbb{I}_N & (K_b+\phi^2)\mathbb{I}_N & \phi\pi\mathbb{I}_N \\ \pi\Delta\mathbb{I}_N & \phi\pi\mathbb{I}_N & \pi^2\mathbb{I}_N+\Delta\phi\mathfrak{b}_3\Gamma \end{bmatrix} \otimes \mathbb{I}_n.$$

Part 2: Here, we show positivity of coefficients $\mathfrak{C}_{\{\}}$, expressed in (A.46), to ensure convergence of the system dynamics in (7.5) which simultaneously addresses concerns on existence of such gains. Let $K_b = \mathfrak{X}_b\phi^2$, $\mathfrak{a}_2 = \Theta\mathfrak{b}_3$ and $\mathfrak{a}_1 = \mathfrak{p}\mathfrak{b}_2$ where scalars $\mathfrak{X}_b,\ \Theta,\ \mathfrak{p} > 0$. First, from $\mathfrak{C}_c > 0$ and $\mathfrak{C}_a > 0$, we can establish bounds of ε_3 as follows:

$$\frac{2\mu}{\mathfrak{a}_2\mathfrak{L}} > \varepsilon_3 > \frac{\Theta\mathfrak{b}_1\mathfrak{L}}{2\Big(\mathfrak{a}_2 - \frac{\lambda_M^\Gamma}{2\zeta_1}\Big)}. \qquad \text{(A.48)}$$

A feasible solution that ensures the order of inequalities in (A.48) is plausible only if the following inequalities are simultaneously satisfied:

$$\begin{cases} \Theta < \frac{4\mu}{\mathfrak{b}_1\mathfrak{L}^2}, \\ \zeta_1 > \frac{2\mu\lambda_M^\Gamma}{\mathfrak{a}_2\left(4\mu - \Theta\mathfrak{b}_1\mathfrak{L}^2\right)}. \end{cases} \qquad \text{(A.49)}$$

To simplify our analysis, we choose $\Theta := 2\mu(\mathfrak{b}_1\mathfrak{L}^2)^{-1}$ and $\zeta_1 := 2\lambda_M^\Gamma(\mathfrak{a}_2)^{-1}$ that comply with (A.49). This choice bounds ε_3 as follows: $2\frac{\mu}{\mathfrak{a}_2\mathfrak{L}} > \varepsilon_3 > \frac{4}{3}\frac{\mu}{\mathfrak{a}_2\mathfrak{L}}$. Let $\varepsilon_3 := 3\mu(2\mathfrak{a}_2\mathfrak{L})^{-1}$; then, $\mathfrak{C}_c = \frac{1}{24}\frac{\mathfrak{a}_2^2\mathfrak{L}^2}{\mu}\mathfrak{b}_1\phi\Delta$. From $\mathfrak{C}_{\text{sym}} > 0$, we have $K_a > \frac{(\lambda_M^\Gamma\mathfrak{L})^2\epsilon_{\mathsf{L}}}{2\mu}\frac{\mathfrak{b}_1}{\mathfrak{a}_2}\phi\Delta$. Define $\mathfrak{R}$ such that $\mathfrak{R} > \mathfrak{R}_{K_a} = \frac{(\lambda_M^\Gamma\mathfrak{L})^2\epsilon_{\mathsf{L}}}{2\mu}$, and let $K_a = \mathfrak{R}\mathfrak{b}_1(\mathfrak{a}_2)^{-1}\phi\Delta$; then,

$$\begin{aligned}\mathfrak{C}_{\text{sym}} &= \mathfrak{R}\mathfrak{b}_1\phi\Delta - \phi\Delta\mathfrak{b}_3\frac{\lambda_M^\Gamma\zeta_1\epsilon_{\mathsf{L}}}{2}\\ &= \Big(\mathfrak{R}\mathfrak{b}_1 - (\lambda_M^\Gamma)^2\epsilon_{\mathsf{L}}\frac{\mathfrak{b}_3}{\mathfrak{a}_2}\Big)\phi\Delta\\ &= \big(\mathfrak{R} - \mathfrak{R}_{K_a}\big)\mathfrak{b}_1\phi\Delta.\end{aligned}$$

Note that $\mathfrak{R}_{k_a}$ depends solely on the network and objective functions involved. Choices made for Θ, ζ_1, ε_3, $\mathfrak{R}$ and K_a ensure that the coefficients $\mathfrak{C}_{\{c,\text{sym}\}}$ are positive. Next, we determine other design parameters in order to ensure that the coefficients $\mathfrak{C}_{\{a,b\}}$ are also positive. For this, we begin by evaluating (A.43) which can be expressed as:

$$\begin{aligned}&\Theta\mathfrak{b}_3\mathfrak{b}_2\big(\mathfrak{p}\Delta^2 - \phi\Delta\big) - (\mathfrak{X}_b+1)\phi^2\mathfrak{b}_3 = 0\\ \implies &\Delta^2 - \frac{1}{\mathfrak{p}}\phi\Delta - \frac{1}{\mathfrak{p}}\frac{\mathfrak{X}_b+1}{\Theta\mathfrak{b}_2}\phi^2 = 0.\end{aligned} \tag{A.50}$$

Note that the quadratic equation in (A.50), in Δ/ϕ, always has two real roots; these lie on either side of the imaginary axis. Let $\mathfrak{S}_{\frac{\Delta}{\phi}}$, given by (7.7), denote the positive solution of (A.50). Through substitutions involving various parameters, we can rewrite $\mathfrak{C}_a$ and $\mathfrak{C}_b$ in (A.46) as

$$\begin{aligned}\mathfrak{C}_a &= \phi^2\mathfrak{b}_1\mathfrak{S}_{\frac{\Delta}{\phi}}\frac{\mu}{4} - K_a\mathfrak{a}_1\frac{\varepsilon_1}{2} - \big(\mathfrak{X}_b+1\big)\phi^2\Big(\frac{\varepsilon_1}{2\Theta} + \frac{\mathfrak{b}_1\mathfrak{L}\varepsilon_2}{2}\Big)\\ &= \mathfrak{b}_1\phi^2\Big(\mathfrak{S}_{\frac{\Delta}{\phi}}\frac{\mu}{4} - \big(\mathfrak{X}_b+1\big)\mathfrak{L}\Big(\frac{\mathfrak{L}}{\mu}\frac{\varepsilon_1}{4} + \frac{\varepsilon_2}{2}\Big) - \mathfrak{R}(\mathfrak{S}_{\frac{\Delta}{\phi}}\mathfrak{p})\frac{\mathfrak{b}_2}{\mathfrak{a}_2}\frac{\varepsilon_1}{2}\Big),\end{aligned} \tag{A.51}$$

and

$$\begin{aligned}\mathfrak{C}_b &= \mathfrak{X}_b\mathfrak{b}_2\phi^2 - K_a\mathfrak{a}_1\frac{1}{2\varepsilon_1} - \big(\mathfrak{X}_b+1\big)\phi^2\Big(\mathfrak{b}_1\frac{\mathfrak{L}}{2\varepsilon_2} + \frac{1}{\Theta}\frac{\phi}{\Delta} + \frac{1}{\Theta}\frac{1}{2\varepsilon_1}\Big)\\ &= \mathfrak{b}_2\phi^2\Big(\mathfrak{X}_b - \mathfrak{R}(\mathfrak{S}_{\frac{\Delta}{\phi}}\mathfrak{p})\frac{\mathfrak{b}_1}{\mathfrak{a}_2}\frac{1}{2\varepsilon_1}\Big) - \big(\mathfrak{X}_b+1\big)\mathfrak{b}_1\phi^2\Big(\frac{\mathfrak{L}}{2\varepsilon_2} + \frac{\mathfrak{L}^2}{2\mu}\frac{1}{\mathfrak{S}_{\frac{\Delta}{\phi}}} + \frac{\mathfrak{L}^2}{2\mu}\frac{1}{2\varepsilon_1}\Big)\\ &= \mathfrak{b}_1\phi^2\Big(\frac{\mathfrak{b}_2}{\mathfrak{b}_1}\mathfrak{X}_b - \big(\mathfrak{X}_b+1\big)\mathfrak{L}\Big(\frac{\mathfrak{L}}{2\mu}\frac{1}{2\varepsilon_1} + \frac{1}{2\varepsilon_2} + \frac{\mathfrak{L}}{2\mu}\frac{1}{\mathfrak{S}_{\frac{\Delta}{\phi}}}\Big) - \mathfrak{R}(\mathfrak{S}_{\frac{\Delta}{\phi}}\mathfrak{p})\frac{\mathfrak{b}_2}{\mathfrak{a}_2}\frac{1}{2\varepsilon_1}\Big),\end{aligned} \tag{A.52}$$

respectively. To provide intuition on solving for positivity of $\mathfrak{C}_a,\ \mathfrak{C}_b$ in (A.51) and (A.52), respectively, we let $\varepsilon_1 = \varepsilon_2 = \varepsilon$; then $\mathfrak{C}_{\{a,b\}} > 0$ can be combined into one inequality expressed in (7.6). From $\mathfrak{S}_{\frac{\Delta}{\phi}}$ in (7.7) we see that a relatively small $\mathfrak{p}$ can inflate the first argument of the min function in (7.6). This affects the second term in (7.6), specifically $\mathfrak{S}_{\frac{\Delta}{\phi}}\mathfrak{p} = (1+\frac{\mathfrak{p}}{\mathfrak{J}})^{\frac{1}{2}}$, favorably; additionally, this term can also be manipulated by picking appropriate ratio $\mathfrak{r}_2 := \mathfrak{b}_2/\mathfrak{a}_2$. The second argument of the min function can be inflated by appropriately choosing the ratio $\mathfrak{r}_1 := \mathfrak{b}_2/\mathfrak{b}_1$. Thus, solving (7.6) ensures positivity of coefficients $\mathfrak{C}_{\{a,b\}}$.

To summarize, the coefficients $\mathfrak{a}_{\{1,2\}},\ \mathfrak{b}_{\{2,3\}}$ in (7.5) can be expressed in terms of the gradient gain $\mathfrak{b}_1$, ratios $\mathfrak{r}_{\{1,2\}},\ \mathfrak{p}$ and (cost) function parameters $\mathfrak{L},\ \mu$ as follows:

$$\begin{cases} \mathfrak{a}_1 = \mathfrak{p}\mathfrak{r}_1\mathfrak{b}_1, & \mathfrak{a}_2 = \frac{\mathfrak{r}_1}{\mathfrak{r}_2}\mathfrak{b}_1, \\ \mathfrak{b}_2 = \mathfrak{r}_1\mathfrak{b}_1, & \mathfrak{b}_3 = \frac{\mathfrak{a}_2}{\Theta} = \frac{\mathfrak{r}_1}{\mathfrak{r}_2}\frac{\mathfrak{L}^2}{2\mu}\mathfrak{b}_1^2. \end{cases} \tag{A.53}$$

In order to ease the design of event-based broadcasting in Section 7.4, we also define $\breve{\mathfrak{C}}_{\{\}}$ such that the coefficients $\mathfrak{C}_{\{\}}$ in (A.45) can be expressed as $\mathfrak{C}_{\{\}} = \mathfrak{b}_1\phi^2\breve{\mathfrak{C}}_{\{\}}$. Here, $\breve{\mathfrak{C}}_{\{\}}$ are given by:

$$\breve{\mathfrak{C}}_a = \mathfrak{S}_{\frac{\Delta}{\phi}}\frac{\mu}{4} - \big(\mathfrak{X}_b+1\big)\mathfrak{L}\Big(\frac{\mathfrak{L}}{4\mu}+\frac{1}{2}\Big) - \mathfrak{R}(\mathfrak{S}_{\frac{\Delta}{\phi}}\mathfrak{p})\frac{\mathfrak{b}_2}{2\mathfrak{a}_2}, \tag{A.54a}$$

$$\breve{\mathfrak{C}}_b = \frac{\mathfrak{b}_2}{\mathfrak{b}_1}\mathfrak{X}_b - \big(\mathfrak{X}_b+1\big)\mathfrak{L}\Big(\frac{\mathfrak{L}}{4\mu}+\frac{1}{2}+\frac{\mathfrak{L}}{2\mu}\frac{1}{\mathfrak{S}_{\frac{\Delta}{\phi}}}\Big) - \mathfrak{R}(\mathfrak{S}_{\frac{\Delta}{\phi}}\mathfrak{p})\frac{\mathfrak{b}_2}{2\mathfrak{a}_2}, \tag{A.54b}$$

$$\breve{\mathfrak{C}}_c = \frac{1}{24}\Big(\frac{\mathfrak{r}_1}{\mathfrak{r}_2}\Big)^2\frac{\mathfrak{L}^2}{\mu}\mathfrak{S}_{\frac{\Delta}{\phi}}\mathfrak{b}_1^2, \tag{A.54c}$$

$$\breve{\mathfrak{C}}_{\text{sym}} = \big(\mathfrak{R}-\mathfrak{R}_{K_a}\big)\mathfrak{S}_{\frac{\Delta}{\phi}}. \tag{A.54d}$$

A.4.3 Effect of the Broadcast Error

Recall that e only affects functions V_a and V_b, defined in Appendix A.4.2; therefore, their derivatives along dynamics in (7.10) are bounded as:

$$\begin{aligned} \dot{V}_a &= \mathfrak{a}_1 a^{\mathrm{T}} b - \mathfrak{a}_2 a^{\mathrm{T}}\mathsf{L}_s^n a - \mathfrak{a}_2 a^T\mathsf{L}^n e \\ &\le \mathfrak{a}_1 a^{\mathrm{T}} b - \mathfrak{a}_2 a^{\mathrm{T}}\mathsf{L}_s^n a + \underbrace{\sigma_{\mathsf{L}}\Big(\frac{\mathfrak{b}_1}{2\varrho_1}|a|^2 + \frac{\varrho_1}{2\mathfrak{b}_1}|e|^2\Big)} \end{aligned}$$

and

$$\begin{aligned}\dot{V}_c &= c^{\mathrm{T}}a + c^{\mathrm{T}}\Gamma^n \mathsf{L}_{ss}^n a + c^{\mathrm{T}}e + c^{\mathrm{T}}\Gamma^n \mathsf{L}_{ss}^n e \\ &\le c^{\mathrm{T}}a + \Big(\frac{\lambda_M^\Gamma}{2\zeta_1} + \underbrace{\frac{\mathfrak{b}_1}{2\iota_1} + \frac{\mathfrak{b}_1\lambda_M^\Gamma}{2\iota_2}}\Big)|c|^2 + \frac{\lambda_M^\Gamma \zeta_1 \epsilon_{\mathsf{L}}}{2} a^{\mathrm{T}} \mathsf{L}_s^n a \\ &\quad + \underbrace{\frac{1}{\mathfrak{b}_1}\Big(\frac{\iota_1}{2} + \frac{\lambda_M^\Gamma \iota_2 \epsilon_{\mathsf{L}}}{2}\lambda_M^{\mathsf{L}_s}\Big)|e|^2},\end{aligned}$$

where the under-brace shows the additional terms as a result of broadcast error. Here, σ_{L} is the spectral norm of L. The derivative of V, defined in (A.41), along (7.10) is then upper bounded as:

$$\dot{V} \le -\hat{\mathfrak{C}}_a|a|^2 - \mathfrak{C}_b|b|^2 - \hat{\mathfrak{C}}_c|c|^2 - \mathfrak{C}_{\mathrm{sym}} a^{\mathrm{T}} \mathsf{L}_s a + \mathfrak{C}_e|e|^2,$$

where

$$\hat{\mathfrak{C}}_a = \mathfrak{C}_a - K_a\sigma_{\mathsf{L}}\frac{\mathfrak{b}_1}{2\varrho_1} = \mathfrak{b}_1\phi^2\Big(\breve{\mathfrak{C}}_a - \Re\mathfrak{S}_{\frac{\Delta}{\phi}}\frac{\mathfrak{r}_2}{\mathfrak{r}_1}\frac{\sigma_{\mathsf{L}}}{2\varrho_1}\Big) \tag{A.55a}$$

$$\begin{aligned}\hat{\mathfrak{C}}_c &= \mathfrak{C}_c - \Delta\phi\mathfrak{b}_3\Big(\frac{\mathfrak{b}_1}{2\iota_1} + \frac{\mathfrak{b}_1\lambda_M^\Gamma}{2\iota_2}\Big) \\ &= \mathfrak{b}_1\phi^2\Big(\breve{\mathfrak{C}}_c - \mathfrak{S}_{\frac{\Delta}{\phi}}\mathfrak{b}_3\Big(\frac{1}{2\iota_1} + \frac{1\lambda_M^\Gamma}{2\iota_2}\Big)\Big) \\ &= \mathfrak{b}_1^3\phi^2\mathfrak{S}_{\frac{\Delta}{\phi}}\frac{\mathfrak{r}_1}{\mathfrak{r}_2}\frac{\mathfrak{L}^2}{2\mu}\Big(\frac{1}{12}\frac{\mathfrak{r}_1}{\mathfrak{r}_2} - \Big(\frac{1}{2\iota_1} + \frac{\lambda_M^\Gamma}{2\iota_2}\Big)\Big),\end{aligned} \tag{A.55b}$$

$$\begin{aligned}\mathfrak{C}_e &= \frac{1}{2\mathfrak{b}_1}\Big(K_a\sigma_{\mathsf{L}}\varrho_1 + \Delta\phi\mathfrak{b}_3(\iota_1 + \lambda_M^\Gamma\iota_2\epsilon_{\mathsf{L}}\lambda_M^{\mathsf{L}_s})\Big) \\ &= \frac{\mathfrak{S}_{\frac{\Delta}{\phi}}\phi^2}{2\mathfrak{b}_1}\Big(\Re\frac{\mathfrak{r}_2}{\mathfrak{r}_1}\sigma_{\mathsf{L}}\varrho_1 + \mathfrak{b}_3(\iota_1 + \lambda_M^\Gamma\lambda_M^{\mathsf{L}_s}\epsilon_{\mathsf{L}}\iota_2)\Big),\end{aligned} \tag{A.55c}$$

and $\breve{\mathfrak{C}}_a$ is from (A.54). Here, positivity of coefficients $\hat{\mathfrak{C}}_{\{a,c\}}$ can be ensured by choosing $\varrho_1,\ \iota_1,\ \iota_2$ as follows:

$$\varrho_1 > \Re\frac{\mathfrak{r}_2}{\mathfrak{r}_1}\frac{2\sigma_{\mathsf{L}}}{\mu}, \tag{A.56a}$$

$$\Big(\frac{1}{\iota_1} + \frac{\lambda_M^\Gamma}{\iota_2}\Big) < \frac{1}{6}\frac{\mathfrak{r}_1}{\mathfrak{r}_2}, \tag{A.56b}$$

and, if deemed necessary, revising the choice of $\mathfrak{p}$ in (7.6). Let the new choice of $\mathfrak{p}$ be denoted by $\bar{\mathfrak{p}}$; if it remains unchanged then $\bar{\mathfrak{p}} = \mathfrak{p}$.

A.4.4 Proof of Theorem 7.2

In this proof, using the η_i dynamics in (7.21), we show that the dynamics in (7.10) asymptotically converges to E.

We begin the proof by establishing some quantities. First, recall that in (7.19) we bounded the growth rate of W_i. Here, we define H_i such that $\dot{W}_i \leq (\mathfrak{a}_2\mathsf{d}_i)W_i + H_i$, where $H_i^2 \coloneqq 2\big(\mathfrak{a}_1^2|b_i|^2 + \mathfrak{a}_2^2|\mathsf{L}_i|^2|a|^2 + \mathfrak{a}_2^2|\mathsf{A}_i|^2|e|^2\big)$. Next, we add and subtract $\sum_{i\forall\mathcal{V}}(\delta_1/\mathfrak{b}_1)H_i^2$, $\delta_1 > 0$, from (7.18) which results in:

$$\begin{aligned}\dot{V} \leq & -\big(\hat{\mathfrak{C}}_a - 2\frac{\delta_1}{\mathfrak{b}_1}\mathfrak{a}_2^2\mathrm{Tr}(\mathsf{L}^{\mathrm{T}}\mathsf{L})\big)|a|^2 - \big(\mathfrak{C}_b - 2\frac{\delta_1}{\mathfrak{b}_1}\mathfrak{a}_1^2\big)|b|^2 \\ & - \hat{\mathfrak{C}}_c|c|^2 - \mathfrak{C}_{\mathrm{sym}}a^{\mathrm{T}}\mathsf{L}_s a + \sum_{i\forall\mathcal{V}}\Big\{\big(\mathfrak{C}_e + 2\frac{\delta_1}{\mathfrak{b}_1}\mathfrak{a}_2^2\mathrm{Tr}(\mathsf{A}^{\mathrm{T}}\mathsf{A})\big)|e_i|^2 - \frac{\delta_1}{\mathfrak{b}_1}H_i^2\Big\}.\end{aligned} \tag{A.57}$$

where $\hat{\mathfrak{C}}_{\{a,c\}}$, $\mathfrak{C}_e$ are defined in (A.55).

Second, to enhance performance of the ETC in (7.13), we use the information that is locally available at the node, namely, $\mathsf{L}_i^n\hat{x}$, to construct an function $\hat{V}_i$ as

$$\hat{V}_i = \mathfrak{c}_{\mathsf{L}}|\mathsf{L}_i^n\hat{x}|^2 \leq \mathfrak{c}_{\mathsf{L}}|\mathsf{L}_i|^2|a|^2 + \mathfrak{c}_{\mathsf{L}}|\mathsf{L}_i|^2|e|^2. \tag{A.58}$$

We add and subtract $\sum_{i\forall\mathcal{V}}\mathfrak{b}_1\hat{V}_i$ from (A.57), resulting in

$$\begin{aligned}\dot{V} \leq & -\underbrace{\Big(\hat{\mathfrak{C}}_a - (2\mathfrak{a}_2^2\frac{\delta_1}{\mathfrak{b}_1} + \mathfrak{b}_1\mathfrak{c}_{\mathsf{L}})\mathrm{Tr}(\mathsf{L}^{\mathrm{T}}\mathsf{L})\Big)}_{\bar{\mathfrak{C}}_a}|a|^2 \\ & - \underbrace{\big(\mathfrak{C}_b - 2\mathfrak{a}_1^2\frac{\delta_1}{\mathfrak{b}_1}\big)}_{\bar{\mathfrak{C}}_b}|b|^2 - \hat{\mathfrak{C}}_c|c|^2 - \mathfrak{C}_{\mathrm{sym}}a^{\mathrm{T}}\mathsf{L}_s a \\ & + \sum_{i\forall\mathcal{V}}\Big\{\underbrace{\Big(\mathfrak{C}_e + \Big(2\mathfrak{a}_2^2\frac{\delta_1}{\mathfrak{b}_1}\mathrm{Tr}(\mathsf{A}^{\mathrm{T}}\mathsf{A}) + \mathfrak{b}_1\mathfrak{c}_{\mathsf{L}}\mathrm{Tr}(\mathsf{L}^{\mathrm{T}}\mathsf{L})\Big)\Big)}_{\gamma_i^2}|e_i|^2 \\ & - \frac{\delta_1}{\mathfrak{b}_1}H_i^2 - \mathfrak{b}_1\hat{V}_i\Big\}.\end{aligned} \tag{A.59}$$

From (A.53), we express $\mathfrak{a}_1$, $\mathfrak{a}_2$ in terms of $\mathfrak{b}_1$ and $\bar{\mathfrak{p}}$; then

$$\begin{aligned}\bar{\mathfrak{C}}_a =& \mathfrak{b}_1\Big(\phi^2\Big(\breve{\mathfrak{C}}_a - \mathfrak{RS}\tfrac{\Delta}{\phi}\frac{\mathfrak{r}_2}{\mathfrak{r}_1}\frac{\sigma_{\mathsf{L}}}{2\varrho_1}\Big) - (2\frac{\mathfrak{r}_1^2}{\mathfrak{r}_2^2}\delta_1 + \mathfrak{c}_{\mathsf{L}})\mathrm{Tr}(\mathsf{L}^{\mathrm{T}}\mathsf{L})\Big), \\ \bar{\mathfrak{C}}_b =& \mathfrak{b}_1\Big(\breve{\mathfrak{C}}_b\phi^2 - 2\bar{\mathfrak{p}}^2\mathfrak{r}_1^2\delta_1\Big),\end{aligned} \tag{A.60}$$

where coefficients $\bar{\mathfrak{C}}_{\{a,b\}}$, $\hat{\mathfrak{C}}_c$ ought to be positive which can be ensured, independent of choice of $\mathfrak{b}_1$, by choosing appropriate ϕ.

Now, we are ready to show the convergence of the hybrid dynamics (7.15). Let the Lyapunov function be defined as follows:

$$U \coloneqq V + \sum_{\forall i \in \mathcal{V}} \big\{ \gamma_i \theta_i W_i^2 + \eta_i \big\}.$$

Stability analysis for hybrid systems has two aspects, namely, convergence in the flow domain when $\mathcal{X} \in C$, and convergence in the jump domain when $\mathcal{X} \in D$.

• *Analysis during flow:*

The derivative of U along the dynamics described in (7.15) is:

$$\begin{aligned}
U^\circ &= \dot{V} + \sum_{\forall i} \big\{ \gamma_i \dot{\theta}_i |e_i|^2 + 2\gamma_i \theta_i \dot{W}_i |e_i| + \eta_i^\circ \big\} \\
&\leq - \bar{\mathfrak{C}}_a |a|^2 - \bar{\mathfrak{C}}_b |b|^2 - \hat{\mathfrak{C}}_c |c|^2 - \mathfrak{C}_{\text{sym}} a^{\mathrm{T}} \mathsf{L}_s a + \sum_{\forall i} \Big\{ \gamma_i^2 |e_i|^2 \\
&\quad + \gamma_i \big(- 2L_\nu^i \theta_i - \gamma_i (\frac{\mathfrak{b}_1}{\delta_1} \theta_i^2 + 1) \big) |e_i|^2 \\
&\quad + 2\gamma_i \theta_i \big(\mathfrak{a}_2 \mathsf{d}_i |e_i| + H_i \big) |e_i| + \dot{\eta}_i - \frac{\delta_1}{\mathfrak{b}_1} H_i^2 - \mathfrak{b}_1 \hat{V}_i \Big\} \\
&\leq - \bar{\mathfrak{C}}_a |a|^2 - \bar{\mathfrak{C}}_b |b|^2 - \hat{\mathfrak{C}}_c |c|^2 - \mathfrak{C}_{\text{sym}} a^{\mathrm{T}} \mathsf{L}_s a \\
&\quad - \sum_{\forall i} \Big\{ 2\gamma_i \theta_i \nu_i |e_i|^2 + \beta_i \eta_i \Big\}.
\end{aligned} \tag{A.61}$$

where U° denotes the Clarke derivative, see [12]. Here, we used Young's inequality to disintegrate $2\gamma_i \theta_i H_i |e_i|$ as:

$$2\gamma_i \theta_i H_i |e_i| \leq \frac{\mathfrak{b}_1}{\delta_1} \gamma_i^2 \theta_i^2 |e_i|^2 + \frac{\delta_1}{\mathfrak{b}_1} H_i^2.$$

Since the coefficients $\bar{\mathfrak{C}}_{\{a,b\}}$, $\hat{\mathfrak{C}}_c$, β_i are positive, there exists a positive definite function Ω such that U° in (A.61) satisfies

$$U^\circ \leq -\Omega(U(\mathcal{X})), \ \forall \mathcal{X} \in C. \tag{A.62}$$

• *Analysis at jumps:*

Prior to examining changes in the Lyapunov function U, over the jump domain

D, we define three index sets to categorize agents based on the sign of their g_s^i at the jump instant $\mathfrak{t}$. Recall that in (7.17), the jump states described by the set-valued mapping in $\mathcal{J}_i$ depend on g_s^i. At jump instant $\mathfrak{t}$, the nodes in the network, which actively take part in the jump, must belong to one of the following sets: a) $\mathcal{P} = \{i \in \mathcal{V} \mid g_s^i > 0\}$, b) $\mathcal{Q} = \{i \in \mathcal{V} \mid g_s^i < 0\}$, and c) $\mathcal{R} = \{i \in \mathcal{V} \mid g_s^i = 0\}$. Here, $\mathcal{P} \cup \mathcal{Q} \cup \mathcal{R} \subseteq \mathcal{V}$. Note that agents which do not take part in the jump, at jump instant $\mathfrak{t}$, do not contribute towards changes in U.

The states (a, b, c), like mentioned in Section 7.4.1, do not change, instantaneously, after the jump; however, states (e, η, τ) instantaneously jump as follows:

$$\begin{cases} \forall i \in \mathcal{P}: & e_i^+ = e_i,\ \eta_i^+ = g_s^i,\ \tau_i^+ = 0, \\ \forall i \in \mathcal{Q}: & e_i^+ = \mathbf{0},\ \eta_i^+ = g_t^i,\ \tau_i^+ = 0, \\ \forall i \in \mathcal{R}: & \begin{cases} \forall i \in \mathcal{R}_1: & e_i^+ = e_i,\ \eta_i^+ = g_s^i,\ \tau_i^+ = 0, \\ \forall i \in \mathcal{R}_2: & e_i^+ = \mathbf{0},\ \eta_i^+ = g_t^i,\ \tau_i^+ = 0, \end{cases} \end{cases}$$

where $\mathcal{R}_1,\ \mathcal{R}_2$ are subsets of $\mathcal{R}$ such that the $\mathcal{R}_1 \cup \mathcal{R}_2 = \mathcal{R}$ and $\mathcal{R}_1 \cap \mathcal{R}_2 = \phi$ (null set). The two sets $\mathcal{R}_1$ and $\mathcal{R}_2$ represent the index subsets of nodes $i \in \mathcal{R}$ that jump to states $\mathcal{J}_i^1$ and $\mathcal{J}_i^2$, respectively. At any jump instant $V^+ = V$, therefore we have:

$$\begin{aligned} U^+ - U &= \sum_{\forall i} \Big\{ \eta_i^+ - \eta_i + \big[\gamma_i \theta_i |e_i|^2\big]^+ - \gamma_i \theta_i |e_i|^2 \Big\} \\ &\leq \sum_{i \in \mathcal{P} \cup \mathcal{R}_1} \Big\{ g_t^i - \eta_i + \gamma_i \Big(\frac{1}{\lambda_i} |e_i^+|^2 - \theta_i |e_i|^2 \Big) \Big\} \\ &\quad + \sum_{i \in \mathcal{Q} \cup \mathcal{R}_2} \Big\{ g_s^i - \eta_i + \gamma_i \Big(\frac{1}{\lambda_i} |e_i^+|^2 - \theta_i |e_i|^2 \Big) \Big\} \\ &\leq -\sum_{i \in \mathcal{P} \cup \mathcal{R}_1} \gamma_i (\theta_i - \lambda_i) |e_i|^2 \leq 0. \end{aligned}$$

Recall that $\theta_i(\tau_i) \geq \lambda_i$ from Lemma 7.3; therefore, from (**??**) we have:

$$U(\mathcal{X}^+) \leq U(\mathcal{X}),\ \mathcal{X} \in D. \tag{A.63}$$

The proof is completed by following the arguments made in Theorem 1 of [69] using (A.62) and (A.63). □